IMPROVING EXTREME PRECIPITATION ESTIMATES CONSIDERING REGIONAL FREQUENCY ANALYSIS(Dissertation_全文)

AUTHOR(S):

Nor Eliza Binti Alias

CITATION:

Nor Eliza Binti Alias. IMPROVING EXTREME PRECIPITATION ESTIMATES CONSIDERING REGIONAL FREQUENCY ANALYSIS. 京都大学, 2014, 博士(工学)

ISSUE DATE:

2014-09-24

URL:

https://doi.org/10.14989/doctor.k18562

IMPROVING EXTREME PRECIPITATION ESTIMATES CONSIDERING REGIONAL FREQUENCY ANALYSIS

Nor Eliza Binti Alias

2014

IMPROVING EXTREME PRECIPITATION ESTIMATES CONSIDERING REGIONAL FREQUENCY ANALYSIS

（地域頻度解析を考慮した極端降水推定値の精度向上に関する研究）

by

Nor Eliza Binti Alias

A dissertation submitted in partial fulfilment of the requirements for the Degree of Doctor of Engineering

Department of Civil and Earth Resources Engineering

Kyoto University, Japan

2014

~~ *To my beloved family and to world peace* ~~

~~ ~~ ⁛ ~~ ~~

Acknowledgements

This PhD research titled "*Improving extreme precipitation estimates considering regional frequency analysis"* was carried out in the Department of Civil and Earth Resources Engineering, Kyoto University during October 2011 to September 2014. It was a pleasure for me to be part of Professor Takara's Laboratory (Innovative Disaster Prevention Technology and Policy Research Laboratory), Division of Disaster Management for Safe and Secure Society of the Disaster Prevention Research Institute (DPRI), Kyoto University, Japan. I gained a great deal of knowledge on the problems and issues related to extreme rainfall conditions and the climate change. Various skills such as writing, communications and human soft skills as a researcher were also gained during this short three-year period as a doctoral student. Involvement of professors and educators in Japan as well as other parts of the world made it possible for the completion of my PhD degree. Thus, my appreciations should be expressed to all of them.

I would like to give the highest degree of appreciation and gratitude to my supervisor Professor Kaoru Takara for his kind generosity to accept me as his student and to be a part of his laboratory. Countless thanks for his guidance, encouragement, and faith towards my research. Due to him I was introduced to the Kyoto University's GCOE-ARS program. The program exposes me to various international and local academic events such as conferences, symposiums, international gatherings and world organizations' meetings. The experience gained from the academic events made me wiser, open-minded and able to think more critically towards global hydrological and extreme climate issues. I would also like to give my appreciation to Associate Professor of GCOE-ARS Masahito Ishihara, Professor Eiichi Nakakita, Associate Professor Sunmin Kim, Professor Bin HE, Dr. Apip, and Dr. Pingping LUO for their direct assistant and constructive suggestions and guidance in improving my research. I would like to express my gratitude to my sub-supervisors Associate Professor Yosuke Yamashiki and Professor Yasuto Tachikawa for showing interests in my research and make me feel valuable as a student. Appreciations and acknowledgements are also towards my internship's supervisor Prof. Hayley Fowler and Dr. Stephen Blenkinsop of Newcastle University, United Kingdom and Dr. Fiona Johnson of University of New South Wales, Sydney who gave me plenty of advices, new perspectives and taught me on climate change analysis. They exposed me to the current problems and issues of extreme rainfalls in Europe and in Australia.

I would also like to express my thanks to the secretaries of Takara Laboratory and secretaries of the GCOE-ARS program. Highest gratitude is towards Ms. Sono Inoue, Ms. Yoko Yonekawa, Ms. Mayumi Nishimura, Ms. Kaori Saidera, and Ms. Saho Matsuda for their kind and excellent assistance and administrative tasks for me and the other students of Takara Laboratory. Lovely thanks are also for all my dear friends and colleagues with whom I had many discussions and debates in order to improve my research and me as a whole. They are Mr. Weili Duan, Mr. Hendy Setiawan, Mr. Josko Troselj, Mr. Bounheing

Vilasane, Mrs. Pham Hong Nga, Mr. Maochuan Hu, Mr. Han Xue (Setsu), Mr. Adnan Arutyunov and Ms. Tomoko Teramoto. Many thanks also to my friends for their companion and assistant of my daily lives in Japan, they are Dr. Remy Rozaini, Dr. Maja Ostric, Mr. Toshiharu Sasaki, Ms. Eun Bi Kang, Ms. Yong-A Shin, Dr. Tsutao Oizumi, Ms. Khai Lin Chong, Ms. Jamilah Rajabi, Ms. Eva Mia Siska, Ms. Yongxue Shi (Seki), Mr. Dang Quang Khang, Mr. Pham Van Tien, and Mr. Doan Huy Loi.

The highest degrees of appreciations are also to my darling husband Ahmad Zaki Bin Kassim for his sacrifices, patience and care towards me and our daughter Adlina chan during the whole period of my PhD life. Without his love and support, I would not have the strong spirit to do the best and survive. Heartiest appreciations and gratitude are also to my parents Alias Bin Mohd Noor and my mother Nor 'Ain Binti Abdullah for their continuous support, love and believing in me throughout my life.

Finally, I gratefully acknowledged the financial support from the Japanese government under the MEXT scholarship program and Universiti Teknologi Malaysia for the family support during my stay in Japan. Acknowledgements are also for the Wakate fund of GCOE-ARS Program and Kyoto University fund for the internships and international scientific events.

Abstract

Extreme precipitation analyses are important for improving flood defence structures and flood risk management. Research conducted around the world reports an increasing trend of extreme precipitation events. Rare extreme-rainfall events produce outliers within the rainfall data records. The outliers can affect the quality of the quantile values when adopting conventional frequency analysis. This is due to the fact that they were not fitted to the frequency analysis model causing underestimation of high return period's quantiles. The underestimation causes design limits of hydraulics and flood defence structures to be exceeded. Thus it is important to obtain reliable quantiles estimates as the problem would be more significant for areas receiving unexpected high amount of rainfall intensities in the future caused by global warming.

There are two main approaches used to deal with future extreme rainfalls for designing hydraulic structures. One of them is predicting the probability of occurrence of an extreme rainfall event, and the other is estimating the highest rainfall amount that could possibly occur. They are the quantiles estimated from frequency analysis and the probable maximum precipitation (PMP) values. Both approaches are important. However, estimation of reliable quantiles and PMP estimates is quite difficult for regions containing limited meteorological data in terms of the observation length or gauged-network densities. Extreme outliers within the recorded data also affect the estimation of the quantiles and PMP estimates. Hence, in order to solve the problems, this research proposes regional frequency analysis to improve both the frequency analysis and statistical PMP estimation method. The regional approach can substitute space for time using observations from different sites in the same region.

Chapter 1 introduces the research purpose and backgrounds. The chapter explains in detail what motivates the research. The increasing trends of extreme rainfall events and the failure of flood-defence structures to accommodate high amounts of rainfalls are the problems that the research wishes to assess. Based on that, the objectives were formed. The main objectives are: 1) To improve the estimation of quantiles by considering regional frequency analysis; 2) To improve the statistical method used for estimating the probable maximum precipitation (PMP) by considering extreme-rainfall homogeneous regions; 3) To identify extreme-rainfall homogeneous regions for Japan; 4) To estimate statistical PMP for Japan by applying the Japanese rainfall data into the proposed method; and 5) To prove the importance to consider PMP estimates besides using high return period's quantiles for designing flood-defence structures.

Chapter 2 presents details of the location and the data used. The data are from approximately 1050 stations belonging to the Japan Meteorological Agency (JMA) of long-term surface stations (1896 to 2008) and AMeDAS network (1976 - 2008). The data were screened and checked to see whether they contain errors and are acceptable to be used for analysis. Reviews on literatures on the description of the Japanese rainfall and its climate conditions were also presented. Heavy rainfall-events usually occur from June to

October in Japan. They are caused by large-scale convective systems instead of localized short-term precipitation.

Chapter 3 introduces the basic theories of the frequency analysis and discusses the limitation when considering conventional frequency analysis alone during the designing of critical structures such as dams or hazardous waste landfills. From that, the significance to consider PMP estimates was highlighted. Finally, a simple method to combine quantile plots with the PMP as an upper boundary using a non-linear regression equation is shown.

Chapter 4 presents the extreme-rainfall homogeneous regions produced using the *L*-moments regional frequency analysis method. Compared to other common cluster analysis, the *L*-moments method considers the means, skewness, and kurtosis of a frequency distribution for the clustering. At the beginning of the chapter, the basic theories of the *L*-moments regional frequency analysis were introduced in order to explain the basic construction of the extreme-rainfall homogeneous regions. A discordancy test and heterogeneity test were used to examine the homogeneity of sites within the proposed homogeneous regions. After achieving satisfactory requirements, the proposed regions are accepted as the homogeneous regions. This chapter also presents the quantiles produced based on the station-year method using the homogenous regions. The SLSC test results prove that the regional frequency distribution has better fit compared to the at-site frequency distribution. The regional approach reduces the probability differences of the outliers by more than 30%. It also significantly reduces the probability differences of the 30-year or 10-year rainfall events to around 90%. In addition, the return period for Hikone extreme rainfall outlier of 596.9 mm was reduced from a 2000-year rain to a 500-year-rain. Similar goes to the outlier of Kyoto (288.6 mm), where its rainfall period was reduced from a 100-year-rain to a 30-year-rain.

Chapter 5 focuses on the PMP. The chapter presents basic theories of the Hershfield statistical method and describes a FORTRAN program developed to calculate the statistical PMP estimates. By using the program codes, analysis time for detail and extensive preliminary PMP estimation can be shortened.

Chapter 6 describes the main contribution of this research by combining the methods explained in Chapter 4 and Chapter 5. The research proposes a new approach by considering the extreme-rainfall homogeneous regions into the statistical PMP method. The essence of the statistical PMP method is transposing the frequency factor, K_m which is highly influenced by the transposition boundaries. Conventional method used the boundaries of river basins or particular administrative regions. Here, however, the new approach proposed the use of boundaries of an extreme-rainfall homogeneous region. In order to test the performance, PMPs were estimated by using two river basins and six administrative regions representing the conventional method, and two homogeneous regions of Region 7 and Region 10 representing the new approach. Results show that the new approach avoids overlooking higher K_m values that can be used for the transposition. Validations of the statistical PMP estimates use current record-breaking rainfalls obtained up to March 2014. Most of the PMPs produced by the conventional method are near to or less than the current record-breaking rainfall values. In contrast, the new approach gives optimal PMP estimates that are much higher than the current record-breaking rainfall values, providing better precaution measures. The PMPs estimated by the new approach are also comparable to PMPs estimated by a longer observation data. This proves that the new approach is able to compensate for the data limitation. The studies also show comparable PMP estimates against the PMPs estimated using projected climate data obtained from a general circulation model of MRI AGCM3.2s until the year 2104. Thus, this research recommends the highest PMP value within a homogeneous region to be used for flood-mitigation project plans and flood-defence structures designs for any sites in that particular homogeneous region.

Finally, Chapter 7 presents the summaries of the main research outcomes and future works. The main contributions from this research are as follows: 1) The research proposed ten extreme-rainfall homogeneous regions for Japan, which have not been proposed before, by using an *L*-moments regional frequency analysis. The regions can be used for future research in relation to extreme rainfall analysis; 2) The research introduces an improved method for statistical PMP estimation. The method considers extreme-rainfall homogeneous regions as the transposition boundaries. Hydro-meteorological PMP estimation method needs long records of meteorological data besides rainfall. If statistical PMP estimates using only precipitation data can provide satisfactory maximum rainfall estimates, it will benefit countries with limited data availability; 3) The research presents the statistical PMP estimates for Japan using the new approach. There is no previous research on PMP for Japan which use the Hershfield statistical method. Since long-term observation records are available, using statistical methods are suitable; 4) A FORTRAN program code for the Hershfield statistical PMP estimation was developed from this research. Using program-codes for calculation will shorten analysis time for detailed and extensive preliminary PMP estimation. The FORTRAN codes are attached in the Appendices; 5) The research proves the Japanese atmospheric general circulation model, MRI-AGCM 3.2 (20 km) outputs to perform adequately in terms of the means of annual maximum series (X_n) by using a simple bias correction method. The AGCM outputs also produce acceptable PMP estimates. The PMPs estimated by the new approach are comparable to PMPs estimated using projected climate data up to the year of 2104.

Contents

List of Figures

List of Tables

Chapter 1 Introduction

1.1 Background

Extreme precipitation analyses are very important. Outcome of such analyses highly influences flood protection and flood risk management. Due to global warming, extreme precipitation has been observed and reported to increase around the world. The Intergovernmental Panel on Climate Change (IPCC) reported that the frequency of heavy precipitation events increases over most areas and had likely occured especially in the late 20th century (IPCC, 2007).

Studies using trend analysis on historical data report an increase of extreme precipitation intensities in various regions, for example, in India (Dasgupta et al., 2010; Pal and Al-Tabbaa, 2010; Subash et al., 2011), in Italy (Brunetti et al., 2000; Brunetti et al., 2001), Australia (Plummer et al., 1999; Suppiah and Hennessy, 1998), United Kingdom (Osborn et al., 2000), South Africa (Mason et al., 1999), Malaysia (Suhaila et al., 2010), China (Fu et al., 2013) and Japan (Fujibe and Yamazaki, 2006; Fujibe et al., 2005). The increasing trend found however varies during season. Most areas have increasing trend of extreme precipitation during the summer season, such as in India, Northern Italy, Southern China and part of Australia (Brunetti et al., 2000; Fu et al., 2013; Pal and Al-Tabbaa, 2010; Subash et al., 2011; Suppiah and Hennessy, 1998). However some are also observed during the winter season for example in the UK (Osborn et al., 2000). In Malaysia, increasing trend of extreme rainfall is observed only in the highly urbanized area around Kuala Lumpur and Selangor. However, in terms of total, mean annual precipitation or number of rainy days a decreasing trend was observed for some areas such as in the southern part of Italy and Malaysia (Cannarozzo et al., 2006; Suhaila et al., 2010). In general most of the studies relate the increasing intensity of extreme rainfall events to global warming due to the increasing rate of greenhouse gases (GHG). In particular, more localized phenomena such as the El Nino-Southern Oscillation trends (Fu et al., 2013; Plummer et al., 1999; Suhaila et al., 2010; Trenberth, 1998), cyclone events (Brunetti et al., 2001; Mason et al., 1999), local atmospheric circulation changes (Brunetti et al., 2001; Fu et al., 2013; Osborn et al., 2000; Pal and Al-Tabbaa, 2009), and the magnitude of Monsoon (Fu et al., 2013) were frankly blamed for the increase of extreme rainfall intensity. Besides studies using historical data, studies using climate model projections and atmospheric processes theories also predict increase of the extreme rainfall intensities in the future due to climate change (Ekström et al., 2005; Karl et al., 1995; Kunkel et al., 2013; Trenberth, 1998).

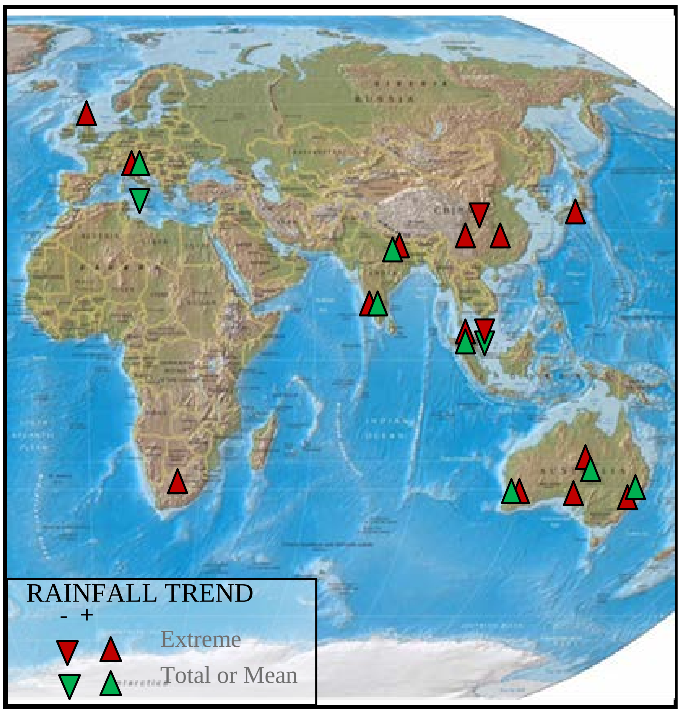

Figure 1-1: Rainfall trends around the Asia Pacific.

International reports such as The Asia Pacific Disaster Report, 2010 published by The Economic and Social Commission for Asia and the Pacific (ESCAP) and the United Nation International Strategy for Disaster Reduction (ISDR) reported that record-breaking extreme rainfalls had been increasing especially since the 2000's (Bhatia et al., 2010). In accordance to the increasing trend of extreme rainfalls, flood occurrences are also observed to increase. A statistical report by the ISDR presented in their website particularly for disaster risk reduction (DRR) showed that the numbers of events reported for flood have been increasing from the year 1980 to 2008 (UNISDR, 2013). An annual report on disaster statistical review also shows an increasing trend of reported disaster from 1990 to 2011 in which disaster categorized as hydrological-subgroup (flood and mass movement) were the most dominant (Guha-Sapir et al., 2012). Some of the recent major or record-breaking extreme rainfall events were the Bangkok flood in November 2011, Queensland flood in December 2010 - January 2011, Malaysian floods in November 2010, January 2011, December 2012, December 2013, Japanese floods in September 2011, July 2012, September 2013 and the Indonesian flood in January 2014. Flood disaster usually involves the lives of thousands of people and could generate millions dollars of economic losses. Thus, countermeasures to deal with problems or disasters generated from the increasing of this extreme rainfall needs to be assessed.

There are various steps and approaches that can contribute to the preparation of future extreme events. One of them is to predict the probability of occurrence of an extreme rainfall event. A popular and conventional method is to use frequency analysis. Another acceptable method is to predict the most possible highest rainfall amount that could occur by using the Probable Maximum Precipitation (PMP) estimates. The thesis focuses on the methods to improve the prediction of extreme rainfall particularly used for hydraulic and flood defence structures; such as the estimation of quantiles for design rainfalls and maximum rainfall estimates, by using statistical approaches and limited meteorological data. This is to consider regions with very limited data availability in term of type of meteorological data (precipitation, temperature, humidity, etc.), observation period and the rain-gauge network density.

1.2 **Problem Statements**

As discussed in Section 1.1, the frequency and intensities of extreme rainfalls and record-breaking flood are observed to be increasing. Flood are becoming more apparent due to design limits of flood defence structures (storm drainage, embankments, dams, etc.) which are being exceeded and areas with high population suddenly having unexpected rainfall amounts. Such cases are during the 2011 Bangkok flood in Thailand, the 2011 Queensland flood in Australia and the 2004 Niigata flood in Japan. The occurrence of the 2011 Bangkok flood was blamed on the dam operation management and the outdated dam capacity due to unexpected rainfall amounts (Jothityangkoon et al., 2013). The 2011 Queensland flood experienced its second highest flood event since 1974 (B.O.M, 2012). High record rainfalls were observed throughout the states together with others primary climatic drivers such as the La Nina event, the Madden Julian Oscillation, and the monsoonal wet season (B.O.M, 2011), making design limits of flood structures exceeded and its dam operations questioned. Another case is the 2004 Niigata flood in Japan which shows an example of a levee breached due to a record-breaking 25-year-rainfall intensity. A total of 216 mm rain fell in a 48-hour period, causing an exceedence of the levee design limit (Huang, 2006). This shows the importance of a reliable and up-to-date return period estimation for the designing of hydraulics and flood protection structures especially in this current changing climate. As a relation to the problem mentioned above, the existence of extreme rainfall values or outliers can affect the quality of the quantiles estimated when using a conventional frequency analysis during the design stages of hydraulics and flood defence structures. This is due to the extreme values which were not fitted to the frequency analysis model. In future, this problem would be more significant for many regions which receive very high rainfall intensities than the normal amount.

As it is well known, the usage of an extreme rainfall population distribution is usually used to estimate the return periods or quantiles for hydraulic structures designs. Common return periods used for flood defence structures and flood risk analysis ranges within 1-, 5-, 10-, 20-, 50- and 100-year rainfalls (ASCE and WEF, 2012). Based on responses by multiple institutions and organizations on a questionnaire asked by the Hydro-meteorological Design Studies Centre (HDSC) of the National Oceanic and Atmospheric Administration, United States in 2007 (NOAA, 2007), the usage of 500-year and 1000-year rainfalls are rarely applied but have been taken into consideration particularly to represent extreme cases for high risk projects such as hazardous waste landfills, flood hazard maps and dam designs. Even though the 500-year and 1000-year designs are thought to be wildly speculative and very statistically uncertain, they are still used to represent benchmark of extreme cases. Apart from using frequency analysis, probable maximum precipitation (PMP) is also being considered and is thought to be an alternative approach particularly to represent the 1000-year rainfall.

Thus, from the literature reviewed above, two types of analyses are being conducted by researchers and practitioners to deal with extreme rainfalls: 1) frequency analysis to obtain quantiles or return-period rainfall values; and 2) PMP analysis to obtain the theoretically maximum rainfall. However there exist two schools of thoughts regarding PMP estimates. Some believe that it will simply be enough to consider frequency analysis to estimate the extreme rainfall values (Koutsoyiannis, 1999; Papalexiou and Koutsoyiannis, 2006); others strongly believe that the PMP can indeed be used to represent maximum rainfall values or representing upper boundary of the extreme rainfall frequency analysis models (Desa M et al., 2001; Elíasson, 1997; Rezacova et al., 2005; Takara and Tosa, 1999; WMO, 2009; Zhan and Zhou, 1984). Despite the thoughts, PMP estimates are being used widely by researchers and practitioners around the world. A more detailed discussion between the frequency analysis approach and the PMP estimates will appear further in the thesis. So does the importance of both frequency analysis and the PMP towards extreme rainfall predictions.

The World Meteorological Organization (WMO) recognizes several methodologies to estimate PMP (WMO, 2009). The two main methods are: 1) a statistical approach known as Hershfield statistical method; and 2) the physical approach known as the hydro-meteorological method. Depending on the availability and limitations of data, both methods are accepted and are widely used. However, WMO (2009) cautiously remarked that the statistical method to be use for preliminary PMP estimates only; since the procedure provide results with minimum effort, and needs support from procedures based on comprehensive meteorological analysis. However, practitioners use the statistical method when they have difficulties in obtaining the meteorological parameters such as the dew-point temperature, relative humidity and surface temperature. In addition, since statistical PMP estimation requires only precipitation data, it is the best option for them. To support the use of statistical method, Casas et al. (2011) and Deshpande et al. (2008) claim that the statistical method is comparable to the hydro-meteorological method. However, their analysis was based on long observation records of rainfall data. According to WMO (2009), more reliable PMP estimates can be calculated via the hydro-meteorological method (physical method) if various meteorological data are available. This is a significant problem for those who have difficulties to acquire the data. A reliable PMP estimates using the statistical method requires long observed data.

Recently, many researchers use a regional approach of the frequency analyses to compensate for data limitation ever since Hosking and Wallis (1993, 1997) introduced the regional frequency analysis based on *L*-moments method. The regional frequency benefited various countries to help explain the condition of their extreme rainfall, to have better quantiles estimation using limited data and improving hydrological practices. The analysis can produce homogeneous regions. Thus, a test can be conducted to see whether the statistical PMP estimates can be improved by adopting the homogeneous region.

In addition, due to the increase of intensities of extreme rainfall events, even regions with long observational data and high densities of gauged-sites can benefit from the method. Japan has data dating from 1886 until now at 51 stations distributed across its country, thus long series of annual maximum rainfalls can be used for the analysis. Significant outliers are included in the rainfall records through the long series of observation data of more than 100 years. These outliers are difficult to be fitted in the frequency analysis model, resulting in to underestimation of the actual quantile values. Thus, regional frequency analysis can be tested to see whether the extreme outliers were fixed into a frequency analysis model.

Fowler and Kilsby (2003), Hassan and Ping (2012), Hailegeorgis et al. (2013), Yang et al. (2010), Awadallah (2013), and Shabri and Jemain (2013) to name a few have adopted the *L*-moments regional frequency analysis into their works. They developed homogeneous regions for extreme rainfalls during the analysis. These indicate the wide-spread usage of the *L*-moments approach for regional frequency analysis. Thus, it could be possible to consider the *L*-moments regional frequency analysis into the statistical PMP estimation method to improve PMP estimates for regions with limited meteorological data.

In summary, more studies are needed to improve the methodology in estimating the quantiles and PMP values. The method should consider regions with limited meteorological data and contains outliers. Regional frequency analysis can be introduced to the improvements on both the quantiles and statistical PMP estimation. The statistical method uses much less variables compared to a physical approach which needs various meteorological data. Thus, we need to consider methodology that could improve the quantiles and the statistical PMP by taking into account limited data availability.

1.3 Research Objectives

Based on the background and problem statements discussed in the previous sections, several main objectives are expected to achieve in order to improve the existing methodology for future extreme rainfall estimates using statistical approaches and limited meteorological data. The main objectives are as follows:

a) To improve the estimation of quantiles by considering regional frequency analysis.
b) To improve the statistical method used for estimating the probable maximum precipitation (PMP) by considering extreme-rainfall homogeneous regions.
c) To identify extreme-rainfall homogeneous regions for Japan.

d) To estimate statistical PMP for Japan by applying the Japanese rainfall data into the proposed method.

e) To prove the importance to consider PMP estimates besides using high return period's quantiles for designing flood-defence structures.

There are several sub-objectives that should be highlighted in assisting the achievements of the main-objectives. They are:

a) To assess the improvements of the quantiles and outliers fitting using regional frequency analysis.

b) To assess improvements using the new approach against conventional method for the statistical PMP estimates.

1.4 Scopes and Limitations

This study focuses on determining new methodologies that could improve the estimations of extreme rainfall particularly for flood defence structures such as storm drainages, detention ponds and dams which use quantiles and maximum precipitation estimates. As mentioned in the previous sections, regional frequency analysis is becoming more popular to compensate for data limitations; it is assumed that it will help in improving existing methodologies especially for statistical PMP estimation which uses rainfall data only. The scope and limitations considered in this study are:

a) *L*-moments regional frequency analysis method is used for determining the extreme-rainfall homogeneous regions by grouping sites with similar rainfall distribution characteristics. Compared to other common cluster analysis such as the component factor analysis, the *L*-moments method considers not just the means of a distribution of one site but also its skewness which reflects extreme conditions or the tail of a distribution. Sites which statistically fit similar extreme population distribution are considered belonging to one homogeneous region or in the same cluster group.

b) Japanese rainfall data is used for the case-study since Japan has reliable and long-term historical observation data dating from 1896. Using sufficient data availability assists in validating and testing any proposed new methodology especially for statistical analysis.

c) The statistical PMP estimates conducted are point values. An aerial average value for PMP estimated requires an area reduction curve which can be conducted based on analysis on multiple extreme storms.

d) Validations of the proposed improved methodology use the daily-rainfall records. This is due to extreme rainfalls cases in Japan are influenced by mesoscale meteorological phenomena such as typhoons. However, tests and validations using sub-daily rainfall are also important and could be included in future works.

1.5 Thesis Organization

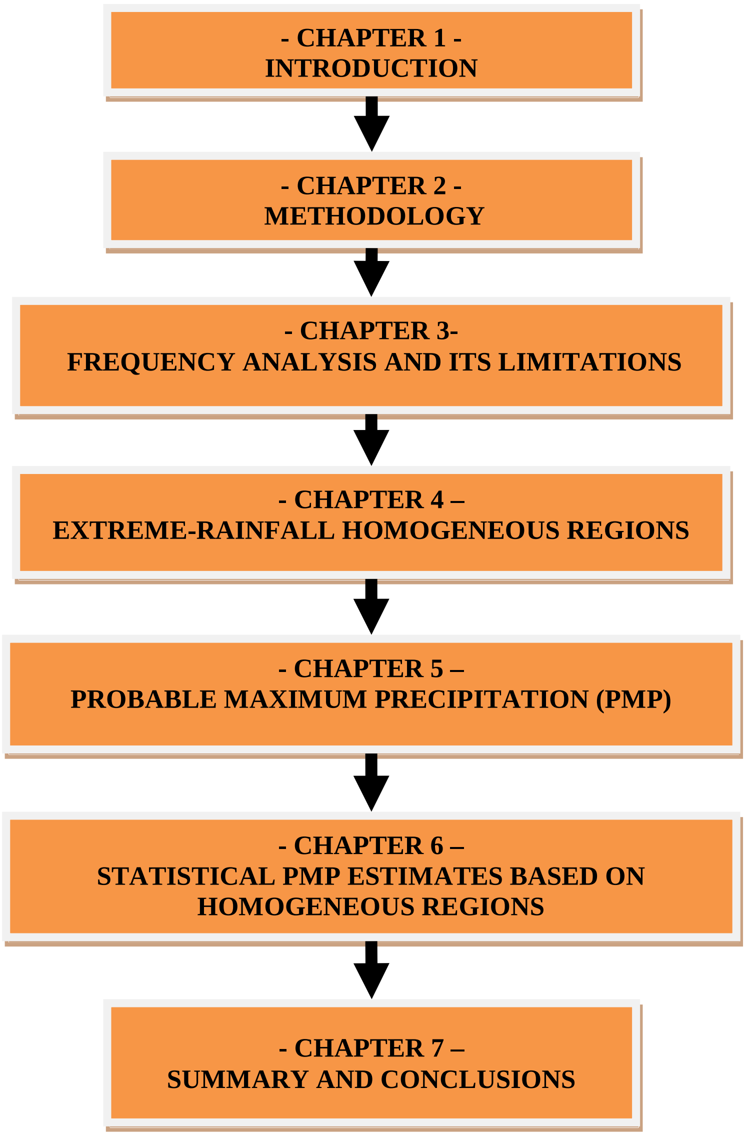

Figure 1-2: Thesis organization flow

The thesis consists of seven chapters. Chapter 1 describes the background, the problem the study wish to assess, the objectives and its scopes and limitations. Chapter 2 contains detailed information on the study site and the data used for the research. Chapter 3, 4, and 5 are the main parts of the research, where description on the theories and procedures used for the analysis are presented in detail. These chapters describe all the important features needed to propose the new methodology to improve the statistical maximum and extreme rainfall estimates. Results from case-studies are also presented in these chapters. Chapter 6 contains the results of the proposed new method and discuss in detail the comparisons and improvements against the conventional method. Lastly, Chapter 7 summarizes the results and presents the future works that can be conducted based on outcomes from this thesis. The research contributions are also highlighted in this chapter.

Chapter 2 Methodology

2.1 Main Research Flow

Main components of the methodology used in the study include frequency analysis, regional frequency analysis and probable maximum precipitations (PMP). Figure 2-1 shows a general flow of the research. The research conducts quantiles estimation from both the conventional frequency analysis and regional frequency analysis using annual maximum rainfalls obtained from observation data between the periods of 1896 to 2008. The extreme-rainfall homogeneous regions obtained use the *L*-moments regional frequency analysis method. The regions are tested first whether it meet the requirements to be considered as a homogeneous region. During this process, stations with gross error can be identified and will not be used for further PMP analysis. Once the homogeneous regions were proven to be adequate, comparisons were made using the quantiles of the at-site analysis and the regional analysis (based on the homogeneous regions). By achieving better quantiles estimations, it proves that the regional frequency analysis is significant and could be useful to improve the statistical PMP estimation. Afterwards, the homogeneous regions are used as the transposition boundaries to estimate the statistical PMP. Finally, the research compares the PMPs estimated by the conventional method and the new approach. Validations and comparisons use updated record-breaking rainfalls and estimations from a bias-corrected atmospheric general circulation model (MRI-AGCM3.2s) outputs.

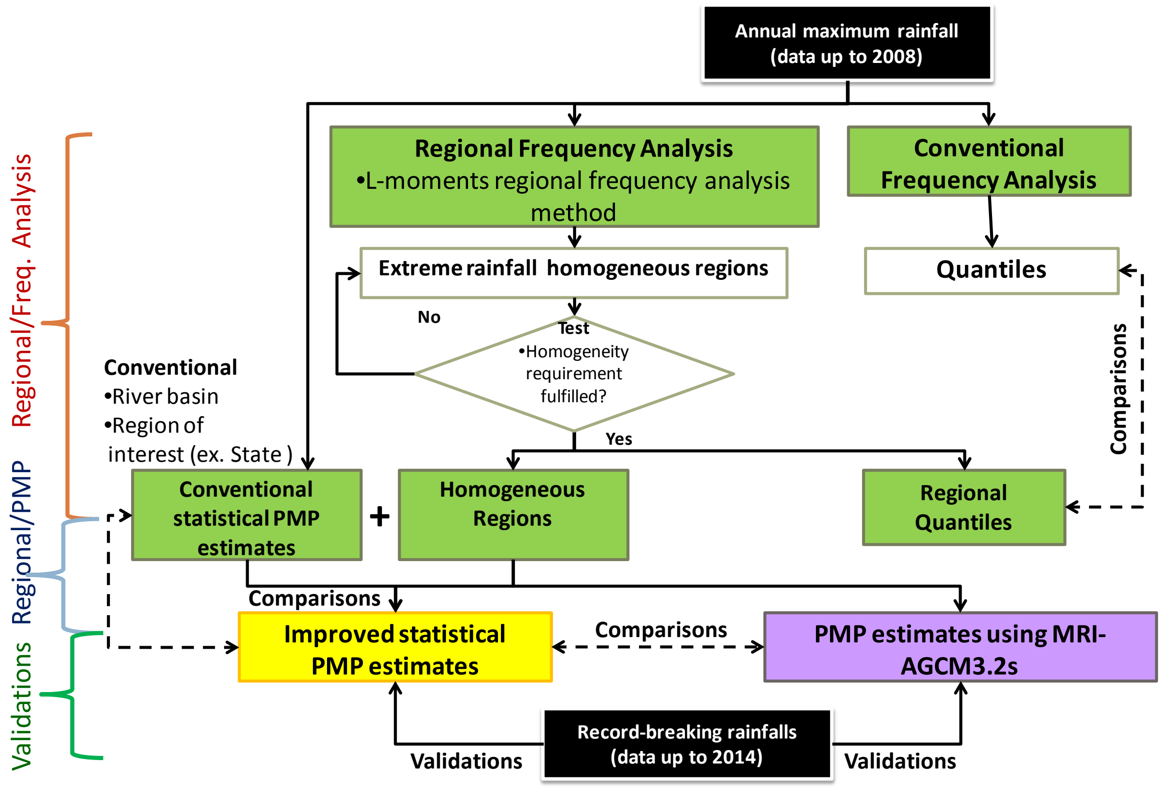

Figure 2-1: Research main-flow diagram

2.2 Study-site

Japan is chosen as the study-site throughout the analysis. In general, Japan is located between 24°N to 46°N latitude and 122°E to 142°E longitudes at the west of the Pacific Ocean (Figure 2-2). Geographical locations highly influence the climate and weather of one place. In term of the Koppen system, Japan has a climate of moist with severe winters (Tsonis et al., 2011). Due to its location in the mid-latitudes, it experiences four season of summer, autumn, winter and spring. According to Emanuel (2011) mid-latitude cyclones or extra tropical cyclones occur in the middle-latitude regions of the globe (roughly 30°N - 70°N latitude), while according to the National Oceanic and Atmospheric Administration (NOAA) of the United State, tropical cyclone forms between the 5°N and 30°N latitude signifying Japan is located within a cyclonic zone. Thus, the extreme rainfall condition in Japan is influenced by four main meteorological phenomena which are: in the order from the most influential to the least, the typhoon, the Baiu front which is a stationary-front during the Baiu season (June to July), the extra-tropical cyclones and the regional thunderstorms. The rainy seasons are usually during summer (June to August) and early autumn (September to October).

The heaviest precipitation was identified to be in June to October (Fujibe and Yamazaki, 2006)while in term of extremes the top daily events are most frequent in September while the top ten-minute and hourly precipitation events are during July and August (Miyajima and Fujibe, 2011). According to Fujibe et al. (2005) the majority of heavy rainfall in Japan are caused by large-scale convective systems instead of localized short-term precipitation under sunny and undisturbed weather which normally would enhance urban influence towards heavy precipitation. However, it is possible that the global warming and increase of water vapour result in increase of localized intense precipitation. The maximum rainfall currently reported by the Japan Meteorological Agency (JMA) in 2014 is 851.5 mm 24-hour rainfall at Yanase, Kochi on 19 July 2011 and 153 mm hourly rainfall at Katori, Chiba on 27 October 1999 and at Nagauradake, Nagasaki on 23 July 1982. Note that informal records by other private companies or organization are also available and exceeds the official records by JMA. They are: 1,317 mm 24-hour rainfall at Kaikawa, Tokushima on 1 August 2004 by Typhoon No. 10, and 187 mm hourly rainfall at Nagayo Town Office, Nagasaki on 25 July 1982.

Extensive trend analyses have been conducted for Japan. Fujibe and Yamazaki (2006) conducted some comprehensive trend analysis on Japan. June to October was identified to have the heaviest precipitation. Results also show higher frequencies of daily precipitation ≥ 100 mm and daily annual maximum mostly distributed in Western Japan. They had identified three major trends. They are; 1) Slightly decreasing trend of annual precipitation amount; 2) Significant increasing trend of heavy precipitation ≥ 100 mm, and annual maximum daily precipitation, and; 3) weak increasing trend and negative trend for lower daily precipitation ≥ 50 mm and ≥ 20 mm respectively. These agrees well with Fujibe et al. (2005) which summarizes in their paper that there exist an increase of intense and decrease of weak precipitation. Fujibe et al. (2005) also summarized that the majority of heavy rainfall in Japan are caused by large-scale convective systems instead of localized short-term precipitation under sunny and undisturbed weather which is normally would enhance urban influence towards heavy precipitation. They also believed that it is possible that the global warming and increase of water vapour result in increase of localized intense precipitation.

In terms of local climate characteristics, general climatic regions have been produced by JMA for Japan and were used by Murazaki et al. (2010) and Sasaki et al. (2006). There are seven types of climatic areas as shown in Figure 2-3. They are Area 1:

cold, snowfall in winter, cool in summer; Area 2: cold and dry in winter, cool in summer; Area 3: heavy snowfall in winter; Area 4: Dry in winter, wet in summer; Area 5: rain or occasionally snowfall in winter, much rain in summer; Area 6: Dry in winter, much rain in summer; Area 7: Oceanic type of climate, warm and humid during all seasons. Their classifications of the regions were mostly influenced by the administrative regions, of which boundaries are often mountain ranges. Extensive studies on homogeneous regions in term of extreme rainfall events have not been conducted yet. Climatic areas may be different from extreme rainfall regions.

Table 2-1: Summary of climate characteristics (Japan)

Climate characteristic	
Max daily rainfall	851.5 mm
Max hourly rainfall	153 mm
Max temperature	40.9 °C
Max relative humidity	83%

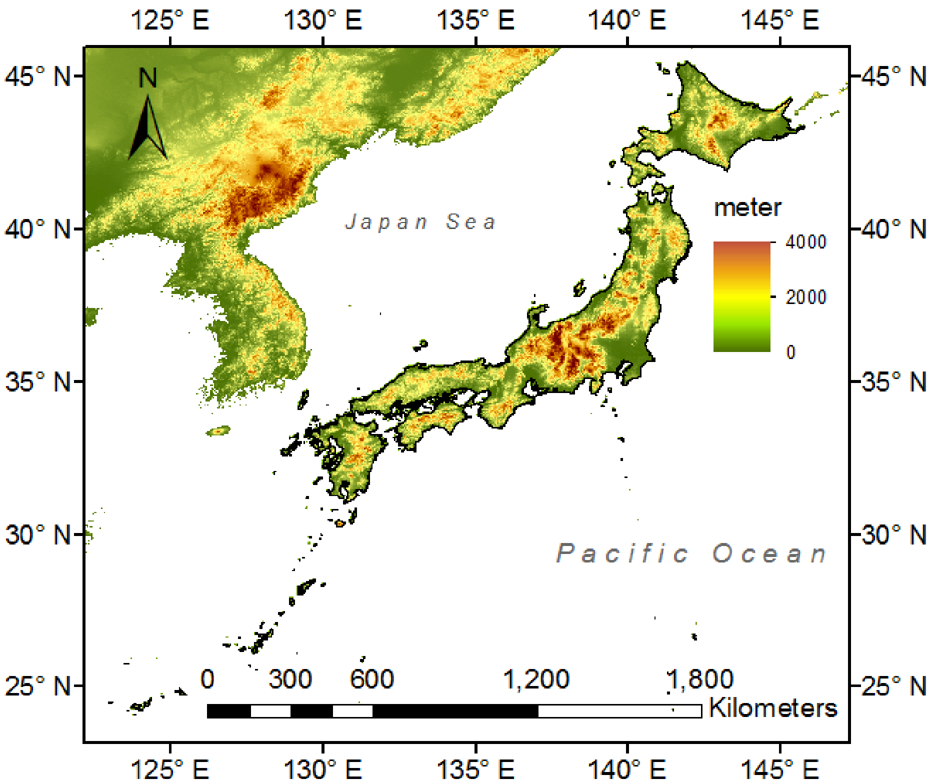

Figure 2-2: Geographical locations of Japan

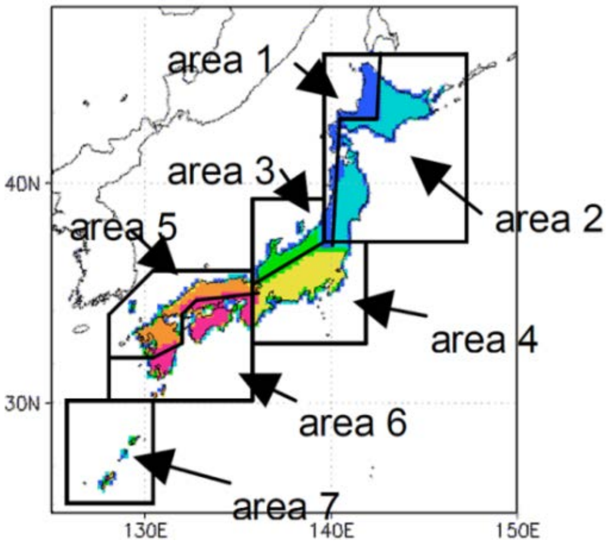

Figure 2-3: Climatic areas of Japan identified (Murazaki et al., 2010; Sasaki et al., 2006)

2.3 **Data**

2.3.1 *Data Sources*

This study uses the annual maximum daily-rainfall and hourly-rainfall to represent the extreme rainfalls. Japan was chosen as the study region due to its sufficient data availability and quality. The study uses daily and hourly rainfall series from the Automated Meteorological Data Acquisition System (AMeDAS) stations and the long historical surface stations by the Japan Meteorological Agency (JMA). Long-term historical data from 1901 to 2008 (with some stations from 1880) of 51 stations belong to the surface weather observation network, while the rest around 1000 stations (1976 - 2008) are from the AMeDAS network. Figure 2-4 shows the dense distributions of the network. There are much more stations owned by JMA within the AMeDAS network, however after data screening only stations with more than 25 years of observation period and no missing data were selected for this study.

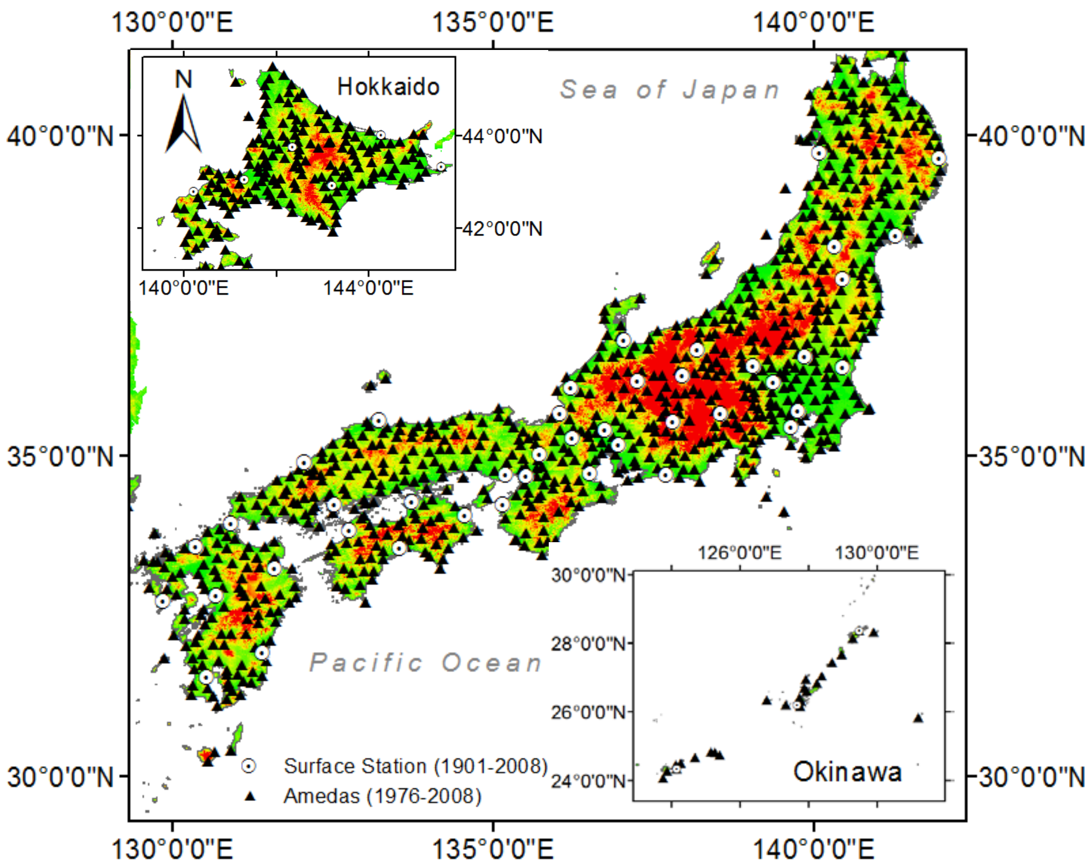

Figure 2-4: Location of the AMeDAS and the surface stations of Japan Meteorological Agency (JMA)

A brief summary of the data management and quality control conducted by the Japan Meteorological Agency (JMA) is presented. The precipitation records of the JMA owned rainfall stations were digitized for the full period of operation, including some stations established before 1900 (Fujibe et al., 2005). The Observation Department of JMA conducted a quality check for the daily precipitation data from 1901 providing a complete daily records with only few missing values (Fujibe and Yamazaki, 2006). Based on previous analysis and discussion, the data were used with confidence and are assumed that they will provide reliable results. Details on the Japanese precipitation measurements and for other precipitation periods such as the hourly and up to 4-minutes period are also available in Fujibe et al. (2005).

2.3.2 *Data Processing*

As described in the previous section, the analysis selects only stations with more than 25 years of observation data. The data screening uses A FORTRAN program called ANNMAX.FOR. The program also analyse the percentage of missing data. Only stations with less than 15% of missing data are considered and re-checked to whether it is suitable to be used for the analysis.

Figure 2-5 shows a flow chart of the ANNMAX.FOR program. The program would first ask how many numbers of stations needed for the analysis. After obtaining the number of station information, it will read one station at a time. The numbers of days per year (for the daily data) and numbers of hours per year (for the hourly data) is calculated. From that information, the number of missing data can be assessed. Afterwards, rainfall values of various periods are calculated. For the daily-data, the 2-, 3-, 5-, and 7-day rainfall is obtained, while for the hourly-data the 2-, 3-, 4-, 6-, 12-, and 24-hour rainfall is obtained. Using the various rainfall periods, the annual maximum of each rainfall periods are then determined. Lastly, all the results are printed into an OUTPUT.TXT file.

Examples of the input and output files are presented in the Appendices. Two types of input files are needed for the ANNMAX.FOR. The first one is the Station_list.TXT which lists all the file names of the data files of all the stations (example is in Appendix A-1). The other is the data files containing the date and rainfall values (daily or hourly). Each stations used for the analysis will have its own data file. Example of the data file's format is presented in Appendix A-2 for daily and A-3 for hourly rainfall data. While, an example of the output file is presented in Appendix A-6 for the hourly data and A-7 for daily data.

Homogeneity tests for time-series were also conducted using the Mann-Kendall trend test using several time slices. Based on the significant level 0.001, very few sites have a significant trend test, thus the time-series are considered homogeneous and can be use for the frequency analysis and regional frequency analysis which requires the data to be stationary. It is acknowledge that there exist increasing trend within the data.

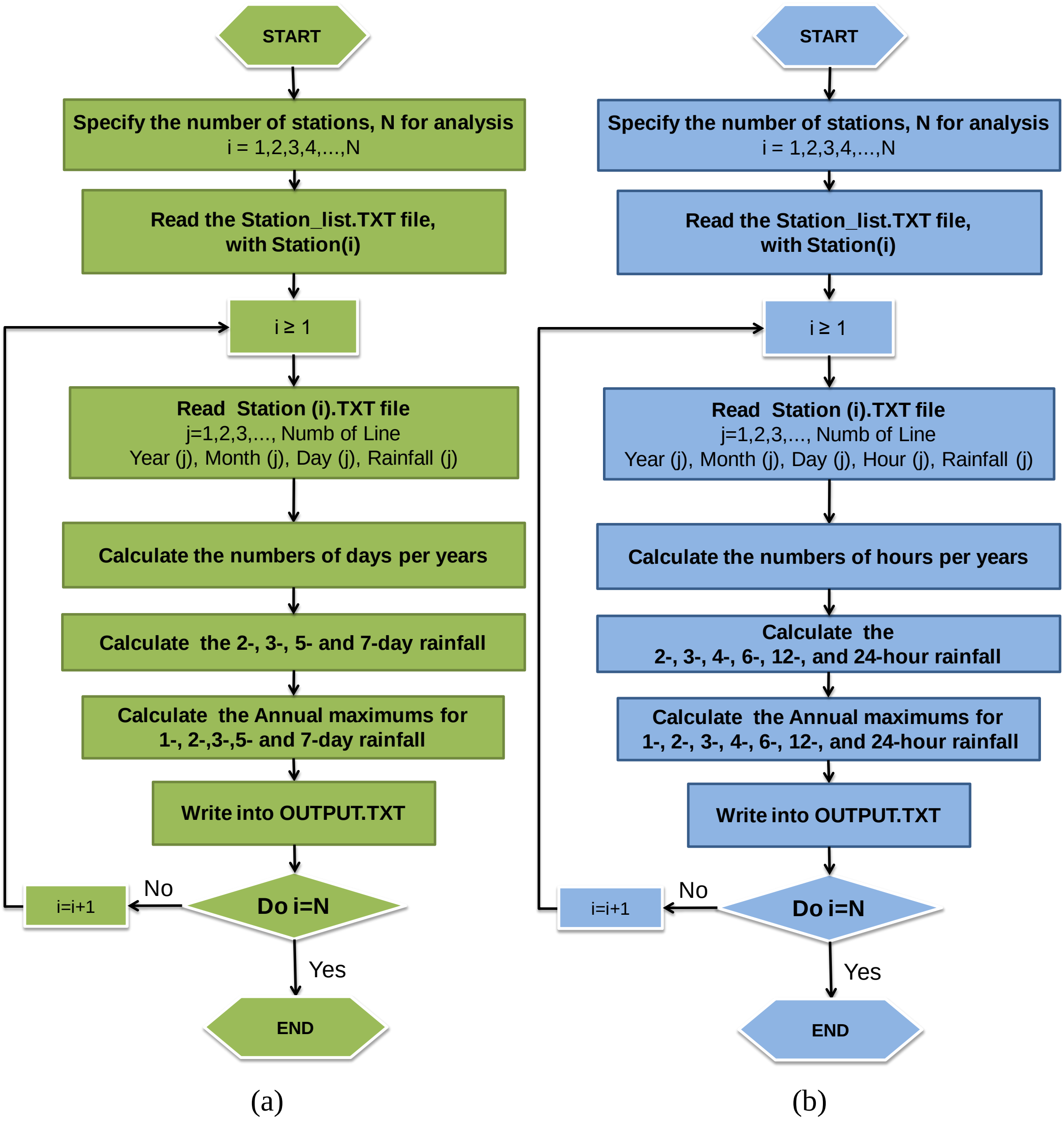

Figure 2-5: Flow chart of the ANNMAX.FOR program for the (a) daily-rainfall and (b) hourly-rainfall.

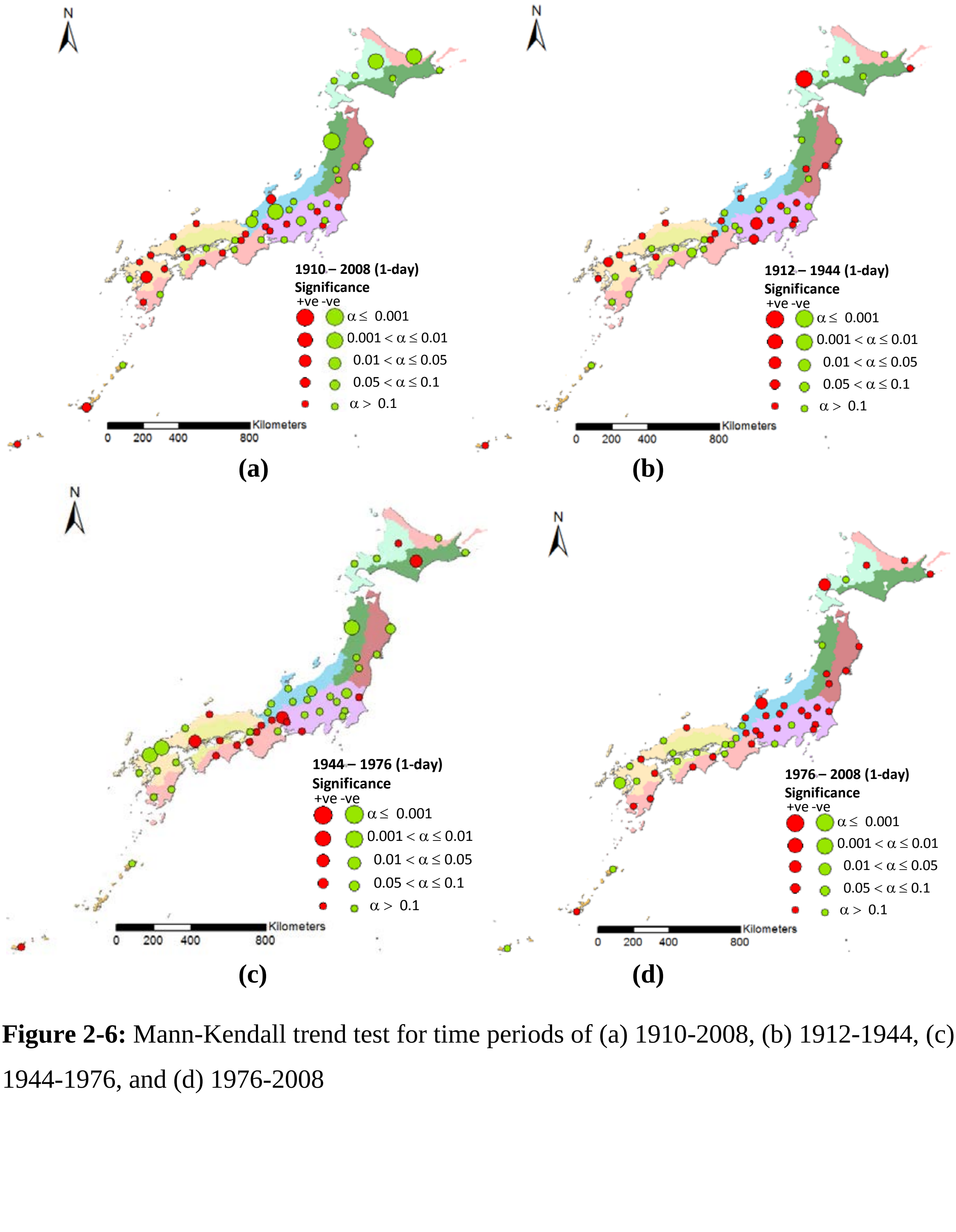

Figure 2-6: Mann-Kendall trend test for time periods of (a) 1910-2008, (b) 1912-1944, (c) 1944-1976, and (d) 1976-2008

Chapter 3 Frequency Analysis and Its Limitation

3.1 Introduction to Frequency Analysis

Most of hydrologic phenomena are stochastic. Since there are no pure deterministic hydrologic processes to fully understand and describe the phenomena, extensive use of probability theory and frequency analysis are needed (Yevjevich, 1972). An example of a hydrologic phenomenon is extreme rainfall. In frequency analysis an extreme rainfall events are considered as random variables which are assumed to be independent and come from identical distribution. The magnitude of the random variables can be related to their frequency of occurrence using probability distribution. Probability distribution could be represented in two forms. One is the probability density function (PDF) and the other is the cumulative distribution function (CDF). PDF and CDF are described in the following equation:

$$F(x) = P[X \leq x] \qquad \textbf{Eq. 3-1}$$

$$\boldsymbol{F(x) = \int_{-\infty}^{x} f(x)dx} \qquad \textbf{Eq. 3-2}$$

with $F(x)$ is the cumulative distribution function (CDF) and $f(x)$ is the probability density function (PDF). The CDF is the probability distribution of a random variable x with a given probability, P found at a value less than or equal to x (Eq. 3-1). It is also regarded as the non-exceedence probability. The CDF is also related to PDF as in Eq.3-2. A cumulative of the PDF produces the CDF. The relationship between a PDF and CDF is shown in Figure 3-1. By plotting the PDF the location parameter, scale parameter, skewness and curtosis of a frequency distribution could be seen more clearly. There are various kinds of frequency analysis models. The most commonly used for extreme random variables is the Generalized Extreme Value family and Exponential/Pearson type family. Details on the distribution suggested for extreme values are presented in Section 3.1.2.

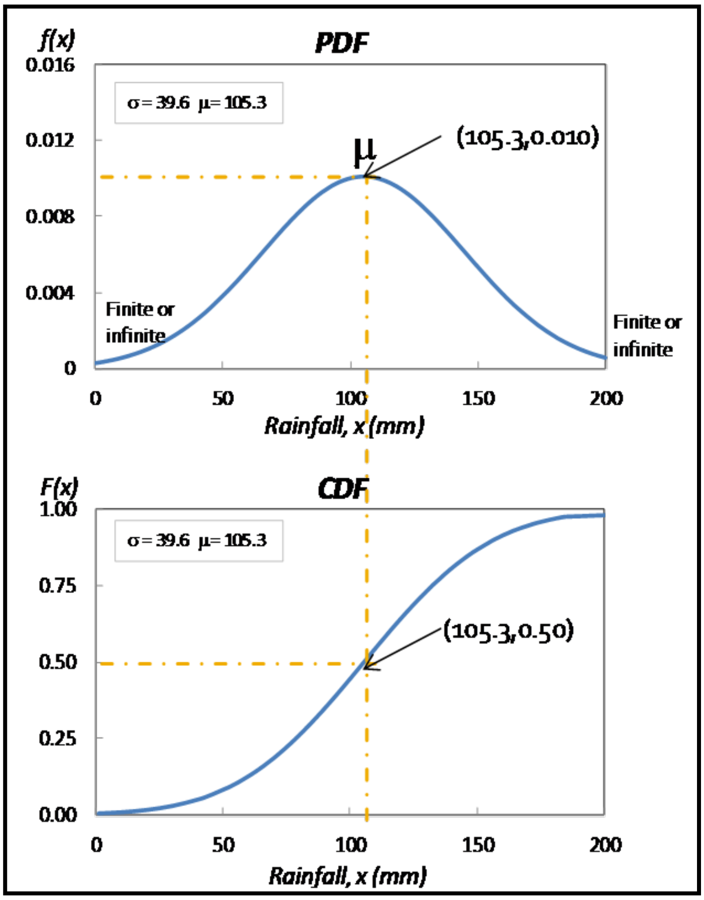

Figure 3-1: PDF and CDF relationship

The best way to describe the random variables is by a proper fit of PDF (Yevjevich, 1972). This is to identify which frequency analysis model the random variables belongs to, afterwards the model is then used to predict the extreme values and its frequency of occurrence or return period, T (e.g., 10-year, 50-year, 100-year rainfall). In other words, the PDF and CDF interpret past records of hydrological events in terms of future probabilities of occurrence (Chow, 1964). PDF and CDF are very important and are useful in flood protection and flood risk management since the design life of hydraulic structures depends on the return Period, T. If a hydrologic event, X equal to or greater than x occurs once in T years, the exceedence probability $P(X \geq x)$ is equal to 1 in T cases, or

$$\boldsymbol{P(X \geq x) = \frac{1}{T}} \qquad \textbf{Eq. 3-3}$$

Hence,

$$T = \frac{1}{P(X \geq x)} = \frac{1}{1 - P(X \leq x)} \qquad \textbf{Eq. 3-4}$$

Note $P(X \leq x)$ is a non-exceedence probability and $P(X \geq x)$ is an exceedence probability. The quantiles, Q are usually determined using the following equation:

$$Q = F^{-1}\left(1 - \frac{1}{T}\right) \quad \textbf{Eq. 3-5}$$

Common exceedence probabilities that correspond to return periods that are usually of interest are 0.5, 0.2, 0.1, 0.04, 0.02, 0.01, 0.002 (McCuen, 1998). The limitation by using frequency analysis is that it is based on the assumption of a stationary event (non-changing climate). However, since now global warming is currently taking its tow towards extreme rainfall distribution, the consequences on using a stationary analysis are making the quantiles being exceeded and return periods shortened. For example a 100-year rain could be observed to occur within 5 years and some cases even twice per year. Examples on such cases are presented in Section 3.3. The next section describes the processes to conduct frequency analysis.

Frequency analysis involves several processes. This thesis focuses on extreme values, thus the methodology to conduct frequency analysis presented here uses methods which suit extreme values analysis. The first step is to fit the data into several hypothesized distribution functions using a parameter estimation method. There are five parameter estimation methods that are recommended in extreme value analysis. They are the; 1) Least square fitting method (SLSC); 2) Method of moments (MOM); 3) Maximum likelihood method (MLM); 4) Graphical method and 5) *L*-moments method. Details on each method could be referred in Yevjevich (1972) and Hosking and Wallis (1997). Each method has different level of simplicity and accuracy and some have limitations. The selection of which method is suitable to be used depends on the type of distribution to be tested. For example the easiest way is to use the Least square fitting method, Method of moments or Graphical method, however these methods only applies for several distribution only especially distribution with less than 3 parameters. The most accurate parameter estimation is by using the Maximum likelihood method yet this method requires a good computer programming skills. The *L*-moments method is also quite comparable with the Maximum likelihood method. It was derived from Probable Weighted method, but then was modified for more simplicity. This method requires quite a lot of calculation steps however, if by using basic computer programming skills, calculations are a brief. Nowadays, computer programming codes for the MLM and *L*-Moments are available and are easy to be used.

Thus, for extreme values analysis, Maximum likelihood method or the *L*-Moments method are the most recommended since distribution function with at least 3 parameters usually best fits extreme values distribution.

After obtaining the parameters of various distribution functions, the goodness of fit test is conducted. The goodness of fit is often subjectively evaluated by visual consistency comparing plotted data with a theoretical (fitted) probability curve on probability paper or comparing the histogram with the probability density functions. Figure 3-2 shows an example of a histogram and tested PDFs. A more accurate and reliable way is by using quantitative method which by using the Goodness of Fit Criterion. The next section (Section 3.1.1 describes each criterion. Based on the Goodness of fit criterion, the best distribution is selected for the quantiles and return period estimation.

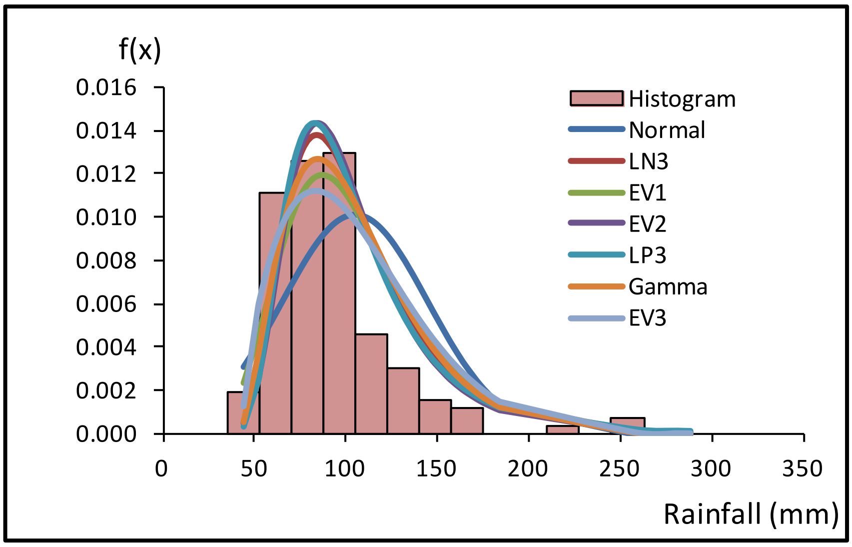

Figure 3-2: Histogram and PDFs comparison

3.1.1 *Goodness of Fit Tests*

Takara and Stedinger (1994) use 4 goodness-of-fit criteria. They are the; 1) SLSC (standard least-square criterion); 2) COR (correlation coefficient); 3) MLL (Maximum log-likelihood);and 4) AIC (Akaike's information criterion). Based on the goodness of fit test, the best fit distribution is used to estimate the return periods and quantiles of the extreme values. Figure 3-3 shows an example of the methodology to conduct frequency analysis using SLSC as the goodness of fit test.

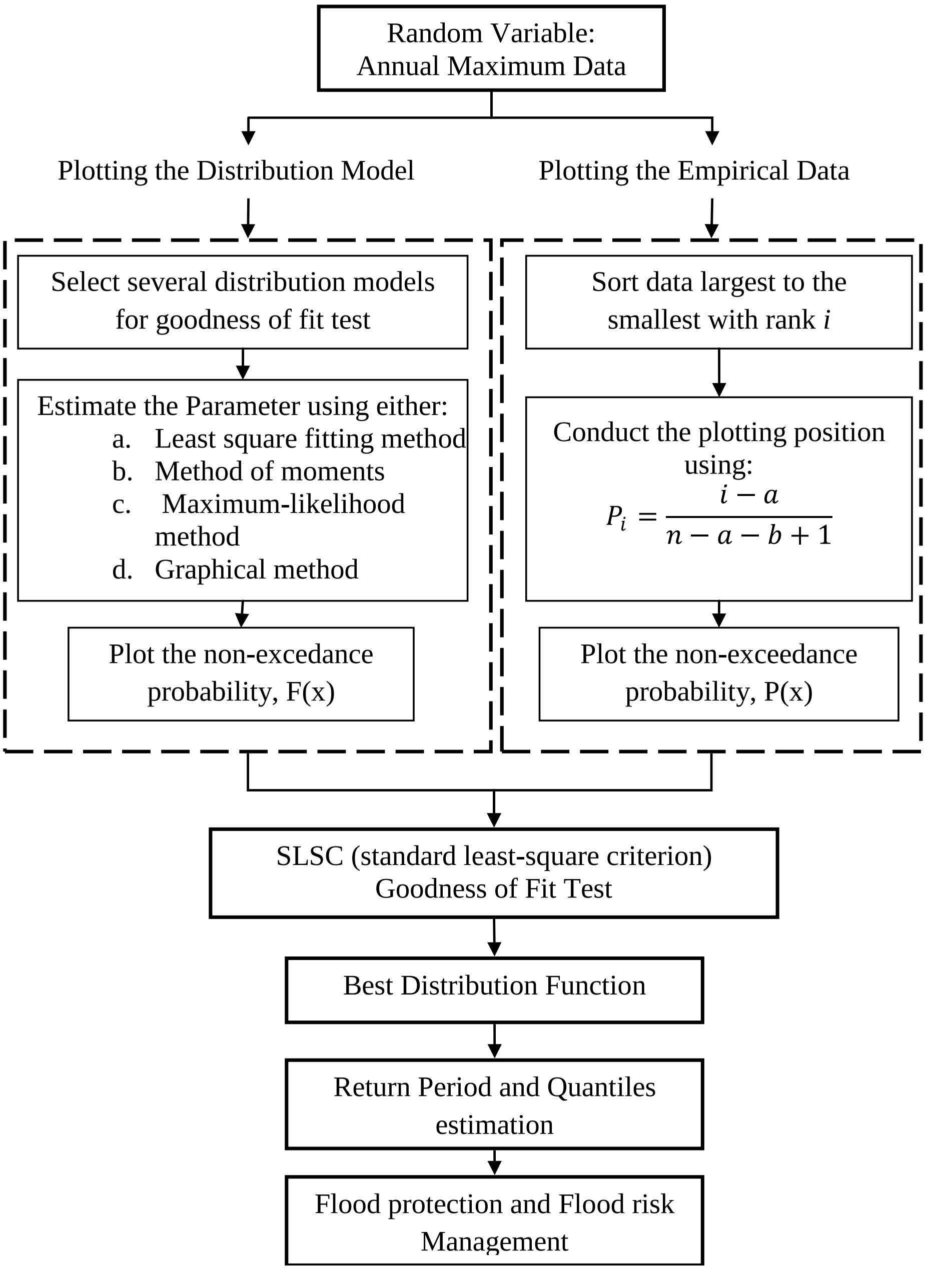

Figure 3-3: Frequency Analysis Flow Chart using SLSC Goodness of Fit Test.

3.1.1.1 *SLSC (standard least-square criterion)*

The easiest and reliable method that could be used without high level of computer programming skills is the SLSC method. The SLSC tests the differences between the reduced standardized variate of the frequency analysis models S_i fitted using the sample, to the empirical data r_i plotted using the plotting position formula. An example of the plot is shown in Figure 3-4. The reduced standardized variate uses a transformation function described as:

$$\mathbf{S_i} = \mathbf{g(y_i)} \qquad \textbf{Eq. 3-6}$$

$$\mathbf{r_i} = \mathbf{g(F^{-1}(y_i))} \qquad \textbf{Eq. 3-7}$$

With S_i is the reduced or standardized variate for the model, y_i is the sorted values of the variables x from the least to the largest values, r_i is the standard variate for the empirical data and q_i is a non-exceedence probability assigned to y_i based on a plotting position formula. The function $g(y_i)$varies among distributions. The SLSC fit test uses the following equations:

$$\mathrm{SLSC} = \frac{\sqrt{\delta^2_{\min}}}{|s^*_{1-q} - s^*_q|} \qquad \textbf{Eq. 3-8}$$

$$\delta^2 = \frac{1}{N}\sum_{i=1}^{N}(s_i - r_i)^2 \qquad \textbf{Eq. 3-9}$$

With s^*_q is a specific value of the reduced variate S_i corresponding to the non-exceedence probability q and $\delta^2_{\min}$ is obtained by minimizing Eq.3-9 is the differences between the reduced variate of the non-exceedence probability of q = 0.99 and 1-q = 0.01= (1-0.99). q = 0.99 is used for data which have samples less than 100 observations. Takara and Stedinger (1994) suggested *q* = 0.99 since most hydrologic samples have less than 100 observations. The fitness of the distribution is considered very good for SLSC ≤ 0.02.The plotting position uses a general equation of:

$$P_i = \frac{i-a}{N+1-2a} \qquad \textbf{Eq. 3-10}$$

With a is a constant that depends on the probability distribution of Weibull, Hazen or Cunnane. There are other types of plotting position formula, however in extreme values analysis those three are the most commonly applied. Takara and Stedinger (1994) suggested the Cunnane formula while Makkonen (2006) however suggested Weibull to be the most suitable for extreme values analysis since it predicts much shorter return periods of extreme events than other commonly used method. Eq. 3-11, Eq. 3-12, and Eq. 3-13 equations take the form for Weibull, Hazen and Cunnane formula respectively.

Weibull ($a = 0$), $P_i = \frac{i}{N+1}$ **Eq. 3-14**

Hazen ($a = 0.5$), $P_i = \frac{i-0.5}{n}$ **Eq. 3-15**

Cunnane ($a = 0.4$), $P_i = \frac{i-0.4}{n+0.2}$ **Eq. 3-16**

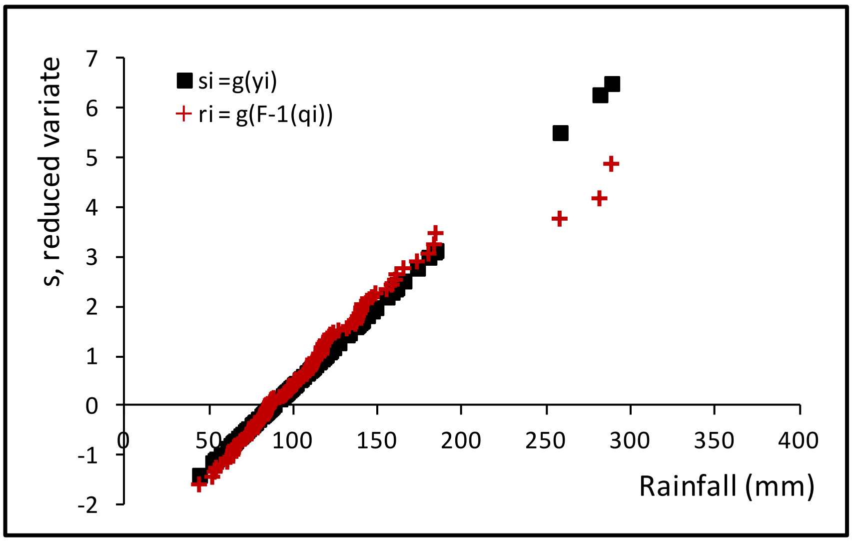

Figure 3-4: Standard reduced variate of S_i and $r_i$versus rainfall value (SLSC method)

3.1.1.2 *COR (correlation coefficient)*

The COR method test the distribution fitting by the correlation coefficient between the ordered statistics y_i and r_i:

$$\mathrm{COR} = \frac{\sum_{i=1}^{N}(y_i-\bar{y})(r_i-\bar{r})}{\left[\sum_{i=1}^{N}(y_i-\bar{y})^2 \sum_{i=1}^{N}(r_i-\bar{r})^2\right]^{\frac{1}{2}}} \qquad \textbf{Eq. 3-17}$$

With y_i is the ordered statistics, r_i is the standard variate for the empirical data (similar with the y_i and r_i of the SLSC method) and $\bar{y}$ and $\bar{r}$ are their means. Values of COR closer to unity corresponds to better fits.

3.1.1.3 *MLL (Maximum log-likelihood)*

The MLL method is most suitably used if the parameter estimation method uses the Maximum Likelihood Method (MLM) as introduced in Section 3.1.

$$\mathrm{MLL} = \sum_{i=1}^{N} \log f(x_i; \hat{\theta}) \qquad \textbf{Eq. 3-18}$$

With $\hat{\theta}$ is the maximum likelihood estimator of θ. When several distributions are fitted to a sample, the distribution that gives the greatest MLL value can be regarded as the best fit.

3.1.1.4 *AIC(Akaike's information criterion)*

The AIC considers the model simplicity as well as the goodness of fit of proposed models. In general, distributions with higher number of parameters fit better however the simplicity of a model would decrease. The AIC was proposed by Akaike. The AIC formula balances the number of parameters, k and the quality of fit by using:

$$AIC = -2\,(MLL) + 2k \qquad \textbf{Eq. 3-19}$$

As k increases, 2k will increases while -2(MLL) will decrease since the goodness of fit becomes better. Akaike (1974) suggests that the model that minimizes the AIC is the best.

3.1.2 *Basic Distributions Functions for Extreme Values*

Takara and Stedinger (1994) had suggested several important families of the basic distributions which is reasonable for modelling extreme events. They are Normal, Log-normal, extreme value type I (EV I or Gumble) and type II (EV II or Frēchet), and Pearson type III (Gamma 3p) distributions. Furthermore, according to Elíasson (1997) and Takara and Tosa (1999), the family of the extreme value distribution are the most commonly applied distribution function for maximum values of hydrologic frequency analysis model. Elíasson (1997) wrote that the distribution function for annual maxima will follow EVI very closely in the medium range of values but deviate for the highest and lowest return periods. He also relates the EVI to the estimation of the probable maximum values (PM). Therefore he had suggested some transformation method in order to use the EVI for precipitation that has a PMP value as an upper limit. Takara and Tosa (1999) suggested that finite lower and upper bounds is scientifically more rational than those with infinite bound in dealing with the physical phenomena. All the modified basic distribution functions are presented in Section 3.1.3. Table 1 shows the properties and equations of the selected distribution functions for extreme values series.

Table 3-1: Properties of the selected distribution functions for extreme values

Distribution	**Parameters**	**Domain**	**Equations** **(f(x) = PDF, F(x) = CDF, y =reduced variate)**
Log Normal *3-parameter* *LN3*	σ, μ, γ $\sigma = scale\ parameter$ $\mu =$ $location\ \ parameter$ $\gamma =$ $lower\ boundary$ $parameter$	$\gamma < x < +\infty$ 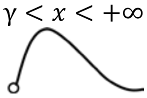	$f(x) = \frac{exp\left(-\frac{1}{2}\left(\frac{ln(x-\gamma)-\mu}{\sigma}\right)^2\right)}{(x-\gamma)\sigma\sqrt{2\pi}}$ $F(x)\ = \Phi\left(\frac{ln(x-\gamma)-\mu}{\sigma}\right)$ $y = \frac{\ln\ (x-\gamma)-\mu}{\sigma}$
Generalized *Extreme* *Value (Gev):* *-EV1* *-EV2* *-EV3*	k,σ, μ k = shape parameter $\sigma = scale\ parameter$ $\mu =$ $location\ \ parameter$	$1 + k\frac{(x-\mu)}{\sigma} >$ 0 for $k \neq 0$ $-\infty < x <$ $+\infty$ for $k = 0$   	$f(x) =$ $\begin{cases} \frac{1}{\sigma} exp(-(1+kz)^{-1/k}(1+kz)^{-1-\frac{1}{k}} & k \neq 0 \\ \frac{1}{\sigma} exp(-z - exp(-z)) & k = 0 \end{cases}$ $F(x) = \begin{cases} exp(-(1+kz)^{-1/k}) & k \neq 0 \\ exp(-exp(-z)) & k = 0 \end{cases}$ where $z = (x-\mu)/\sigma$ k,u,α are parameters to be determined. The three limiting cases are: 1) k = 0 EV1 (Gumbel) x unbounded 2) k < 0 EV2 (Frechet) in which $(u + \alpha/k) \leq x \leq \infty$ x is bounded from below 3) k > 0 EV3 (Weibull) in which $-\infty \leq x \leq (u + \alpha/k)$ x is bounded from above Reduced variate for GEV $y = -ln\left[ln\left(\frac{1}{F(x)}\right)\right]$
Gamma 3p	α, β, γ $\alpha = shape\ parameter$ $\beta = scale\ \ parameter$ $\gamma = lower\ boundary$ $parameter$	$\gamma < x < +\infty$ 	$f(x) = \frac{(x-\gamma)^{\alpha-1}}{\beta^\alpha \Gamma(\alpha)} exp(-(x-\gamma)/\beta)$ $F(x) = \frac{\Gamma_{(x-\gamma)/\beta}(\alpha)}{\Gamma(\alpha)}$ Γ is the Gamma Function $\Gamma(\alpha)\ = \int_0^\infty t^{\alpha-1}e^{-t\ dt} \qquad (\alpha > 0)$ Γ_x is the Incomplete Gamma Function $\Gamma_x(\alpha)\ = \int_0^x t^{\alpha-1}e^{-t\ dt} \qquad (\alpha > 0)$ Reduced variate : $y = \frac{x-\gamma}{\alpha}$ $\gamma = \bar{x} - \alpha\varepsilon \qquad \bar{x} = \ mean$ $\alpha = \frac{\sqrt{v}}{\sqrt{\varepsilon}}$ $\alpha = standard\ deviation$, v=variance , g=skewness $\varepsilon = \left(\frac{2}{g}\right)^2$

Log Pearson 3-parameter LP3	α, β, γ $\alpha = shape\ parameter$ $\beta = scale\ \ parameter$ $\gamma = lower\ boundary\ parameter$	$0 < x < e^{\gamma}$ $for\ \ \beta < 0$ $e^{\gamma} \leq x < +\infty$ $for\ \ \beta > 0$ 	$f(x) = \frac{1}{x\lvert\beta\rvert\Gamma(\alpha)} \frac{(\ln x - \gamma)^{\alpha-1}}{\beta} \exp(-(\ln x - \gamma)/\beta)$ $F(x) = \frac{\Gamma_{(\ln x - \gamma)/\beta}(\alpha)}{\Gamma(\alpha)}$ where Γ is the Gamma Function $\Gamma(\alpha) = \int_0^{\infty} t^{\alpha-1} e^{-t\,dt} \qquad (\alpha > 0)$ Γ_x is the Incomplete Gamma Function $\Gamma_x(\alpha) = \int_0^{x} t^{\alpha-1} e^{-t\,dt} \qquad (\alpha > 0)$ Reduced variate: $y = \frac{\ln x - \gamma}{\beta}$

3.1.3 *Modified Distributions Functions for Extreme Values*

This section introduces modified distributions suggested for extreme values analysis. They are the transformed extreme value (TDF) distribution by Elíasson (1997), log normal 4-parameter (LN4) distribution by Slade (1936), and extreme value distribution with lower and upper bounds (EVLUB or EV4) by Kanda (1981). Most of the modified distributions have been derived earlier but then was used for extreme hydrological analysis years after.

Elíasson (1997) recommended from the EV1, the TDF and ODF (cut-off distribution functions) and introduce the PMP value into the TDF. While Takara and Tosa (1999) suggested that from the viewpoint of scientific rationality, physical variate such as river discharge and rainfall should take positive values (non-negative lower bound) and have a finite physical maximum limit as an upper bound which is also the PMP value. Traditionally, however the negative lower bound has often been accepted because the lower bound is regarded as a location parameter (a free parameter) used for achieving better fitting to the data. They also suggested that when dealing with physical phenomena, the use of finite lower and upper bounds is scientifically more rational than the use of those with infinite bound. The properties of the recommended modified distribution functions are as follows:

(a) Eliasson EV1 transformed distribution Elíasson (1997)

i) TDF(Transformed Distribution Function)

Using the TDF in data analysis is equivalent to using the data transformation:

$$\tilde{X} = X - \frac{a^2 k}{X_{PM} - X} \qquad \textbf{Eq. 3-20}$$

The EVI distribution for the transformed variable is then estimated. Its CDF could also be presented as:

$$F(x) = exp\left[-exp(-z + \frac{k}{y_{lim} - z})\right] \qquad \textbf{Eq. 3-21}$$

ii) ODF (Cut Off Distribution Function)

ODF is the limit of the TDF when k → 0

$$F(x) = exp[-exp(-z)] \qquad z < y_{lim} \qquad \textbf{Eq. 3-22}$$

$$F(x) = 1 \qquad z \geq y_{lim} \qquad \textbf{Eq. 3-23}$$

$$z = \frac{x}{a} + b \qquad \textbf{Eq. 3-24}$$

$$y_{lim} = \frac{x_{PM}}{a} + b \qquad \textbf{Eq. 3-25}$$

With y = EVI's reduced variate = log (-log [P(X<x)]), y_{lim} is the limiting reduced variate, a the scale parameter, b location parameter, x_{PM} the probable maximum value, k a negative constant. Particularly for the EVI transformation, the PDF is as follows:

$$F(x) = exp\left[-exp(-\frac{x}{a} + \frac{ak}{x_{PMP} - x} - b)\right] \qquad \textbf{Eq. 3-26}$$

(b) Log Normal type 4-parameter, LN4 (Slade, 1936)

The parameters are σ_Y, μ_y, a, and g. While the domain is a $< x < g$ and the PDF:

$$f(x) = \frac{g - a}{(x - a)(g - x)\sigma_Y\sqrt{2\pi}} exp\left[-\frac{1}{2}\left(\frac{\{ln(x - a)/(g - x)\} - \mu_Y}{\sigma_Y}\right)^2\right] \qquad \textbf{Eq. 3-27}$$

(c) Extreme value distributions with lower and upper bounds, EV4 or EVLUB (Kanda, 1981; Takara and Tosa, 1999)

The parameters are $\mathrm{v}, \kappa, \mathrm{a}, \mathrm{g}$ with a as the lower limit = 0 and g is the upper limit or the PMP value. The domain is $a < x < g$ and PDF ad CDF as follows:

$$f(x) = \frac{\kappa(g-x)^{\kappa-1}(g-a)}{v^{\kappa}(x-a)^{\kappa+1}} exp\left[-\left\{\frac{g-x}{v(x-a)}\right\}^{\kappa}\right] \quad \textbf{Eq. 3-28}$$

$$F(x) = exp\left[-\left\{\frac{g-x}{v(x-a)}\right\}^{\kappa}\right] \quad \textbf{Eq. 3-29}$$

These modified distribution functions however have more than 3 parameters thus decreasing the simplicity of the function. The functions are not included in most available frequency analysis software's, thus complicating the used of it. To use this modified distribution functions, custom PDF and CDF equations need to be build into numerical modeling software such as MATLAB or FORTRAN in order to conduct their parameters estimation using Maximum Likelihood Estimate (MLE) or other estimation methods. To measure the best fit by considering these distribution functions against others distribution functions, AIC criterion is recommended since it takes into account the number of parameters (representing the distribution functions simplicity) and the Maximum log-likelihood (MLL), (Takara and Stedinger, 1994).

3.2 **Limitation of Frequency Analysis**

Conventional frequency analysis of extreme rainfalls can under estimate its quantiles. Some extreme rainfall events are observed to occur more than once within its estimated return period. This is due to the existence of extreme outliers which will be more significant in the future for many regions around the world. An example of such event is the case of Kochi.

The annual maximum series are extracted from Kochi daily rainfall observations from 1901 to 2008 (108 years). The annual maximum series are fitted to three frequency analysis models using the Method of Moments (MOM) and Maximum Likelihood (MLE) parameter estimation methods. They are Gumbel, Generalized Extreme Value (GEV) and

Log-Normal 3p (LN3). Gumbel and GEV were chosen due to the two distributions are commonly used in extreme values frequency analysis. While, LN3 was chosen because it has the best goodness of fit test using the SLSC criterion for sites close to Kochi (Alias and Takara, 2012). Figure 3-5 (a) shows the annual maximum rainfalls from 1901 to 2008 while Figure 3-5 (b) shows its density plot. Two extreme cases were observed (see Table 3-2 and Figure 3-5(a)).

Using the fitted parameters, the return periods R and quantiles Q are calculated and plotted. Figure 3-5 (c)-(e) and Table 3-3 display the quantiles estimated by the frequency models for commonly used return periods. The 20, 50 and 100-year rainfall are commonly used for flood defence structures and flood risk analysis. While the 500 and 1000-year are rarely applied but have been taken into consideration particularly to represent extreme cases hazardous waste landfills, flood hazard map and dam designs. Even though the 500-year and 1000-year designs are thought to be wildly speculative and very statistically uncertain, they are still used to represent benchmark of extreme cases. Apart by using frequency analysis, probable maximum precipitation (PMP) is also being considered and is thought to be an alternative approach particularly to represent the 1000-year rainfall (NOAA, 2007).

The quantiles plots (Figure 3-5 (c)-(e)) of all the three distributions illustrate two extreme cases were underestimated by the frequency models. While Table 3-2 shows the 524.5 mm events should have occurred at least in 175-years (according to the GEV model), even though in reality another extreme case of 628.5 mm rainfall event occurred less than 20 years later. Since the commonly used return periods particularly for flood defence structures is 20 or 50-years which have the quantiles between 300 mm and 400 mm, these extreme cases usually produced extreme flood events since the design limits has been exceeded.

If a dam or hazardous waste landfills are to be constructed, based on frequency analysis alone engineers would probably use the 500-year or 1000-year rainfall for the design limit. In this case they will select the extreme rainfall around 500 mm to 750 mm (depending on the frequency analysis model). However in real situation, a maximum rainfall of 628.5 mm have already occurred thus increasing the possibility that the design limit would be exceeded as well. Thus, it is surely safer to assume a much higher benchmark. This is where the purpose of the probable maximum precipitation (PMP) is significant.

Table 3-2: Two extreme daily-rainfall events in Kochi

Rainfall value (mm)	Year	RETURN PERIOD, T (year)		
		Gumbel	GEV	LN3
524.5	1976	400	175	469
628.5	1988	2213	449	2103

Table 3-3: Quantiles estimated by the frequency model of Kochi

Distribution	$P(X \leq x)$	QUANTILES , Q (mm)					
		0.95	**0.98**	**0.99**	**0.998**	**0.999**	**0.9995**
	T	**20**	**50**	**100**	**500**	**1000**	**2000**
GEV		334	407	469	642	730	829
GUMBEL		341	397	440	538	580	622
LN3		326	382	424	529	576	625

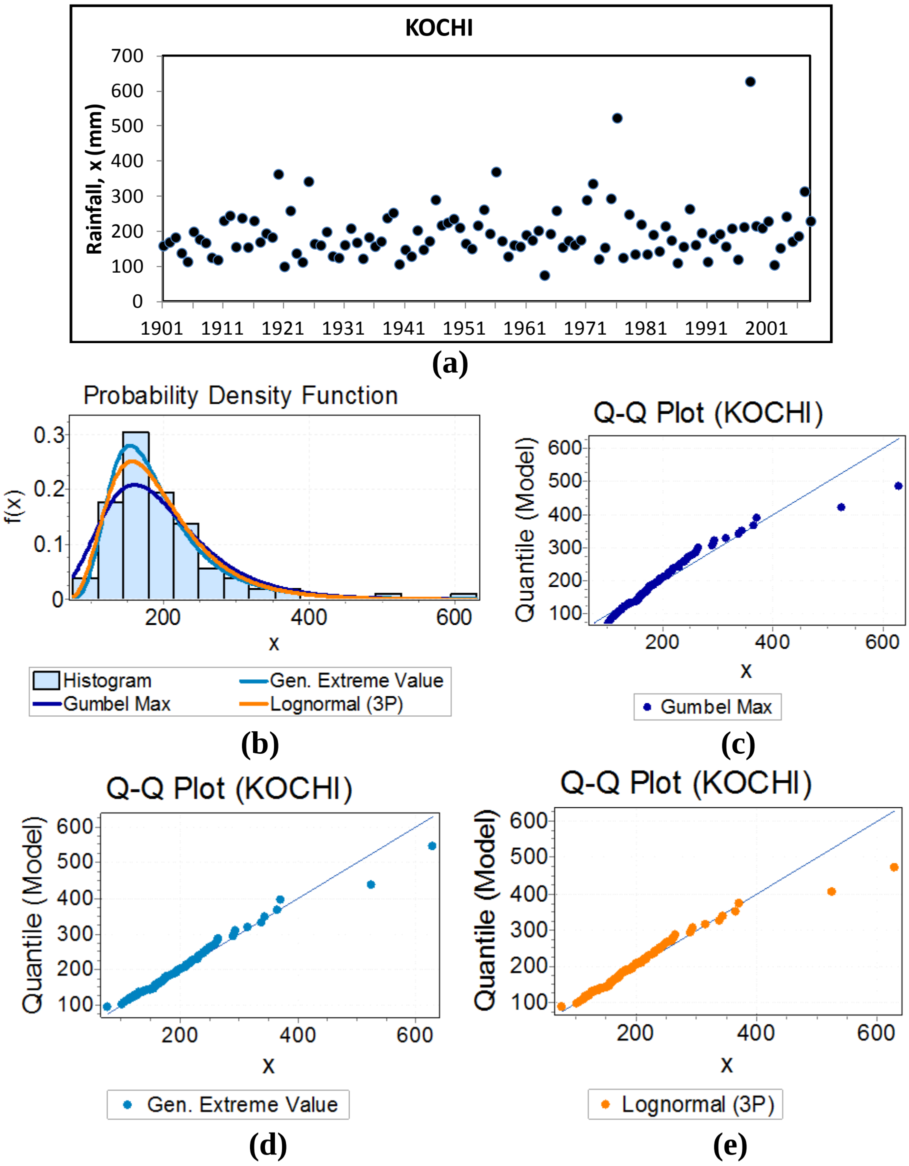

Figure 3-5: Annual maximum rainfall distributions of Kochi (1901-2008)

3.3 **Frequency Analysis with PMP**

Limitation on using the basic frequency analysis has been highlighted in the previous section, thus some of the ways to assess this problem is to implement a non-stationary frequency analysis or use an alternative method for example using the probable maximum precipitation (PMP) to predict future extreme rainfalls. PMP is used widely by practitioners and policy makers and is accepted by the World Meteorological Organization (WMO). Chapter 5 presents details and methodology on PMP. Combinations of frequency analysis and PMP can be conducted as reviewed in Section 3.1.3.

Another method by using basic frequency analysis models and a PMP estimates is tested. A sample of data is first fitted to a distribution function. Calculation of the return period of selected quantiles (until the maximum value of the sample) and the PMP (T_{PMP}) uses the fitted parameters. Based on the relationship between the return periods, its quantiles and the PMP return period a new non-linear regression equation (NLR) were produced in a form of:

$$Y = \alpha X^{\beta},\ 0 < Y < PMP \qquad \textbf{Eq. 3-30}$$

Where Y is quantiles, X is the return period, α and β are constants obtained from the NLR equation and PMP is the probable maximum precipitation. Since Y is the extreme rainfall and is a physical variate, it should be defined as a positive value with an upper boundary as PMP. This agree with Takara and Tosa (1999) who signify that physical variate such as river discharge and rainfall should take positive values (non-negative lower bound) and have a finite physical maximum limit as an upper bound which is also the PMP. The idea of the method is to plot the quantiles up to the maximum recorded value and its return period and then connecting it with the PMP value. This is to try to stabilize the distribution function using a new non-linear regression relationship by including the PMP values and its return period into the equation since most of extreme value distribution has no upper boundary.

A test on the method was conducted by fitting a GEV distribution to the annual maximum 1-day rainfall series of Kyoto, Hikone and Kochi (all have long rainfall observation, 108, 115 and 108 years respectively). The return periods and quantiles up to the maximum sample value (green circle in Figure 3-6) were plotted together with the PMP and its return period estimates. The plots are shown in Figure 3-6. From the plots, non-linear regression equations (NLR) were produced. This is conducted for each station (Hikone, Kyoto and Kochi). The NLR equation produced for Hikone is $Y = 78.131X^{0.2682}$, $Y = 95.367X^{0.2045}$ for Kyoto and $Y = 135.62X^{0.2541}$ for Kochi.

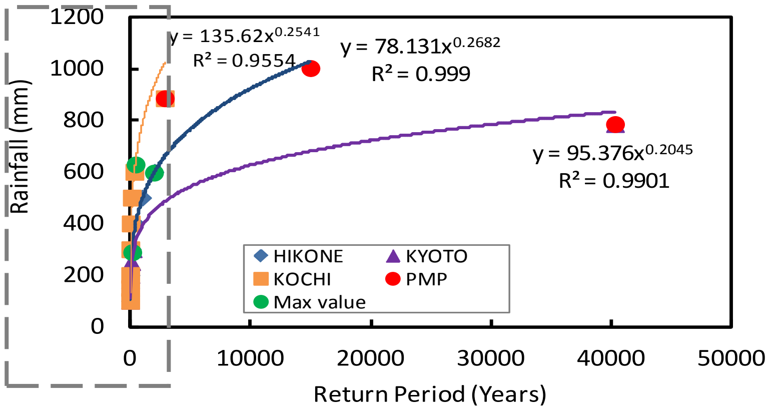

Figure 3-6: Quantiles (rainfall) versus the return periods

Table 3-4: Results on the non-linear regression equation (NLR) and the GEV.

Station (Observed Years)	X_{max} (mm)	PMP (mm)		Return Period (Years) X_{max}	200	300	500	700	1000
HIKONE (115)	596.9	1002	GEV	1977	31	140	994	3679	14863
			NLR	1962	33	151	1013	3553	13433
KYOTO (108)	288.6	785	GEV	172	37	209	3145	20847	165451
			NLR	225	17	271	3300	17102	97840
KOCHI (108)	628.5	885	GEV	449	3	13	138	797	5705
			NLR	418	5	23	170	638	2598

Table 3-4 presents the results. The NLR appear to reduce the return period of the distribution for quantiles near its PMP value. Similar results are observed for Kyoto and Kochi. Unfortunately, the current method introduced does not solve the problem stated in Section 3.2. However it can be concluded that GEV overestimates the RPs for high quantiles values (more than 700 mm) because GEV's upper bound is infinite. The NLR with upper bound given by PMP stabilizes the return period estimates. In other words, we can avoid (or reduce) overestimation by using NLR. To solve the problem in Section 3.2 another test was conducted by introducing regional frequency analysis in Chapter 5.

Chapter 4 Extreme Rainfall Homogeneous Regions

4.1 Introduction

According to the dictionary homogeneous is *'same or similar nature or kind'*. Extreme-rainfall homogeneous regions refer to regions containing sites with similar characteristics of extreme rainfall distribution such as the means, skewness and kurtosis. This means that any areas within the homogeneous region are considered to have similar climatic exposure, conditions and source of extreme rainfalls. There are various methods to identify the homogeneous regions such as using the cluster analysis. However the most recent and popular method is using the regional frequency analysis based on the *L*-moments method by Hosking and Wallis, 1997 (Fowler and Kilsby, 2003; Jones et al., 2010; Kysely and Picek, 2007). According to Hosking and Wallis (1997) the method uses an approach that is statistically efficient and reasonably straight forward to implement.

The need for a regional frequency analysis is that even though procedures for statistical frequency analysis of a single set of data are well established, however for some fitted distribution, its quantiles estimates were exceeded due to unexpected extreme rainfalls. In other cases it is quite difficult to obtained many available samples for analysis and getting a good fit especially if the samples has an extreme outlier. The other common reason to adopt regional frequency analysis (or obtaining climatological and extreme-rainfall homogeneous region) is that the availability of rainfall records in one site are not enough for a good fit due to short period of observation. Thus, by identifying extreme homogeneous regions using regional frequency analysis, short time-series or series with one or two extreme outliers records at individual sites can be compensated by substituting space for time by using observations from different sites in a region. Kysely and Picek, (2007) claims that the regional frequency analysis approach is most advantageous for variables (e.g., precipitation) exhibiting high and largely random spatial variability. The procedures for the regional frequency analysis are based on the *L*-moments method. The advantages by using the *L*-moments methods are discussed in the following section.

4.2 Basics of *L*-moments

This section introduces the basic concept and theories of the *L*-moments in regarding the usage for identifying the homogeneous regions. Details on the *L*-moments can be referred in Hosking and Wallis (1997). *L*-moments are an alternative system of describing the shapes of probability distributions apart from the parameter estimation method as described in Section 3.1. They are modified from the 'probability weighted moments (PWM)' of Greenwood et al. (1979). Detail description of the PWM are not describe in this thesis and can be find in Hosking and Wallis (1997) and Greenwood et al. (1979). The next paragraph describes the structure of *L*-moments as described in Hosking and Wallis (1997).

The main structure of the *L*-moments considers linear combinations of the observations in a sample of data arranged in ascending order. Take an example a sample as $X_{k:n}$ with *k*th the smallest observation from a sample of size *n*, so the ordered sample is $X_{1:n} \leq X_{2:n} \leq \cdots \leq X_{n:n}$. A sample of size 1 is the single observation $X_{1:1}$. It contains information about the location of the distribution. If the distribution is shifted toward a larger value, larger value of $X_{1:1}$ would be expected. See Figure 4-1 (a)-(b). A sample of size 2 contains two observations $X_{1:2}$ and $X_{2:2}$. The sample contains the information about the scale, or dispersion of the distribution. If the distribution is tightly bunched around a central value, then the two observations will be close. If it is widely dispersed then the two distributions would be far apart. See Figure 4-1 (c)-(d). Thus the difference between the two distributions $X_{2:2} - X_{1:2}$, is a measure of its scale. A sample of size of 3, $X_{1:3} \leq X_{2:3} \leq X_{3:3}$ contains information about the skewness of the distribution. If the distribution is symmetric about a central value, then the two extremes observations will be approximately equidistant from the central. Thus, $X_{3:3} - X_{2:3} \approx X_{2:3} - X_{1:3}$ or $X_{3:3} - 2X_{2:3} + X_{1:3} \approx 0$. If the distribution is skewed to the right, so that the upper tail is heavier than the lower tail, then typically $X_{3:3} - X_{2:3}$ will be larger than $X_{2:3} - X_{1:3}$, and so $X_{3:3} - 2X_{2:3} + X_{1:3}$ will be positive. See Figure 4-1 (e)-(f). Similarly if the distribution is skewed to the left than $X_{3:3} - 2X_{2:3} + X_{1:3}$ will typically be negative. Thus $X_{3:3} - 2X_{2:3} + X_{1:3}$, the second difference of the ordered sample is a measure of the skewness of the distribution. For a sample of 4, $X_{1:4} \leq X_{2:4} \leq X_{3:4} \leq X_{4:4}$, it measures how much further apart the two extreme values of the sample are than the two central values, writing it as $(X_{4:4} - X_{1:4}) - 3(X_{3:4} - X_{2:4})$. If the distribution has a flat density function, then the sample values will typically be approximately equally spaced and the central third difference will be close to zero. If the distribution has a high central peak and long tails, then the central third difference is typically large. See Figure 4-1 (g)-(h). Thus $(X_{4:4} - X_{1:4}) - 3(X_{3:4} - X_{2:4})$ is the measure of the kurtosis of the distribution.

Linear combinations of the elements of an ordered sample are shown to contain information about the location, scale, and shape of the distribution from which the sample are drawn. L-moments are defined to be the expected values of these linear combinations, multiplied for numerical convenience by scalar constants. The "L" in L-moments emphasizes the construction of L-moments from linear combinations of order statistics. The L-moments of a probability distribution are defined by:

$$\boldsymbol{\lambda_1 = E(X_{1:1})} \quad \textbf{Eq. 4-1}$$

$$\lambda_2 = \frac{1}{2}E(X_{2:2} - X_{1:2}) \quad \textbf{Eq. 4-2}$$

$$\lambda_3 = \frac{1}{3}E(X_{3:3} - 2X_{2:3} + X_{1:3}) \quad \textbf{Eq. 4-3}$$

$$\lambda_4 = \frac{1}{4}E(X_{4:4} - 3X_{3:4} + 3X_{2:4} - X_{1:4}) \quad \textbf{Eq. 4-4}$$

and in general

$$\lambda_r = r^{-1}\sum_{j=0}^{r-1}(-1)^j \binom{r-1}{j} E\left(X_{r-j:\,r}\right) \quad \textbf{Eq. 4-5}$$

$$E(X_{r:n}) = \frac{n!}{(r-1)!(n-r)!}\int_0^1 x(u)u^{r-1}(1-u)^{n-r}du \quad \textbf{Eq. 4-6}$$

Details on the theories describing the L-moments can be referred in Hosking and Wallis, 1997.

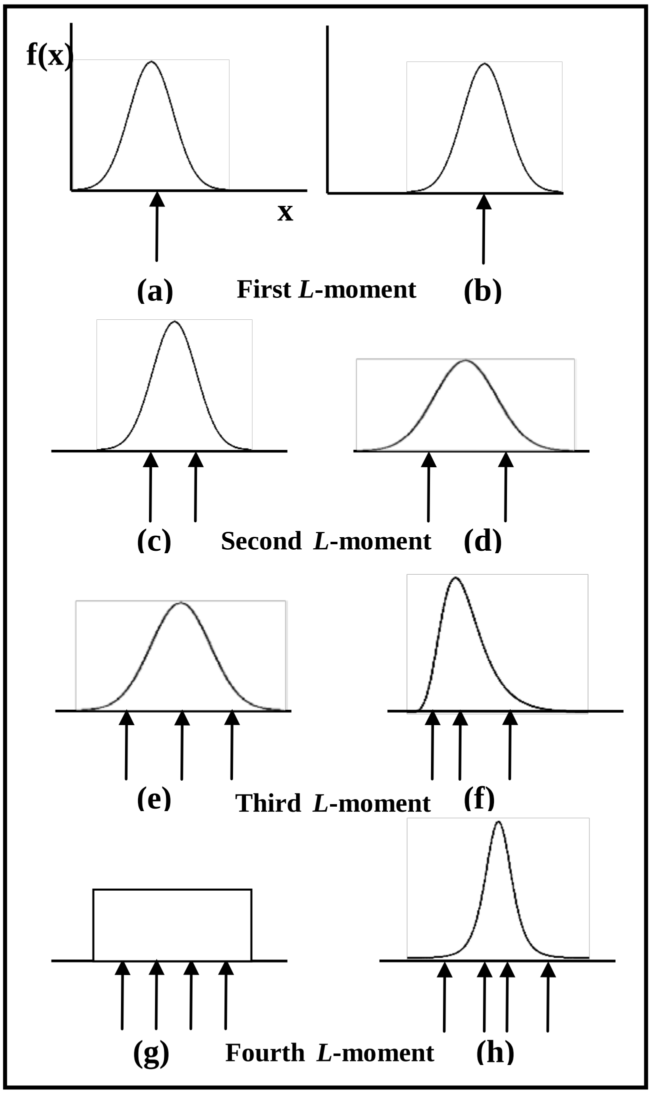

Figure 4-1: Definition sketch of *L*-moments (based on Hosking and Wallis, 1997)

4.2.1 *Properties of L-moments*

There are five most useful quantities in the *L*-moments for summarizing probability distributions and for the regional frequency analysis. They are the *L*-moments and the *L*-moment ratios:

L-moments

- ❖ λ_1 the *L*-location or mean of the distribution, λ_1 can take any value
- ❖ λ_2 the *L*-scale, $\lambda_2 \geq 0$

L-moment ratios:

- τ the L-CV
- τ_3 the L-skewness
- τ_4 the L-kurtosis

The L-moment ratios were developed since it is more convenient to define dimensionless versions of L-moments which are achieved by dividing the higher-order L-moments by the scale measure λ_2 . Thus it measures the shape of a distribution independently of its scale of measurement. The L-moment ratios are defined by

$$\tau_r = \frac{\lambda_r}{\lambda_2}, \qquad r = 3, 4, \ldots \qquad \textbf{Eq. 4-7}$$

$$\tau = \frac{\lambda_2}{\lambda_1} \qquad \textbf{Eq. 4-8}$$

4.2.2 *Sample L-moments*

L-moments have been defined for a probability distribution, but in practice must be estimated from a finite sample. Estimation based on a sample of size n, arranged in ascending order. Let $X_{1:n} \leq X_{2:n} \leq \cdots \leq X_{n:n}$ be the ordered sample. It is said to be convenient to begin with an estimator of the probability weighted moment β_r. An unbiased estimator of β_r is

$$b_0 = n^{-1} \sum_{j=1}^{n} x_{j:n}\,, \qquad \textbf{Eq. 4-9}$$

$$b_1 = n^{-1} \sum_{j=2}^{n} \frac{(j-1)}{(n-1)} x_{j:n}\,, \qquad \textbf{Eq. 4-10}$$

$$b_2 = n^{-1} \sum_{j=3}^{n} \frac{(j-1)(j-2)}{(n-1)(n-2)} x_{j:n}\,, \qquad \textbf{Eq. 4-11}$$

and in general,

$$b_r = n^{-1} \sum_{j=r+1}^{n} \frac{(j-1)(j-2)\ldots(j-r)}{(n-1)(n-2)\ldots(n-r)} x_{j:n} \qquad \textbf{Eq. 4-12}$$

In terms of samples, the L-moments of λ_1, λ_2, λ_3, and λ_4 are defined as l_1, l_2, l_3, and l_4 respectively. Thus, the sample L-moments are:

L-location: $l_1 = b_0$, **Eq. 4-13**

L-scale: $l_2 = 2b_1 - b_0$, **Eq. 4-14**

L-skewness: $l_3 = 6b_2 - 6b_1 + b_0$, **Eq. 4-15**

L-kurtosis: $l_4 = 20b_3 - 30b_2 - 12b_1 - b_0$, **Eq. 4-16**

The sample *L*-moment ratios are analogously to Eq.4-7 and Eq. 4-8 defined by:

$t_r = l_r/l_2$ **Eq. 4-17**

L-CV = $t = l_2/l_1$ **Eq. 4-18**

4.3 **Forming the Homogeneous Regions**

Based on the *L*-moments method, 3 main processes are undertaken to form the homogeneous regions. Step 1 is forming preliminary regions based on '*site characteristics*'; Step 2 is calculating at-site statistics using the *L*-moments and; Step 3 is homogeneity testing of the proposed regions. The homogeneity criterions are not expected to be exactly satisfied. Approximate homogeneity is sufficient to ensure that regional frequency analysis is much more accurate than at-site analysis (single site frequency analysis).

4.3.1 *Determining the Site Characteristics*

After data quality checking as described in Section 2.3, initial forming of the regions were carried out by considering each '*site characteristics*'. According to Hosking and Wallis, 1997 the site characteristics should be characteristics which are thought to influence the frequency distribution. The '*site characteristics*' chosen particularly for identifying the extreme-rainfall homogeneous region in this study are

- Topography influences (e.g DEM, nearest water body)
- Existing administrative regions or climatological boundary proposed by the Meteorological Agency or previous studies.
- The annual maximum rainfall distribution
- The annual maximum rainfalls' trend distributions

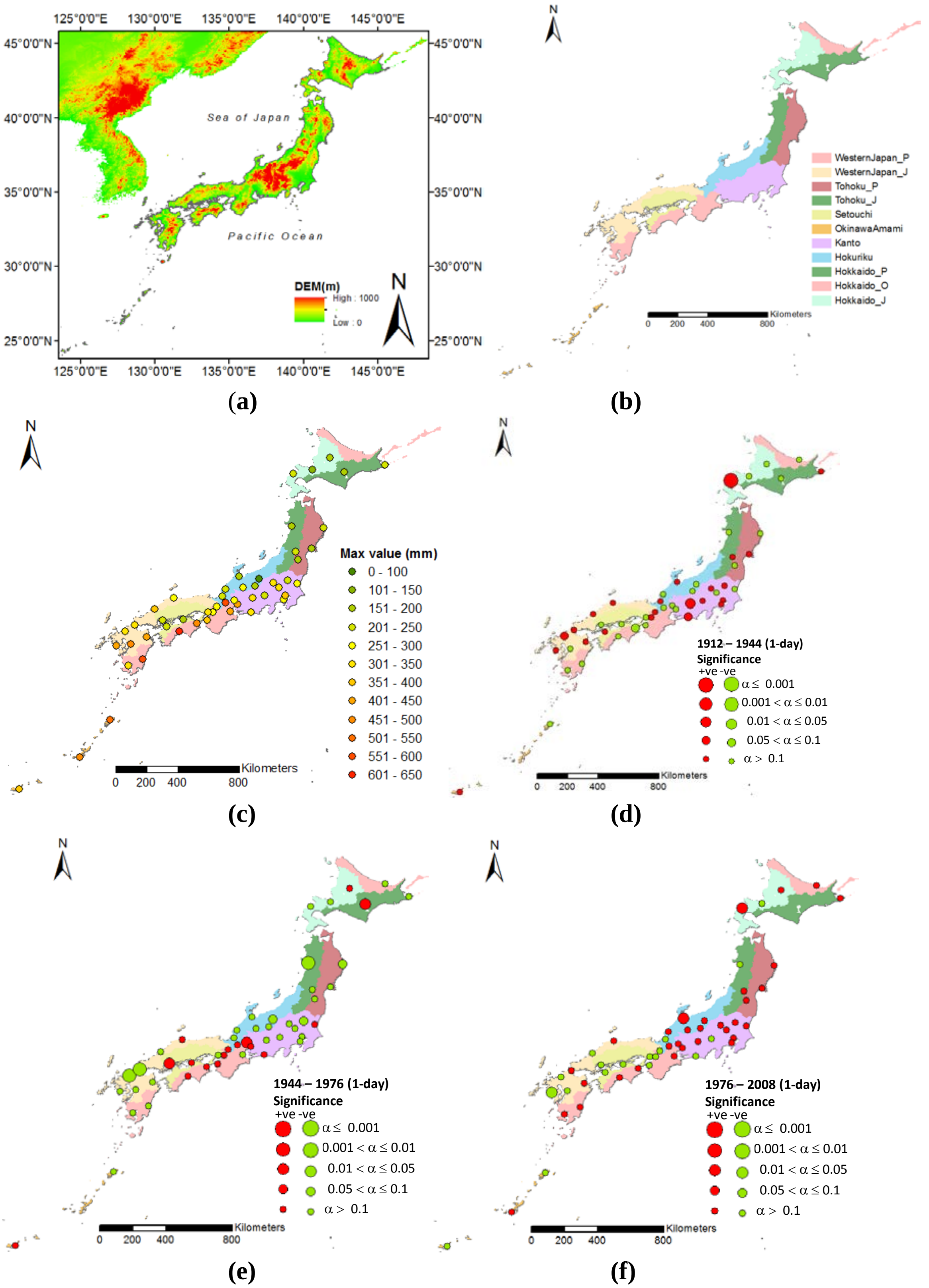

Figure 4-2: Site characteristics used for forming regions; (a) the topography influences, DEM; (b) Japanese climatic regions in term of heavy snowfall and high rainfall by Chaffe et al. (2014); (c) the annual maximum rainfall distribution; (d)-(f) the trend statistic distributions of every 33 years.

Figure 4-2 (a) represents the DEM. The DEM is an SRTM data V4 of the International Centre for Tropical Agriculture (CIAT) with a 250 meter grid (Jarvis et al., 2008). Figure 4-2 (b) is the Japanese climatic regions divided by Chaffe et al. (2013) based on the regions used for the seasonal forecast by JMA and cluster analysis related to the main climatic influences of the Sea of Japan (with heavy snowfall in the winter) and the Pacific Ocean (high summer rainfall). It is unknown whether the boundaries could represent homogeneous regions for extreme rainfall cases since no statistical test were conducted, thus the regional frequency analysis in this thesis was conducted for this purpose. Figure 4-2 (c) is the annual maximum rainfall distribution while Figure 4-2 (d-f) is the trend statistics distributions. Using data described in Section 2.3 of the Japanese surface station observation data, long records from 1901 up to 2008 were used for determining the annual maximum series and the trend statistics. Since long observation data are available, multiple trend analysis was conducted. The trend analysis was conducted using the Mann-Kendall non-parametric test. The test analyzed whether there exists an increasing or decreasing monotonic trend. Based on the test statistic Z (trend statistic), an increasing or decreasing trend was obtained. Using data from 1901 to 2008, 3 separate trend analysis for the years 1912-1944, 1944-1976, and 1976-2008 was conducted. Any spatial correlation in the trends were hoped to assess whether the sites are exposed to similar climate characteristics.

Based on all the site characteristics proposed, preliminary regions were formed by grouping sites with similar extreme rainfall patterns taking consideration the topography and the nearest source of moisture. The extreme rainfall patterns are observed visually from the annual maximum rainfall distributions and the trend distributions. Some weak patterns can be seen from the 3 year-groups of trend distributions. Some areas are showed to be decreasing or increasing analogous to each observation period (spatial correlation in trends). This information can be use as a guide for the formation of the preliminary homogeneous regions since it indicates stations exposing to similar climate characteristics.

Using the above site characteristics the regions were formed roughly by first considering the highest mountainous ranges (using the DEM) (Figure 4-2 (a)) and the initial climatologically boundary (Figure 4-2 (b)). Then, the preliminary boundary regions were adjusted by considering the extreme rainfall distribution patterns (Figure 4-2 (c-f)). Sites within the regions were identified and used for the next processes which are the estimations of the at-site statistics and the homogeneity or heterogeneity test.

4.3.2 *At-site Statistics*

After forming the preliminary regions, at site statistics based on L-moments are determined for all the sites within the region. The at site statistics are the L-moments,l_1, L-CV, t_3, t_4, and t_5. All have been described in Section 4.2.2

4.3.3 *Homogeneity Tests*

Using the at site statistics obtained, two tests are conducted to test the proposed regions' homogeneity. They are the discordancy test and heterogeneity test. Discordancy test will produce a discordancy measure, D_i while heterogeneity test produces the heterogeneity measure, H. The discordancy test was conducted first followed by the heterogeneity test alternately until the requirements for homogeneity are qualified.

i) Discordancy Test

The main function of the discordancy test is to detect sites with gross errors and to detect outliers in the proposed homogeneous region. When sites exceed some critical value of D_i, then the site needs to be check whether it is due to some gross errors or it is an outlier within the region. Gross errors could be due to gauge being moved at certain time or man induced changes. Sites with gross errors in its observed data are excluded from further analysis. However, if the site is an outlier (without any gross errors due to man-induced changes), then the site will either be kept or move to neighbouring region. It is kept if the surrounding sites have acceptable D_i values. This could be due to an existence of an extreme localized meteorological event. The discordancy measure for one site is determined by the following formulas. Suppose that there are N sites in the group. Let $u_i = \left[t^{(i)} t_3^{(i)} t_4^{(i)}\right]^T$ be a vector containing the L-moments t, t_3, and t_4 values for site i: the superscript T denotes transposition of a vector or matrix. Let $\bar{u}$ be the unweighted group average, A the matrix of sums of squares and cross-products and D_i the discordancy measure for site i.

$$\bar{u} = N^{-1} \sum_{i=1}^{N} u_i \qquad \textbf{Eq. 4-19}$$

$$A = \sum_{i=1}^{N} (u_i - \bar{u})(u_i - \bar{u})^T \qquad \textbf{Eq. 4-20}$$

$$D_i = \frac{1}{3} N (u_i - \bar{u})^T A^{-1} (u_i - \bar{u}) \qquad \textbf{Eq. 4-21}$$

Hosking and Wallis (1997) initially suggested the critical value of D_i to be 3 for regions having more than 15 sites. This means that site *i* is declared to be discordant if D_i exceeds 3. However, in this study-case even though all the regions have more than 15 numbers of sites, using the critical value as 3 was not suitable. During analysis, it was more practical to use the critical value 2 since no improvement on the heterogeneity test was obtained by using the critical value 3. It was also observed in some region the discordance values (D_i) did not have D_i values 3 or higher during the first test for discordancy. This makes it impossible to improve the *H* value to fulfil the homogeneity requirement.

ii) Heterogeneity Test

In a homogeneous region all sites have the same population *L*-moment ratios. The between-site dispersion of the sample *L*-moment ratios for the group of sites under consideration can be used to measure the homogeneity. A visual assessment of the dispersion of the sample *L*-moment ratios are obtained by plotting them on graphs of *L*-skewness (t_3) versus *L-CV* (t) and *L*-skewness (t_3) versus *L*-kurtosis (t_4). Refer Figure 4-3. A reasonable numerical measures of dispersion based on this plots are the average distance from a site's plotted point on such a graph to the group average point. The group averages are weighted proportionally to the sites' record lengths.

In term of mathematical expression of the dispersion measures, suppose the proposed region has *N* sites, with site *i* having record length n_i and sample *L*-moment ratios $t^{(i)} t_3^{(i)} t_4^{(i)}$. Denote t^R, t_3^R, and t_4^R the regional average *L-CV*, *L*-skewness, and *L*-kurtosis, weighted proportionally to the sites' record length and *V* the weighted standard deviation of the at-site sample *L-CV*s.

$$t^R = \sum_{i=1}^{N} n_i t^{(i)} / \sum_{i=1}^{N} n_i \qquad \textbf{Eq. 4-22}$$

$$V = \left\{ \sum_{i=1}^{N} n_i \left(t^{(i)} - t^R\right)^2 / \sum_{i=1}^{N} n_i \right\}^{1/2} \qquad \textbf{Eq. 4-23}$$

To test whether the region is homogeneous, any distribution is fitted to the regional average *L*-moment ratios (t^R, t_3^R, and t_4^R). Even so, Hosking and Wallis (1997) suggested the kappa distribution to be used. This is because the *L*-moments of kappa distribution cover a large area of the τ_3 and τ_4 plane. The kappa distribution is a four-parameter distribution that includes as special cases the generalized logistic, generalized extreme value, and generalized Pareto distributions. For these reason it is useful as a general distribution with which to compare the fit of two- and three-parameter distributions and for use in simulating artificial data in order to assess the accuracy of statistical methods.

Using the distribution fitted, large number of simulation N_{sim} of the region are realized. The simulated regions have sites with similar record lengths as the real-samples. This is done by adopting the Monte Carlo simulation. For each simulated region, its V is calculated. The mean and standard deviation of the N_{sim} values of V were determined. These are called μ_V and σ_V. The heterogeneity measure are then calculated as

$$H = \frac{(V - \mu_V)}{\sigma_V} \qquad \textbf{Eq. 4-24}$$

Region was declared to be heterogeneous if H is sufficiently large. Hosking and Wallis (1997) suggested the region be regarded as "acceptably homogeneous" if $H < 1$, "possibly heterogeneous" if $1 \leq H < 2$, and "definitely heterogeneous" if $H \geq 2$. Figure 4-3 (a) is an example of the distribution of the L-moment ratios of all the sites in one proposed region. After the discordancy and heterogeneity test were conducted alternately by discarding sites with D_i higher than 2, until H is less than 1, resulting plots of the L-moment ratios are as in Figure 4-3 (b). Alternatively dispersion measure could also be used based on L-skewness (t_3) and L-kurtosis (t_4) using equations

$$V_2 = \frac{\sum_{i=1}^{N} n_i \left\{ \left(t^{(i)} - t^{R}\right)^2 + \left(t_3^{(i)} - t_3^{R}\right)^2 \right\}^{\frac{1}{2}}}{\sum_{i=1}^{N} n_i} \qquad \textbf{Eq. 4-25}$$

$$V_3 = \frac{\sum_{i=1}^{N} n_i \left\{ \left(t_3^{(i)} - t_3^{R}\right)^2 + \left(t_4^{(i)} - t_4^{R}\right)^2 \right\}^{\frac{1}{2}}}{\sum_{i=1}^{N} n_i} \qquad \textbf{Eq. 4-26}$$

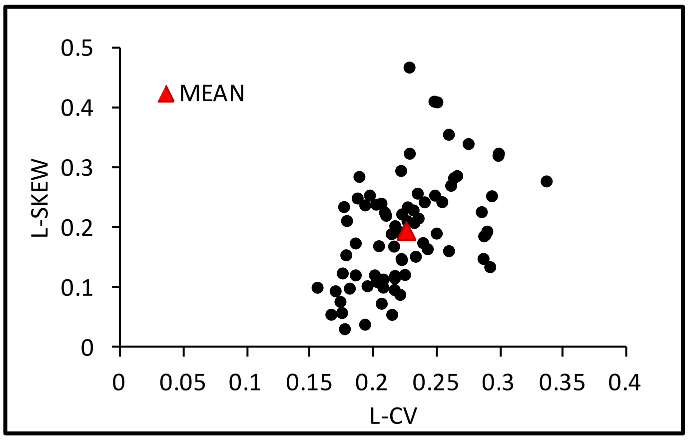

(a) L-skew versus L-CV (Before test)

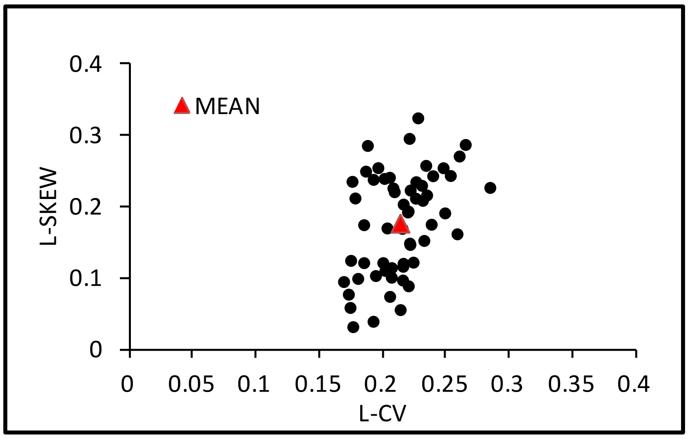

(b) L-skew versus L-CV (After test)

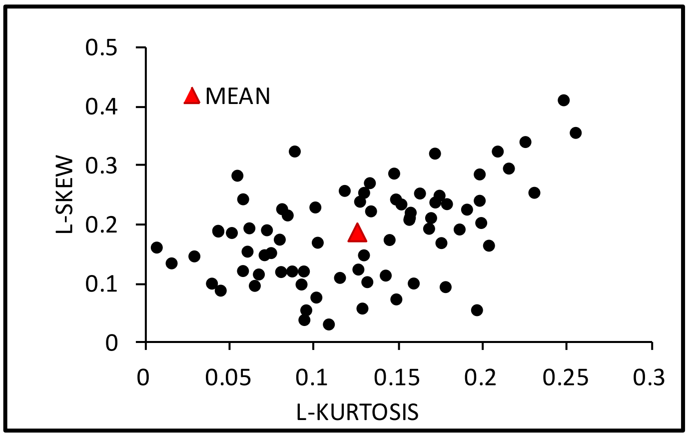

(c) L-skew versus L-kurtosis

Figure 4-3: Visual assessment on the *L*-moment ratios

Eq. 4-25 is based on the *L-CV* and *L*-skewness and Eq. 4-26 is based on *L*-skewness and *L*-kurtosis. However, according to Hosking and Wallis (1997), the H statistic based on V_2 and V_3 lack power to discriminate between homogeneous and heterogeneous regions. The H statistic based on V has much better discriminatory power. This study uses H statistic based on V only.

4.4 The Extreme-Rainfall Homogeneous Regions

4.4.1 *Region Description*

Ten extreme-rainfall homogeneous regions were identified using the *L*-moments regional frequency analysis method. Table 4-1 shows the information of H statistics obtained and percentage of sites discarded due to its high discordancy measure D_i (above 2). All the stations discarded were checked for any man-induced gross errors. The stations with high D_i due to local extreme weather event and orographic effects during typhoons are kept. According to Hosking and Wallis (1997), *'it must be considered that an extreme but localized meteorological event may have affected only a few sites in a region. If such event equally likely to affect any of the sites in the future, then it is correct to treat the entire group of sites as a homogeneous region, even though some sites appear to be discordant with the region as a whole'*.

The homogeneous regions could be divided into three major sections with their own source of moisture. The sections are separated by the Japanese mountain ranges. Section 1 contains the regions which faces the Pacific Ocean thus rainfalls distributed in this section has its winds carrying moisture from the Pacific Ocean. They are regions 4, 6, 7 and 10. While Section 2 contains the regions which faces the Sea of Japan, thus the source of its rainfall is obtained from the Sea of Japan. They are regions 2, 3, 5, and 8. The third section include only Region 9 which has its source of moisture from the Setonaikai sea (located in the middle of Region 9) and is surrounded by mountain ranges, thus most of the moistures carried by winds from the Sea of Japan and the Pacific Ocean were shielded. Due to this, it has a climate similar to a Mediterranean climate. See Figure 4-4.

Table 4-1: Heterogeneity information for the homogeneous regions

Region	No. of stations (Amedas and Surface stations)	Heterogeneity test, H (excluding high D stations)				Heterogeneity test, H (all acceptable stations)		
		Qualified H_1	% of Discarded stations (qualified)	Best H_1	% of Discarded stations (best)	H_1	H_2	H_3
Region 1	79	-0.19	0%	-0.19	0%	-0.14	-1.33	-2.18
Region 2	118	1.00	20%	0.36	26%	2.60	1.32	0.60
Region 3	89	0.85	12%	0.43	15%	4.06	3.23	3.12
Region 4	100	1.00	0%	0.77	15%	1.15	-0.08	-0.89
Region 5	82	0.92	0%	-0.35	6%	0.06	1.00	0.89
Region 6	162	-0.21	30%	-0.21	30%	6.94	1.26	-0.50
Region 7	100	0.76	5%	-0.04	8%	2.59	1.36	0.65
Region 8	143	0.72	11%	0.61	13%	2.44	1.38	0.52
Region 9	75	0.84	21%	0.84	21%	9.82	6.54	5.30
Region 10	105	0.48	6%	0.48	6%	5.26	1.85	2.12

Table 4-2: Distribution Information for the homogeneous regions

Region	Distribution (excluding high D stations)		Distribution (all acceptable stations)	
	Z statistic	Type	Z statistic	Type
Region 1	-0.66	Log normal	-0.60	Log normal
Region 2	0.56	Log normal	0.43^1, -1.42^2	Gen. Extreme value[1], Log normal[2]
Region 3	-0.17	Log normal	0.66	Log normal
Region 4	-1.17	Pearson type III	0.70^1, -2.19^2	Log normal[1], Pearson type III[2]
Region 5	0.51	Gen. Extreme value	0.62	Gen. Extreme value
Region 6	1.32	Pearson type III	-1.12	Pearson type III
Region 7	-0.93	Gen. Extreme value	-0.8	Gen. Extreme value
Region 8	-0.51	Log normal	-0.04^1, -1.68^2	Gen. Extreme value, Log normal[2]
Region 9	0.85	Log normal	0.10^1, -0.72^2	Gen. Extreme value, Log normal[2]
Region 10	0.31	Log normal	0.33^1, -0.90^2	Gen. Extreme value, Log normal[2]

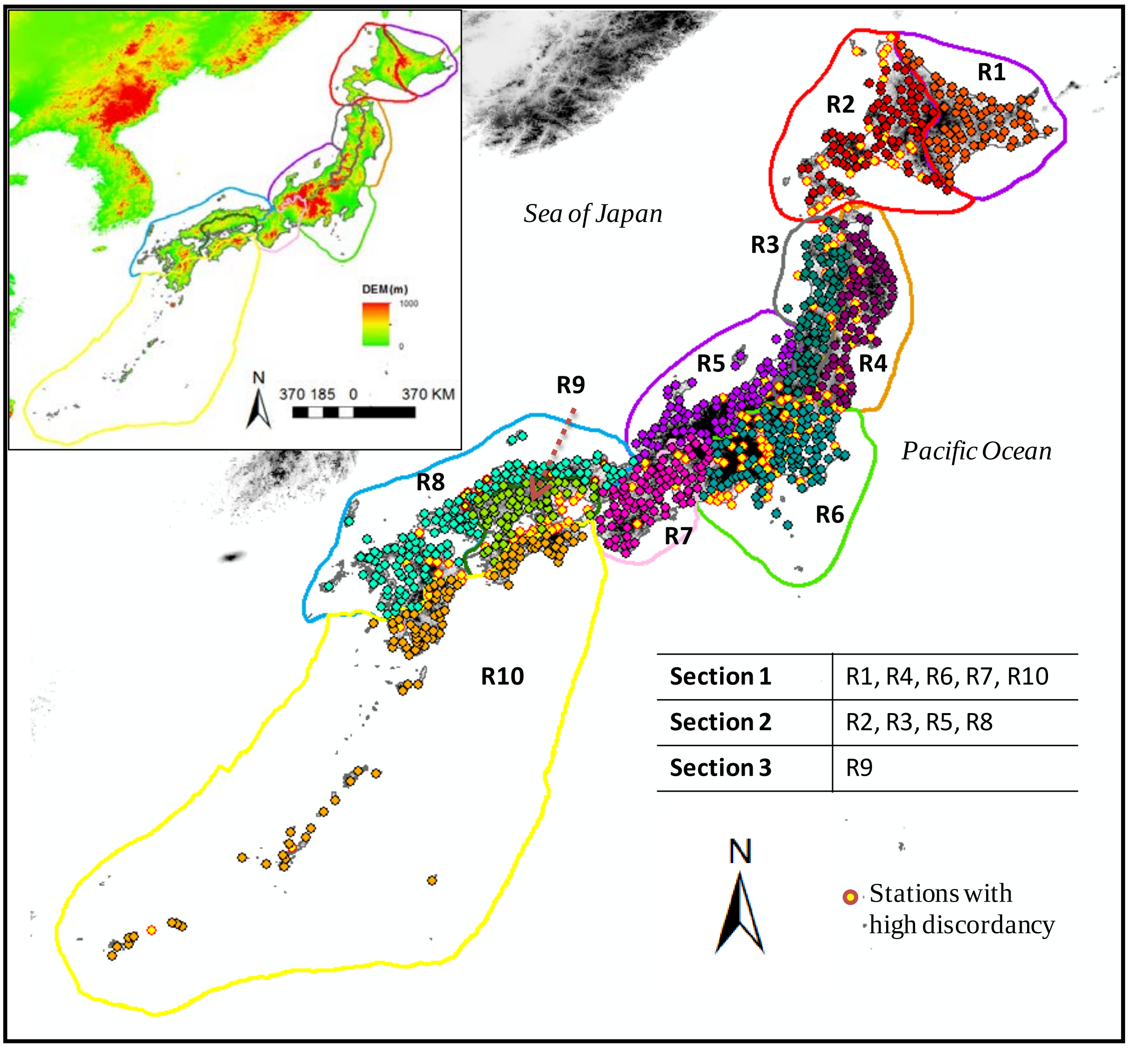

Figure 4-4: Extreme-rainfall homogeneous regions for Japan

Most of the regions are quite similar to the climate regions divided by Chaffe et. al (2014), differences are due to some combination or splitting of the regions. Examples of the differences are the regions 1 and 2 (R1 and R2 respectively in Fig. 4). In this case the Hokkaido region (the most north island of Japan) is separated into two instead of three. R1 and R2 are separated by mountainous ranges with its heights around 1000 meters. This shows that the high mountainous ranges effect the extreme rainfall distributions quite significantly, acting as a barrier from wind carrying moisture influenced by large scale convective system (e.g. typhoons) from the Pacific ocean to the Sea of Japan.

In Section 1, all the regions except Region 6 has very good heterogeneity test with the discarded stations being less than 10% for *H* to be qualified Region 6 is the only region which consist of about 50% of mountainous ranges and is directly exposed to typhoons. See Figure 4-4. Majority of sites with high discordances could be observed to cluster at areas on slopes of the mountains. Most of the sites have an altitude higher than 200 meters. This could suggest the possibility that those high discordances' sites are highly influenced by orographic effects. During the typhoons, sites near the mountain ranges could experience significant orographic effects thus producing intense rainfalls compared to sites further from the mountain ranges. Take for an example sub-region (sub-1) of Region 6 in Figure 4-5, the H values obtained is 0.05 and 0% of discarded sites. As shown in Figure 4-6, by analysisng the *L*-moment ratios, sub-1 has high L-CV values compared to all sites in Region 6 in general. L-CV is the ratio of the standard deviation (dispersion) towards the means. The standard deviation (l_2) of most sites in sub-1 indeed has the highest standard deviation (l_2) values compared to all sites in Region 6 as a whole. This could suggest that everytime a typhoon event occurs, sub-1 sites experienced an orographic phenomea thus creating its own extreme rainfall distribution densities compared to other sites further from the montain ranges. According to Miyajima and Fujibe (2011) orographic enhancement are more conspicuous for precipitation of a longer time scale.

Different from sub-1, sites in sub-2 are scattered across Region 6 without any geographical significant similarities. The only similarities they have is that their skewness ratio,t_3 (l_3/l_2) are very high compared to other sites (Figure 4-6). This could suggest they have more outliers then the others. For example one or two very large annual maximum value compared to the whole recorded annual maximum series. This could be due to local extreme value event.

For regions in Section 2, in general 0 - 12 % of sites having high discordancy values were discarded to obtain qualified *H* values. This shows a very good heterogeneity assessment. However, only Region 2 has a very high percentage of 20%. It is located at the most north part of the Japanese archipelago and partially faces the Pacific Ocean and the Sea of Japan. Thus, it also experienced heavy rainfalls due to its direct exposure from typhoons generated at the Pacific Ocean. The other regions within Section 2 were shielded mostly by the mountainous ranges trough out the middle of the Japanese islands. Besides typhoons, the region also experiences extra tropical cyclone and heavy snowfall. A study by Duan et al. (2014) shows that the trend distribution of rainfalls in Region 2 is highly influenced by seasonal variations where significant increasing trend are observed in Region 2 during the winter season. Much study are needed to assess the reason on why it has a lot of high discordances sites, however we could suggest that it could be due to the effect of diversity of the climate in Region 2 which are combinations of the influence from various large scale meteorological phenomena (typhoon, extra tropical cyclone, and Baiu-front) and due to the geographical properties (existence of the Hidaka Mountain range).

For Section 3 which consists of only Region 9, the percentage of high discordances sites are quite high which reaches 21%. Section 3 has a unique climate of a Mediterranean climate. This is due to its geographical location and its surrounding topography. It is surrounded by high mountainous ranges thus limiting winds carrying moisture from either the Pacific Ocean or the Sea of Japan to enter into its area. The high discordances sites within Region 9 have very few rainfalls where drought seldom occurs due to the existence of the mountain range at its south. Most of the wind carrying moisture from the South was blocked by those mountain ranges.

As a conclusion, regions which have very good heterogeneity assessments and with high confidence accepted as an extreme-rainfall homogeneous region are Region 1, Region 3, Region 4, Region 5, Region 7, Region 8 and Region 10. Region 2, Region 6 and Region 9 are proven to be acceptably homogeneous, however with quite a large numbers of discordances sites. These sites- as discussed in the previous paragraphs are either due to localized extreme rainfall event or due to some orographic phenomena. Further assessment and changes can be conducted by introducing sub-regions. However, for this particular research all the regions are assumed to be acceptably homogenous. The regions are used for calculating the statistical PMP estimates considering homogeneous regions as the transposition boundaries.

Table 4-3: Sub-regions analyzed within Region 6

Sub-1		Sub-2	
42396	46076	40406	48561
43091	49251	41011	48731
43156		41091	49086
43151		42046	50466
43157		42186	50476
44046		42286	50506
44051		42396	50536
49171		45346	50551
49161		48331	

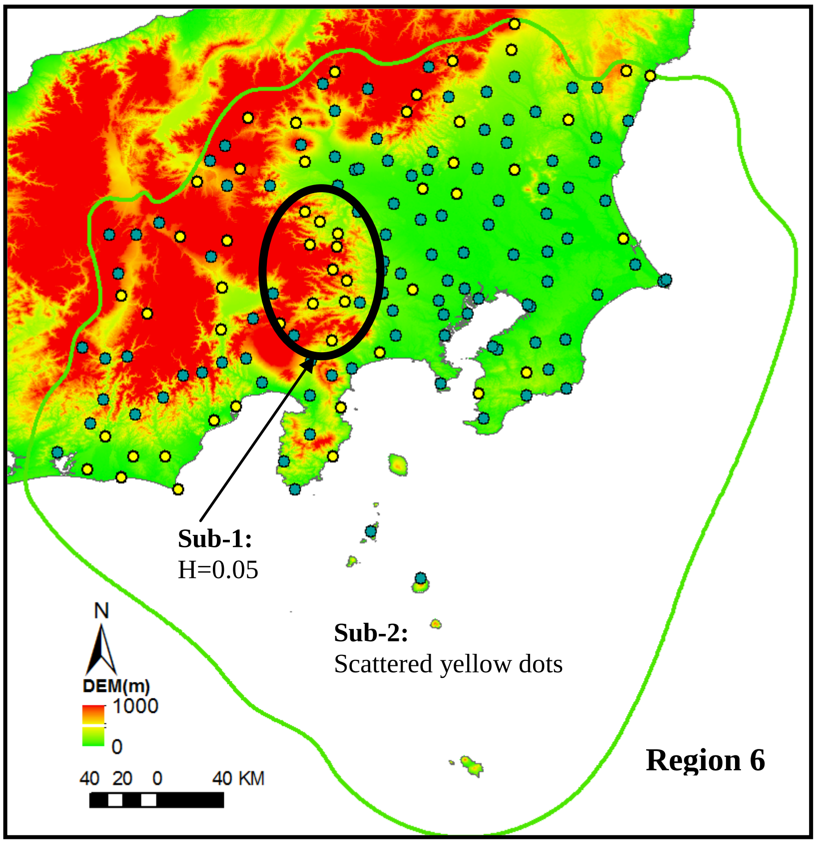

Figure 4-5: High discordances' sites (yellow dots) in Region 6.

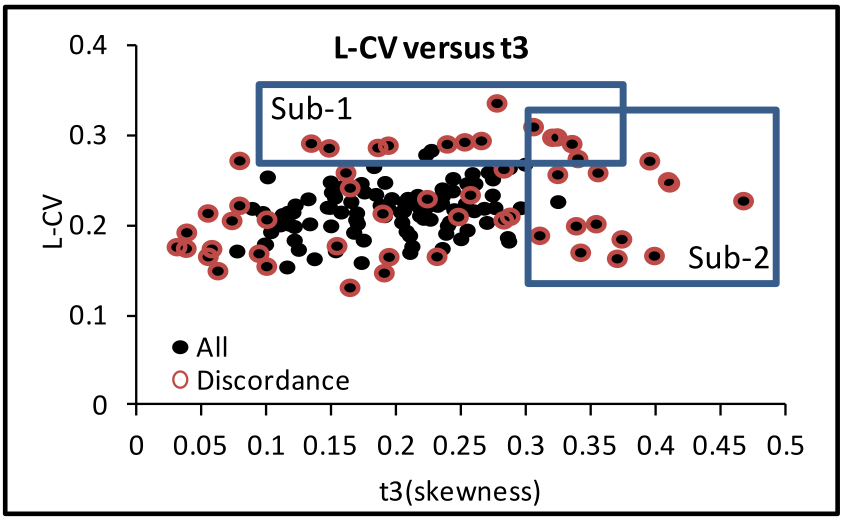

Figure 4-6: *L*-moment ratio's plot for Region 6

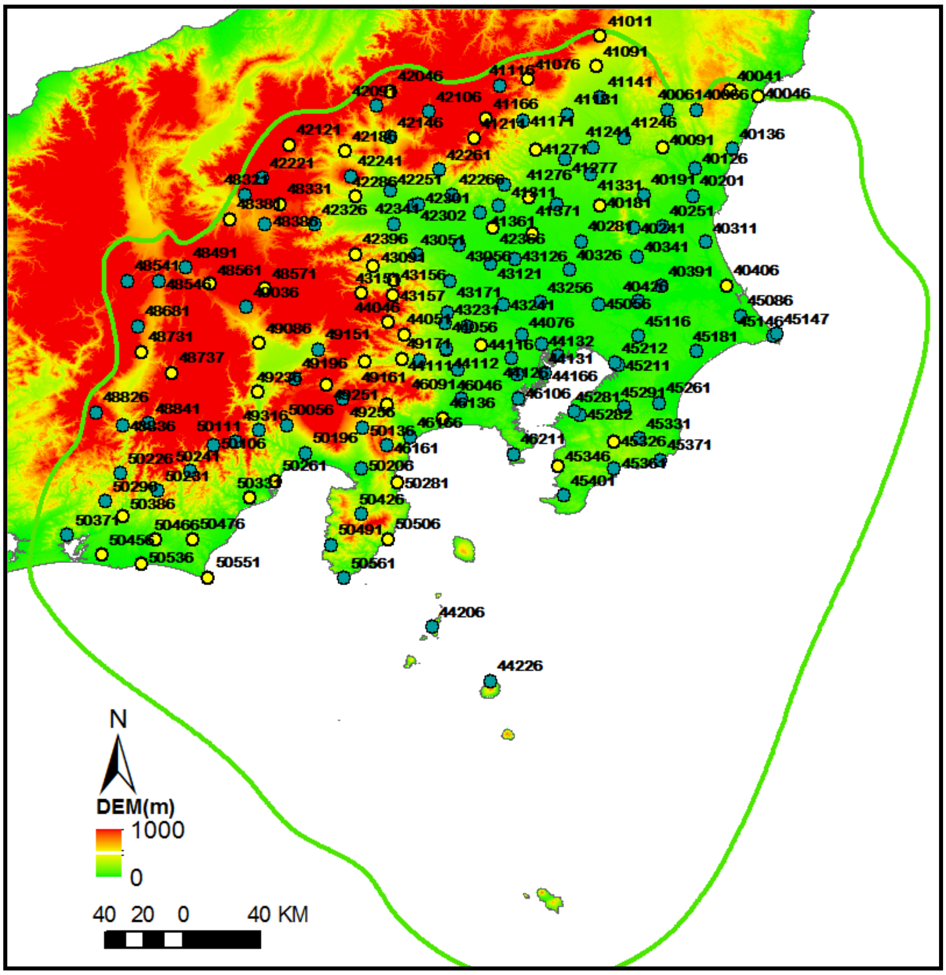

Figure 4-7: Stations within Region 6 (yellow dots are stations with high discordances)

4.5 Fitting the Extreme Outliers

All the stations from the AMeDAS (data from 1976 to 2008) and the surface stations (data from as early as 1896 to 2008) network were used for the testing of the homogeneous regions. The high discordances sites which appear to be discordant with the region as a whole but experienced an extreme but localized meteorological event which are equally likely to affect any of the sites in the future are kept and used for this analysis. Based on the 10 homogeneous regions mentioned in Section 4.1, Region 7 and Region 10 are used as representative examples for comparison between the at-site and regional frequency analysis. The comparison is conducted to assess the improvement of the distribution fitting especially towards the extreme outliers. The fitting of the regional distribution and its quantiles estimations uses the station-years method in which the sample size is equal to the total number of observation years of all the sites within the homogeneous region. Region 7 and Region 10 were chosen because; 1) they have the largest numbers of historical highest recorded 1-day rainfall sites in Japan 2013 according to the national ranking by J.M.A (2014), refer Figure 4-8; 2) both regions have at least one site with significant outliers and; 3) both regions have very good heterogeneity test assessment. All the JMA stations including both long observation data and AMeDAS datasets were used for the distribution fitting and quantiles estimations. Six sites were chosen to represent at-site frequency analysis, with three within Region 7 (Hikone, Kyoto and Miyagawa) and three in Region 10 (Kochi, Yanase, Miyazaki). See Figure 4-9.

The *EASYFIT 5.5 Professional* software was used for the distribution frequency analysis. Figure 4-10 and Figure 4-11 show the quantile-quantile (Q-Q) plot and probability difference plot of several sites in Region 7 and Region 10 respectively. The Q-Q plot is a graph of the quantiles of the empirical values against the quantiles of the frequency analysis model. While, the probability difference plot is the plot of the difference between the empirical cumulative distributions function (CDF) and the theoretical CDF. By considering n as the number of observations and x, the empirical values, the empirical CDF is based on the following equation:

$$F_n(x) = \frac{1}{n}.\left[Number\ of\ observations \leq x\right] \qquad \textbf{Eq. 4-27}$$

From the graphs of Figure 4-10 and Figure 4-11, we can clearly see several significant outliers within the quantiles plots of Hikone (Region 7), Kyoto (Region 7) and Kochi (Region 10). All three sites have long observation data series (at least 108 years). The fitting of the distribution including the outliers need to be assessed in order to obtain a more reliable quantiles estimates. Using data samples based on a station-year method of the homogeneous region the fittings of the outliers are assessed. The at-site samples were also fitted to the GEV model. All of them (at-site sample) have been tested to fit to other type of distributions such as the Log Normal 3 parameter, Log Pearson 3 parameter and the Gumbel, however not much difference were observed between the fittings especially for the samples with the outliers. Since the GEV model was found to fit the homogeneous Region 7 and 10 (Table 4-2), GEV model was used throughout the analysis.

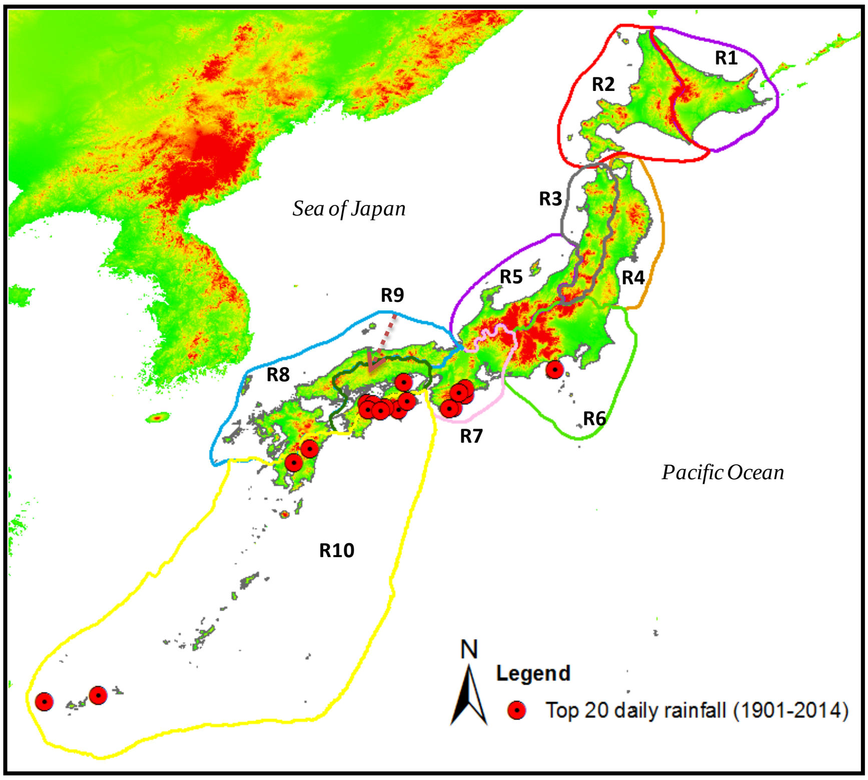

Figure 4-8: Location of top 20 daily rainfalls by Japan Meteorological Agency as in 2014

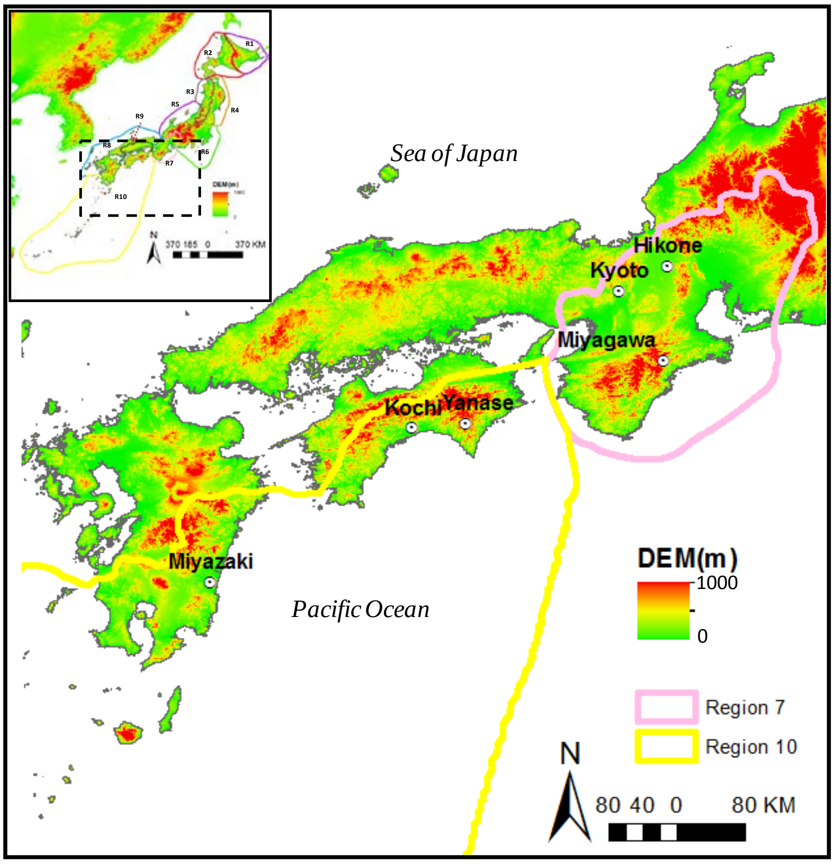

Figure 4-9: Location of selected stations within Region 7 and Region 10

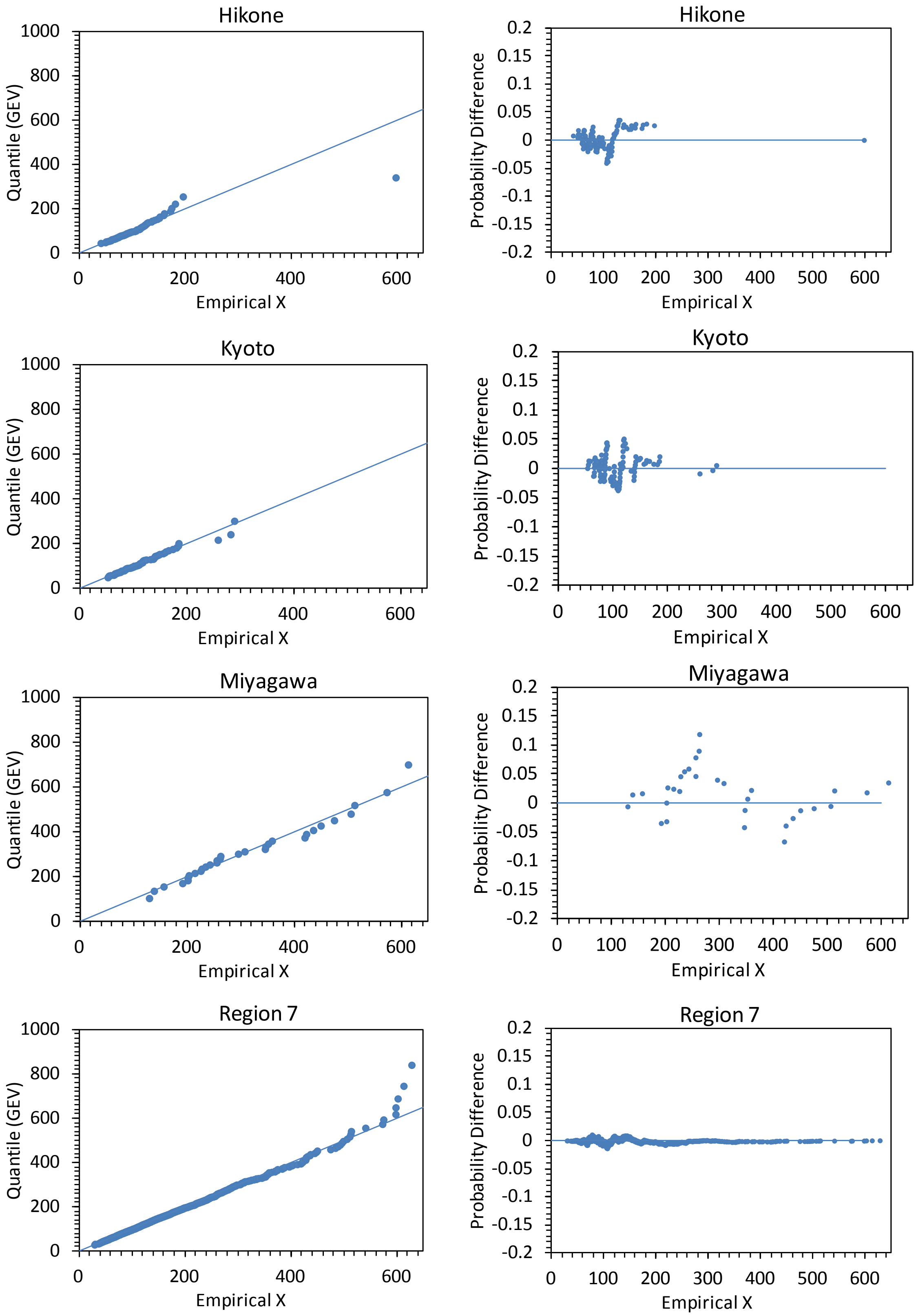

Figure 4-10: Quantile-quantile plots (Q-Q plot) (left side) and its probability difference plot (right side) based on the General Extreme Value (GEV) model of several sites in Region 7 (Hikone, Kyoto and Miyagawa) and all sites within the homogeneous region combined (Region 7). All units in mm.

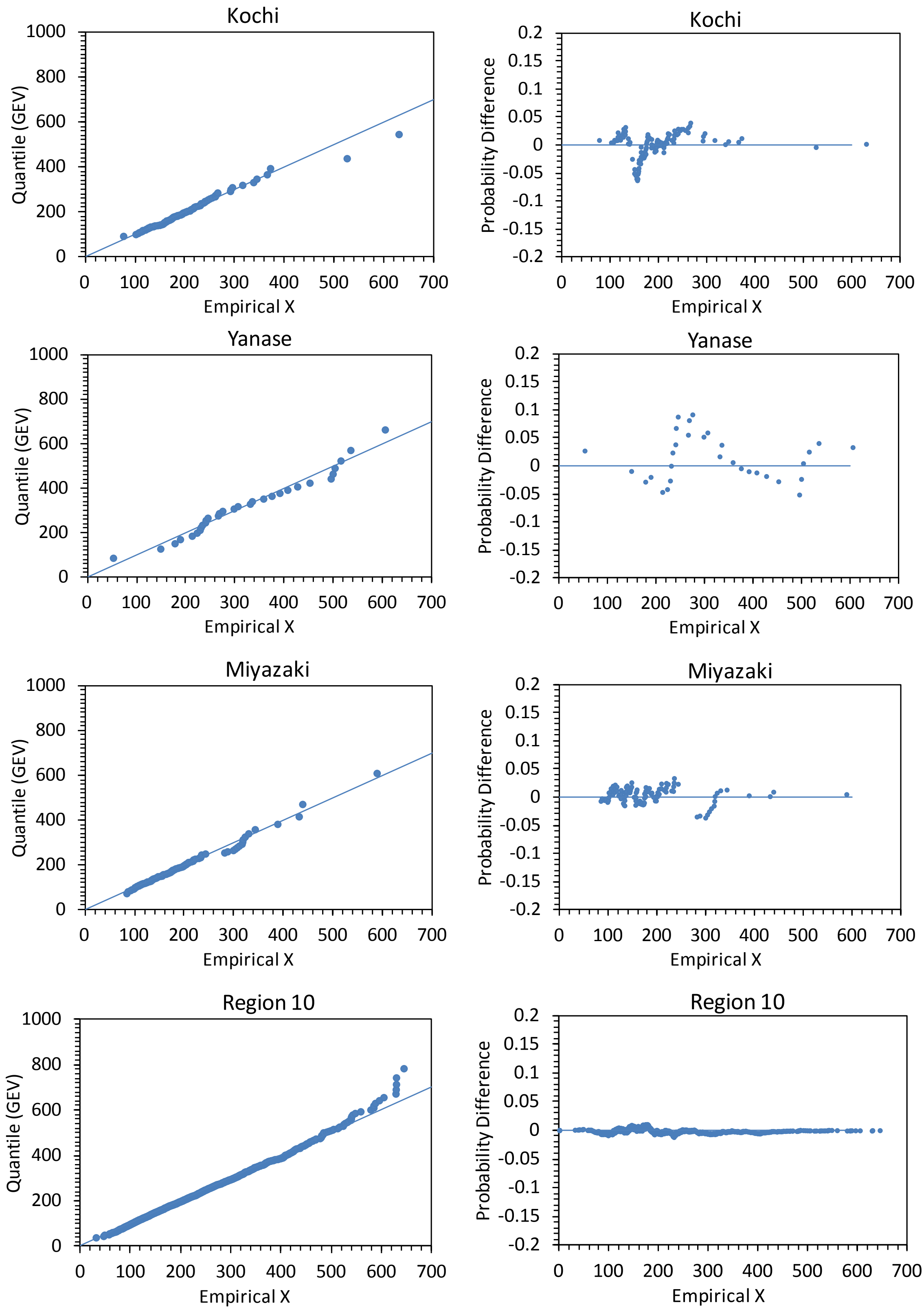

Figure 4-11: Quantile-quantile plots (Q-Q plot) (left side) and its probability difference plot (right side) based on the General Extreme Value (GEV) model of several sites in Region 10 (Kochi, Yanse and Miyazaki) and all sites within the homogeneous region combined (Region 10). All units in mm.

In general, qualitatively we can conclude that the regional distributions illustrate a better fitting for the whole data sample for Region 7 and Region 10 (Q-Q plots of Region 7 in Figure 4-10 and Region 10 in Figure 4-11) compared to their at-site distributions (Q-Q plots of Hikone, Kyoto and Miyagawa for Region 7; Kochi, Yanase and Miyazaki for Region 10). The probability difference plots also provide similar information where the probability differences for Region 7 is between -0.016 to 0.016 which is much less than its at-site probability differences (Hikone 0.04 to -0.04, Kyoto 0.05 to -0.05, and Miyagawa 0.15 to -0.15). The same conclusion could be made for Region 10 where its probability differences are much smaller than its at-site probability differences (Region 10 0.011 to -0.011, Kochi 0.05 to -0.055, Yanase 0.1 to 0.055, and Miyazaki 0.04 to -0.04).

To obtain quantitative evidence of the fittings among the sample datasets (at-site and regional), the goodness of fit test was conducted. Guides by Takara and Stedinger (1994) suggested four types of goodness of fit test suitable for extreme values analyses. They are: 1) SLSC (Standard least square criterion); 2) COR (Correlation of coefficient); 3) MLL (Maximum log-likelihood) and 4) AIC (Akaike information criterion). Since this study focuses on comparison between the at-site and regional fitting instead of determining which frequency analysis model fits the best, only SLSC test was used since it is one of the simplest and comparable with the other method suggested. The smaller the SLSC value is, the better the fitting of the distribution. The results of the SLSC test are presented in Table 4-4. The SLSC test results also prove that the regional datasets has the best fit compared to its at-site frequency distribution. Region 7 has its SLSC value of 0.0124 which is much less than its at-site SLSC value. The same goes to Region 10 which has its SLSC value of 0.0118.

Results presented from Figure 4-10, Figure 4-11 and Table 4-4 have proven that the regional datasets has the best distribution fit. This would highly be the case since the regional datasets have extremely much more sample data compared to the at-site datasets due its number of station-years, 4060 years for Region 7 and 3981 years for Region 10 (refer Table 4-4). The important thing is do the regional distributions provide a better fitting for the outliers and thus providing a more reliable quantiles estimates. This is answered by results presented in Table 4-5 and Table 4-6. Table 4-5 and Table 4-6 present the reduction of the probability differences by the regional distribution against the at-site distribution for the maximum recorded rainfall event (representing the outliers) and for a 30-year-rain (Hikone, Kyoto, Kochi, Miyazaki) or a 10-year-rain (Miyagawa, Yanase) event. With $PDiff_{Regional}$ as the probability difference based on the regional approach and $PDiff_{at-site}$ as the probability difference based on the at-site approach, the reductions are shown in term of percentages using the following equation

$$\%\,Reduction = \left|PDiff_{Regional} - PDiff_{at-site}\right| / PDiff_{at-site} \qquad \textbf{Eq. 4-28}$$

All the probability differences of the outliers were reduced quite significantly by adopting the regional frequency analysis. More than 30% of reductions are obtained for the outliers (Hikone 30.24%, Kyoto 78.03%, and Kochi 58.23%), and almost all of the probability differences of the 30-year or 10-year rainfall events have a reduction around 90%: Hikone's 30-year-rain, 91.92%; Kyoto's 30-year-rain, 95.15%; Miyagawa's 10-year-rain, 99.40%; Kochi's 30-year-rain, 90.51%; Yanase's 10-year-rain, 80.72% and; Miyazaki's 30-year-rain, 42.93% . While, the probability differences reductions for the highest recorded event of each station are: Hikone (596.9 mm rain event), 30.24%; Kyoto (288.6 mm rain event), 78.03%; Miyagawa (612.0 mm rain event), 97.29%; Kochi (628.5 mm rain event), 58.23%; Yanase (604.0 mm rain event), 96.80% and Miyazaki (587.2 mm rain event), 66.21%.

The quantiles produced by both regional and at-site frequency analysis are presented in Table 4-4. Since the distribution fit of the regional approach and the at-site approach has been assessed and the fitting of the extreme outliers were improved for the regional probability distribution, the quantiles estimated by the regional frequency analysis model (Region 7 and Region 10) are considered to be more accurate and reliable. However, there are some stations such as Miyagawa and Yanase have their quantiles reduced. It can be questioned whether these stations are reasonable to be put within the same homogeneous regions as Hikone and Kyoto for Region 7, and Kochi and Miyazaki in Region 10. As been proven in the discordancy test and heterogeneity test using data from 1976 to 2008 from all stations, both Miyagawa and Yanase are not high discordancy sites. It is also acknowledged that another method to improve the regional quantile estimation can be conducted using the indexed flood procedure by Hosking and Wallis (1997). The procedure considers a weighted estimation of the quantiles by taking consideration of the L-location of each site.

In order to highlight the important of regional frequency analysis to improve quantile fittings of extreme outliers, the station-year approach was implemented. Three stations with extreme outliers are focused on (Hikone, Kyoto and Kochi), the return period for Hikone extreme rainfall outlier of 596.9 mm was reduced from a 2000-year rain to a 500-year-rain. Similar goes to the outlier of Kyoto (288.6 mm), where its rainfall period was reduced from a 100-year-rain to a 30-year-rain. However not much difference was observed for Kochi case where its outlier remains within the 500-year-rain.

We could conclude that from the assessments, regional frequency analysis can be used to improve the methodology for extreme rainfall frequency distribution especially in fitting extreme outliers. However, detail analysis can be conducted using other suitable homogeneous regions. Better identification of the extreme-rainfall homogeneous regions could provide higher assurance in estimating the quantiles of the regional frequency analysis models. This study also highlights the benefits of using regional frequency analysis for region with long historical data, not just for regions with limited data availability and number of gauged-sites locations.

Table 4-4: Quantiles of regional against at-site analysis

(a) Region 7

Datasets (station-years)	**SLSC**	**Quantiles (mm)**					
		30-yr	**50-yr**	**100-yr**	**500-yr**	**1000-yr**	**2000-yr**
Hikone (*115*)	0.1174	199	228	275	419	501	599
Kyoto (*108*)	0.0313	201	224	259	355	405	460
Miyagawa (*31*)	0.0291	619	676	754	936	1016	1096
Region 7 (*4060*)	0.0124	274	315	378	564	666	785

(b) Region 10

Datasets (station-years)	**SLSC**	**Quantiles (mm)**				
		50-yr	**100-yr**	**500-yr**	**1000-yr**	**2000-yr**
Kochi (*108*)	0.0382	407	469	642	730	829
Yanase (*31*)	0.0397	647	701	812	855	895
Miyazaki (*108*)	0.0193	432	511	738	859	998
Region 10 (*3981*)	0.0118	428	490	650	727	809

Table 4-5: Reduction of the probability differences (model versus empirical) of Region 7

(a) Hikone

Datasets (station-years)	SLSC	Probability Difference (*PDiff*)	
		Max. recorded: 596.9 mm	**30-year: 195.8 mm**
Hikone (*115*)	0.1174	0.000506	0.026581
Region 7 (*4060*)	0.0124	0.000353	0.002148
Reduction %		30.24 %	91.92 %

(b) Kyoto

Datasets (station-years)	SLSC	Probability Difference (*PDiff*)	
		Max. recorded: 288.6 mm	**30-year: 184.5 mm**
Kyoto (*108*)	0.0313	0.005816	0.020906
Region 7 (*4060*)	0.0124	0.001278	0.001014
Reduction %		78.03 %	95.15 %

(c) Miyagawa

Datasets (station-years)	SLSC	Probability Difference (*PDiff*)	
		Max. recorded: 612.0 mm≈(30-yr)	**10-year: 495.0 mm**
Miyagawa (*31*)	0.0291	0.035555	0.0050623
Region 7 (*4060*)	0.0124	0.000965	0.00003
Reduction %		97.29 %	99.40 %

Table 4-6: Reduction of the probability differences (model versus empirical) of Region 10

(a) Kochi

Datasets (station-years)	SLSC	Probability Difference (*PDiff*)	
		Max. recorded: 628.5 mm	**30-year: 343.5 mm**
Kochi (*108*)	0.0382	0.002229	0.00692
Region 10 (*3981*)	0.0118	0.000931	0.000657
Reduction %		58.23 %	90.51 %

(b) Yanase

Datasets (station-years)	SLSC	Probability Difference (*PDiff*)	
		Max. recorded : 604.0 mm ≈(50-yr)	**10-year: 502.0 mm**
Yanase (*31*)	0.0397	0.033605	0.004948
Region 10 (*3981*)	0.0118	0.001076	0.000954
Reduction %		96.80 %	80.72 %

(c) Miyazaki

Datasets (station-years)	**SLSC**	**Probability Difference (*PDiff*)**	
		Max. recorded: 587.2 mm	**30-year: 387.3 mm**
Miyazaki (*108*)	0.0193	0.003329	0.003329
Region 10 (*3981*)	0.0118	0.001125	0.001900
Reduction %		66.21 %	42.93 %

Chapter 5 Probable maximum precipitation

5.1 Background

In 1959, the American Meteorological Society defined probable maximum precipitation (PMP) as “the theoretically greatest depth of precipitation for a given duration that is physically possible over a particular drainage area at a certain time of year” (American Meteorological Society, 1959). However the current definition by the World Meteorological Organization is "the theoretical maximum precipitation for a given duration under modern meteorological conditions. Such a precipitation is likely to happen over a design watershed, or a storm area of a given size, at a certain time of year" (WMO, 2009). There are two main techniques to estimate the PMP. They are the statistical approach and the hydro-meteorological approach. The statistical technique uses statistical procedures based on rainfall distributions while the hydro-meteorological technique uses procedures based on comprehensive meteorological analysis. In summary, the statistical technique is suggested to be used for quick estimation or preliminary estimates and many national meteorological services utilize these results only in reconnaissance or feasibility studies. It is important to be aware that the statistical technique assumes that the PMP has been observed at the stations (that provided the envelopment of an abstracted statistic K_m value) used for the analysis. It is also considered to be not as reliable compared to the hydro-meteorological approach especially for regions with short rainfall records (WMO, 2009). Even so, the statistical approach is still being used widely by practitioners around the world especially for areas with limited meteorological data. Some studies have stated that the results of PMP using both the statistical technique and physical technique show very similar and comparable PMP estimates (Casas et al., 2011; Deshpande et al., 2008). Japan has very long observation data dating from 1890's, thus it is a good opportunity to test the PMP estimates using both techniques based on the Japanese data.

5.2 **The Hershfield Statistical Method**

The statistical methpd was adopted from Hershfield (1965). According to the manual of probable maximum precipitation by the World Meteorological Organization (WMO), the method is basically a frequency analysis method and the essence of the method is storm transposition. It is different from the traditional frequency analysis in two important aspects. First it focuses on a wide region, rather than a single station or single watershed, in order to seek a storm that approximates the physical upper limit of precipitation (the maximum observed rainfall). Second, this method involves the application of the process enveloping and transposition.

The envelopment of an abstracted statistic K_m is conducted instead of the specific rainfall amount of one storm. The transposition is achieved by looking up the value of the transposed K_m (envelop) of the design station's mean annual maximum rainfall, $\bar{X}_n$ using a curve such as in Figure 5-1 (WMO, 2009). Based on the transposed K_m, the PMP is calculated. More information on the calculations for the abstracted statistic K_m is explained later. An important assumption should be realized upon using the Hershfield statistical method. The method assumes that the PMP has been observed at the station that provided the envelopment of the K_m values.

The manual did not stated clearly how the envelopment should be conducted. An example was presented of the smooth envelopment of around 2700 stations (90% located in the Unites State) by Hershfield (1965). See Figure 5-1. There are various ways of enveloping conducted by researchers before. Some uses the maximum value of K_m within the study area (usually one watershed basin) for the transposition (Casas et al., 2011; Desa M et al., 2001; Desa M and Rakhecha, 2007). This is recognized as 1-point envelopment throughout this thesis. At first, 1-point envelopment was conducted by Hershfield (1961) which uses the greatest value of K_m based on records of 24-hour rainfall for some 2700 stations for the storm transposition. After modification by Hershfield (1965), values of K_m for other rainfall durations were later determined together with its variation with $\bar{X}_n$ producing a monograph as in Figure 5-1. The curves in Figure 5-1 was then used to obtain the K_m values needed for the PMP calculations relative to the design stations mean annual maximum rainfall. They are initially produced to represent extreme rainfall for the whole world, however it was found not suitable for some regions. Thus, it was recommended for further studies to be done to obtain more reliable values of K_m particularly using data obtained from the target regions itself. This kind of envelopment technique is recognized as a 2-point or multiple point envelopment throughout this thesis. It was used by various researchers such as Deshpande et al. (2008); Rakhecha and Soman (1994); Sherif et al. (2013); NAHRIM (2007); Nobilis et al. (1991).

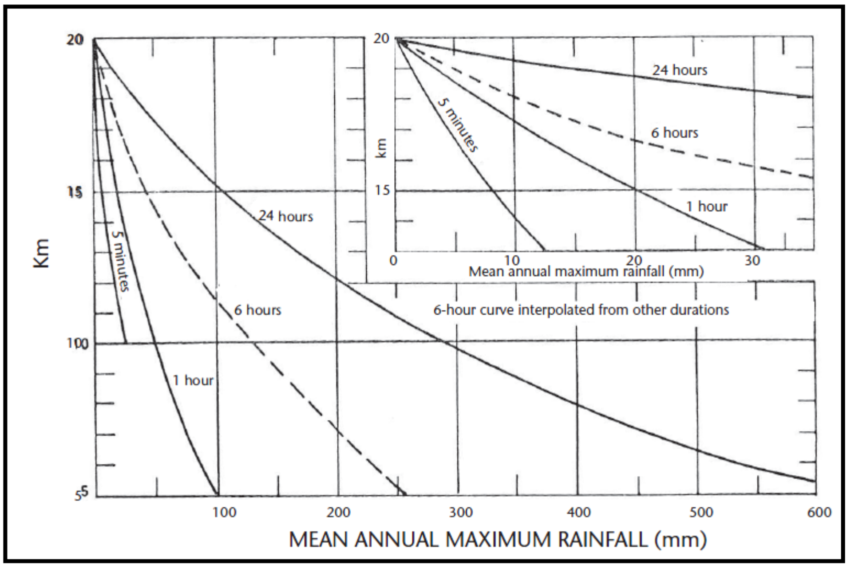

Figure 5-1: Envelopment by Hershfield (1965), (WMO, 2009)

5.2.1 *Basic Theories*

The procedure as developed by Hershfield (1961, 1965) is based on the general frequency equation by Chow (1951) in the form of

$$X_T = \overline{X}_n + KS_n \qquad \textbf{Eq. 5-1}$$

Where X_T is the rainfall for return period T, $\overline{X}_n$ and S_n are respectively, the mean and standard deviation of a series of n annual maxima, and K is a common statistical variable, which varies with the different frequency distributions fitting extreme value hydrological data. See Figure 5-2. If the maximum observed rainfall X_m is substituted for X_T, and K_m for K, K_m is then the number of standard deviations to be added to obtain X_m, or

$$X_m = \overline{X}_n + K_m S_n \qquad \textbf{Eq. 5-2}$$

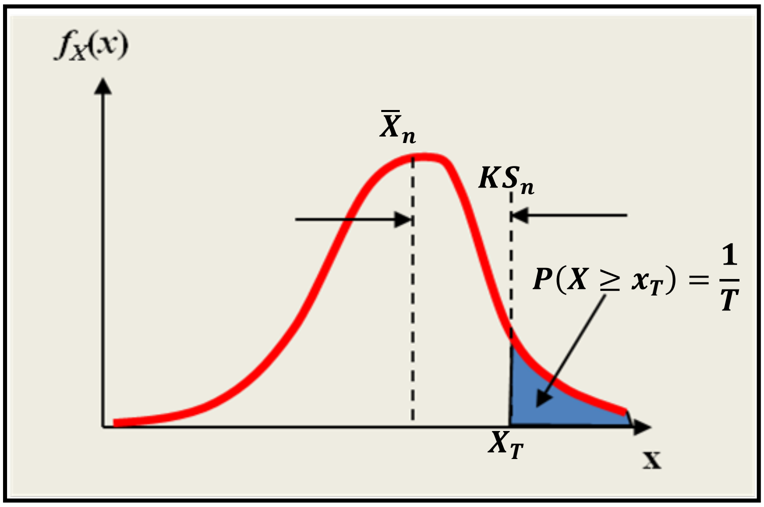

Figure 5-2: Sketch describing the general frequency equation by Chow (1951)

5.2.2 *Method's Procedure*

The Hershfield technique for estimating the PMP value for a station uses the following equations.

$$X_{PMP} = \bar{X}_n + S_n \times K_m \qquad \textbf{Eq. 5-3}$$

$$K_m = \frac{X_{max} - \bar{X}_{n-1}}{S_{n-1}} \qquad \textbf{Eq. 5-4}$$

where, X_{PMP} is the PMP estimates for a station, $\bar{X}_n$ is the mean of the annual extreme series, S_n is the standard deviation of the annual extreme series, K_m is the frequency factor which depends on the availability of data period, X_{max} is the highest rainfall value at the station, $\bar{X}_{n-1}$ is the mean of the annual extreme series without the largest value, and S_{n-1} is the standard deviation of the annual extreme series without the largest value.

First, the parameters X_n, S_n and K_m are calculated. Then, K_m values for all stations are plotted against the X_n values respectively and an envelope curve is drawn. The new K_m value is picked up from the envelope line for each station's $\overline{X}_n$. Finally, the PMP values for each station are calculated using Eq. 5-3 by replacing K_m with the new transposed value.

Adjustment factors are recommended in the manual for series with outliers (extreme rainfall of rare magnitude, e.g. 500-year rainfall which occurred during a much shorter period such as 30 years) and for samples with record length less than 50 years. These adjustment factors are excluded from the analysis since the Japanese data has long record lengths (30 to 100 years). Even for a 30 year record length the adjustment factor for the mean and standard deviation is less than 5%. See Figure 5-3. Adjustments for fixed observational time intervals are also available. However this too is excluded since the factor suggested effects only a maximum of 13% of the PMP estimates only. For example if a PMP estimated is 1000 mm. Thus by applying the highest factor recommended the adjusted PMP estimates is only 1130 mm.

A summary on the procedures for the PMP estimates using Hershfield statistical method is illustrated in Figure 5-5.

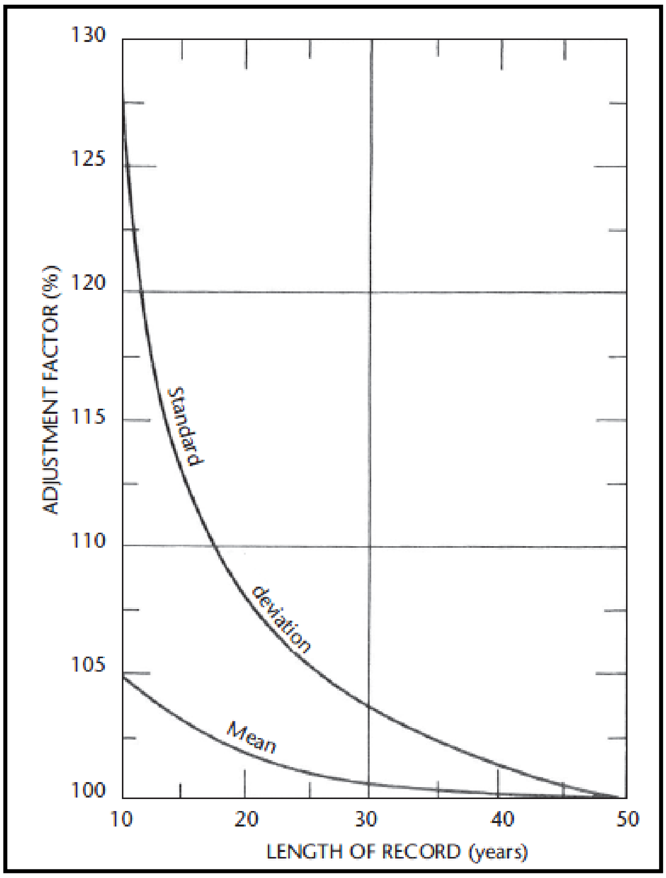

Figure 5-3: Adjustment of mean and standard deviation of annual series for length of record (Hershfield, 1961).

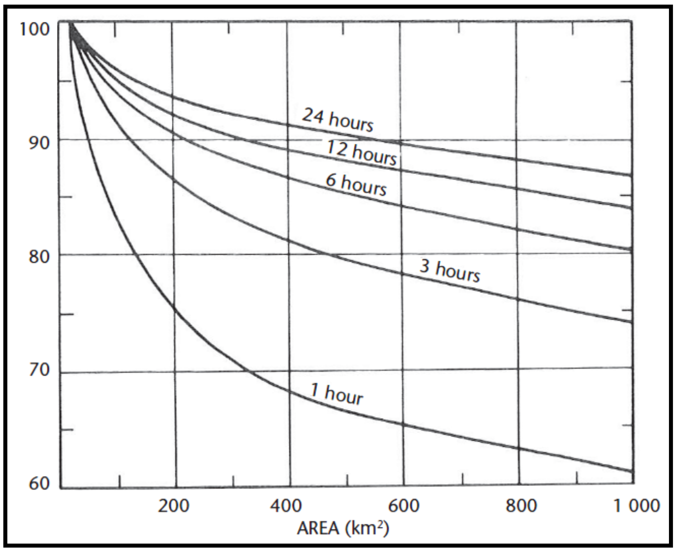

Figure 5-4: An example of an area reduction curve (WMO, 2009).

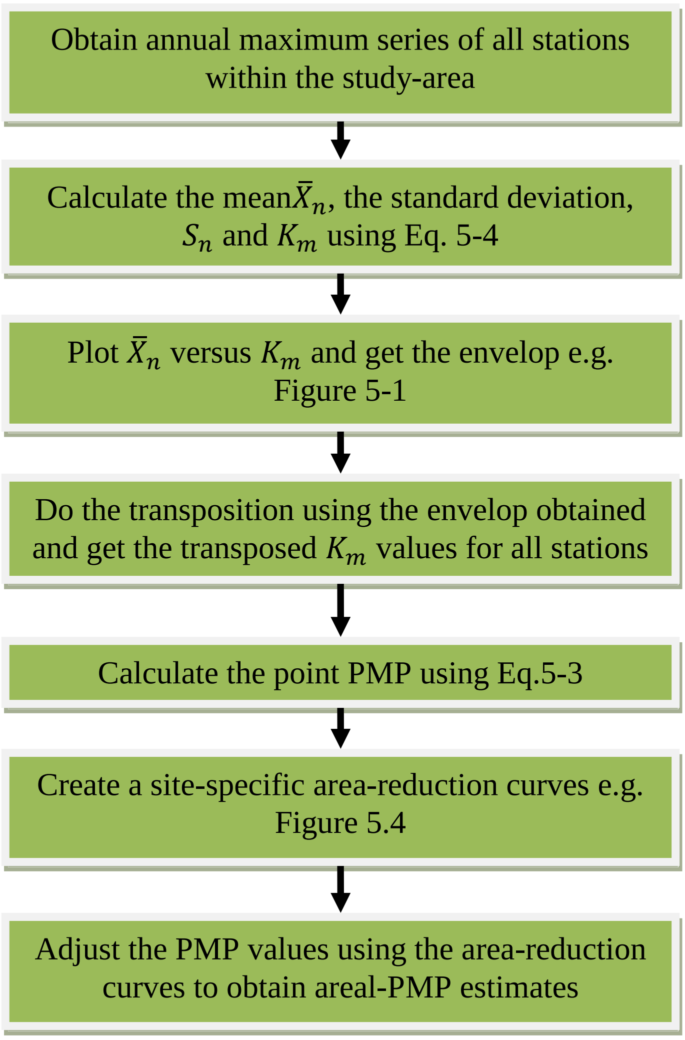

Figure 5-5: Hershfield statistical procedure as recommended by WMO (2009).

5.2.3 *FORTRAN program - HERSHPMP.FOR*

Two input files are required for the program. One is the .TXT file containing the list of stations needed for the PMP study region. Second, is the .TXT file of each station containing the rainfall data. The format of the .TXT files are presented in appendices A-1 and A-2. The main framework for HERSHPMP.FOR is presented in Figure 5-7. The PMPs estimated using HERSHPMP.FOR is based on the theories and equations presented in Section 5.2.

In summary, the HERSHPMP.FOR program reads the data from the data files, calculate the 2-day, 3-day, 5-day and 7 day rainfall automatically and extract the annual maximum series for all the rainfall periods. Similar algorithm is used for the ANNMAX.FOR explained in the previous section, Section 2.3. The annual maximum series are then written into the OUTPUT.TXT file. This is done so that the user could check the quality of the annual maximum series and see if any suspicious or extreme annual maximum value contains in the series. The program then calculates the Hershfield parameters which are the $\overline{X}_n$, S_n, X_{max}, $\bar{X}_{n-1}$, S_{n-1}, and K_m of all the stations. Again the parameters will be written into the OUTPUT.TXT file for optional data checking and handling. The program then determine the envelope line (EL) by identifying the maximum points of K_m and $\overline{X}_n$. Using the two sets of values a linear equation (based on Reg_M and Reg_C) representing the envelope line is formed. The K_m of each station is then transposed using the EL equation corresponding to its $\overline{X}_n$. The statistical PMP estimates of all the stations are then calculated using Eq. 5-3 by using the transposed K_m values. Finally the PMP estimates are written to the OUTPUT.TXT file.

The limitation of HERSHPMP.FOR is that it uses a linear relationship for the envelope instead of a smooth curve or a multiple regression line. This is due to the complexity of the FORTRAN code involved if a multiple regression line equation would be used. However, further version of HERSHPMP.FOR could be constructed to cater this limitation. As for the current study the PMP analysis conducted (Japanese extreme rainfall case) by using the linear equation is appropriate for the envelope. However, it is advisable to plot the K_m versus $\overline{X}_n$ and observe whether appropriate envelope line was formed. If the envelope provided by the program is not suitable, custom envelope line was constructed using EXCEL spreadsheets. Figure 5-6 (a) and (b) show example of the envelope lines with the red continues line representing the envelope produced by the program and the green dashed line representing a custom envelope. The custom envelope line was constructed using an EXCEL built-in linear trend line function. Figure 5-6 (a) is an example of a not-so-suitable envelope line produced by the HERSHPMP.FOR program, thus a custom line was used as the EL for the PMP estimation. While, Figure 5-6 (b) shows an example of a good envelope line produced by the program. Figure 5-7 shows the example of the framework of the HERSHPMP.FOR. Other option for the envelopment is to adopt a one-point envelope where the highest K_m value is used for the PMP calculation. Depends on the plots of the K_m versus $\overline{X}_n$, sometimes it is better to use the one-point envelopment.

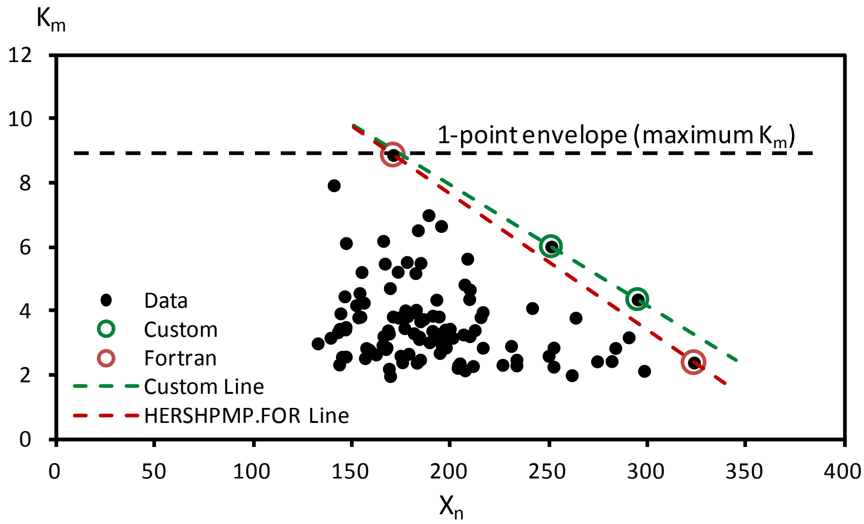

(a)

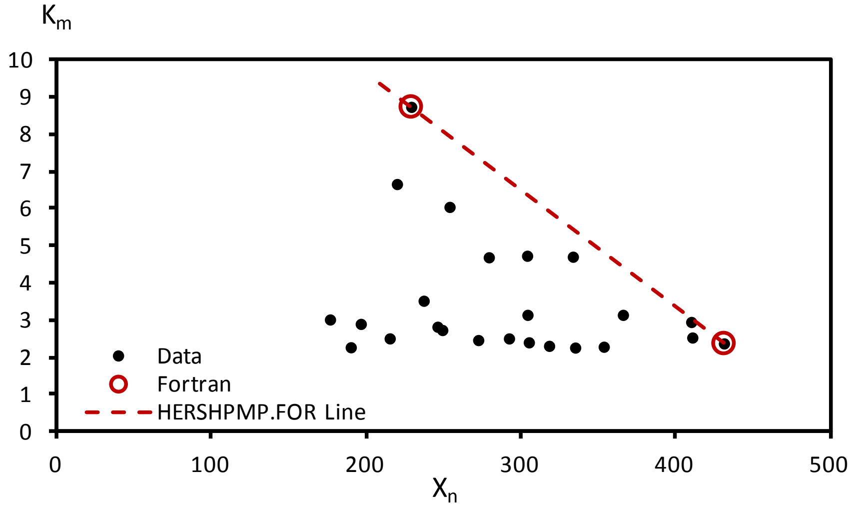

(b)

Figure 5-6: K_m versus $\overline{X}_n$ plots and envelope line (EL) constructed by HERSHPMP.FOR (red continues line) and custom line drawn using EXCEL (green dashed line).(a) adjusted envelop line, (b) non-adjusted envelope line.

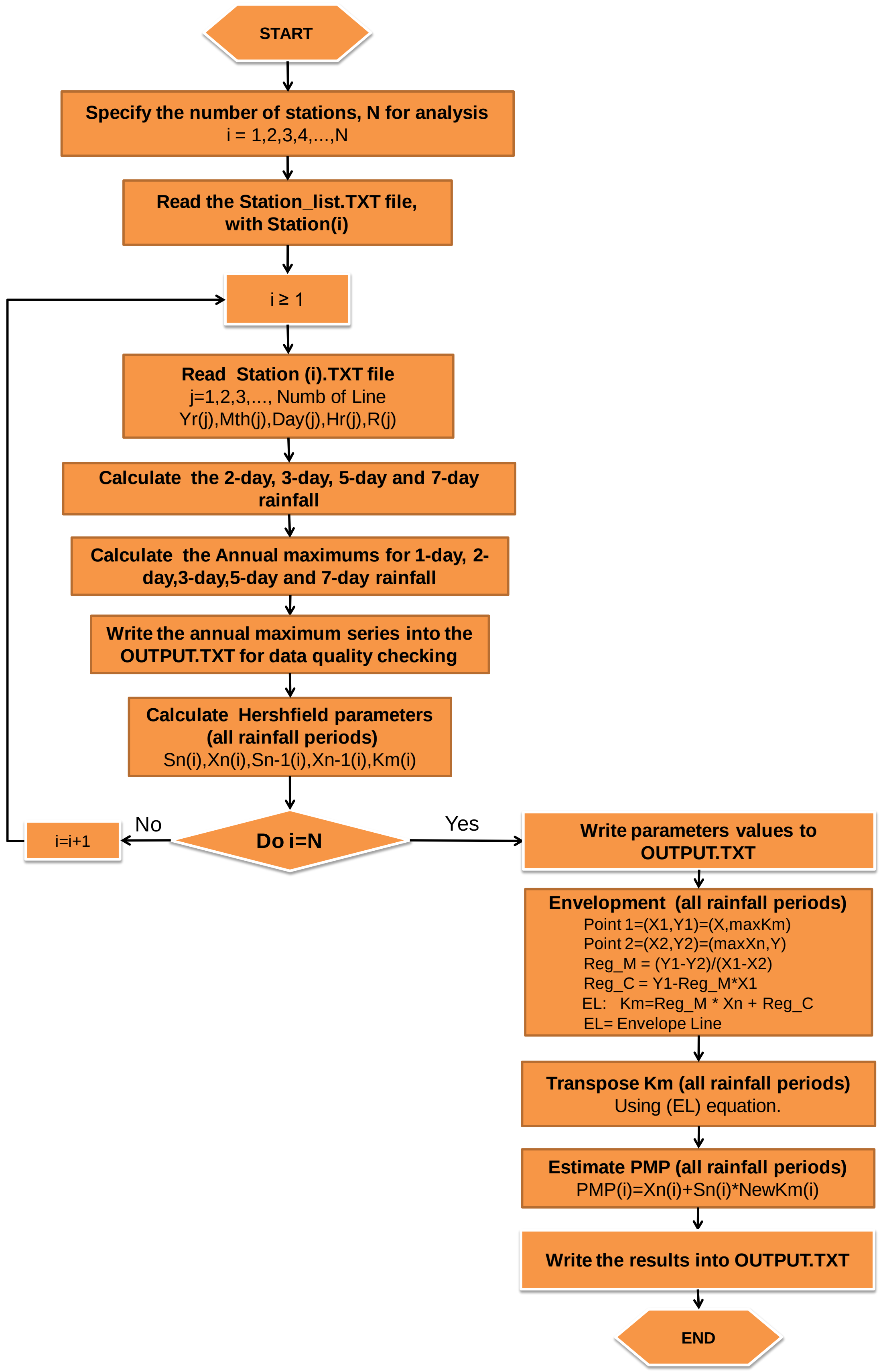

Figure 5-7: HERSHPMP.FOR program framework

5.3 **Case Study - PMP Japan**

Hershfield statistical PMP estimations were conducted for the whole Japan. All the long-observation stations (51 stations from JMA) was used for the 1-day PMP estimation. No transposition boundaries were used, instead all of the data was used for the envelopment. However, according to the manual (WMO, 2009) this would not be appropriate for the statistical estimation since it involves a very large area (about 400 000 km^2). However, for preliminary assessment the statistical PMP estimates for the whole Japan were conducted.

5.3.1 *Envelope for the Statistical PMP Estimates*

Figure 5-8 and Figure 5-9 show the envelope drawn for the statistical PMP estimation method for daily- and hourly-rainfall respectively. The calculations of the Hershfield parameters are conducted using the HERSHPMP.FOR program. Some of the slope of the envelope lines could be seen to vary for different rainfall periods. For the daily-rainfall, the envelope line for the 7-day rainfall is slightly much steeper than for the 1-, 2-, 3-, and 5-day rainfalls' (Figure 5-8). While, for the hourly-rainfall the slope of the envelope line of the 1-, and 2-hour rainfall are much more gentle than the 3-, 4-, and 6-hour rainfall. This could indicate non-uniformity of the rainfall distribution between the stations used for the PMP estimation. The K_m and $\overline{X}_n$ values represents a frequency distribution based on a general frequency equation by Chow (1951) as explained in Section 5.2.1. Thus, if the annual maximum rainfall series of the stations used have a significantly different type of frequency distribution between each other and the extreme rainfalls are influenced by different meteorological phenomena (local storm, typhoon, snow storm during winter, etc.) it will influenced the envelopment process. This effects the PMP estimation significantly.

It can be seen clearly in Figure 5-10, where the maximum Hershfield PMP estimates are seen to be not uniformly increased as the rainfall period increases. It is also shown in Figure 5-11 and Figure 5-12. By referring to Figure 4-8, the top 20 extreme rainfall event in Japan is located at areas with the least difference between its maximum recorded rainfall values and the PMP estimates of Figure 5-11 and Figure 5-12 . Instead, others have very high percentage differences. This shows the non-uniformity of the K_m values being transposed, thus producing a questionable PMP estimates. Therefore, it would be much more appropriate to consider a more focused region such as a river basin area or some administrative regions as recommended by the PMP manual by WMO (2009). Another way is to use a homogeneous region which are tested and discussed in the next section.

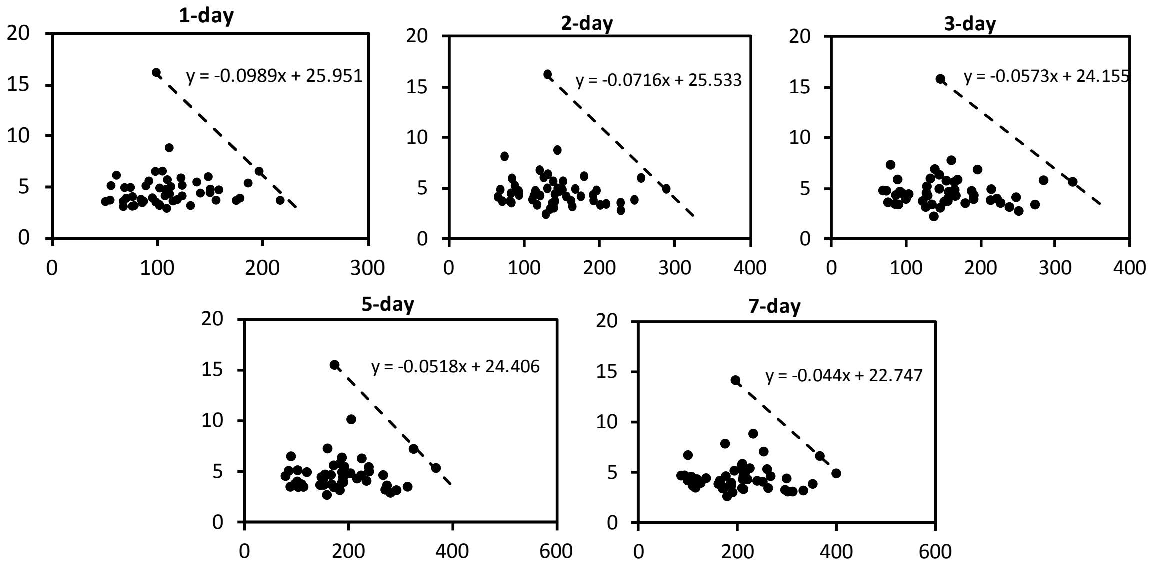

Figure 5-8: K_m versus $\overline{X}_n$ plots and envelope line for the Hershfield PMP statistical estimations for daily rainfall.

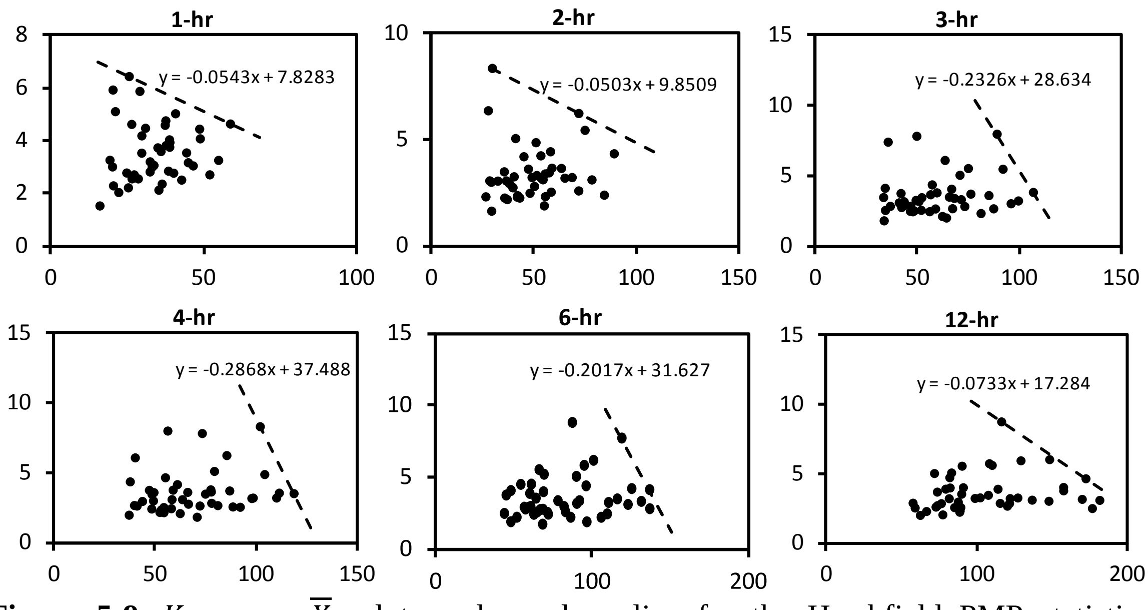

Figure 5-9: K_m versus $\overline{X}_n$ plots and envelope line for the Hershfield PMP statistical estimations for hourly rainfall.

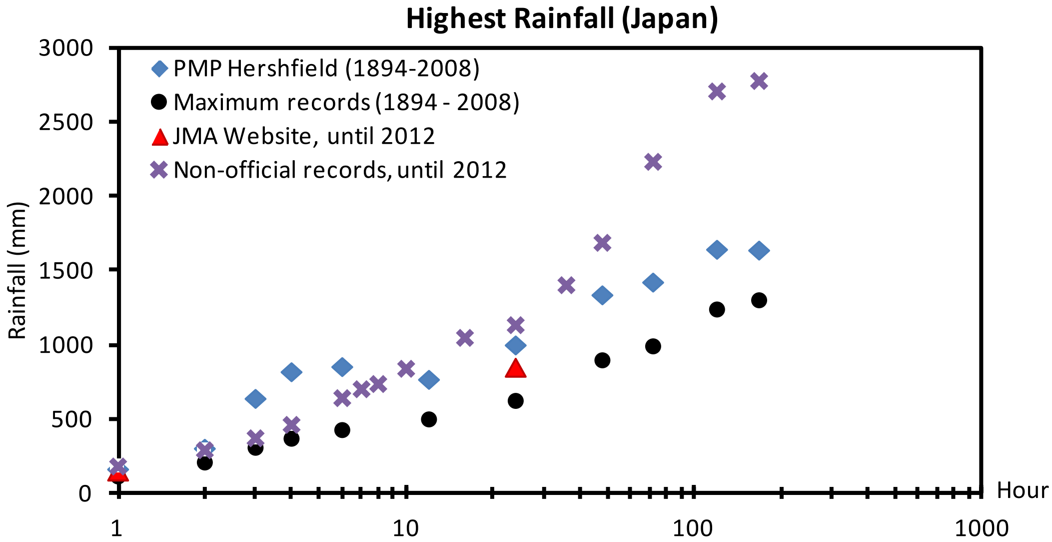

Figure 5-10: Highest recorded rainfalls in Japan and the statistical PMP estimates

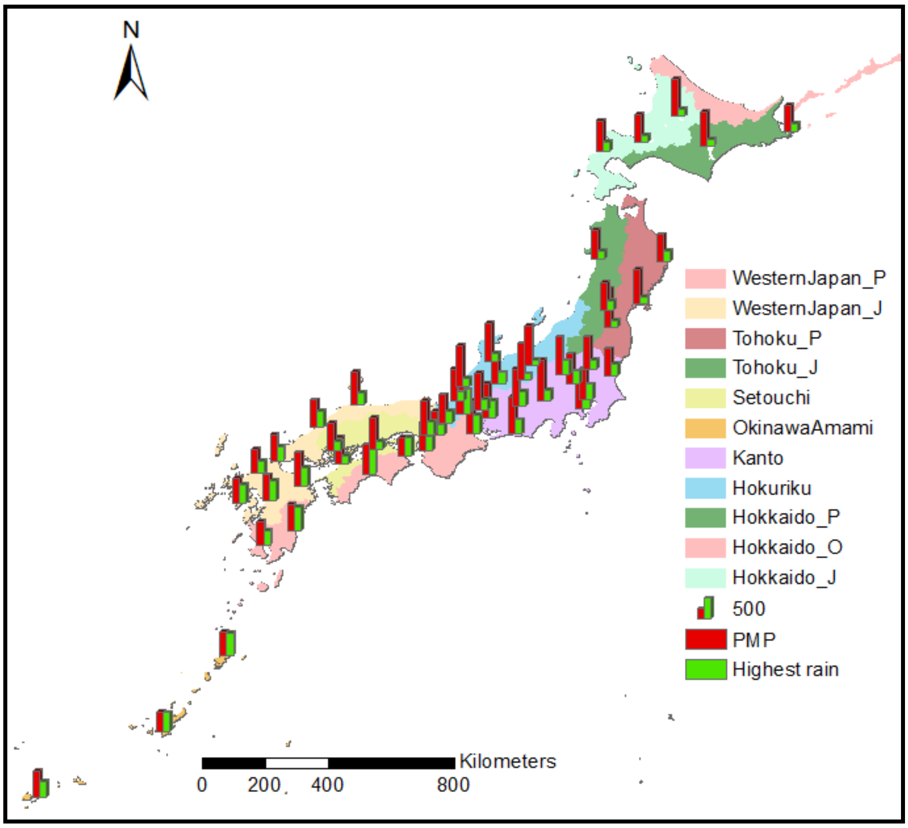

Figure 5-11: Distribution of the point PMP and highest rainfall observed for whole Japan based on long observation data (1886 to 2008)

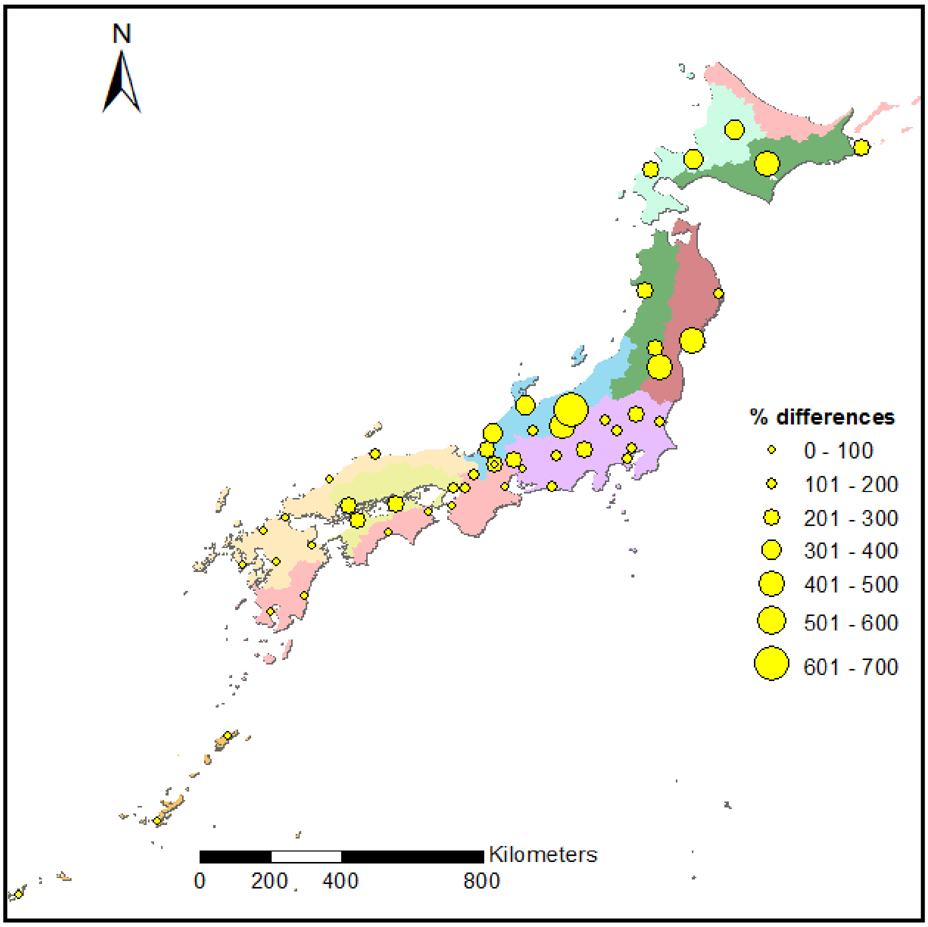

Figure 5-12: Distribution of the percentage difference between the point PMP and highest rainfall observed for whole Japan based on long observation data (1886 to 2008)

Chapter 6 Statistical PMP Estimates Based on the Homogeneous Regions

6.1 Introduction

As mentioned in Section 5.2, statistical PMP estimates are calculated based on the general frequency equation by (Chow, 1951). K_m value representing the maximum storm of one station is calculated using the general frequency equation. The envelope of the K_m versus $\overline{X}_n$ values of all the stations within the study area is then used for the transposition process. Finally, the maximum rainfall or PMP are calculated using the transposed K_m value using Eq. 5-3. The transposition areas or boundary of the stations selected are usually based on the river basin's boundary or particular administrative regions (Desa M et al., 2001; Desa M and Rakhecha, 2007; Rakhecha and Soman, 1994; WMO, 2009). Possibility of a higher observed rainfall outside the basin or administrative regions being over looked could occur. Thus, this study proposes to consider extreme-rainfall homogeneous regions (obtained by regional frequency analysis) into the statistical PMP estimation method. Since the statistic K_m obtained using general frequency equations are based on a frequency distribution (Figure 5-2), it is suitable to consider regional frequency analysis as part of the statistical PMP method.

For this particular test, only the daily rainfalls are used to test the new methodology. Based on the 10 homogeneous regions proposed in Chapter 4, two regions were chosen for the statistical PMP estimates considering homogeneous regions. Region 7 and Region 10 are chosen since both regions have the largest numbers of historical highest recorded 1-day rainfall sites in Japan by the 2013 national ranking of JMA. See Figure 6-1 and Table 6-1.

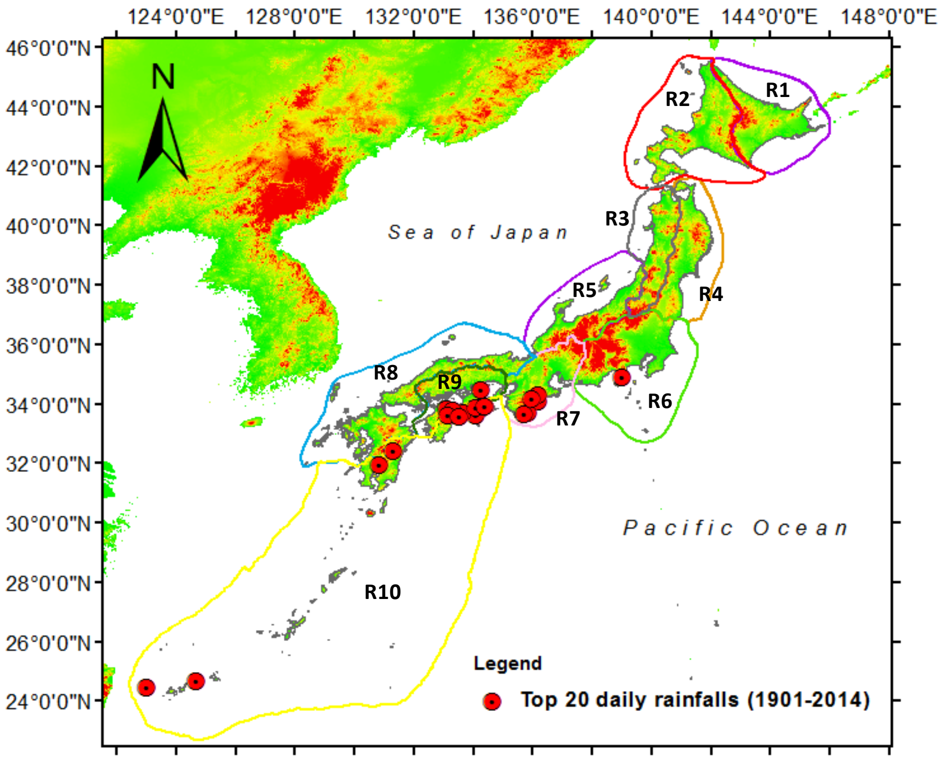

Figure 6-1: Location of the historical highest 1-day rainfall in Japan by JMA (2013) and the extreme homogeneous regions.

Table 6-1: Historical top 20 highest 1-day rainfalls in Japan by JMA (2013)

Observation point	Lat.	Long.	Rainfall (mm)	Date	Region
Yanase	33.615	134.108	851.5	19/07/2011	R10
Hidegadake	34.185	136.108	844	01/08/1982	R7
Owase	34.070	136.193	806	26/09/1968	R7
Uchinomi	34.472	134.275	790	11/09/1976	R9
Yonagunijima	24.467	123.010	765	13/09/2008	R10
Miyagawa	34.278	136.207	764	19/07/2011	R7
Jojusha	33.793	133.132	757	06/09/2005	R9
Shigeto	33.678	133.685	735	24/09/1998	R10
Tsurugisan	33.853	134.097	726	11/09/1976	R10
Ebino	31.945	130.840	715	18/07/1996	R10
Hongawa	33.765	133.338	713	06/09/2005	R10
Irokawa	33.675	135.848	672	21/08/2001	R7
Kamikitayama	34.137	136.005	661	03/09/2011	R7
Ikegewa	33.608	133.168	644	06/09/2005	R10
Fukuharaasahi	33.878	134.388	641.5	19/07/2011	R10
Tarama	24.665	124.697	629	28/04/1988	R10
Kochi	33.567	133.548	628.5	24/09/1998	R10
Mikado	32.385	131.332	628	06/09/2005	R10
Amagisan	34.872	139.023	627	17/08/1983	R6
Nishikawa	33.637	135.710	626	03/09/2011	R7

Focusing on Region 7, there are two major river basins. They are the Yodo River Basin and the Kiso River Basin (Figure 6-2). In practice, a PMP study would consider a basin-scale approach, whereby only stations within the basin boundary will be included for the PMP estimation calculations. However a region's homogeneity is not considered for the analysis. Homogeneous regions are regions that are exposed to similar meteorological condition for example in this case, similar exposure towards the same extreme rainfall conditions, thus all the stations with the same homogenous regions has its extreme rainfall distribution in the same frequency analysis model or population group.

As proven and discussed before Section 4.5, by considering the regional datasets the fitting of the extreme outliers and quantiles were able be improved significantly. The goodness of fit tests and the differences between the quantiles estimated by the frequency analysis model and empirical data were reduced significantly (around 90% for standard return period values and around 30% for extreme outliers). Thus, it would be reasonable to consider all the stations within the homogeneous regions for the statistical PMP estimation in order to avoid missing the sites with the highest maximum rainfall. Sites containing the highest rainfall amount usually has it's K_m versus $\overline{X}_n$ plots as the envelopment point.

6.2 **Conventional Versus New Methodology**

Comparison results from the conventional methodology and proposed new methodology use two approaches: First, is by comparing the envelopment based on a homogeneous region against a river basin; second, is conducting comparison against the envelopment based on an administrative region.

For the first comparison, Figure 6-3 presents the K_m versus $\overline{X}_n$ plots of the stations within Region 7, the Yodo River Basin and Kiso River Basin. 103 stations were used for Region 7, 23 stations were used for Yodo River Basin and Kiso River Basin. By adopting the extreme-rainfall homogeneous region of Region 7, the stations which represent the envelopment are Hikone and Miyagawa (Figure 6-3 (a)). By this, based on the assumptions made by the Hershfield statistical method, it is assumed that the PMP has been obtained at both sites of Hikone and Miyagawa. From that, the K_m values of all the other sites within the homogeneous region are transposed using the envelop equation obtained. For example in this case the K_m transposition uses the envelope equation of:$K_m = -0.063\overline{X}_n + 22.446$.

In addition, Figure 6-3 (a) also highlights the sites used for the envelopment of the conventional method (based on river basin boundary or administrative region). In this case if the Yodo river basin is to be used as the transposition boundaries (by selecting all the stations within Yodo River Basin for the statistical PMP estimates), then Hikone and Soni would be chosen as the sites for the envelopment (Figure 6-3 (b)). As shown in Figure 6-3 (b) the slope of the envelope for Yodo River Basin is very steep and Hikone's K_m versus $\overline{X}_n$ plot is located very far from the other plots. However, if the homogeneous region of Region 7 is to be used, a more gentle envelopment and uniform plots can be obtained Figure 6-3 (a). As for the Kiso River Basin case, it can be clearly seen that without considering the homogeneous regions higher envelopment will be missed Figure 6-3 (a) and (c). In general, this shows that overlooking sites with higher maximum rainfall values or K_m and $\overline{X}_n$ values can be avoided by considering the homogeneous region.

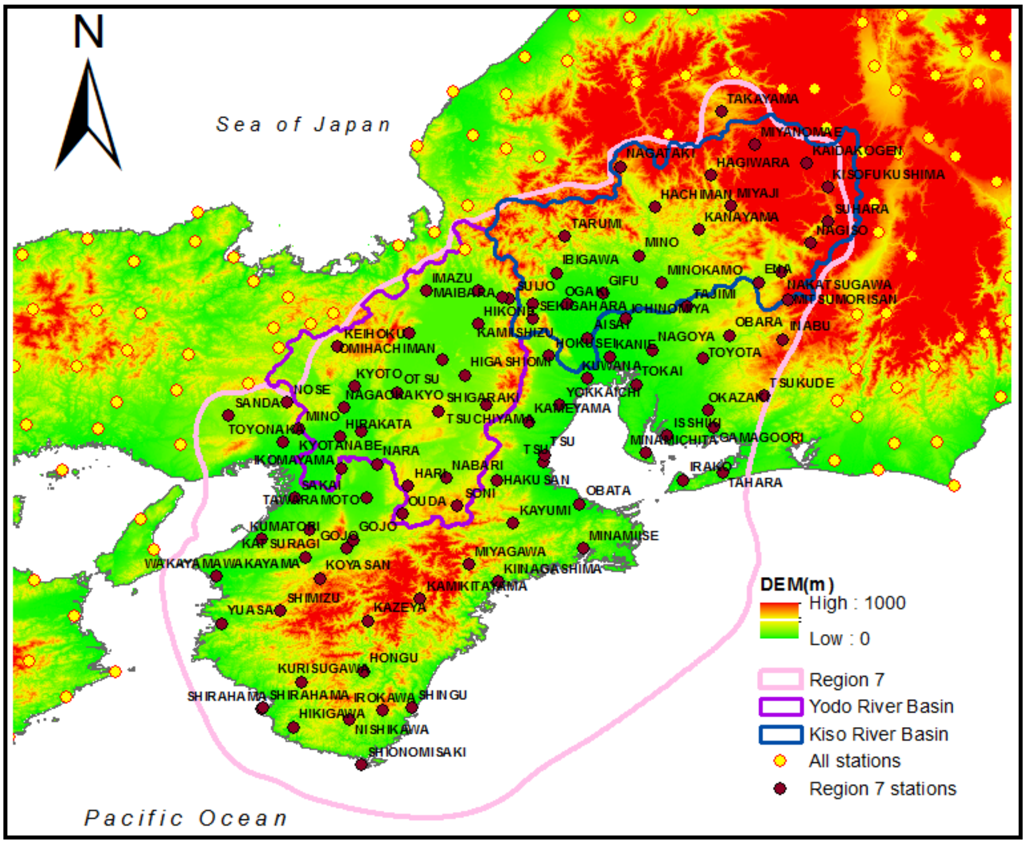

Figure 6-2: Yodo and Kiso River Basin in Homogeneous, Region 7

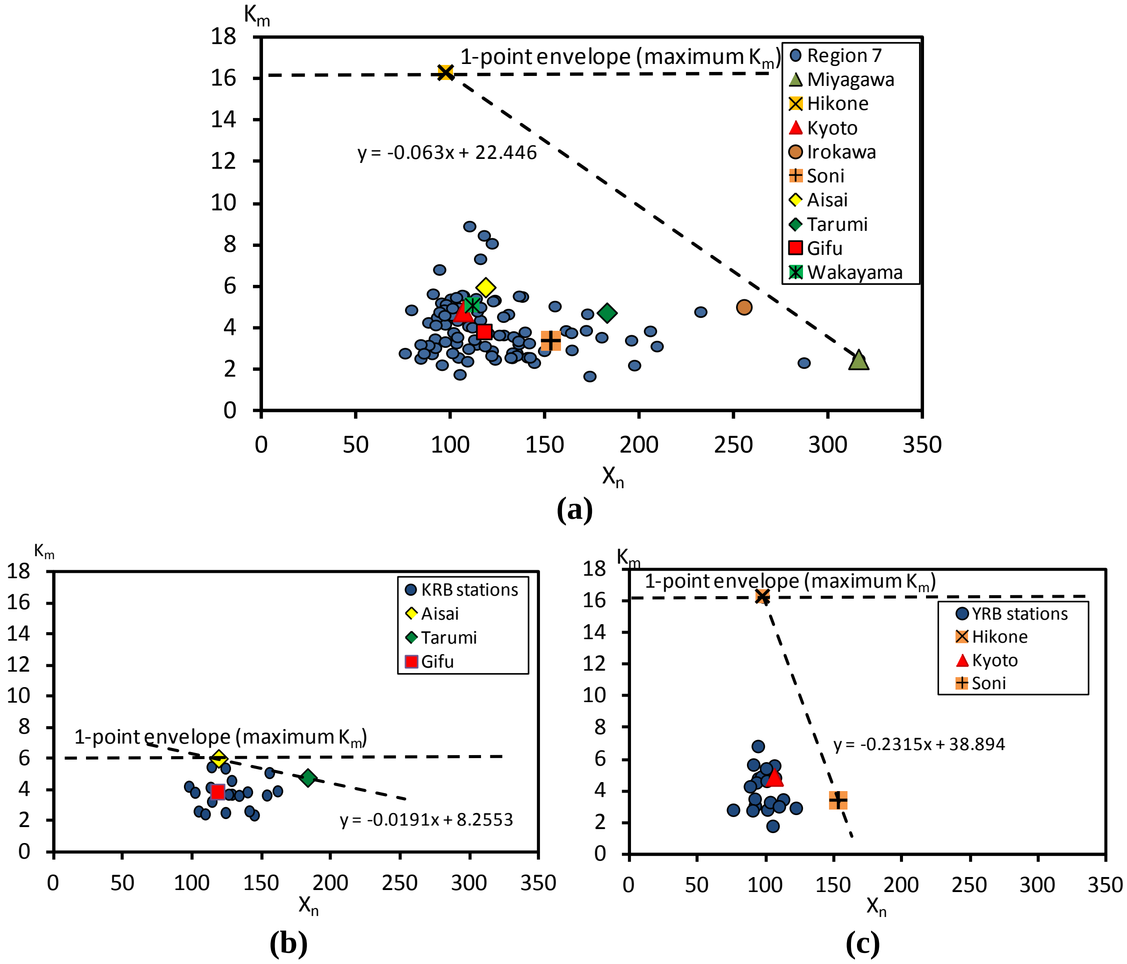

Figure 6-3: Envelopment of K_m for (a) Region 7, (b) Yodo River Basin and (c) Kiso River Basin

Similar tests are done for Region 10. However comparisons are conducted in terms of administrative regions instead of a river basin. Two prefectures are used for the comparisons. One is Kochi and the other is Miyazaki. 24 stations were selected within Kochi prefecture, while 21 stations for Miyazaki prefecture. For Region 10, 109 stations were selected. Figure 6-4 shows the location of the prefectures within Region 10. By referring to Figure 6-5(a) - (c), the K_m versus $\overline{X}_n$ plots for Kochi and Miyazaki prefectures fits perfectly within Region 10 plots. Similar to the comparison made for Region 7-case, by considering a homogeneous region for the statistical PMP estimation method, improvement can be made for the envelopment process by avoiding sites with higher mean annual maximum, $\overline{X}_n$ and K_m values being overlooked.

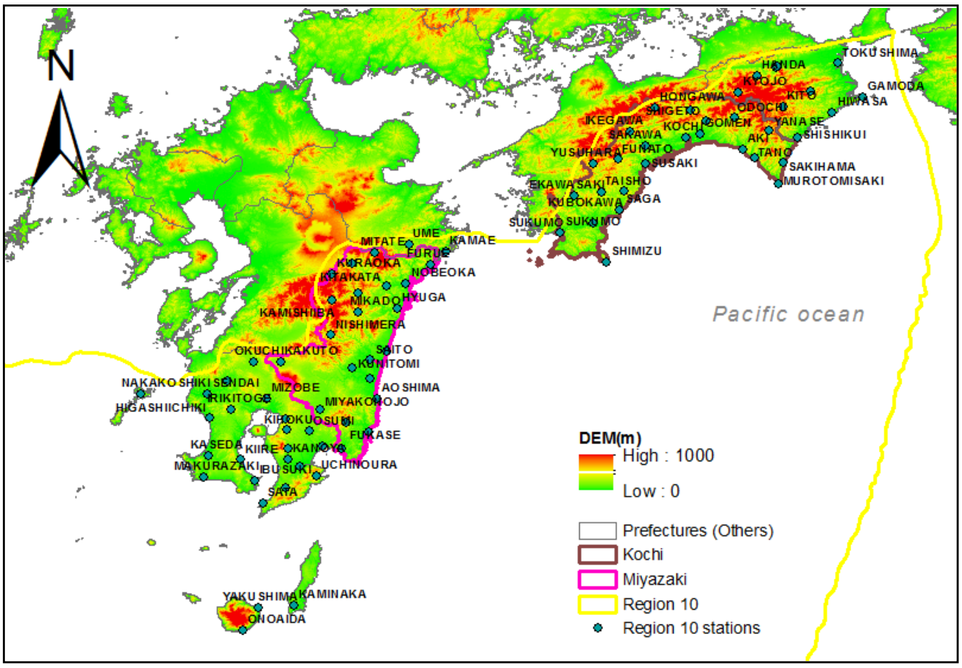

Figure 6-4: Kochi and Miyazaki prefectures in homogeneous region, Region 10

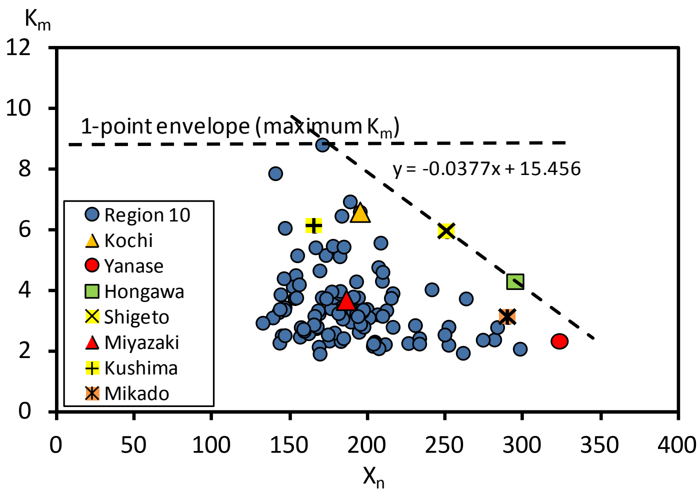

(a)

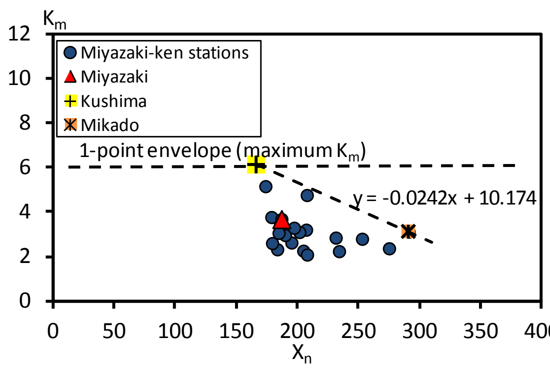

(b)

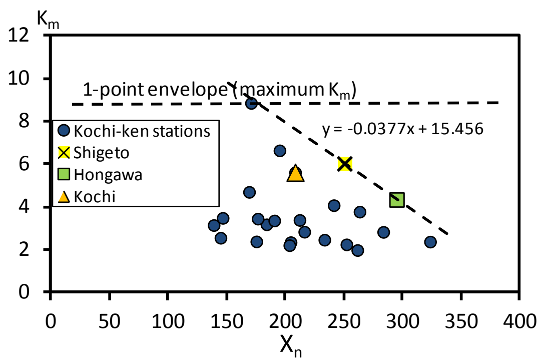

(c)

Figure 6-5 : Envelopment of K_m for (a) Region 10, (b) Kochi-prefecture and (c) Miyazaki-prefecture.

After the determination of the envelopes and obtaining the transposed K_m values, the statistical PMP estimated for both Region 7 and 10 were conducted using the procedures explained in Section 5.2.2. The results are presented in Figure 6-7 for Region 7 and Figure 6-8 for Region 10. The highest maximum rainfall, point PMP estimates and the PMP differences between the conventional methodology and new methodology are presented. The differences are calculated by subtracting the new-methodology PMP estimates to the conventional PMP estimates and then divided by the conventional PMP estimates. Thus, a negative value would indicate a reduction, while a positive value indicates an increment of the PMP estimates. As shown in Table 6-2, the reduction values for all the rainfall periods are between -12 % to -22 %, while the increments are between 172 % and 235 % for the comparison case against river basin's approach. For the administrative region approach the reductions are -1 % and -3 %, while the increments are between 5% and 45 %. Quite similar outcomes were obtained if the one-point envelopment were used.

It is proven that the new method or approach have higher PMP estimates compared to the conventional method. However, the main question is whether it improves the statistical PMP estimates in order to compensate for data limitations in terms of the observation length. A comparison is made for stations within Region 7. The PMP estimated by the conventional method (Yodo river basin as the transposition boundary) and the new approach (Homogeneous region, Region 7 as the transposition boundary) using data from 1976 - 2008 are compared to the conventional method which uses data from 1896 - 2008. Figure 6-6 illustrates the results.

The PMPs estimated by the conventional method using shorter observation data (1976 - 2008) are very low compared to the PMPs estimated using the long observation data (1896-2008). By adopting homogeneous region as the transposition boundary, the PMP estimated were generally increased (however, not so much) for the stations within the Yodo River Basin. While other stations outside the river basin boundary have much higher PMP estimates and could be seen to be near to the PMPs estimated by the long observation data. Thus, for flood structure designing purposes, the highest PMP value within the homogeneous region could represent the PMP values for any flood-mitigation project plan to be implemented in that particular homogeneous region.

Table 6-2: Comparisons of statistical PMP estimated based on conventional and proposed method

	PMP percentage differences

Rainfall Period	[1]New versus [2]conv. (river basin) -2-point envelopment	[1]New versus [2]conv. (river basin) -1-point envelopment	[1]New versus [2]conv. (administrative region) -2-point envelopment
1-day	-14% to 172%	0% to 127%	5% to 43%
2-day	-14% to 235%	0% to 223%	-1% to 45%
3-day	-12% to 228%	0% to 199%	0% to 44%
5-day	-17% to 183%	0% to 17%	0% to 29%
7-day	-22% to 176%	0% to 14%	-3% to 29%

Note: [1]New= based on homogeneous regions, [2]conv. = conventional

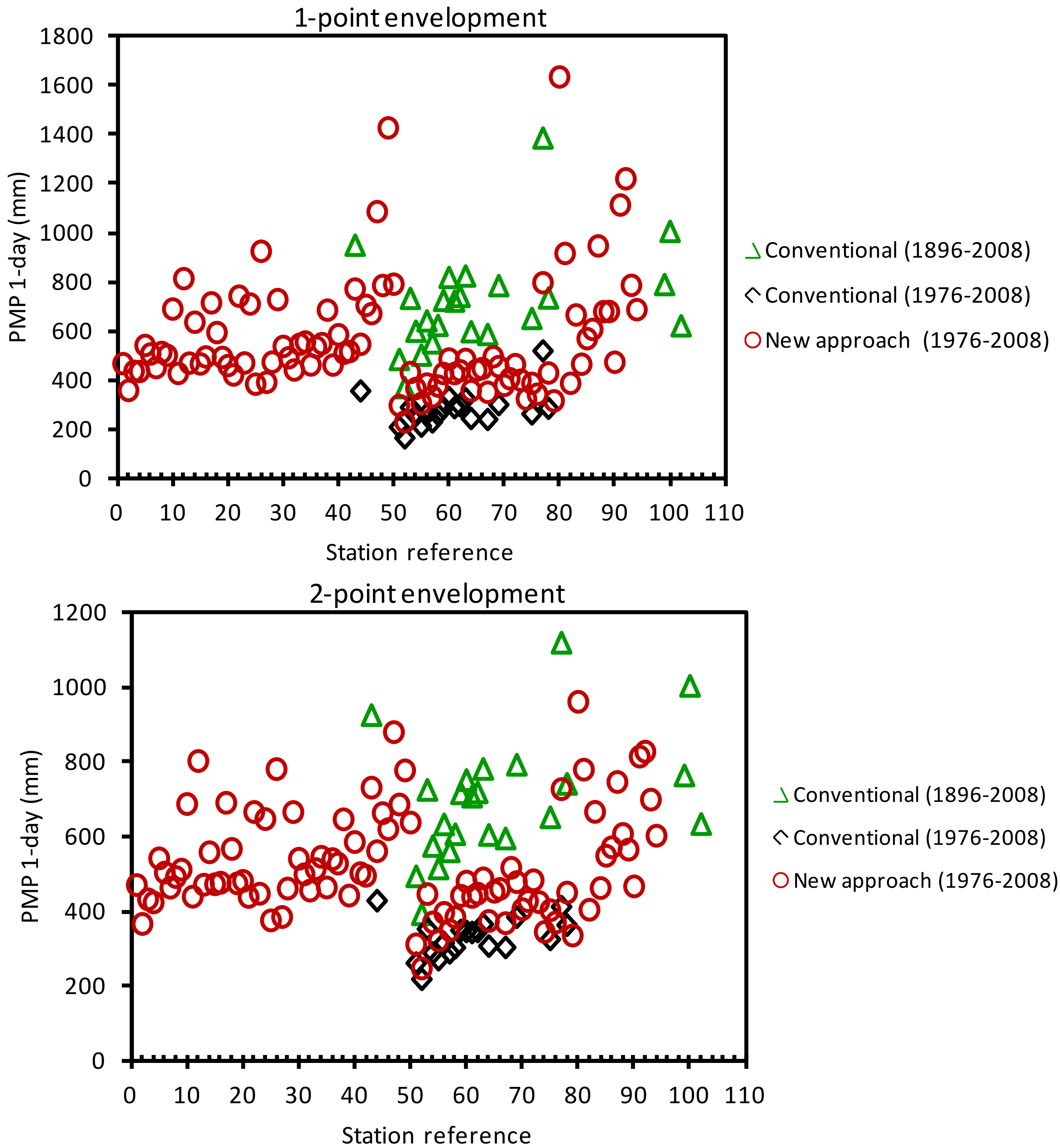

Figure 6-6: Comparison of the PMP estimates according to the observation length

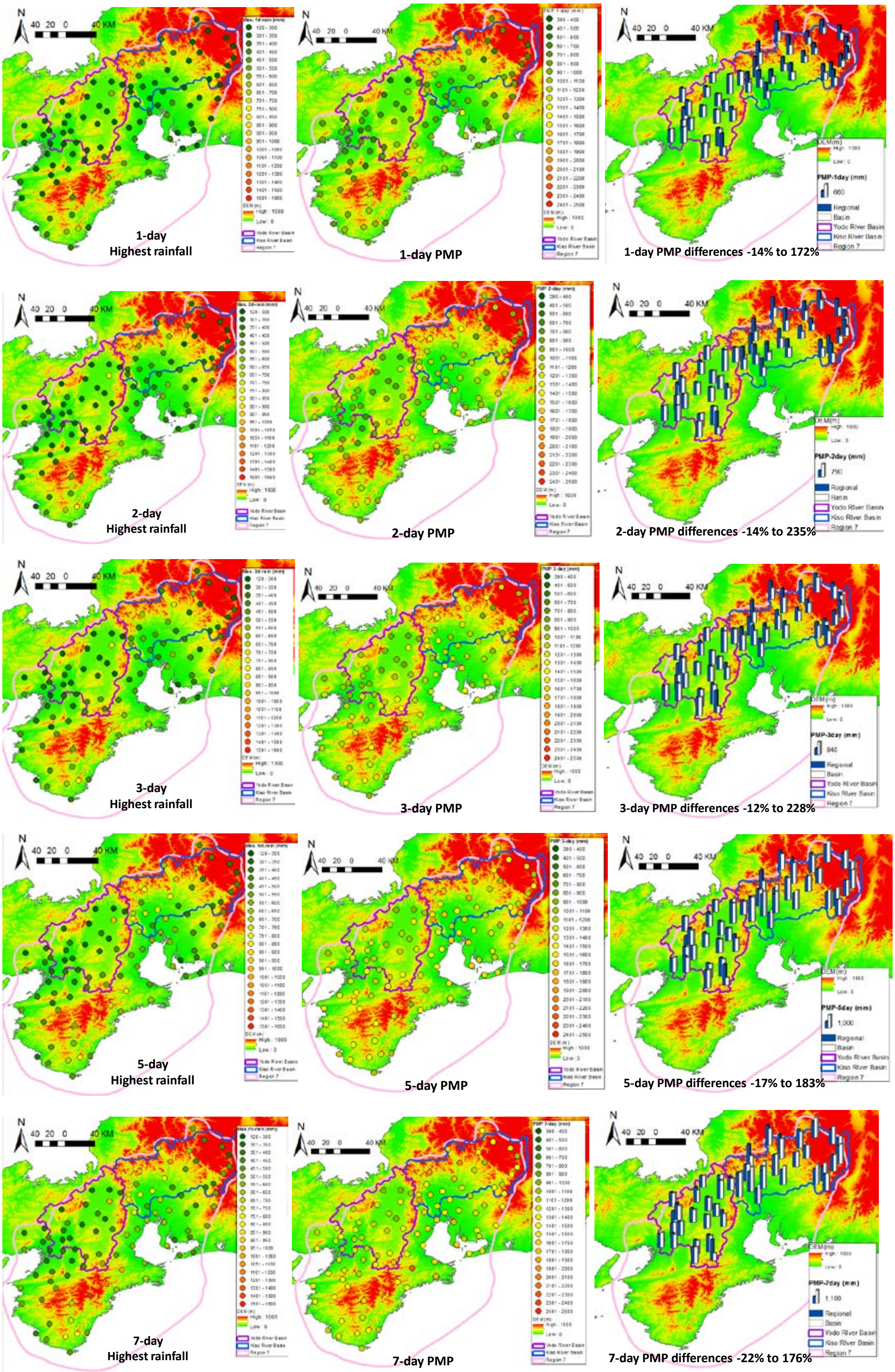

Figure 6-7: Comparison of conventional and improved method for PMP (Region 7)

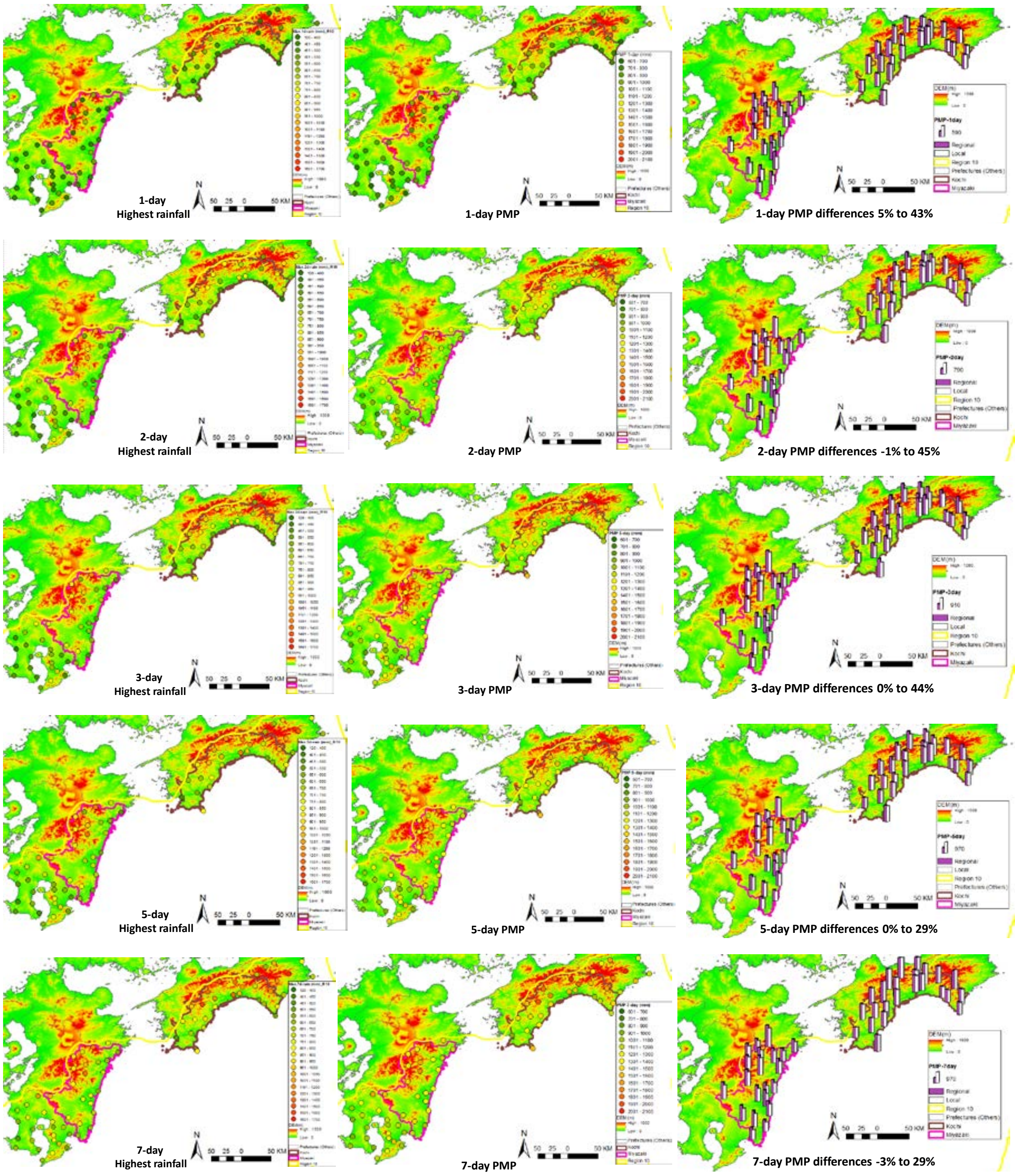

Figure 6-8: Comparison of conventional and improved method for PMP (Region 10)

6.3 Validations of the PMP Statistical Estimates

Validations of the statistical PMP estimates are conducted using current observation records. Additional case-studies are conducted for the conventional method besides using Yodo River Basin, Kiso River Basin, Kochi-prefecture and Miyazaki-prefecture as transposition boundaries mentioned before. The additional boundaries representing the conventional method are Mie, Wakayama, Nara, and Tokushima prefectures. Mie, Wakayama and Nara prefectures are located within the homogeneous region of Region 7, while only Tokushima prefecture is located within Region 10. They are considered for the validations due to recent record-breaking daily rainfall events occurred after the analysis period (2008 to 2014).

By referring to the summary of the validation analysis presented in Table 6-3, for PMP estimated using the 2-point envelopment technique (a regression equation was used for the K_m transposition), in general all of the PMP estimates based on the new method have higher values except for Miyagawa point. This is due to Miyagawa was used as the point for the envelopment which reflects the limitation of the Hershfield statistical PMP estimation which assume points used for the envelopment already received its maximum precipitation condition (refer Chapter 5). However, other results show the improvement of the PMP estimates by considering the homogeneous regions as the transposition boundary. For example, significant improvements can be observed for Kamikitayama point where if the conventional method is to be used (by considering Nara prefecture as the boundary), the PMP estimates of 661 mm would then be reached from the rainfall event on 21/8/2011, of coincidently similar value of 661 mm daily-rainfall amount. However, if the homogeneous region is to be used as the boundary, the PMP estimated is 978 mm. This provides higher precautions measure if the PMP estimate is to be used for flood defence structures' designs. Similar assessment can be made for point Fukuharaasahi, and Miyaji. The PMPs estimated using conventional method for both points are very close to their record-breaking rainfall events (542 mm and 301 mm PMP estimates to 641 mm and 283 mm record-breaking rainfall event of Fukuharaasahi and Miyaji respectively). For Fukuharaasahi, the conventional PMP estimates were even exceeded by the 19/7/2011 record-breaking rainfall event. If the new method is considered, then the statistical PMP estimates will not be reached yet (860 mm PMP estimate against the 641 mm record-breaking rainfall amount). For Yanase point, both the conventional and new-method statistical PMP estimates were exceeded by the 20/7/2011 rainfall event.

However in terms of the PMP estimated using the 1-point envelopment technique (maximum observed K_m value used for the transposition), all of the record-breaking rainfalls still remain below the conventional PMP estimates. By adopting the new method, higher PMP estimates were obtained compared to the conventional. In this case, validations can be conducted in the future to see whether the conventional PMP estimates will be exceeded or not. In addition, Section 6.4 discusses the PMP estimated based on a projected climate data using the general circulation model of the Japanese MRI-AGCM3.2 (20km). It is validated from the results that the new method is closely comparable to the projected PMP estimates.

The 1-point envelopment technique however wasn't clearly mentioned and recommended in the manual on estimation of probable maximum precipitation (PMP) by WMO (2009) for the statistical PMP estimation method. However it was used by Casas et al. (2008); Casas et al. (2011); Desa M et al. (2001); Desa M and Rakhecha (2007) and by Hershfield (1961). Hershfield (1961) uses the 1-point technique at first for a 24-hour rainfall PMP estimate, later he determined the K_m value for other rainfall durations and its variation with X_n. Thus, recommending the K_m envelopment using multiple points and a particular curved or a regression line. There exist some limitations though, by considering the curved (2-point or multiple points' envelopment) for different rainfall durations, if different transposition values (transposed K_m) were conducted for different rainfall durations, the PMP estimated in the end will be unreasonable. For example, at similar point or site a 1-day PMP can be higher than a 2-day PMP estimates if different transposition values were used. Thus, it could be more reasonable to consider the highest observed K_m for all the rainfall durations and use the same value for the transposition. This was conducted and considered by Casas et al. (2011).

In addition, the one-point envelopment technique also produces better relative comparisons between the rainfall means and the PMPs estimates. This can be shown in Figure 6-10. An example of the analysis taken from one of the homogeneous region, Region 5 is presented. Based on the 2-point envelopment, the transposed frequency factors, K_m depends on the regression line (2-point or multiple points' envelopment) produced from the envelope line, thus the frequency factors, K_m of stations with higher means would be transposed much less than stations with lower mean values. Whereas by adopting a 1-point envelopment (highest observed K_m value), then all the frequency factors of all stations will be transposed using a similar factor. This contributes to a PMP estimate which has similar annual mean trends as the stations. For example Figure 6-10 (b) uses a 2-point envelope, thus trends of stations with higher annual maximum means will not have higher PMP estimates.

The PMP estimates of all stations were '*uniformalized*'. However, for a 1-point envelop, Figure 6-10 (c), the frequency factor K_m for all the stations are transposed to a constant K_m value, thus stations with higher annual maximum means will generally have higher PMP estimates. Both methods however are acceptable and is used in various PMP studies (Casas et al., 2008; Casas et al., 2011; Desa M et al., 2001; Desa M and Rakhecha, 2007; WMO, 2009).

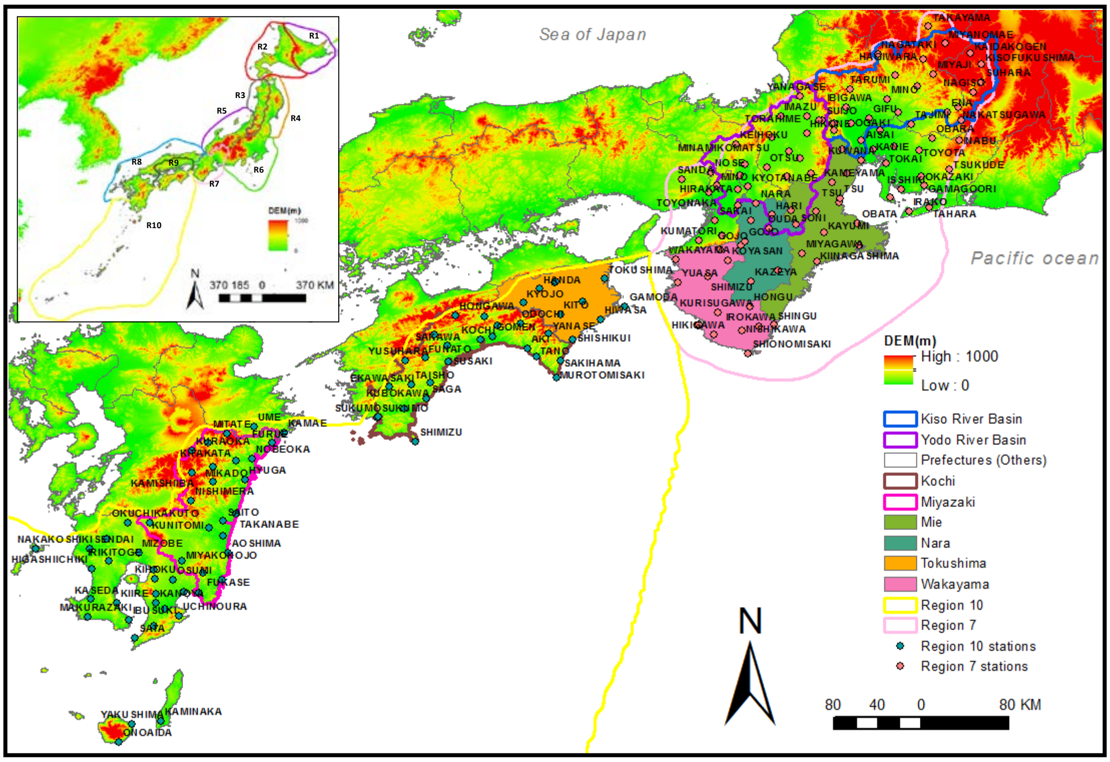

Figure 6-9: Locations of river basins, prefectures and homogeneous regions used for the statistical PMP estimations.

Table 6-3: Validations of the statistical PMP estimates to current observation records

Daily-rainfall (mm) 1894-2014 (Validation period)			*1-day statistical PMP estimates (mm) 1894-2008 (Analysis period)*					
Max.	*Point*	*Date (d/m/y)*	*Conv. (2-point)*	*Conv. (1-point)*	*Region (No. of sta., Area)*	*New (2-point)*	*New (1-point)*	*Region (No. of sta., Area)*

764	Miyagawa	19/7/11	648	1276	Mie-ken (12, 5991 km^2)	648	2442	Region 7 (103, 38340 km^2)
626	Nishikawa	3/9/11	755	762	Wakayama-ken (12, 4803 km^2)	1040	1916	Region 7 (103, 38340 km^2)
661	Kamikita.	21/8/11	661	1370	Nara-ken (9, 3810 km^2)	978	2866	Region 7 (103, 38340 km^2)
852	Yanase	20/7/11	750	1484	Kochi-ken (24, 7201 km^2)	836	1523	Region 10 (109, 31854 km^2)
641	Fukuhara.	19/7/11	542	1002	Tokushima-ken (9, 4237 km^2)	860	1354	Region 10 (109, 31854 km^2)
171	Otsu	15/9/13	566	619	Yodo Riv. Basin (23, 7971 km^2)	605	619	Region 7 (103, 38340 km^2)
283	Miyaji	20/9/11	301	305	Kiso Riv. Basin (23, 9406 km^2)	561	614	Region 7 (103, 38340 km^2)
265	Sekigahara	18/9/12	403	426	Kiso Riv. Basin (23, 9406 km^2)	772	909	Region 7 (103, 38340 km^2)

Conv. = conventional method (considering river basin's or administrative region's boundaries for the transposition). *New*= new method (considering homogeneous regions as the transposition boundaries).
2 point = regression line used for the transposition, *1-point* = maximum K_m value used for the transposition

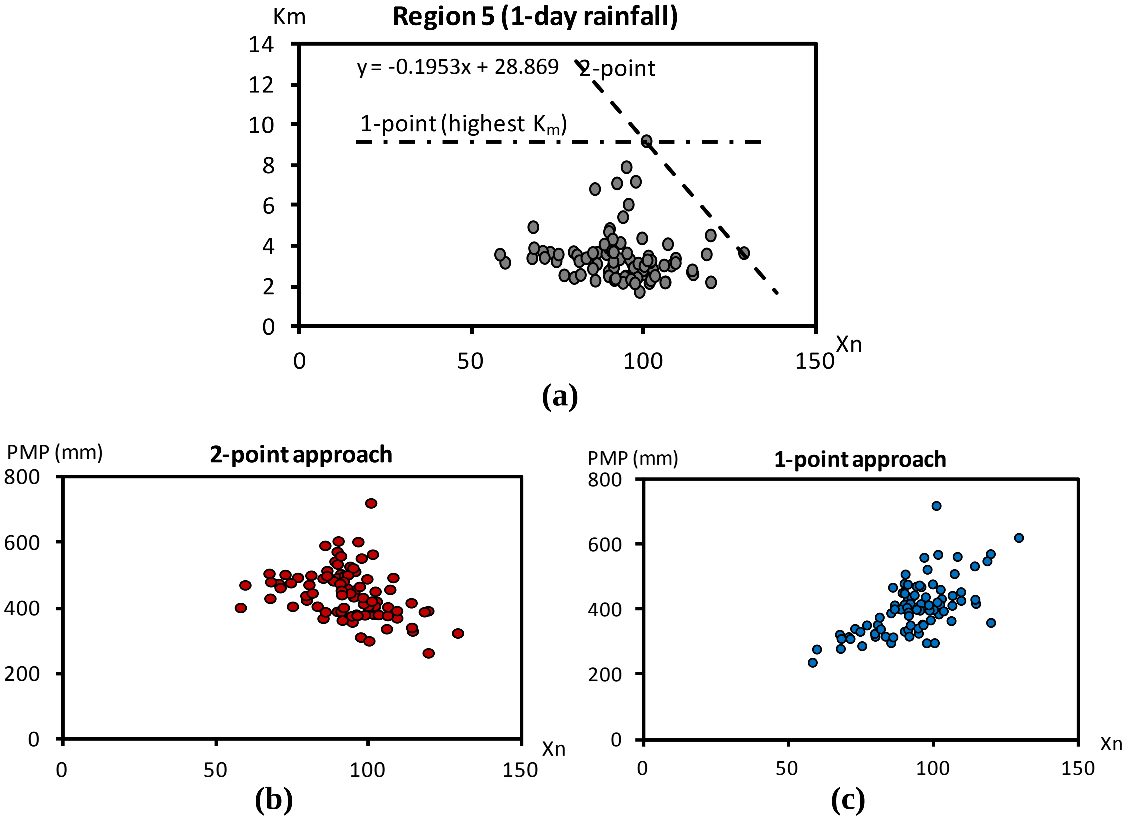

Figure 6-10: PMP estimates based on a 1-point envelopment (largest observed K_m value) and two-point envelopment (regression line)

6.4 PMP and the MRI-AGCM3.2

MRI-AGCM3.2s (AGCM3.2) is an improve version of the atmospheric general circulation model developed by the Meteorological Research Institute (MRI), Japan with a super-high-resolution having a 20-km spatial and 1-hour temporal resolution. The AGCM3.2 provides two terms of future projection run output based on the A1B climate change scenario (IPCC, 2007) which are the near-future term (2015 - 2044) and the far-future (2075 - 2104). For validations and bias corrections, a present term is available for the year 1979 - 2008. Its previous version MRI-AGCM3.1, was developed from an operational numerical weather-prediction model which has provided information on possible climate change induced global warming, including future changes in tropical cyclones, the East Asian Monsoon, extreme events, and blockings. The new MRI-AGCM3.2s was improved by various parameterization schemes (Mizuta et al., 2012). It was proven that the model shows improvements simulating heavy monthly-mean precipitation around the tropical Western Pacific, the global distribution of tropical cyclones, the seasonal East Asian summer monsoon, and blockings in the Pacific (Mizuta et al., 2012). However in terms of spatial distribution of annual precipitation amount the model output shows smoothen spatial pattern due to the rather flatten topographic information (Kim and Nakakita, 2010).

In terms of extreme rainfalls Kim and Nakakita (2010) tests the 100 maximum values of daily and hourly maximum (4 maximum values of each year during 25 years) of each grid for the whole Japanese Islands. As a direct and clear evaluation of the overall model performance desirable reproducibility on the extreme value should have a 1.0 regression coefficient. However they have found that almost all of the regression coefficients for the extreme values were between 0.6 and 0.9 and concluded that the AGCM3.2s output has underestimated the daily and hourly maximum in most part of Japan. Tests on the annual maximum daily output of the AGCM3.2s (which are mainly used for the probable maximum precipitation analysis in this thesis) have yet to be tested before. Thus, a simple bias-correction method usable particularly for determining statistical point PMP estimates in this research were developed and conducted. The MRI-AGCM3.2 outputs used in this study were obtained through the Kakushin and Sousei projects by Japan's Ministry of Education, Culture, Sports, Science, and Technology trough Kyoto University.

6.4.1 *Bias Correction and Validation*

Since the statistical PMP estimates rely on the means of the annual maximum series (X_n), the bias corrections were based on it. A simple and direct bias correction was implemented for all the AGCM3.2s (GCM) grid-points outputs within the homogeneous region, Region 7. Region 7 contains 78 GCM-grid points which were associated to the nearest 100 AMeDAS stations located inside the region (Figure 6-11). After considering the best AMeDAS stations to represent the GCM grid-points, 85 AMeDAS-GCM points were obtained with several grid-points were associated to more than one AMeDAS stations (Figure 6-12). The bias corrections were based on the annual maximum hourly rainfall within the period 1979 to 2008. AMeDAS-GCM points which have its' R-squared value of X_n more then 0.9 was considered to be reliable and were used for the PMP projections of the near-future and far-future time slices. R-squared is a statistical measure of how well a regression line approximates the real data points. The R-squared value is calculated using the following equation.

$$R^2 = 1 - \frac{SS_E}{SS_T}, \qquad SS_E = \sum(x_i - y_i)^2\, , SS_T = \sum(x_i - \bar{x})^2 \qquad \text{Eq. 6-1}$$

$$Local\ R^2 = 1 - \frac{SS_E}{SS_T}, \qquad SS_E = (x_i - y_i)^2,\ SS_T = (x_i - \bar{x})^2 \qquad \text{Eq. 6-2}$$

The bias-correction was conducted by using the annual maximum series of the rainfall period 1-, 2-, 3-, 4-, 6-, 12-, and 24-hour. As an example, Figure 6-13 presents the initial annual maximum plots of the observed versus the GCM output (1979-2008) of several rainfall periods conducted during the analysis. Using a bias-correction factor obtained by plotting a regression line (Figure 6-14), the GCM's annual maximum series (AMS) were divided by the bias-correction factor. As an example, the 1-, 2-, 12- and 24-hr rainfalls' bias-correction factor was found to be 0.3555, 0.4551, 0.5047, and 0.4521 respectively as shown in Figure 6-14.

The bias-corrected annual maximum plots of the observed versus the GCM output (1979-2008) are presented in Figure 6-15 while the fittings are represented in Figure 6-16. Similar processes were conducted for all the 85 AMeDAS-GCM points. After the bias correction, all the annual maximum series of the 85 points produced R-squared more than 0.9 as represented in Figure 6-16. When the means of the annual maximum series of each rainfall periods were plotted (Figure 6-17), high R-squared values were also produced. From this, we can conclude that in terms of the means of annual maximum series (X_n), the bias corrected GCM outputs performs quite well. This is a good indication for the GCM outputs to be used for statistical PMP estimation.

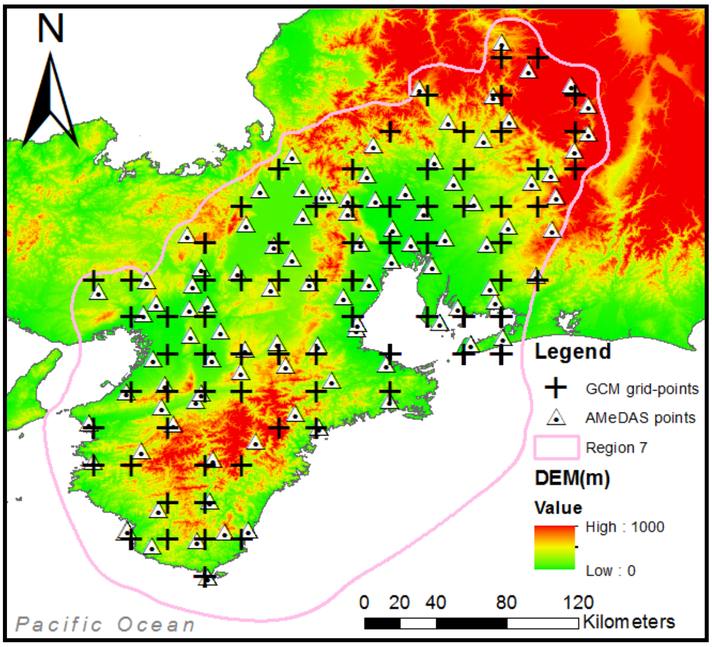

Figure 6-11: Location of the 78 MRI-AGCM3.2 (GCM) grid-points and associated 100 AMeDAS stations within Region 7.

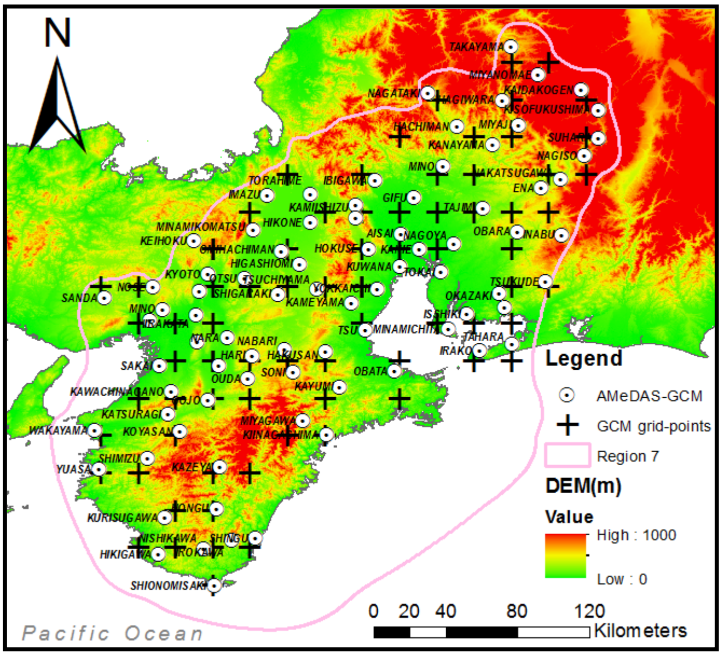

Figure 6-12: Location of the 85 AMeDAS-GCM points used for the bias-correction and future PMP estimates.

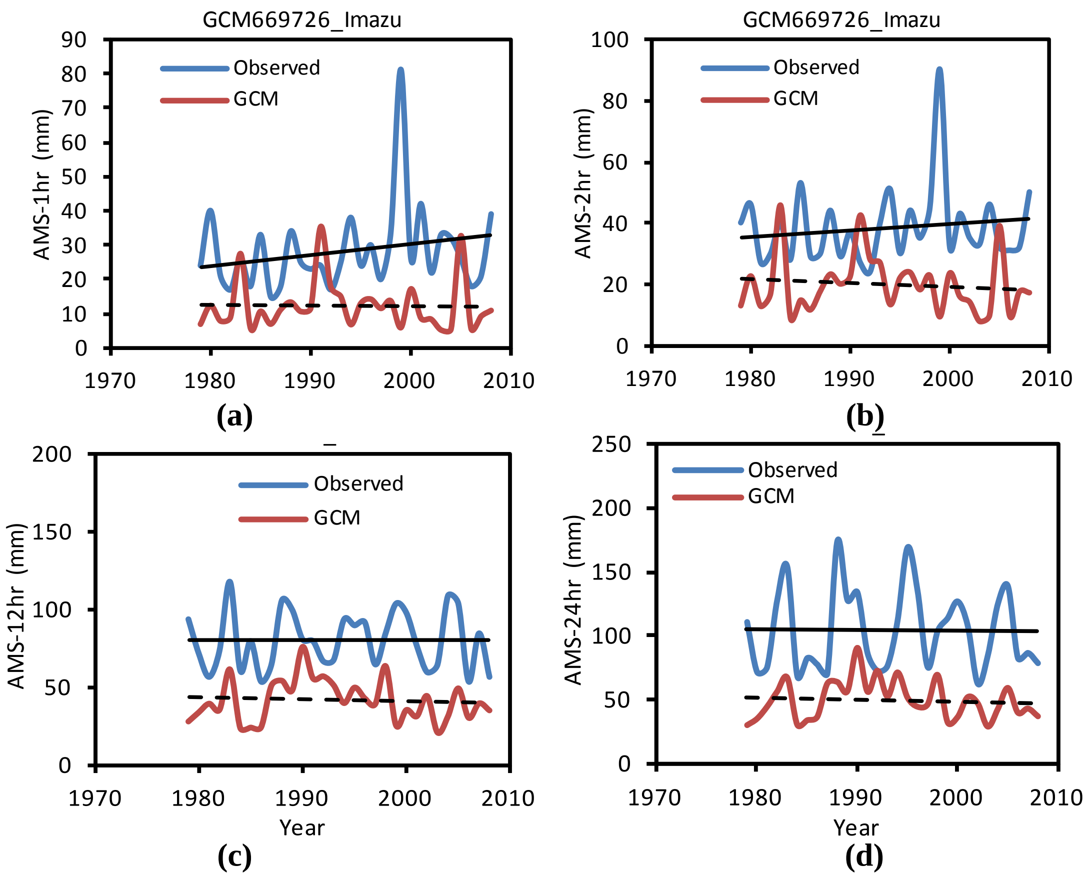

Figure 6-13: Annual maximum series (AMS) of the Amedas (Observed) and the MRI-AGCM3.2 (GCM) before bias-correction (e.g. 1-hr, 2-hr, 12-hr and 24-hr of Imazu).

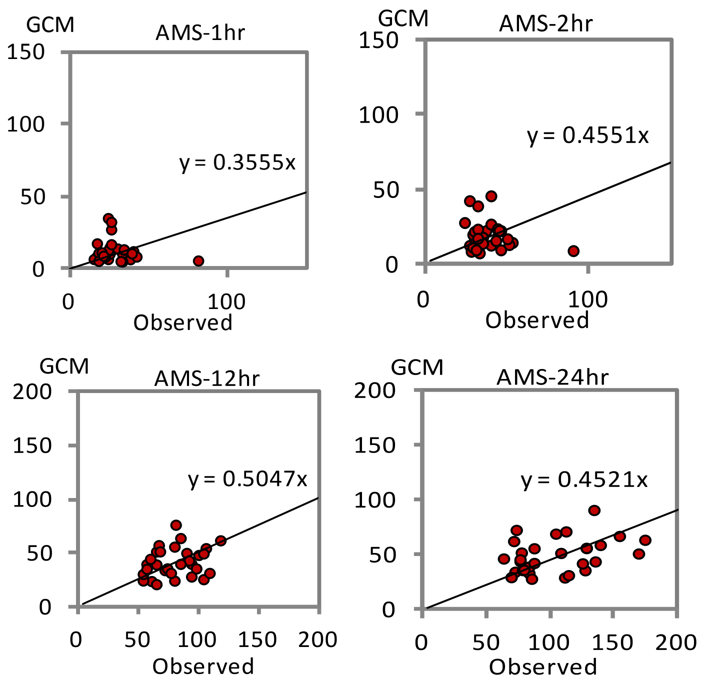

Figure 6-14: Bias correction factor estimation (e.g. 1-hr, 2-hr, 12-hr and 24-hr of Imazu).

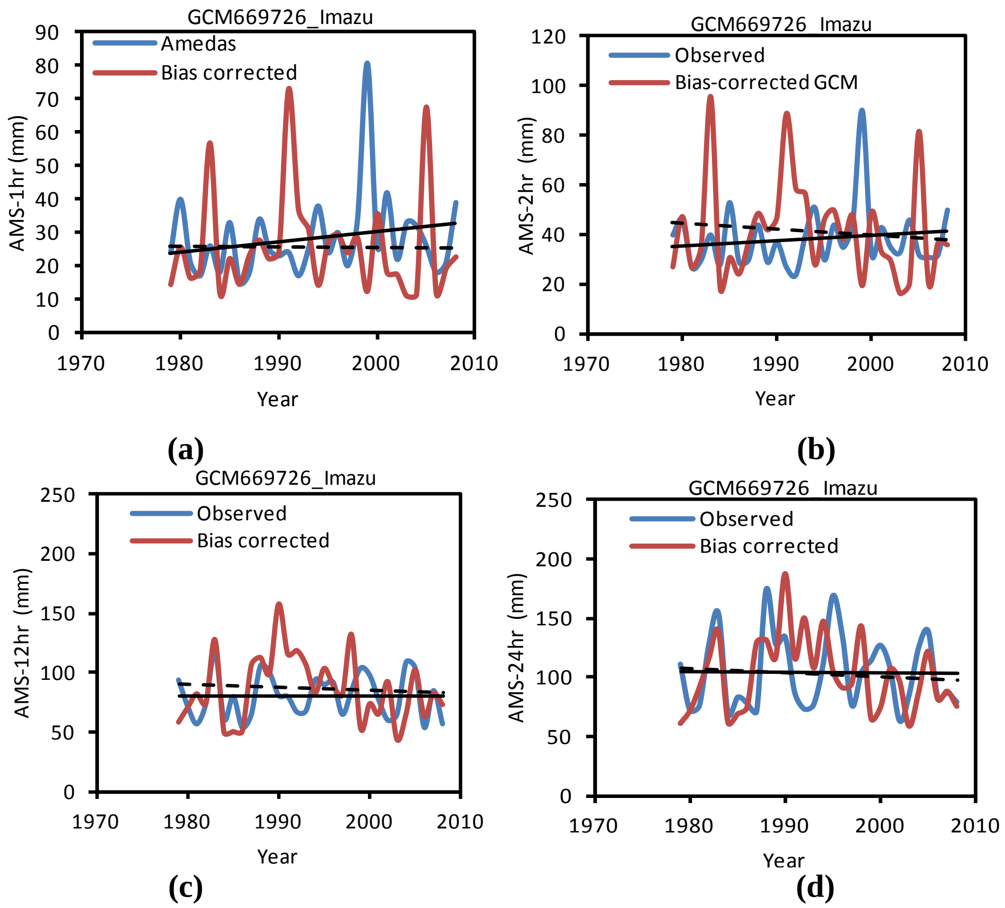

Figure 6-15: Annual maximum series (AMS) of the Amedas (observed) and the MRI-AGCM3.2 (GCM) after bias-correction (e.g. 1-hr, 2-hr, 12-hr and 24-hr).

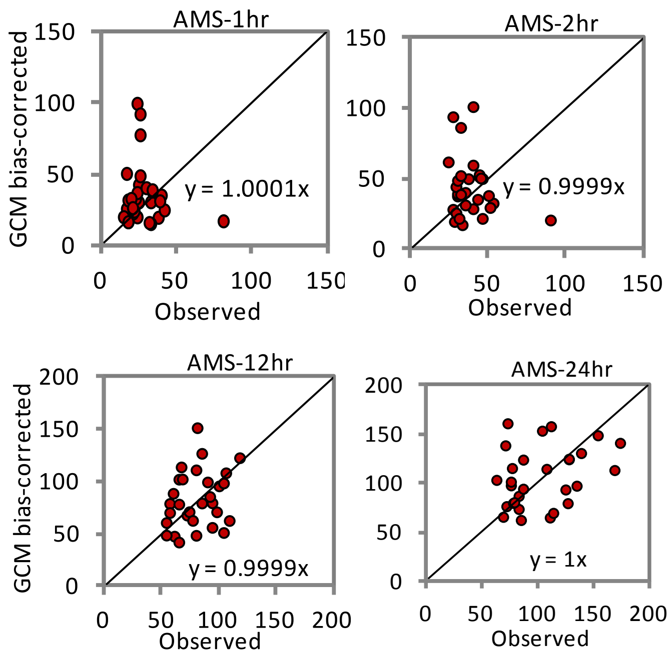

Figure 6-16: Fitting test after bias-correction (e.g. 1-hr, 2-hr, 12-hr and 24-hr of Imazu).

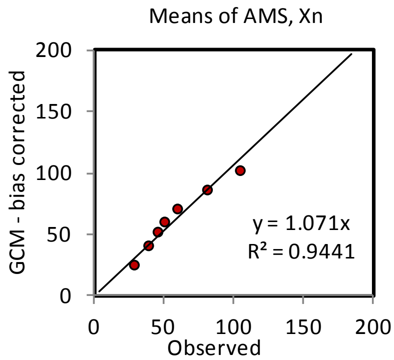

Figure 6-17: R-squared for the means of the annual maximum series (AMS) for Imazu.

6.4.2 *Validation of the GCM's PMP Estimates*

Using all the 84 AMeDAS-GCM points, PMP estimation was conducted similar to the procedures described in Section 6.5. Using the Hershfield parameters obtained, the means of the annual maximum series (X_n) were plotted again to see the R-squared value based on all the sites within Region 7. Reasonable R-squared value were produced (R-squared = 0.761) as shown in Figure 6-18 (b). However, the PMPs estimated produced a lower R-squared value of 0.638. This shows that in general the GCM outputs underestimate or overestimate the PMPs for about 36.2% of variability. However, if we observe the plots in Figure 6-18 (a), regardless of the R-squared value, a lot of the GCM outputs have quite a good fit with the observation (Some points are on the X=Y line, and a majority near to the line). In order to obtain better fit, sites with its local PMP R-squared (Eq. 6-2) value less than 0.35 were excluded resulting into an R-squared value from 0.638 (Figure 6-19(a)) to 0.819 with 54 stations (Figure 6-19(b)). The distribution of the stations which were excluded is illustrated in Figure 6-20.

Using the 54 stations the PMP analysis was conducted again to obtain a new set of transposed frequency factor (K_m). The fitting of the 54 PMPs are presented in Figure 6-21. Similar fitting test was conducted based on the R-square. Surprisingly, the PMPs R-squared value was reduced to 0.680. Thus, it is assumed that this is the best and optimum fit which can be obtained for the PMP estimation using the GCM outputs for this region. Thus, all the 84 AMeDAS-GCM points were used for the future PMP calculations. Knowing the limitations and errors from the bias-corrected GCM outputs, the projected PMPs were conducted using near-future and far-future time slices.

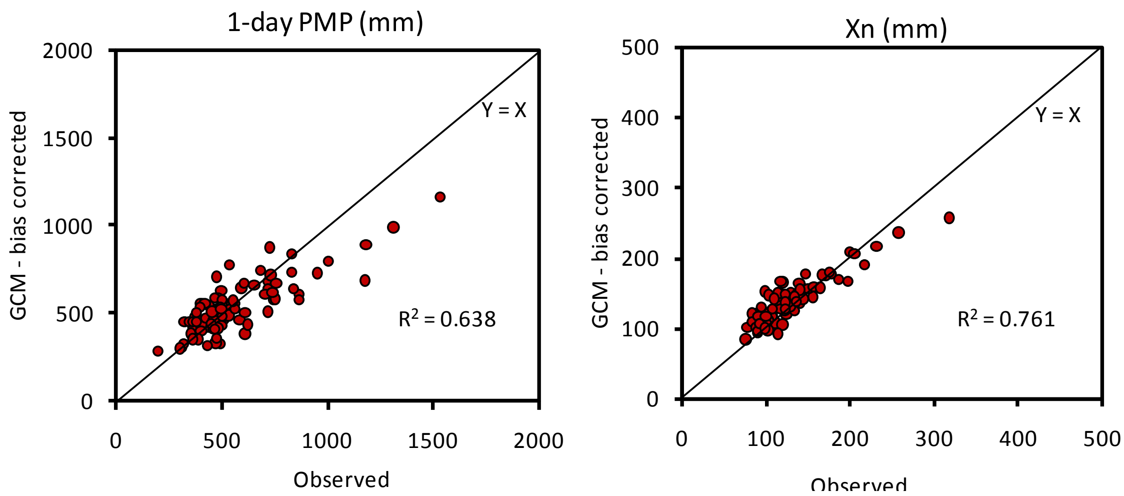

(a) **(b)**

Figure 6-18: R-squared fitting of the bias-corrected AGCM data (1979-2008) and observations (1979-2008) for the **(a)** PMP estimates and **(b)** means of the annual maximum series, Xn.

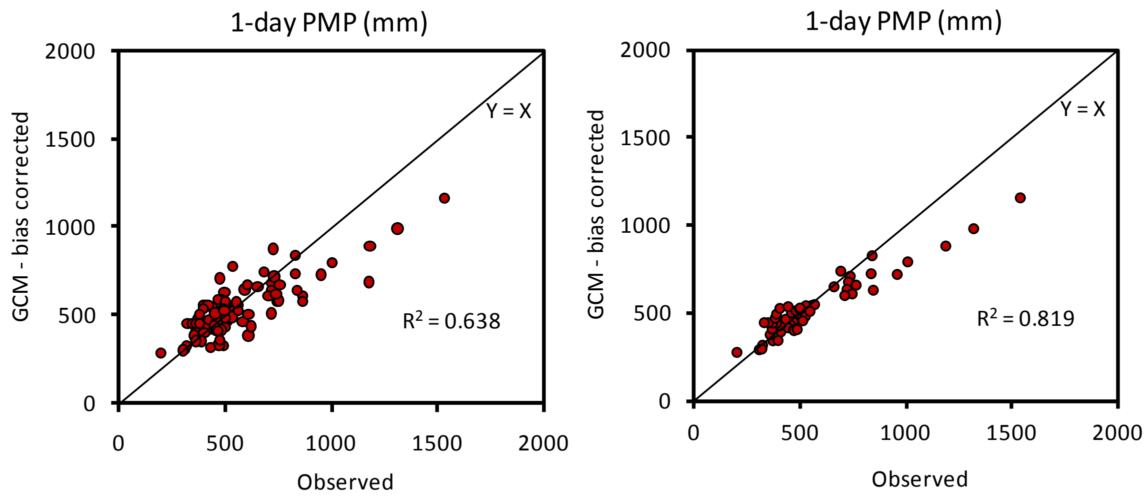

(a) **(b)**

Figure 6-19: PMP fitting of stations producing (a) R-squared = 0.638 (All stations) and (b) R-squared = 0.819 (54 stations with *local* R_2 > 0.35)

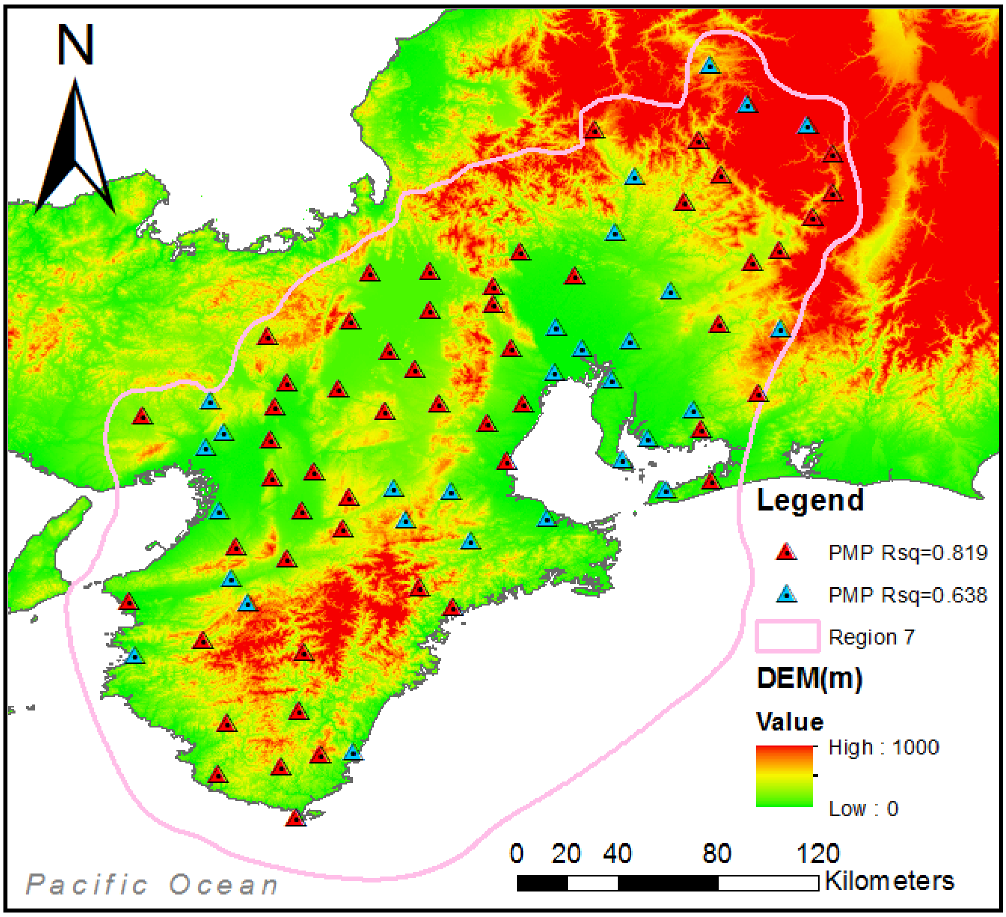

Figure 6-20: R-squared fitting of stations producing R-squared = 0.819 (54 stations with *local* $R_2 > 0.35$) and R-squared = 0.638 (All 85 stations)

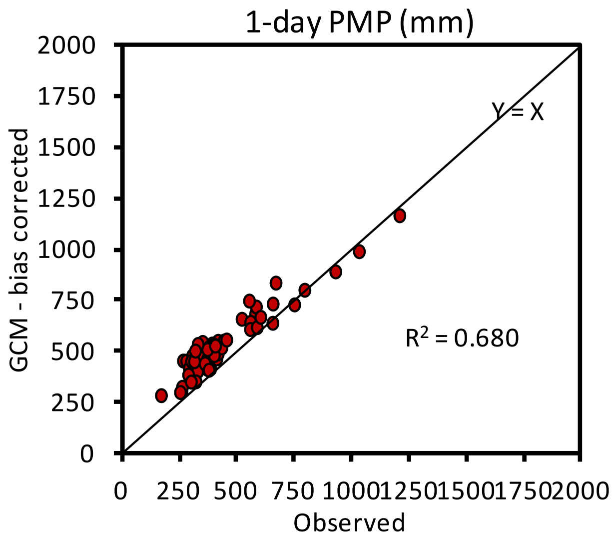

Figure 6-21: Re-estimating of the PMPs based on 54 stations with *local* $R_2 > 0.35$

6.4.3 *Projected PMPs using MRI-AGCM3.2s Model*

Figure 6-22 presents the PMPs obtained based on all available JMA long observation data (1901-2008), the AMeDAS data (1979-2008), the GCM-spa data (1979-2008) which were used for the bias correction and validation, the GCM-sna or near-future projection data (2015-2044) and the GCM-sfa or far-future projection data (2075-2104). The PMPs estimated using the long-observation data (1901-2008) have produced ranges of PMP estimates comparable to the PMPs estimated by the projected climate data (GCM-sna and GCM-sfa). However the PMPs based on a shorter observation period does not.

Several outcomes can be summarized from these findings. First, as proven in Section 6.2, the new methodology by considering homogeneous regions as the transposition boundaries is acceptable also for the 1-point envelopment since the PMPs estimated are much larger than the conventional method and is proven to be comparable to the projected PMPs. However, it should be acknowledged that the PMPs estimated by the GCM data have an error variability of about 30%. Second, the range of PMPs estimated by the near-future (2014-2044) and far-future scenario (2075-2104) has not much difference as compared to the present condition (1979-2008).

From this results and assessment, it can be suggested that the PMP estimates based on the homogeneous regions and the 1-point envelopment for Region 7 of Japan has been proven not just from record-breaking rainfall events but also using projections of an atmospheric general circulation model. The PMPs estimated for Region 7 will hopefully be not exceeded with a confidence level of 70% (around 30% of errors variability).

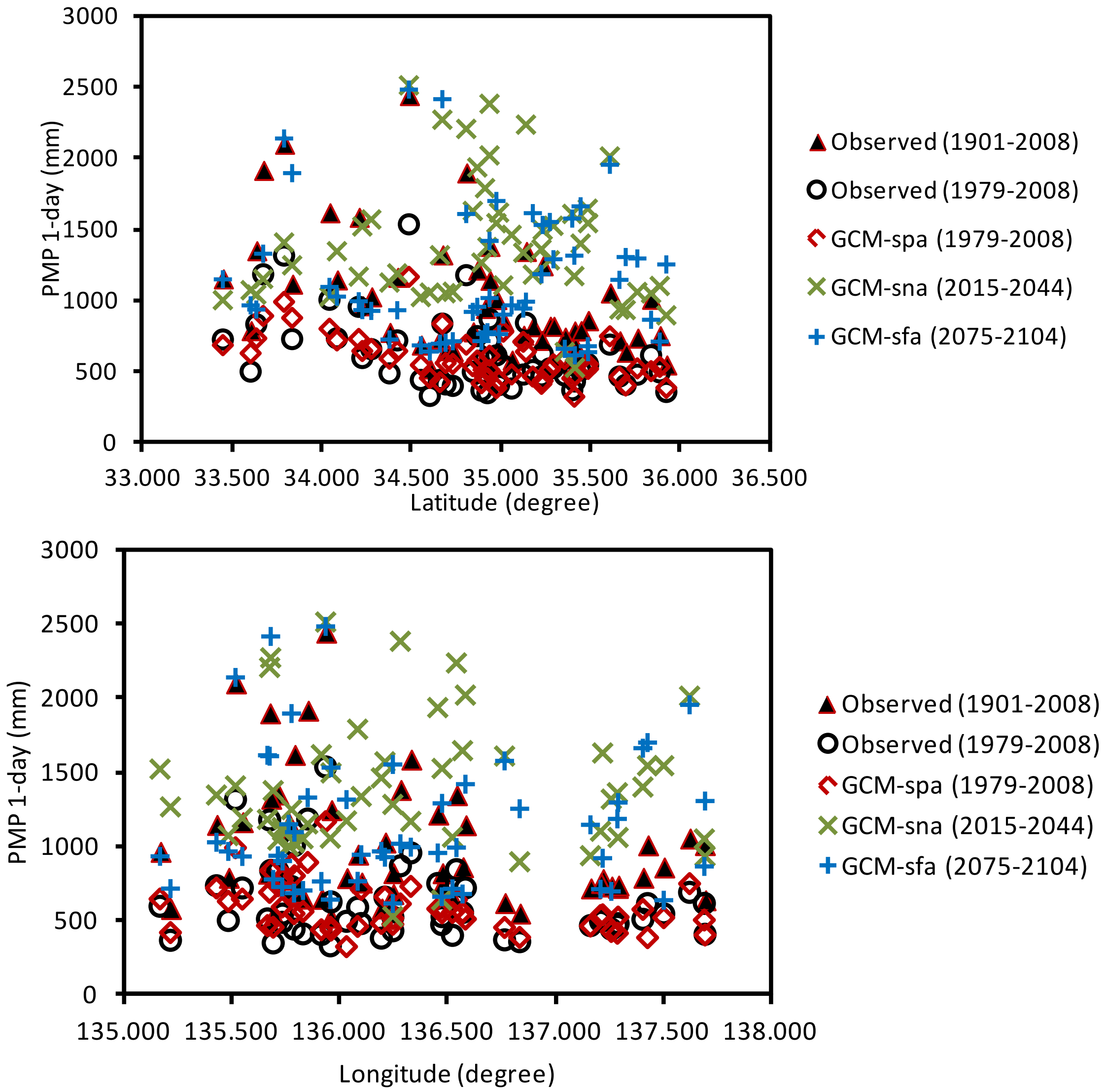

Figure 6-22: Probable maximum precipitation (PMP) plots based on Amedas (Observed) and the multiple time-slices of the MRI-AGCM3.2 projected climate data (GCM-).

6.5 **Statistical PMP Estimates for Japan**

The PMP statistical estimates for all the stations within the homogeneous regions identified are presented in this section based on the new methodology which considers the homogeneous regions as the transposition boundaries of the frequency factor K_m. The one-point envelopment (highest K_m values) where chosen as the technique for the envelopment. Sites having the highest K_m value within a particular homogeneous region are made sure not to be one of the high discordant sites as characterized in Chapter 4. Advantage by using the one-point envelope technique is that consistent envelopment can be conducted to consider other rainfall durations. Other benefits as described in the previous section, section 6.3. A 2-point envelope produces '*uniformalized*' PMP estimates whereby stations with higher annual maximum means will not necessarily have higher PMP estimates. However, for a 1-point envelop, the frequency factor K_m for all the stations are transposed to a constant K_m value, thus stations with higher annual maximum means will generally have higher PMP estimates. Thus, since the PMP estimation will be conducted for all the rainfall durations, the highest frequency factor, K_m regardless of the rainfall durations will be used for the statistical PMP estimation of the stations in the particular homogeneous region.

In the next section, results for the statistical PMP estimates for all the homogeneous regions are presented. First is the plot of the observed frequency factors, K_m of all the rain period obtained by all the stations within the region. Information on the highest observed K_m value used as the transposition factor is presented; second is the table containing the list of stations used for the analysis and; third are the point PMP plots, plotted according to the least latitude to the highest.

As a reminder, all the PMP estimates are point values. Areal values averages can be estimated using an area-reduction curve. The method to construct the area-reduction curve can be found in the manual of the probable maximum precipitation published by the World Meteorological Organization, (WMO, 2009). The area-reduction curve can be constructed using selected storms capable of producing the PMP values. The areal values averages can also be determined based on depth-area-duration (DAD) curves constructed.

6.5.1 *Region 1*

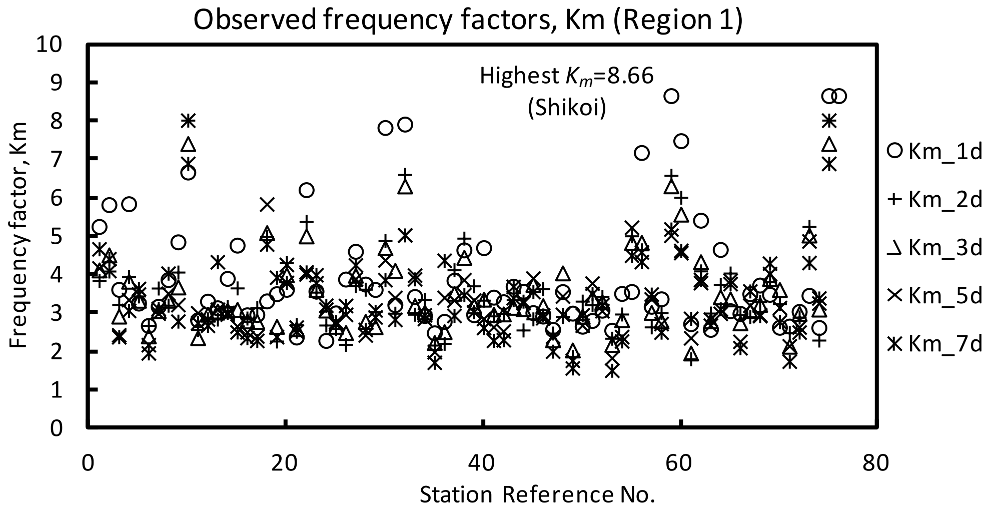

Figure 6-23: Observed frequency factors, K_m for Region 1

Table 6-4 Stations list and 1-day PMP estimates for Region 1

No.	Point (*1-d PMP*)	No.	Point (*1-d PMP*)	No.	Point (*1-d PMP*)	No.	Point (*1-d PMP*)
1	Abashiri (*296*)	*20*	Kamimobetsu (*393*)	*39*	Nishiokoppe (*377*)	*58*	Shibetsu (*370*)
2	Abashiri (ss) (*239*)	*21*	Kamirawan (*316*)	*40*	Nukabira (*576*)	*59*	Shikaoi (*441*)
3	Akan (*469*)	*22*	Kamisatsunai (*574*)	*41*	Nukanai (*490*)	*60*	Shintoku (*447*)
4	Akankohan (*492*)	*23*	Kamishihoro (*350*)	*42*	Obihiro (*363*)	*61*	Shiranuka (*344*)
5	Ashoro (*270*)	*24*	Kashiwakura (*356*)	*43*	Obihiro (ss) (*316*)	*62*	Shirataki (*315*)
6	Attoko (*455*)	*25*	Kawayu (*295*)	*44*	Okoppe (*302*)	*63*	Shotoshibetsu (*361*)
7	Betsukai (*384*)	*26*	Kenebetsu (*323*)	*45*	Omu (*306*)	*64*	Taiki (*595*)
8	Bihoro (*273*)	*27*	Kitami (*270*)	*46*	Oshoppu (*305*)	*65*	Takinoue (*341*)
9	Chippomanai (*411*)	*28*	Kitamiesashi (*257*)	*47*	Ota (*365*)	*66*	Teshikaga (*317*)
10	Engaru (*349*)	*29*	Komaba (*274*)	*48*	Otsu (*418*)	*67*	Tokoro (*299*)
11	Futamata (*469*)	*30*	Koshimizu (*357*)	*49*	Rausu (*357*)	*68*	Toro (*303*)
12	Hamaonishibetsu (*242*)	*31*	Meguro (*551*)	*50*	Rikubetsu (*296*)	*69*	Tsubetsu (*321*)
13	Hamatombetsu (*236*)	*32*	Memuro (*455*)	*51*	Rubeshibe (*294*)	*70*	Tsurui (*358*)
14	Higashimokoto (*314*)	*33*	Mombetsu (*320*)	*52*	Sakaino (*304*)	*71*	Urahoro (*362*)
15	Hiroo (*630*)	*34*	Nakashibetsu (*389*)	*53*	Sakakimachi (*447*)	*72*	Utanobori (*308*)
16	Hombetsu (*320*)	*35*	Nakateshibetsu (*409*)	*54*	Sarabetsu (*563*)	*73*	Utoro (*527*)
17	Ikeda (*315*)	*36*	Nakatombetsu (*247*)	*55*	Saroma (*348*)	*74*	Yubetsu (*285*)
18	Ikutahara (*285*)	*37*	Nemuro (*432*)	*56*	Shari (*325*)		
19	Itokushibetsu (*341*)	*38*	Nemuro (ss) (*351*)	*57*	Shibecha (*346*)		

**ss = surface stations (stations with records from 1890's), others are from 1970's*

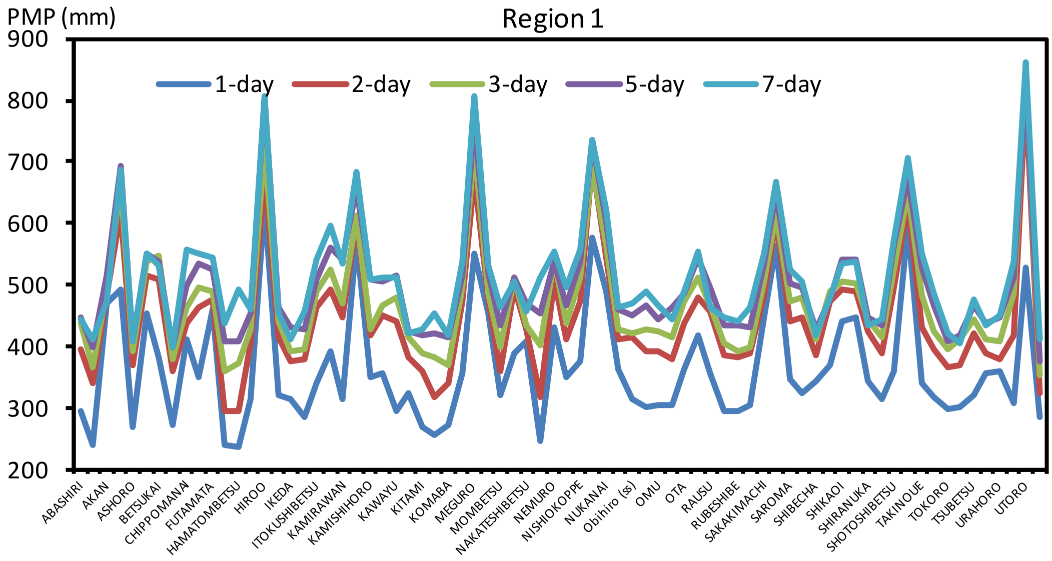

(a)

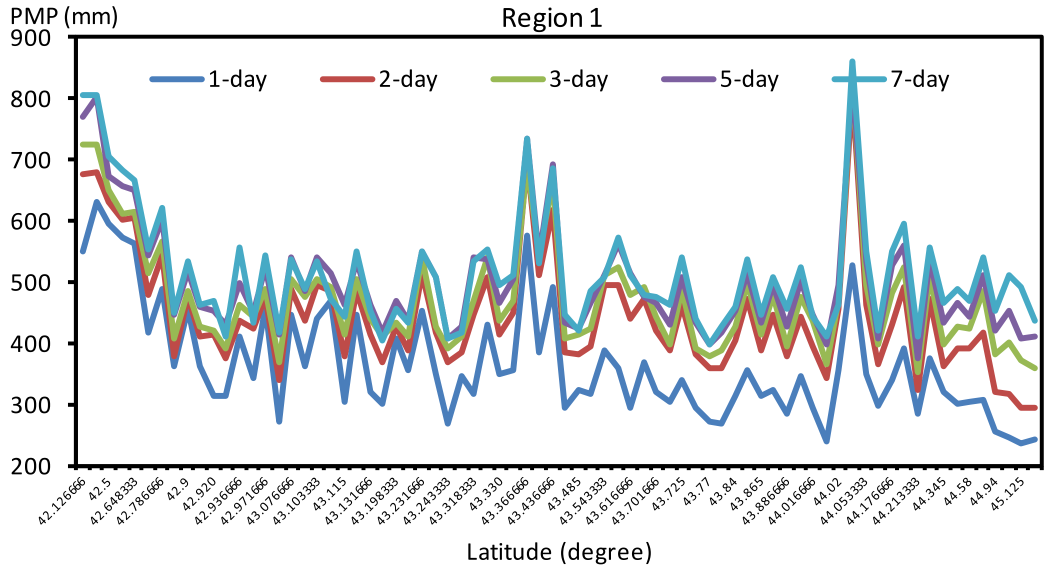

(b)

Figure 6-24: Point statistical PMP estimates for Region 1: (a) by station name, and (b) by latitudes

6.5.2 *Region 2*

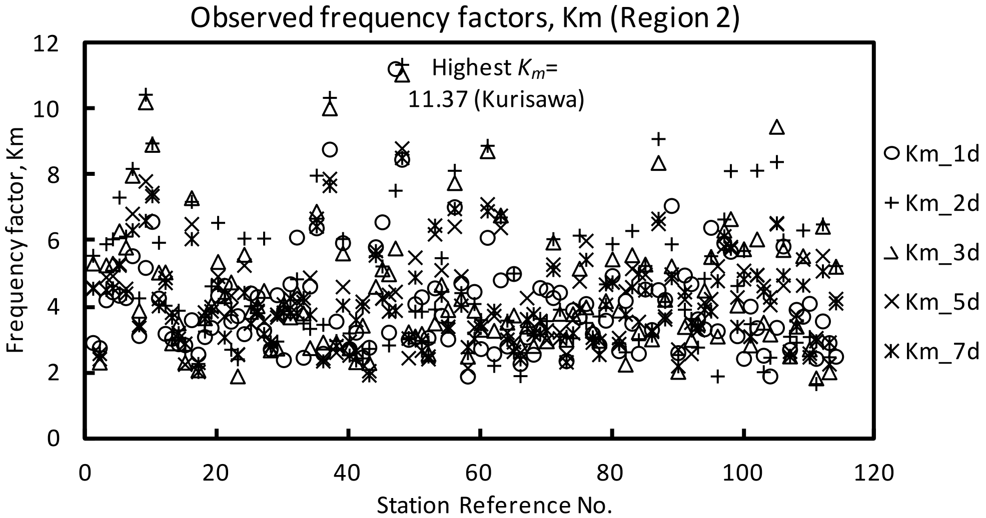

Figure 6-25: Observed frequency factors, K_m for Region 2

Table 6-5 Stations list for Region 2

No.	Point (*1-d PMP*)	No.	Point (*1-d PMP*)	No.	Point (*1-d PMP*)	No.	Point (*1-d PMP*)
1	Abira (495)	*30*	Horoman (484)	59	Muroran (360)	88	Shiraoi (942)
2	Akaigawa (364)	*31*	Horonuka (494)	60	Naganuma (593)	89	Shirogane (401)
3	Asahi (437)	*32*	Ikutora (532)	61	Nakagawa (308)	90	Shizunai (600)
4	Asahikawa (425)	*33*	Imakane (484)	62	Nakakineusu (682)	91	Shosambetsu (323)
5	Asahikawa (ss) (413)	*34*	Ishikarinumata (472)	63	Nayoro (332)	92	Shumarinai (493)
6	Ashibetsu (434)	*35*	Ishizaki (482)	64	Noboribetsu (964)	93	Sorachiyoshino (428)
7	Atsuma (515)	*36*	Iwamizawa (540)	65	Numakawa (252)	94	Sounkyo (414)
8	Atsuta (303)	*37*	Kakkumi (802)	66	Numanosawa (468)	95	Soyamisaki (285)
9	Bibai (567)	*38*	Kamifurano (467)	67	Okishi (372)	96	Suttsu (ss) (378)
10	Biei (320)	*39*	Kamikawa (335)	68	Onuma (444)	97	Takikawa (436)
11	Bifuka (283)	*40*	Kamoenai (316)	69	Oshamambe (413)	98	Tappu (410)
12	Bikuni (444)	*41*	Kashima (474)	70	Osokinai (402)	99	Teimiyama (484)
13	Date (344)	*42*	Kikonai (402)	71	Otaki (667)	100	Teshio (345)
14	Embetsu (291)	*43*	Kimobetsu (352)	72	Otaru (329)	101	Tomakomai (486)
15	Eniwashimamatsu (635)	*44*	Koganeyu (571)	73	Otoineppu (334)	102	Toyakoonsen (346)
16	Erimomisaki (393)	*45*	Kotambetsu (339)	74	Pippu (410)	103	Toyotomi (261)
17	Esashi (481)	*46*	Kumaishi (626)	75	Rankoshi (319)	104	Tsukigata (365)
18	Etambetsu (439)	*47*	Kurisawa (534)	76	Rokugo (512)	105	Urakawa (406)
19	Fukagawa (427)	*48*	Kuromatsunai (371)	77	Rumoi (370)	106	Urausu (352)
20	Furano (475)	*49*	Kutchan (314)	78	Rumoi (355)	107	Uzura (493)
21	Haboro (343)	*50*	Kutsugata (358)	79	Sapporo (ss) (416)	108	Wassamu (396)
22	Hakodate (294)	*51*	Kyowa (327)	80	Sengen (453)	109	Yagishiri (414)
23	Hamamasu (274)	*52*	Makkari (330)	81	Setana (429)	110	Yakumo (463)
24	Hidaka (810)	*53*	Mashike (313)	82	Shibetsu (419)	111	Yamaguchi (420)
25	Hidakamombetsu (766)	*54*	Matsumae (317)	83	Shikotsukohan (692)	112	Yoichi (359)
26	Higashikawa (317)	*55*	Mitsuishi (504)	84	Shimokawa (414)	113	Yubari (438)
27	Hobetsu (779)	*56*	Mori (570)	85	Shimukappu (691)		
28	Hokuto (417)	*57*	Morino (717)	86	Shinshinotsu (412)		
29	Horokanai (408)	*58*	Mukawa (765)	87	Shinwa (814)		

**ss = surface stations (stations with records from 1890's), others are from 1970's*

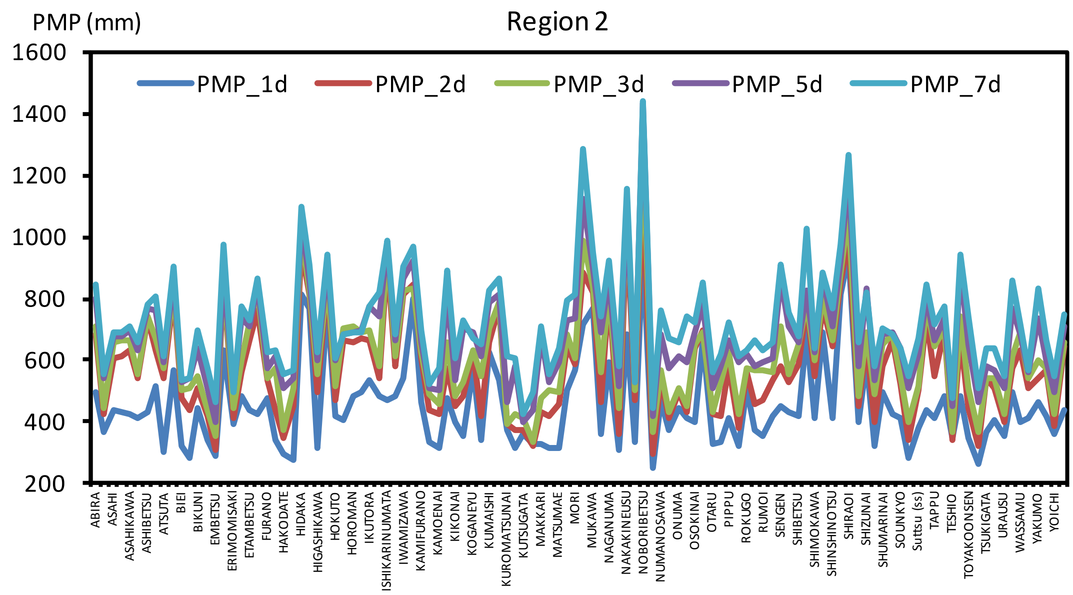

(a)

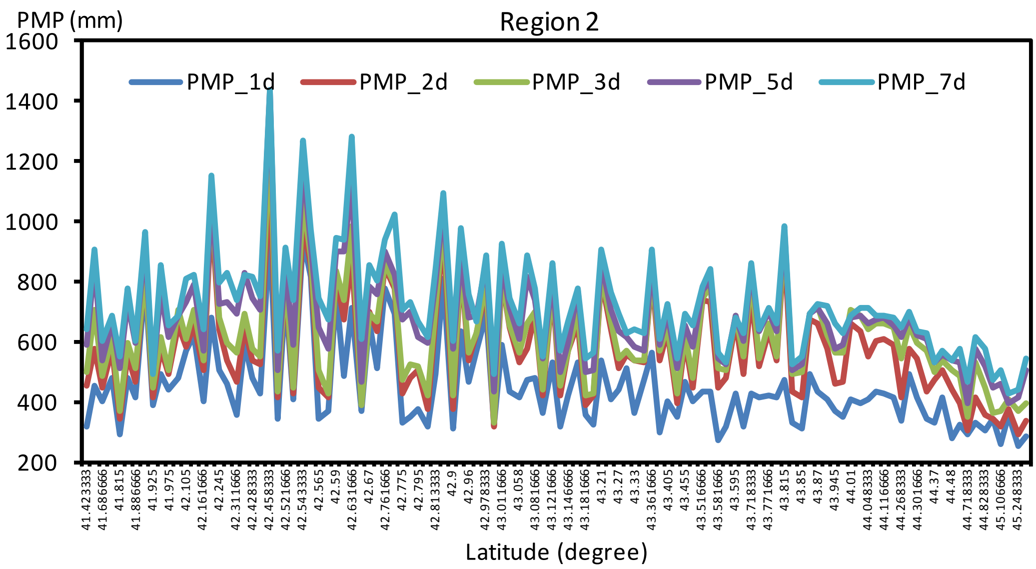

(b)

Figure 6-26: Point statistical PMP estimates for Region 2: **(a)** by station name, and **(b)** by latitudes

6.5.3 *Region 3*

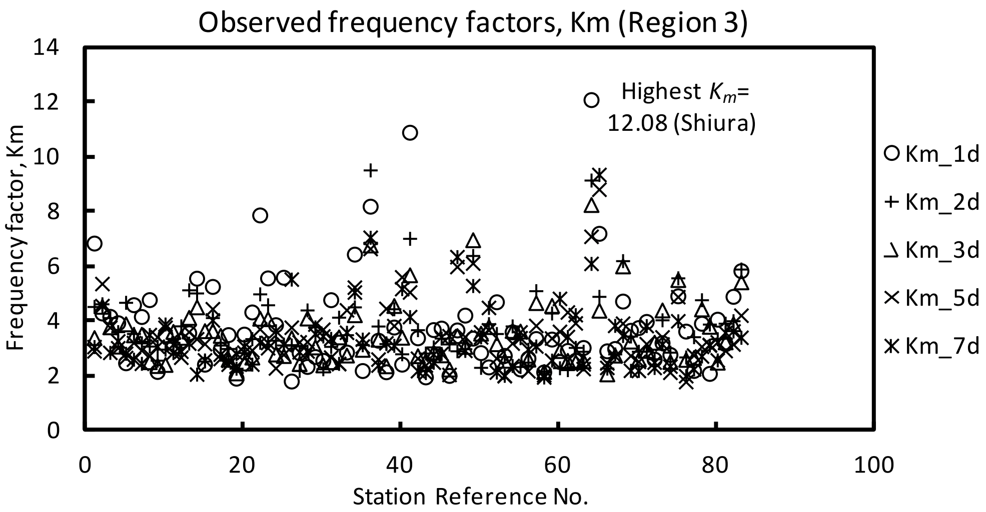

Figure 6-27: Observed frequency factors, K_m for Region 3

Table 6-6: Stations list for Region 3

No.	Point (*1-d PMP*)	No.	Point (*1-d PMP*)	No.	Point (*1-d PMP*)	No.	Point (*1-d PMP*)
1	Ajigasawa (387)	*22*	Hirosaki (528)	*43*	Murayama (367)	*64*	Tadami (731)
2	Akita (ss) (401)	*23*	Hitachinai (493)	*44*	Nagai (412)	*65*	Tajima (556)
3	Aniai (471)	*24*	Honjo (434)	*45*	Nakatsugawa (332)	*66*	Takahata (387)
4	Aomori (584)	*25*	Horohayama (370)	*46*	Nango (405)	*67*	Takamine (370)
5	Arasawa (496)	*26*	Ikarigaseki (360)	*47*	Nibetsu (533)	*68*	Takanosu (414)
6	Aterazawa (482)	*27*	Imabetsu (369)	*48*	Nishiaizu (458)	*69*	Tateiwa (595)
7	Daishoji (452)	*28*	Inawashiro (386)	*49*	Noshiro (352)	*70*	Tazawako (584)
8	Dake (467)	*29*	Iwamisanna (460)	*50*	Nurukawa (325)	*71*	Tsuruoka (400)
9	Fujisato (510)	*30*	Jimba (451)	*51*	Obanazawa (354)	*72*	Wakamatsu (449)
10	Fujiwara (416)	*31*	Kakunodate (524)	*52*	Odate (465)	*73*	Yamagata (342)
11	Fukaura (403)	*32*	Kamikusatsu (597)	*53*	Oga (432)	*74*	Yamagata (ss) (467)
12	Gojome (399)	*33*	Kaneyama (548)	*54*	Ogashinzan (461)	*75*	Yashima (360)
13	Goshogawara (356)	*34*	Kaneyama (402)	*55*	Ogata (445)	*76*	Yasumiya (436)
14	Hachimantai (465)	*35*	Kanita (358)	*56*	Oguni (629)	*77*	Yokote (459)
15	Hachimori (446)	*36*	Karikawa (684)	*57*	Oisawa (482)	*78*	Yonezawa (339)
16	Hibara (454)	*37*	Kazuno (350)	*58*	Omagari (509)	*79*	Yoroibata (613)
17	Higashinaruse (341)	*38*	Kitakata (504)	*59*	Owani (360)	*80*	Yunotai (316)
18	Higashiyuri (371)	*39*	Konan (531)	*60*	Sasunabe (557)	*81*	Yuzawa (363)
19	Hijiori (427)	*40*	Kuroishi (544)	*61*	Semi (302)	*82*	Yuze (466)
20	Hinoemata (580)	*41*	Moriyoshiyama (451)	*62*	Shinjo (367)	*83*	Tadami (731)
21	Hinokinai (569)	*42*	Mukaimachi (317)	*63*	Shiura (617)		

**ss = surface stations (stations with records from 1890's), others are from 1970's*

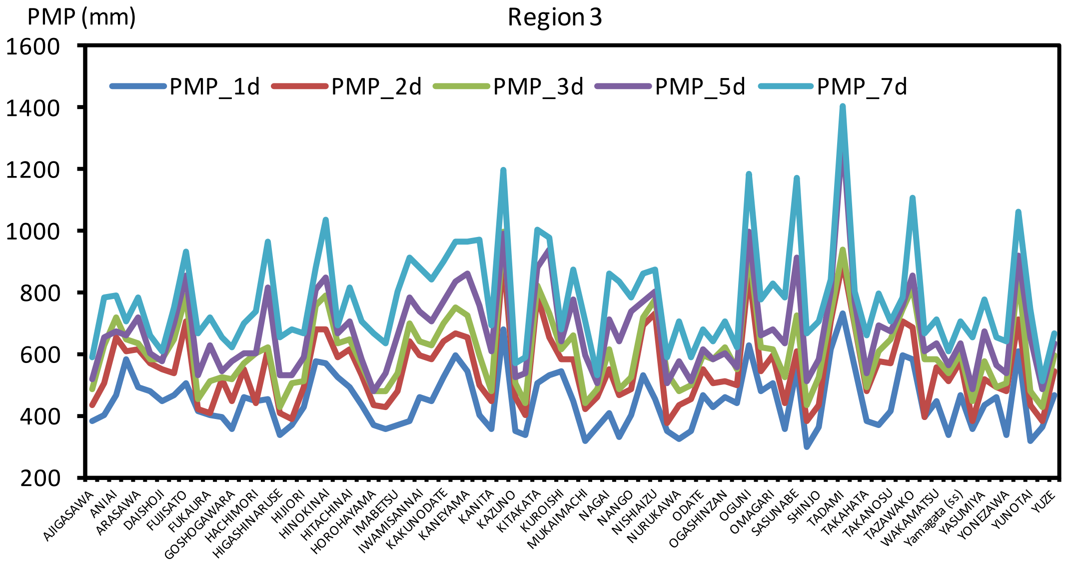

(a)

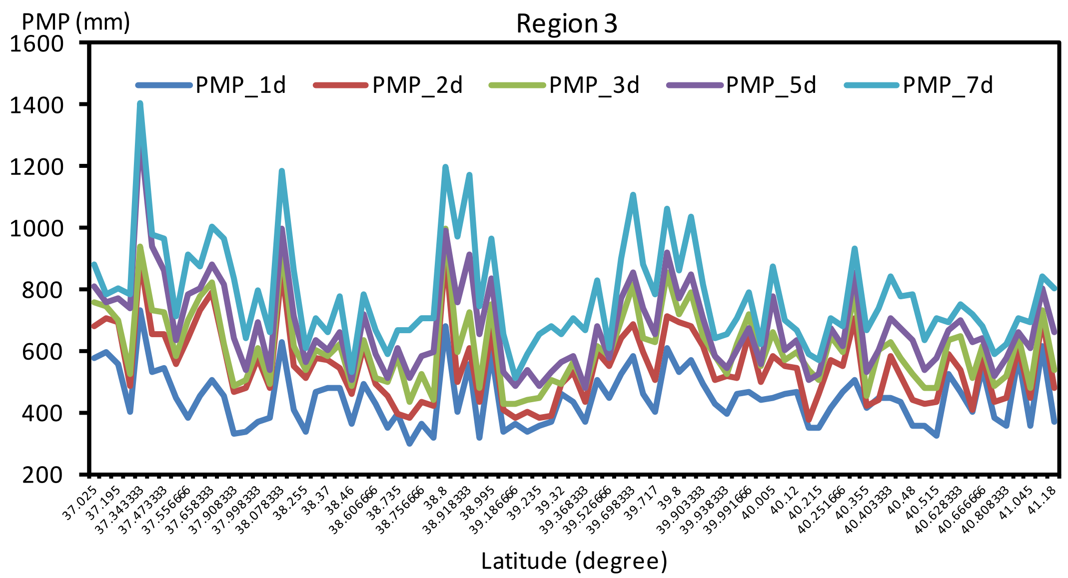

(b)

Figure 6-28: Point statistical PMP estimates for Region 3: **(a)** by station name, and **(b)** by latitudes

6.5.4 *Region 4*

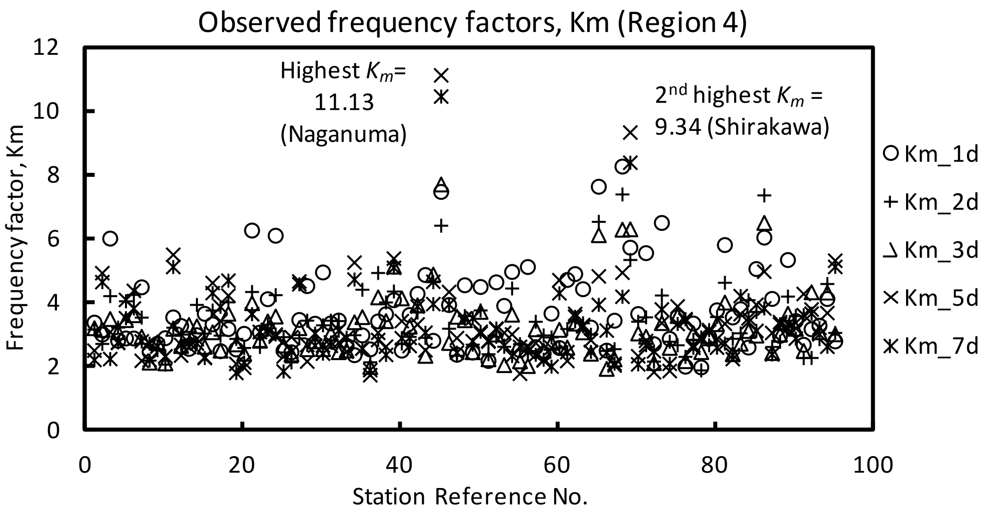

Figure 6-29: Observed frequency factors, K_m for Region 4

Table 6-7 Stations list for Region 4

No.	Point (*1-d PMP*)	No.	Point (*1-d PMP*)	No.	Point (*1-d PMP*)	No.	Point (*1-d PMP*)
1	Araya (379)	*25*	Kawai (416)	*49*	Odanosawa (428)	*73*	Soma (653)
2	Enoshima (507)	*26*	Kawamae (625)	*50*	Ofunato (464)	*74*	Sumita (488)
3	Esashi (400)	*27*	Kawatabi (340)	*51*	Ogatsu (717)	*75*	Taira (507)
4	Fudai (716)	*28*	Kawauchi (739)	*52*	Ohasama (317)	*76*	Taneichi (527)
5	Fukushima (376)	*29*	Kesennuma (453)	*53*	Ohira (381)	*77*	Tomioka (666)
6	Furukawa (347)	*30*	Kitakami (498)	*54*	Okunakayama (391)	*78*	Toono (373)
7	Hachinohe (382)	*31*	Koma (319)	*55*	Oma (288)	*79*	Towada (497)
8	Haramachi (633)	*32*	Komanoyu (550)	*56*	Omoto (637)	*80*	Toyosawa (501)
9	Herai (514)	*33*	Kooriyama (316)	*57*	Onahama (506)	*81*	Tsukidate (311)
10	Higashi. (378)	*34*	Koromogawa (302)	*58*	Ono (564)	*82*	Tsushima (551)
11	Hippo (855)	*35*	Kuji (568)	*59*	Ononiimachi (372)	*83*	Wakayanagi (336)
12	Hirono (628)	*36*	Kuzumaki (317)	*60*	Rokkasho (417)	*84*	Wakinosawa (370)
13	Ichinoseki (335)	*37*	Marumori (492)	*61*	Sannohe (471)	*85*	Watari (576)
14	Iitate (695)	*38*	Matsurube (619)	*62*	Sawauchi (526)	*86*	Yabukawa (282)
15	Ishikawa (315)	*39*	Misawa (379)	*63*	Semmaya (276)	*87*	Yamada (571)
16	Ishinomaki (343)	*40*	Miyako (704)	*64*	Sendai (512)	*88*	Yamagata (476)
17	Ishinomaki(*ss*) (331)	*41*	Miyako (*ss*)(589)	*65*	Shichinohe (393)	*89*	Yamatoyama (546)
18	Iwaizumi (507)	*42*	Morioka (382)	*66*	Shimotokusari (736)	*90*	Yanagawa (350)
19	Iwatematsuo (429)	*43*	Mutsu (373)	*67*	Shiogama (519)	*91*	Yonesato (294)
20	Kakkonda (445)	*44*	Naganuma (584)	*68*	Shirakawa (495)	*92*	Yoneyama (337)
21	Kamaishi (746)	*45*	Nihommatsu (408)	*69*	Shiroishi (450)	*93*	Yuda (536)
22	Karumai (462)	*46*	Nikkawa (419)	*70*	Shiwa (420)	*94*	Yumoto (549)
23	Kashimadai (386)	*47*	Ninohe (415)	*71*	Shizugawa (357)		
24	Katoono (653)	*48*	Noheji (406)	*72*	Shizukuishi (429)		

**ss = surface stations (stations with records from 1890's), others are from 1970's*

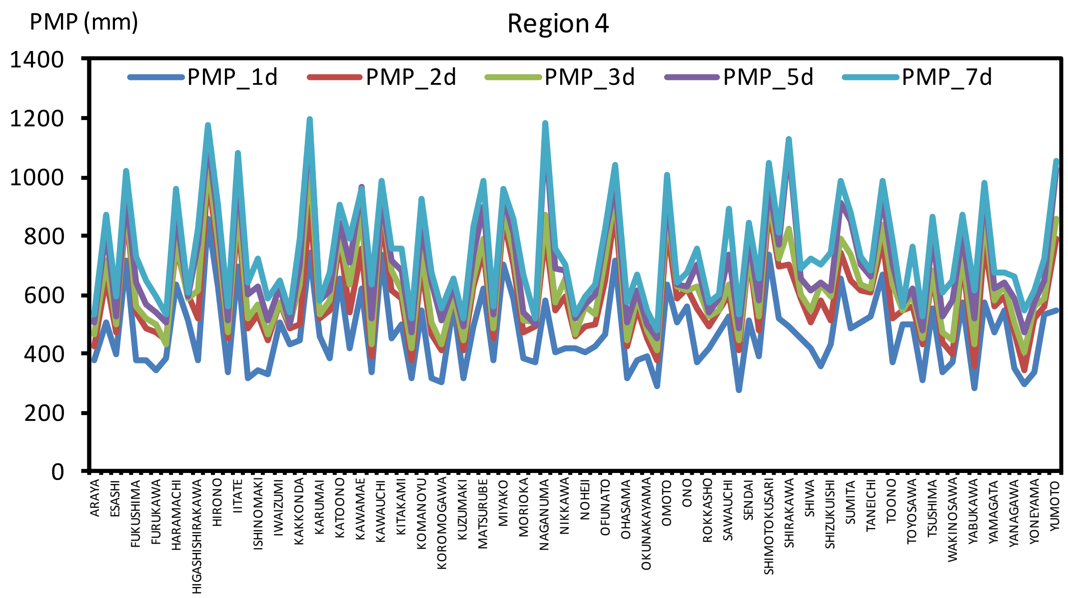

(a)

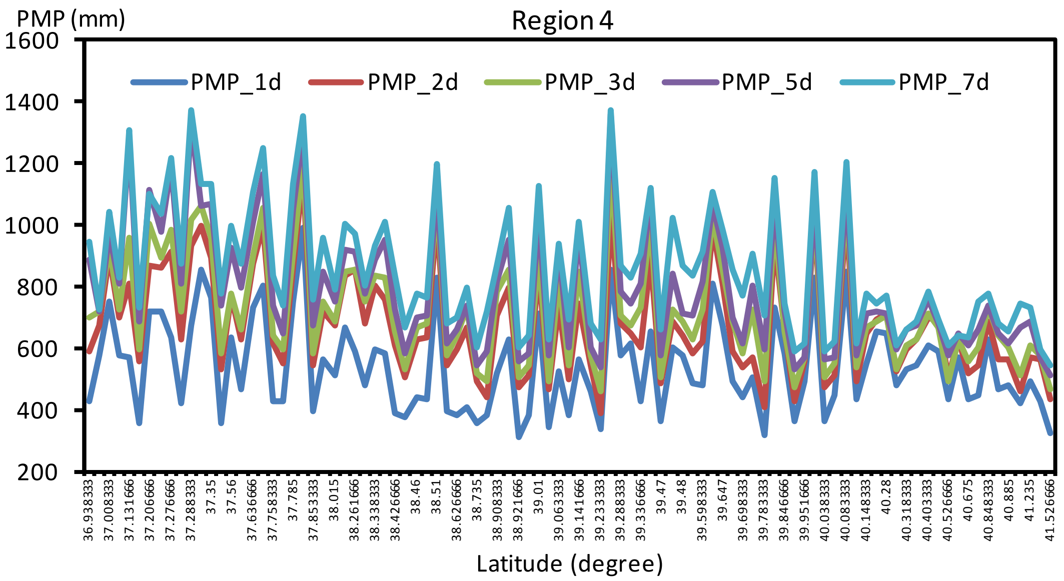

(b)

Figure 6-30: Point statistical PMP estimates for Region 4: **(a)** by station name, and **(b)** by latitudes

6.5.5 *Region 5*

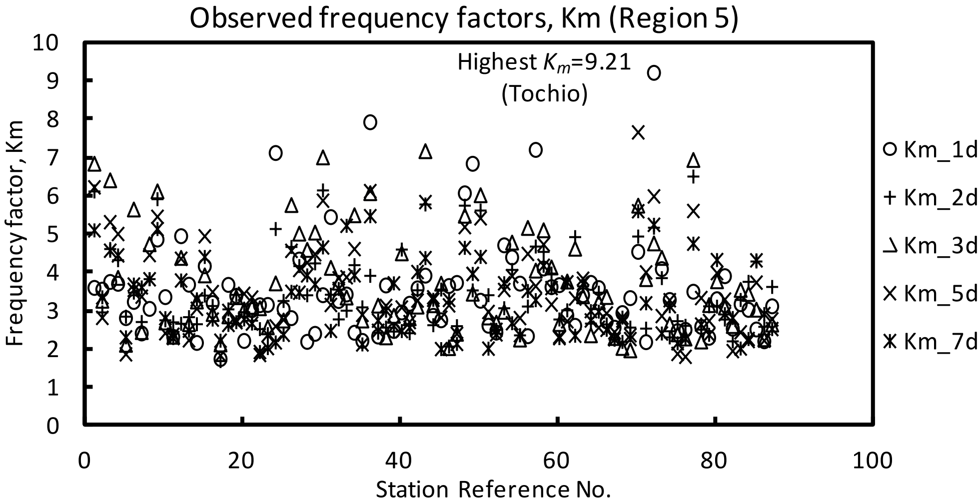

Figure 6-31: Observed frequency factors, K_m for Region 5

Table 6-8: Stations list for Region 5

No.	Point (*1-d PMP*)	No.	Point (*1-d PMP*)	No.	Point (*1-d PMP*)	No.	Point (*1-d PMP*)
1	Akadani (552)	*23*	Kasadake (563)	*45*	Nakajo (418)	*67*	Shirakawa (536)
2	Awashima (356)	*24*	Kashiwazaki (438)	*46*	Nanao (400)	*68*	Sugadaira (354)
3	Fukui (409)	*25*	Kawai (565)	*47*	Nantotakamiya (340)	*69*	Suzu (441)
4	Fukui (ss) (384)	*26*	Kayano (433)	*48*	Nezugaseki (472)	*70*	Takada (357)
5	Fushiki (401)	*27*	Koide (480)	*49*	Niigata (470)	*71*	Takane (574)
6	Fushiki (ss) (394)	*28*	Komatsu (403)	*50*	Niitsu (378)	*72*	Tochio (722)
7	Hakui (354)	*29*	Koshino (421)	*51*	No (420)	*73*	Tokamachi (403)
8	Hakusanyo. (368)	*30*	Maki (320)	*52*	Nozawaonsen (319)	*74*	Tomari (464)
9	Hamochi (511)	*31*	Matsudai (474)	*53*	Ogata (452)	*75*	Tonami (345)
10	Himi (410)	*32*	Matsumoto (335)	*54*	Oguni (481)	*76*	Toyama (329)
11	Hiraiwa (417)	*33*	Matsumoto (ss) (312)	*55*	Omachi (328)	*77*	Tsugawa (572)
12	Hotaka (282)	*34*	Mikuni (416)	*56*	Ono (355)	*78*	Tsunan (342)
13	Iiyama (343)	*35*	Miomote (445)	*57*	Oyu (526)	*79*	Tsuruga (317)
14	Imajo (299)	*36*	Miyama (477)	*58*	Ryotsu (512)	*80*	Tsuruga (ss) (425)
15	Irihirose (447)	*37*	Monzen (320)	*59*	Sanjo (454)	*81*	Ueda (313)
16	Itoigawa (411)	*38*	Mumaya (624)	*60*	Sekiyama (392)	*82*	Uozu (398)
17	Kahoku (370)	*39*	Murakami (419)	*61*	Shika (300)	*83*	Wajima (457)
18	Kakeyu (416)	*40*	Muramatsu (394)	*62*	Shimoseki (404)	*84*	Yanagase (300)
19	Kamiichi (430)	*41*	Nagano (280)	*63*	Shinanomachi (325)	*85*	Yasuzuka (335)
20	Kamikochi (362)	*42*	Nagano (ss) (240)	*64*	Shinshushim. (318)	*86*	Yatsuo (415)
21	Kamioka (435)	*43*	Nagaoka (482)	*65*	Shiozawa (290)		
22	Kanazawa (400)	*44*	Nagawa (435)	*66*	Nakajo (418)		

**ss = surface stations (stations with records from 1890's), others are from 1970's*

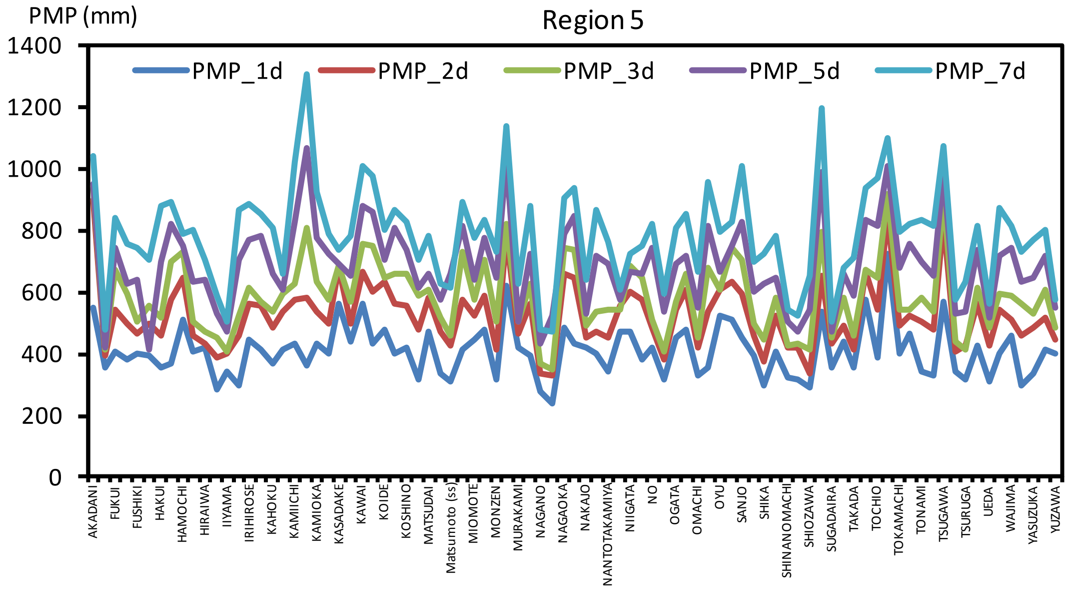

(a)

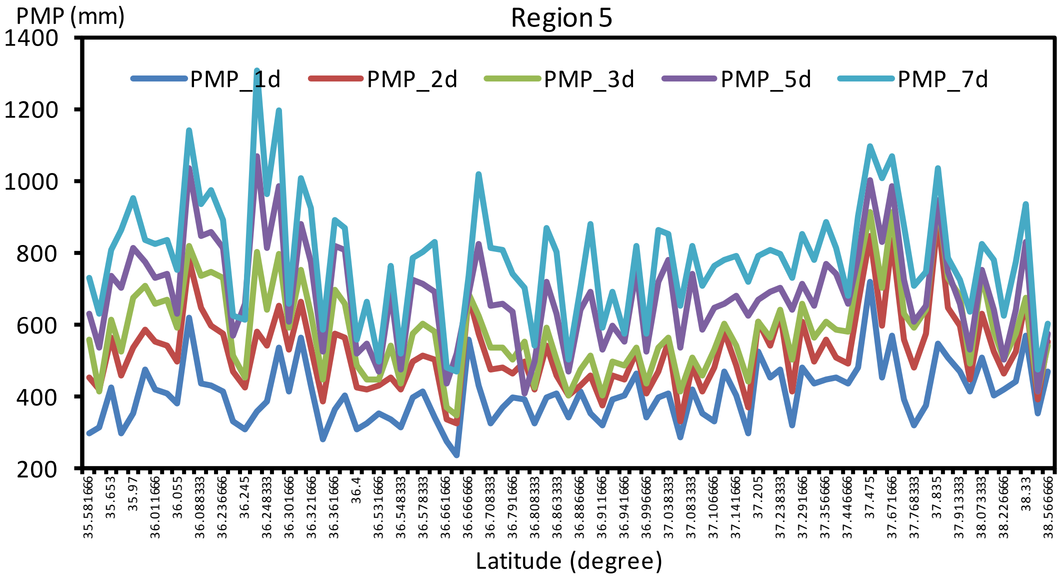

(b)

Figure 6-32: Point statistical PMP estimates for Region 5: **(a)** by station name, and **(b)** by latitudes

6.5.6 *Region 6*

Nasu is a high discordance site, thus the K_m value used are taken from Minamikami station which is the station having the largest frequency factor, K_m after Nasu.

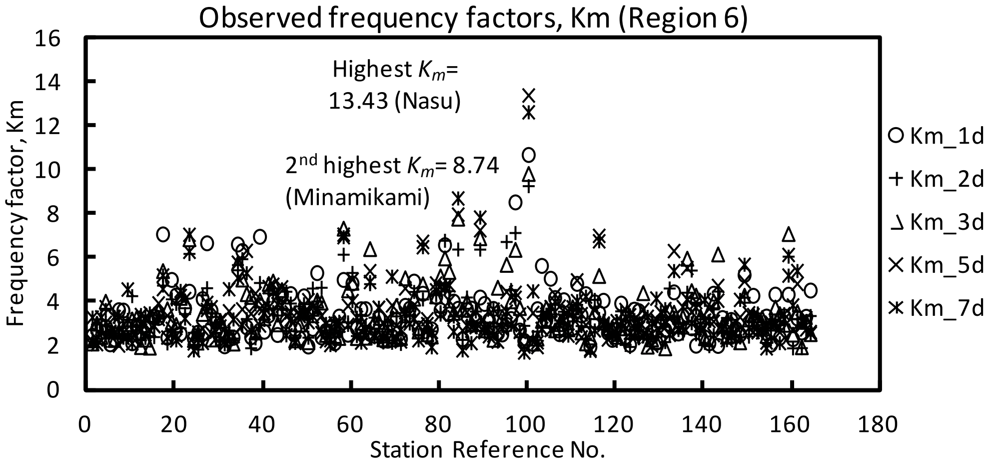

Figure 6-33: Observed frequency factors, K_m for Region 6

Table 6-9: Stations list for Region 6

No.	Point (*1-d PMP*)	No.	Point (*1-d PMP*)	No.	Point (*1-d PMP*)	No.	Point (*1-d PMP*)	No.	Point (*1-d PMP*)
1	Abiko (575)	*34*	Iida (ss) (452)	*67*	Koga (345)	*100*	Nasu (962)	*133*	Shioya (468)
2	Ajiro (523)	*35*	Iijima (539)	*68*	Konosu (466)	*101*	Nerima (581)	*134*	Shiraito (759)
3	Anan (599)	*36*	Ikari (445)	*69*	Koshigaya (500)	*102*	Niijima (788)	*135*	Shizuoka (767)
4	Ashikaga (531)	*37*	Ikawa (1123)	*70*	Koshikidaira (717)	*103*	Nirasaki (635)	*136*	Suwa (316)
5	Ashio (695)	*38*	Imaichi (564)	*71*	Kuki (490)	*104*	Nishinom. (567)	*137*	Takanezawa (373)
6	Bando (472)	*39*	Inatori (774)	*72*	Kuma (823)	*105*	Nobeyama (440)	*138*	Tanzawako (784)
7	Chiba (534)	*40*	Irozaki (613)	*73*	Kumagai (ss) (585)	*106*	Numata (301)	*139*	Tashiro (503)
8	Chichibu (848)	*41*	Isesaki (410)	*74*	Kumagaya (554)	*107*	Odawara (485)	*140*	Tatebayashi (326)
9	Choshi (521)	*42*	Iwata (478)	*75*	Kurohone (439)	*108*	Ogochi (1023)	*141*	Tateshina (349)
10	Daigo (393)	*43*	Kadoi (425)	*76*	Kuroiso (726)	*109*	Oizumi (368)	*142*	Tateyama (592)
11	Dorobu (789)	*44*	Kakegawa (551)	*77*	Kusatsu (553)	*110*	Okunikko (1138)	*143*	Tatsuno (349)
12	Ebina (579)	*45*	Kakioka (467)	*78*	Kuzuu (399)	*111*	Omaezaki (649)	*144*	Tenryu (462)
13	Edosaki (543)	*46*	Kamisatomi (615)	*79*	Kyonan (866)	*112*	Ome (570)	*145*	Tochigi (351)
14	Fuchu (591)	*47*	Kamiyoshida (659)	*80*	Maebashi (404)	*113*	Ootaki (683)	*146*	Tokorozawa (534)
15	Fuji (616)	*48*	Kamogawa (588)	*81*	Maebashi (ss) (478)	*114*	Ose (429)	*147*	Tokuda (452)
16	Fujioka (532)	*49*	Kanna (757)	*82*	Matsuzaki (586)	*115*	Oshika (379)	*148*	Tokyo (629)
17	Fujiwara (450)	*50*	Kanuma (350)	*83*	Mikkabi (534)	*116*	Otawara (427)	*149*	Tokyo (ss) (590)
18	Furuseki (802)	*51*	Karasuyama (377)	*84*	Minakami (355)	*117*	Otsuki (834)	*150*	Tomi (300)
19	Gotemba (959)	*52*	Karuizawa (528)	*85*	Minamishin. (579)	*118*	Oyama (334)	*151*	Tonosho (534)
20	Hachioji (674)	*53*	Kasama (417)	*86*	Minori (523)	*119*	Ozawa (881)	*152*	Tsuchiura (431)
21	Hakone (1290)	*54*	Kashima (761)	*87*	Mishima (630)	*120*	Ryugasaki (499)	*153*	Uenohara (739)
22	Hamamatsu (395)	*55*	Katashina (323)	*88*	Mito (530)	*121*	Sagamih. (692)	*154*	Umegashima (1319)
23	Hamamatsu (ss) (575)	*56*	Katsunuma (516)	*89*	Mito (ss) (489)	*122*	Sagamiko (800)	*155*	Urayama (1066)
24	Hanazono (795)	*57*	Katsuura (688)	*90*	Mitsumine (927)	*123*	Saitama (532)	*156*	Ushiku (620)
25	Haneda (564)	*58*	Kawaguchiko (890)	*91*	Miura (544)	*124*	Sakahata (763)	*157*	Utsunomiya (386)
26	Hanno (567)	*59*	Kawaneh. (827)	*92*	Miyakejima (784)	*125*	Saku (440)	*158*	Utsunomiya (ss) (417)
27	Haramura (313)	*60*	Kikugawa. (777)	*93*	Miyatakogen (461)	*126*	Sakuma (752)	*159*	Yamanaka (965)
28	Harunasan (901)	*61*	Kiriishi (850)	*94*	Mobara (541)	*127*	Sakura (545)	*160*	Yokohama (584)
29	Hatoyama (565)	*62*	Kiryu (396)	*95*	Mooka (350)	*128*	Sano (341)	*161*	Yokohama (ss) (572)
30	Hiratsuka (428)	*63*	Kisarazu (620)	*96*	Nakano (423)	*129*	Setagaya (578)	*162*	Yokoshib. (532)
31	Hitachi (541)	*64*	Kisohirasawa (368)	*97*	Nakanojo (602)	*130*	Shimizu (593)	*163*	Yorii (603)
32	Hiyoshi (603)	*65*	Kitaibaraki (521)	*98*	Nambu (995)	*131*	Shimkiba (578)	*164*	Yugashima (1138)
33	Hokota (536)	*66*	Kofu (ss) (504)	*99*	Namiai (605)	*132*	Shimotsuma (445)		

**ss = surface stations (stations with records from 1890's), others are from 1970's*

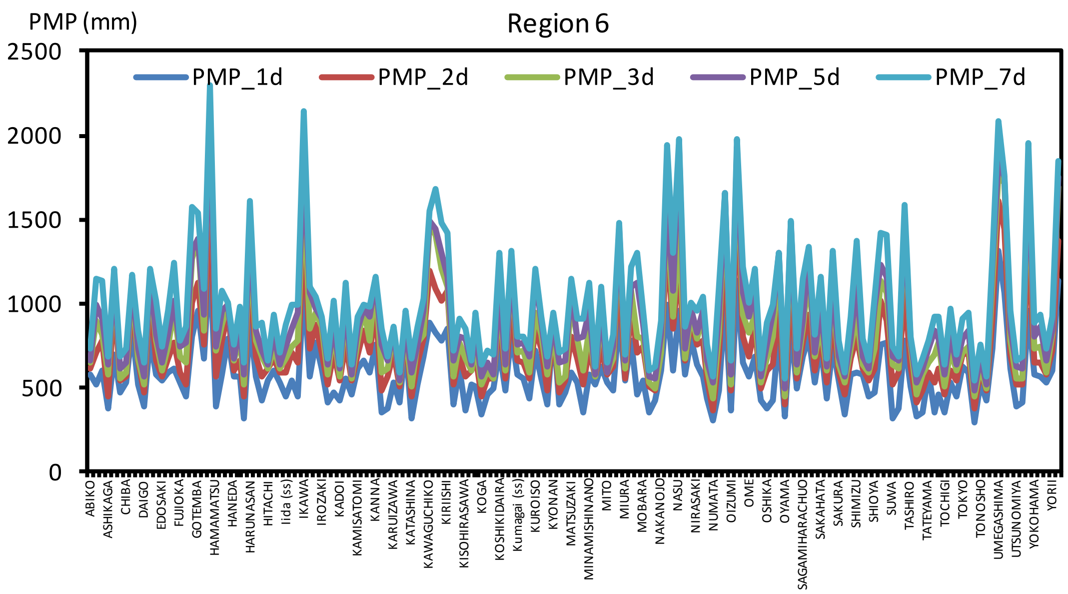

(a)

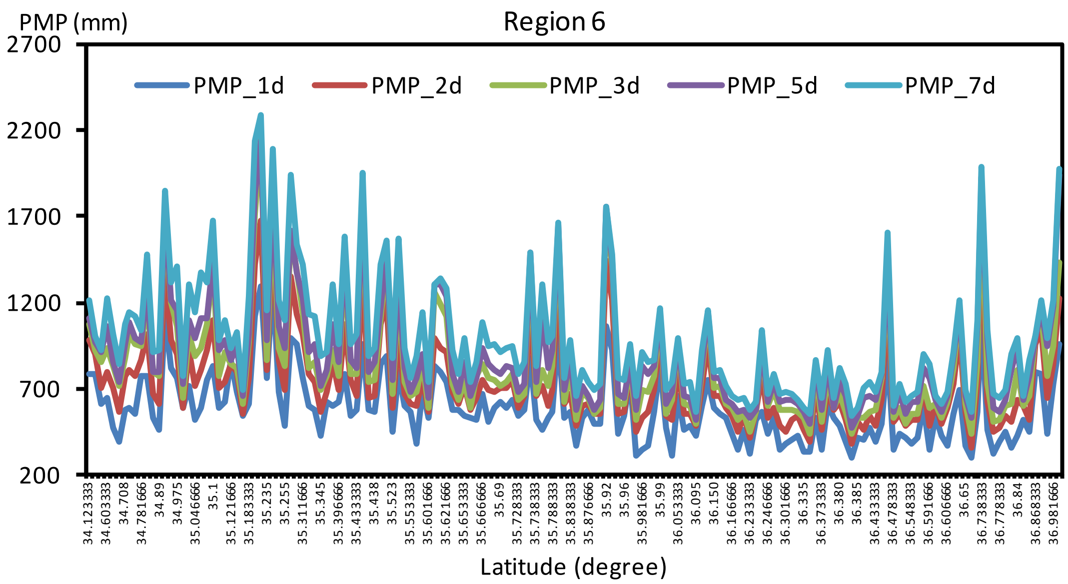

(b)

Figure 6-34: Point statistical PMP estimates for Region 6: **(a)** by station name, and **(b)** by latitudes

6.5.7 *Region 7*

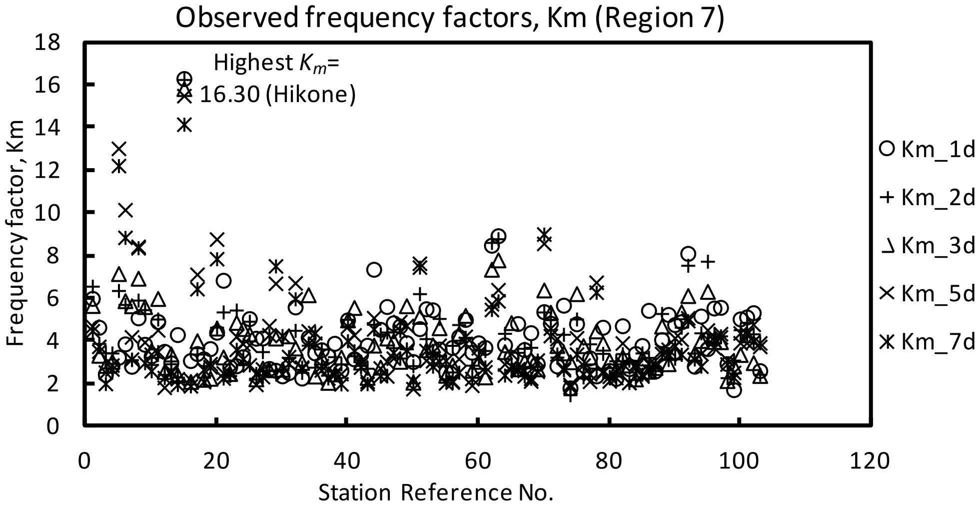

Figure 6-35: Observed frequency factors, K_m for Region 7

Table 6-10: Stations list for Region 7

No.	Point (*1-d PMP*)	No.	Point (*1-d PMP*)	No.	Point (*1-d PMP*)	No.	Point (*1-d PMP*)
1	Aisai (857)	27	Kaidakogen (787)	*53*	Mitsumorisan (924)	*79*	Shimizu (1027)
2	Alpine (ss) (752)	28	Kameyama (861)	*54*	Miyagawa (2442)	*80*	Shingu (1116)
3	Ena (836)	29	Kamiishizu (1179)	*55*	Miyaji (614)	*81*	Shionomisaki (1153)
4	Gamagoori (821)	30	Kamikitayama (2866)	*56*	Miyanomae (712)	*82*	Shirahama (789)
5	Gifu (775)	31	Kanayama (631)	*57*	Nabari (945)	*83*	Soni (1381)
6	Gifu (ss) (763)	32	Kanie (857)	*58*	Nagaokakyo (820)	*84*	Suhara (720)
7	Gojo (521)	33	Katsuragi (649)	*59*	Nagataki (1269)	*85*	Suijo (729)
8	Hachiman (1214)	34	Kawachin. (688)	*60*	Nagiso (711)	*86*	Tahara (817)
9	Hagiwara (768)	35	Kayumi (1898)	*61*	Nagoya (1209)	*87*	Tajimi (916)
10	Hakusan (1215)	36	Kazeya (1586)	*62*	Nagoya (ss) (880)	*88*	Takayama (788)
11	Hari (648)	37	Keihoku (718)	*63*	Nakatsugawa (747)	*89*	Tarumi (1600)
12	Higashiomi (548)	38	Kiinagashima (1322)	*64*	Nara (537)	*90*	Tawaramoto (579)
13	Hikigawa (1351)	39	Kisofukushima (585)	*65*	Nishikawa (1916)	*91*	Tokai (1442)
14	Hikone (498)	40	Kobe (ss) (897)	*66*	Nose (744)	*92*	Torahime (366)
15	Hikone (ss) (1002)	41	Koyasan (777)	*67*	Obara (764)	*93*	Toyonaka (854)
16	Hirakata (582)	42	Kumatori (793)	*68*	Obata (1143)	*94*	Toyota (719)
17	Hokusei (754)	43	Kurisugawa (1146)	*69*	Ogaki (946)	*95*	Tsu (1346)
18	Hongu (1618)	44	Kuwana (1010)	*70*	Okazaki (789)	*96*	Tsu (ss) (1107)
19	Ibigawa (1250)	45	Kyotanabe (593)	*71*	Omihachiman (638)	*97*	Tsuchiyama (814)
20	Ichinomiya (926)	46	Kyoto (737)	*72*	Osaka (ss) (617)	*98*	Tsukude (1054)
21	Ikomayama (781)	47	Kyoto (ss) (785)	*73*	Otsu (619)	*99*	Wakayama (1164)
22	Imazu (481)	48	Minamichita (1245)	*74*	Ouda (731)	*100*	Wakayama (ss) (975)
23	Inabu (854)	49	Minamiiese (1343)	*75*	Sakai (643)	*101*	Yokkaichi (859)
24	Irako (1008)	50	Minamikomatsu (595)	*76*	Sanda (680)	*102*	Yuasa (964)
25	Irokawa (2100)	51	Mino (784)	*77*	Sekigahara (909)		
26	Isshiki (787)	52	Minokamo (921)	*78*	Shigaraki (721)		

**ss = surface stations (stations with records from 1890's), others are from 1970's*

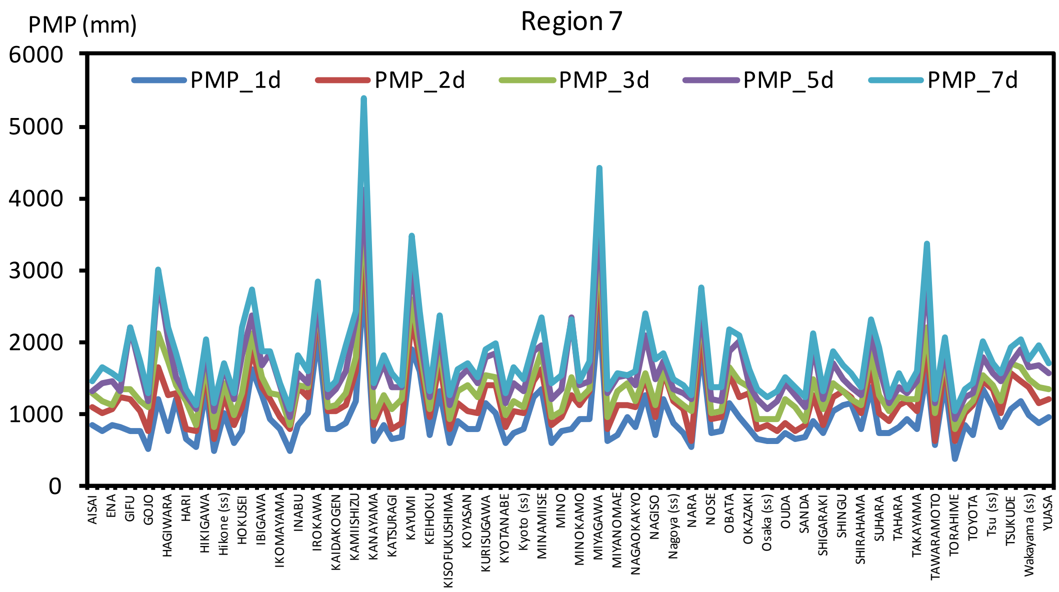

(a)

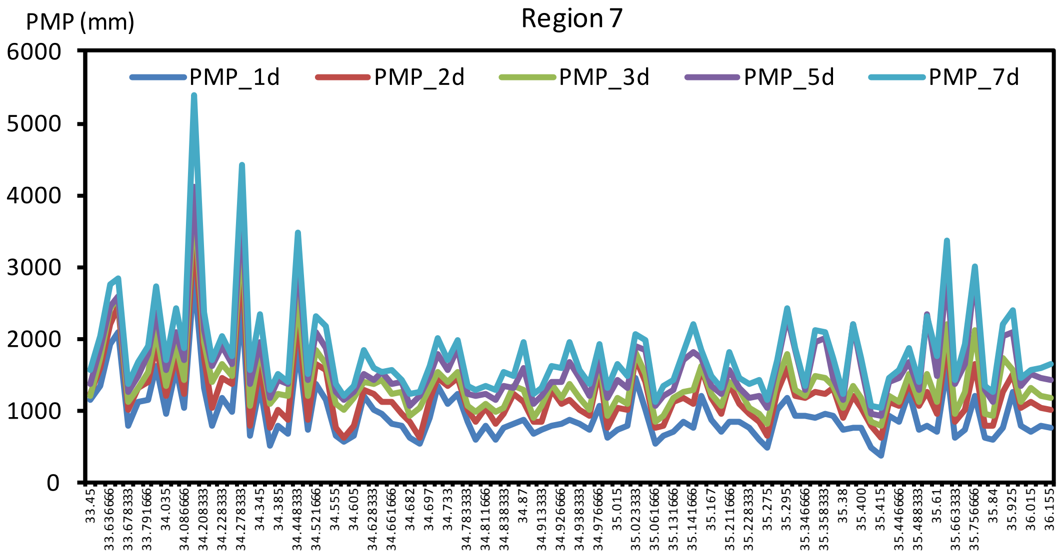

(b)

Figure 6-36: Point statistical PMP estimates for Region 7: **(a)** by station name, and **(b)** by latitudes

6.5.8 *Region 8*

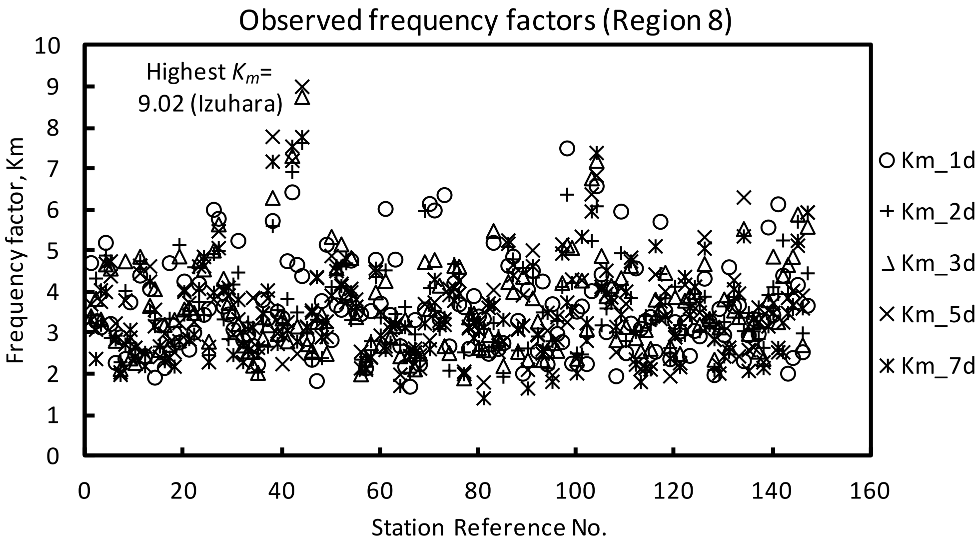

Figure 6-37: Observed frequency factors, K_m for Region 8

Table 6-11: Stations list for Region 8

No.	Point (*1-d PMP*)	No.	Point (*1-d PMP*)	No.	Point (*1-d PMP*)	No.	Point (*1-d PMP*)	No.	Point (*1-d PMP*)
1	Agenosho (634)	*31*	Hita (487)	*61*	Kumamoto (848)	*91*	Omura (560)	*121*	Tottori (431)
2	Akana (413)	*32*	Hitoyoshi (728)	*62*	Kumam. (ss) (829)	*92*	Omuta (757)	*122*	Toyooka (479)
3	Akiyoshidai (487)	*33*	Hofu (494)	*63*	Kunimi (587)	*93*	Oseto (558)	*123*	Toyota (504)
4	Akune (977)	*34*	Hondo (729)	*64*	Kurayoshi (504)	*94*	Otake (477)	*124*	Tsuwano (493)
5	Ama (541)	*35*	Honjo (461)	*65*	Kurogi (577)	*95*	Oya (495)	*125*	Ube (413)
6	Aoya (480)	*36*	Iizuka (555)	*66*	Kurume (489)	*96*	Rakanzan (801)	*126*	Ue (760)
7	Asakura (425)	*37*	Ikuno (646)	*67*	Kusu (474)	*97*	Sada (412)	*127*	Ureshino (749)
8	Ashibe (640)	*38*	Imari (718)	*68*	Maebaru (579)	*98*	Saganoseki (706)	*128*	Ushibuka (744)
9	Asootohime (902)	*39*	Innai (721)	*69*	Maizuru (489)	*99*	Saigo (466)	*129*	Wada (627)
10	Asosan (954)	*40*	Isahaya (743)	*70*	Masuda (593)	*100*	Saiki (860)	*130*	Wadayama (504)
11	Bungotakada (441)	*41*	Iwai (627)	*71*	Matsue (463)	*101*	Saji (601)	*131*	Wakasa (382)
12	Chizu (504)	*42*	Iwakuni (542)	*72*	Matsushima (678)	*102*	Sakai (488)	*132*	Watada (685)
13	Cyaya (410)	*43*	Izuhara (656)	*73*	Matsuura (676)	*103*	Sakurae (542)	*133*	Yabakei (579)
14	Daisen (689)	*44*	Izumi (700)	*74*	Mihama (547)	*104*	Sekigane (601)	*134*	Yahata (416)
15	Daito (330)	*45*	Izumo (403)	*75*	Minamata (825)	*105*	Shikano (1049)	*135*	Yamaguchi (516)
16	Dazaifu (589)	*46*	Kagumey. (560)	*76*	Minamioguni (764)	*106*	Shimon. (406)	*136*	Yanagawa (623)
17	Ebi (310)	*47*	Kahoku (806)	*77*	Mineyama (428)	*107*	Shimon. (ss) (499)	*137*	Yanai (634)
18	Ezarugi (524)	*48*	Kaibara (474)	*78*	Misumi (706)	*108*	Shinobu (556)	*138*	Yasaka (619)
19	Fukue (868)	*49*	Kakeya (401)	*79*	Miyama (417)	*109*	Shiotsu (448)	*139*	Yatsushiro (622)
20	Fukumitsu (425)	*50*	Kamin. (626)	*80*	Miyazu (398)	*110*	Shiroishi (637)	*140*	Yawata (653)
21	Fukuoka (497)	*51*	Kashima (428)	*81*	Mizuho (459)	*111*	Shitsukawa (521)	*141*	Yokota (381)
22	Fukuoka (ss) (553)	*52*	Kasumi (586)	*82*	Munakata (415)	*112*	Shuchi (449)	*142*	Yonago (405)
23	Hagi (557)	*53*	Kawamoto (444)	*83*	Naganoyama (550)	*113*	Soeda (721)	*143*	Yufuin (995)
24	Hakuta (387)	*54*	Kikuchi (752)	*84*	Nagasaki (896)	*114*	Susa (516)	*144*	Yukuhashi (505)
25	Hamada (739)	*55*	Kitsuki (465)	*85*	Nagas. (ss) (763)	*115*	Taimei (739)	*145*	Yuya (624)
26	Hamada (ss) (621)	*56*	Kosa (711)	*86*	Nakatsu (431)	*116*	Taiza (336)		
27	Haza (707)	*57*	Koyaoka (536)	*87*	Oda (422)	*117*	Takamori (638)		
28	Hikimi (437)	*58*	Kuchinotsu (566)	*88*	Oita (875)	*118*	Taketa (712)		
29	Hirado (724)	*59*	Kudamatsu (591)	*89*	Oita (ss) (793)	*119*	Tanoura (737)		
30	Hirose (625)	*60*	Kuga (676)	*90*	Ombara (544)	*120*	Tokusa (489)		

**ss = surface stations (stations with records from 1890's), others are from 1970's*

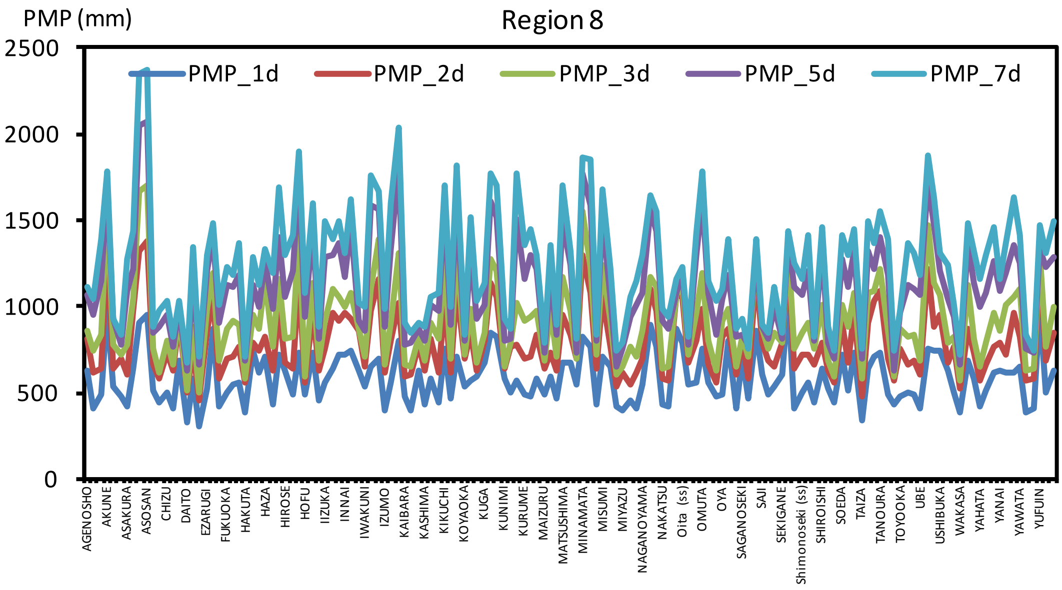

(a)

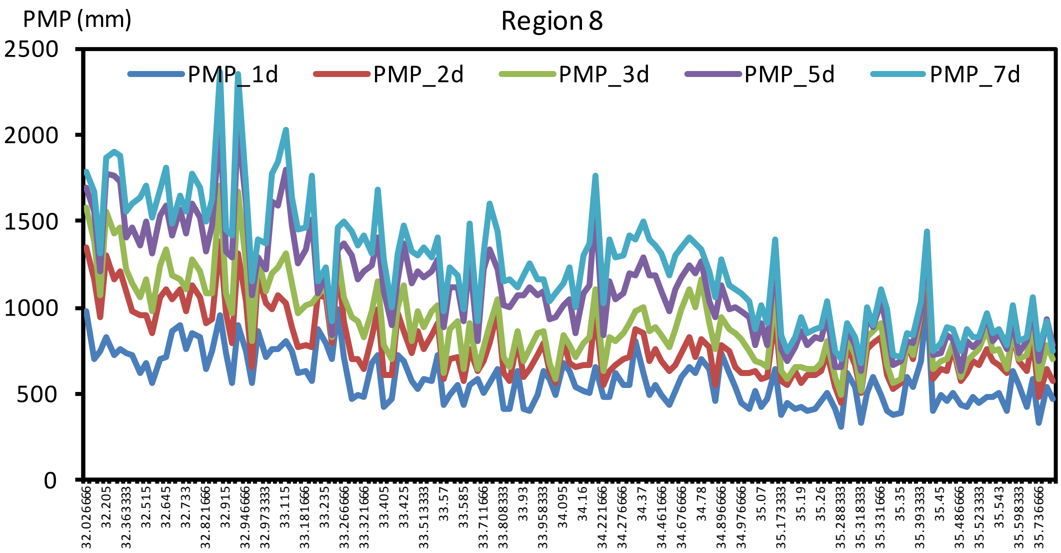

(b)

Figure 6-38: Point statistical PMP estimates for Region 8: **(a)** by station name, and **(b)** by latitudes

6.5.9 *Region 9*

Ieshima and Uchinomi are islands with both are high discordancy sites within Region 9. To represent the transposition point for K_m in Region 9, Kamigori K_m value was selected for the PMP calculation.

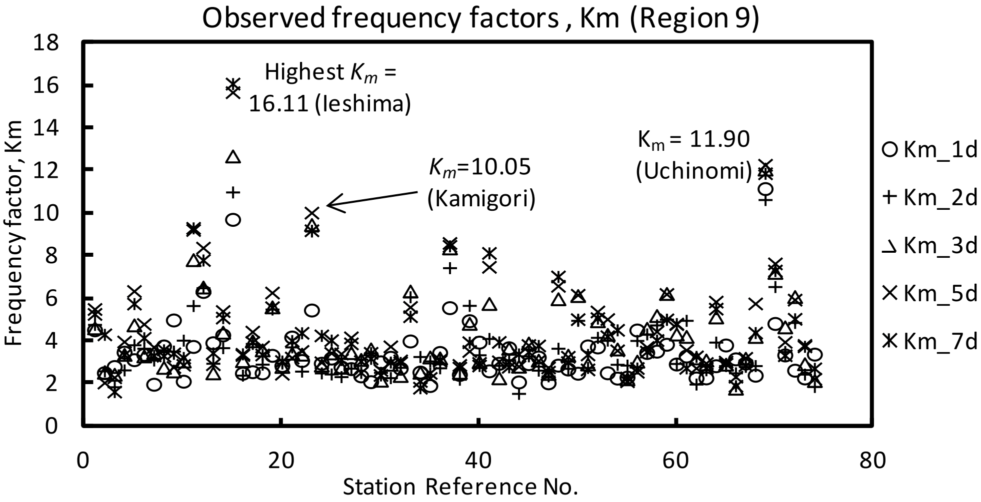

Figure 6-39: Observed frequency factors, K_m for Region 9

Table 6-12: Stations list for Region 9

No.	Point (*1-d PMP*)	No.	Point (*1-d PMP*)	No.	Point (*1-d PMP*)	No.	Point (*1-d PMP*)
1	Akaiwa (554)	*21*	Jojusha (1772)	*41*	Niihama (929)	*61*	Takano (372)
2	Chikanaga (786)	*22*	Kake (530)	*42*	Nishiwaki (382)	*62*	Takehara (360)
3	Chiya (426)	*23*	Kamigori (592)	*43*	Oasa (547)	*63*	Takinomiya (623)
4	Fuchu (372)	*24*	Kasaoka (278)	*44*	Odomari (489)	*64*	Tamagawa (644)
5	Fukusaki (426)	*25*	Koda (437)	*45*	Okayama (375)	*65*	Tamano (437)
6	Fukuwatari (426)	*26*	Kubi (417)	*46*	Omishima (348)	*66*	Tojo (385)
7	Fukuyama (381)	*27*	Kuma (655)	*47*	Ozu (502)	*67*	Tomisato (1107)
8	Gunge (739)	*28*	Kurahashi (426)	*48*	Saijo (772)	*68*	Tsuyama (454)
9	Hatsukaichitsuta (707)	*29*	Kurashiki (343)	*49*	Saita (534)	*69*	Uchinomi (1473)
10	Higashihiroshima (440)	*30*	Kure (483)	*50*	Saya (408)	*70*	Wake (707)
11	Hiketa (898)	*31*	Kuse (337)	*51*	Sera (375)	*71*	Wu (ss) (454)
12	Himeji (585)	*32*	Matsuyama (470)	*52*	Shikoku-chuo (765)	*72*	Yakage (309)
13	Hiroshima (471)	*33*	Matsuyama (ss) (420)	*53*	Shimoazae (373)	*73*	Yawatahama (494)
14	Ichinomiya (566)	*34*	Miki (403)	*54*	Shiwa (410)	*74*	Yuki (423)
15	Ieshima (991)	*35*	Misho (458)	*55*	Shobara (365)		
16	Ikeda (575)	*36*	Miyoshi (396)	*56*	Sumoto (674)		
17	Ikuchijima (365)	*37*	Mushiage (866)	*57*	Tadotsu (461)		
18	Imabari (350)	*38*	Nagahama (466)	*58*	Tadotsu (ss) (428)		
19	Imaoka (487)	*39*	Nagi (400)	*59*	Takahashi (353)		
20	Joge (371)	*40*	Nakayama (513)	*60*	Takamatsu (540)		

**ss = surface stations (stations with records from 1890's), others are from 1970's*

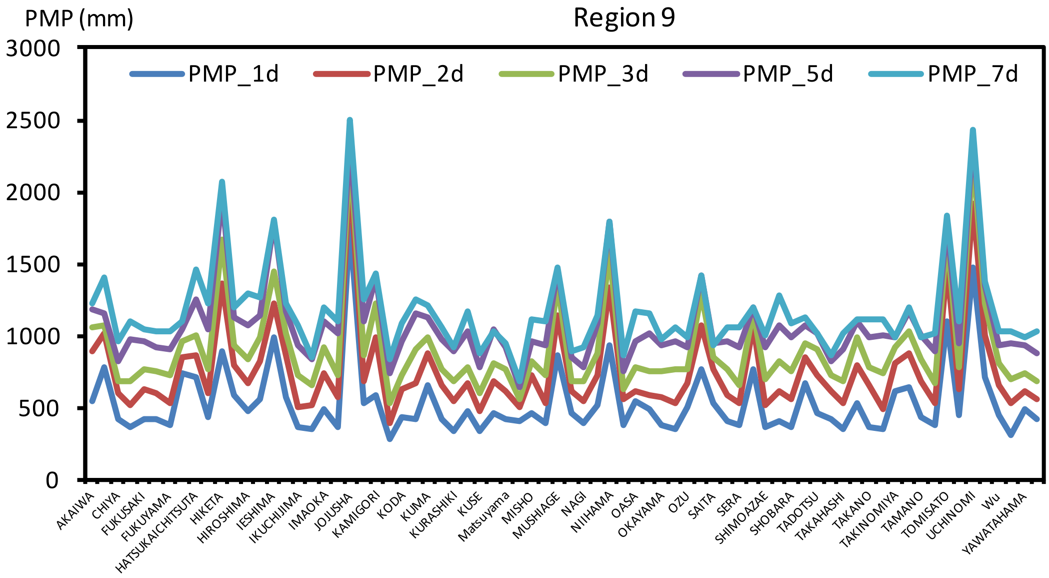

(a)

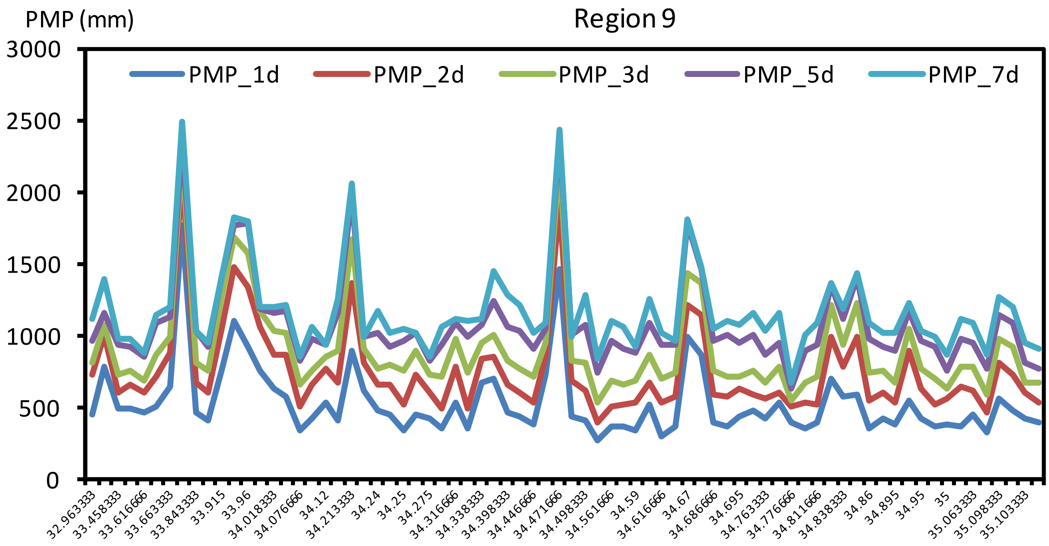

(b)

Figure 6-40: Point statistical PMP estimates for Region 9: **(a)** by station name, and **(b)** by latitudes

6.5.10 *Region 10*

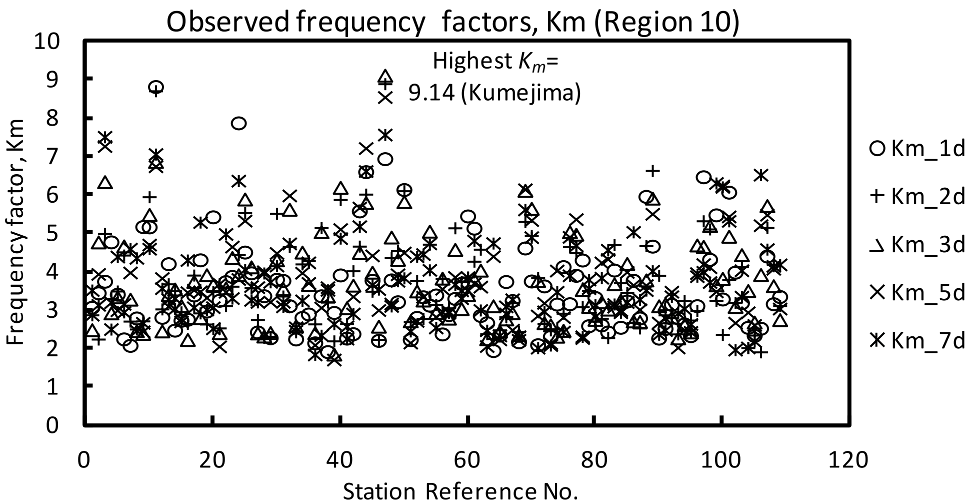

Figure 6-41: Observed frequency factors, K_m for Region 10

Table 6-13: Stations list for Region 10

No.	Point (*1-d PMP*)	No.	Point (*1-d PMP*)	No.	Point (*1-d PMP*)	No.	Point (*1-d PMP*)	No.	Point (*1-d PMP*)
1	Aburatsu (737)	*23*	Irabu (611)	*45*	Koniya (1035)	*67*	Nakakosh. (690)	*89*	Shimizu (813)
2	Aki (605)	*24*	Irikitoge (692)	*46*	Kubokawa (1187)	*68*	Nakamura (802)	*90*	Shishikui (796)
3	Anabuki (1021)	*25*	Isen (819)	*47*	Kumejima (1019)	*69*	Naze (1061)	*91*	Sukumo (576)
4	Aoshima (1048)	*26*	Ishigaki is. (ss) (674)	*48*	Kunitomi (844)	*70*	Naze (ss) (1073)	*92*	Susaki (773)
5	Ekawasaki (1002)	*27*	Ishigakijima (673)	*49*	Kuraoka (1018)	*71*	Nishimera (897)	*93*	Taisho (1095)
6	Fukase (1024)	*28*	Itokazu (613)	*50*	Kushima (774)	*72*	Nobeoka (723)	*94*	Takachiho (812)
7	Fukuhar.(1354)	*29*	Izena (612)	*51*	Kyojo (930)	*73*	Odochi (933)	*95*	Takanabe (843)
8	Funato (1428)	*30*	Kabira (943)	*52*	Makinohara (825)	*74*	Ohara (839)	*96*	Tano (689)
9	Furue (769)	*31*	Kagoshima (ss) (591)	*53*	Makurazaki (737)	*75*	Okinoerabu (656)	*97*	Tarama (1172)
10	Gamoda (917)	*32*	Kakuto (890)	*54*	Mikado (1443)	*76*	Oku (730)	*98*	Tashiro (953)
11	Gomen (995)	*33*	Kaminaka (793)	*55*	Minamidaito (695)	*77*	Okuchi (805)	*99*	Tokashiki (951)
12	Goya (630)	*34*	Kamishiiba (1054)	*56*	Mitate (1470)	*78*	Onoaida (711)	*100*	Tokushima (578)
13	Gusukube (708)	*35*	Kanoya (803)	*57*	Miyakojima (725)	*79*	Osumi (655)	*101*	Tokushima (ss) (700)
14	Handa (978)	*36*	Kaseda (709)	*58*	Miyakonojo (948)	*80*	Saga (961)	*102*	Uchinoura (657)
15	Hateruma (791)	*37*	Kihoku (753)	*59*	Miyazaki (934)	*81*	Saito (835)	*103*	Ume (1028)
16	Higashiich. (626)	*38*	Kiire (587)	*60*	Miyazaki (ss) (948)	*82*	Sakawa (1055)	*104*	Yakushima (864)
17	Hiwasa (911)	*39*	Kikaijima (661)	*61*	Mizobe (834)	*83*	Sakihama (909)	*105*	Yanase (1523)
18	Hongawa (1445)	*40*	Kimotsuki. (1156)	*62*	Morotsuka (1097)	*84*	Sata (727)	*106*	Yomitan (542)
19	Hyuga (808)	*41*	Kitakata (849)	*63*	Motobu (679)	*85*	Satsumaka. (794)	*107*	Yoronjima (744)
20	Ibaruma (734)	*42*	Kito (1334)	*64*	Motoyama (1290)	*86*	Sendai (757)	*108*	Yoshigabeppu (794)
21	Ibusuki (696)	*43*	Kochi (1188)	*65*	Murotomisaki (766)	*87*	Shibushi (700)	*109*	Yusuhara (1075)
22	Ikegawa (1396)	*44*	Kochi (ss) (908)	*66*	Naha (ss) (942)	*88*	Shigeto (1343)		

**ss = surface stations (stations with records from 1890's), others are from 1970's*

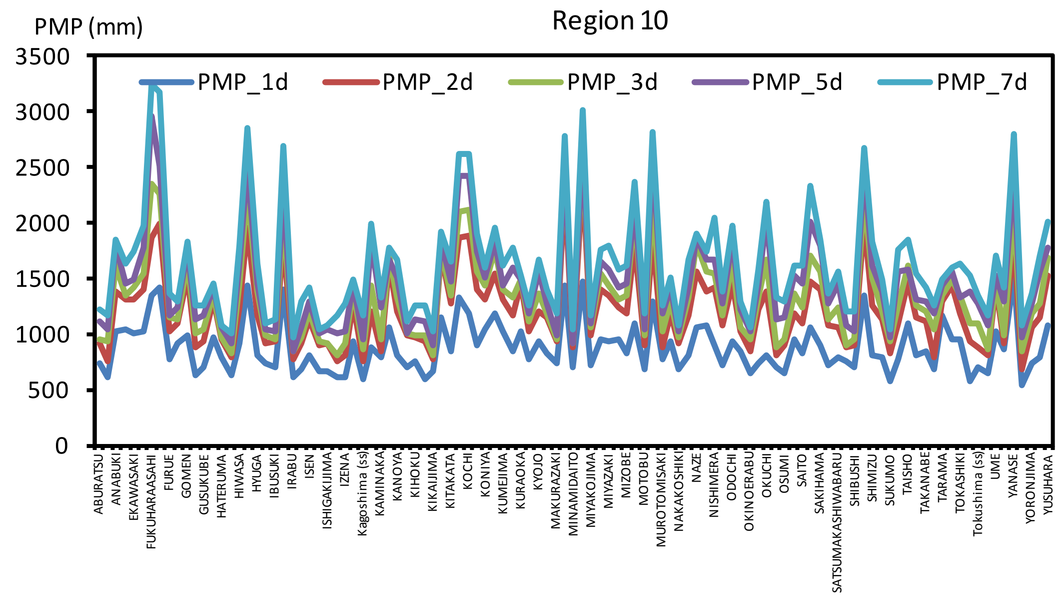

(a)

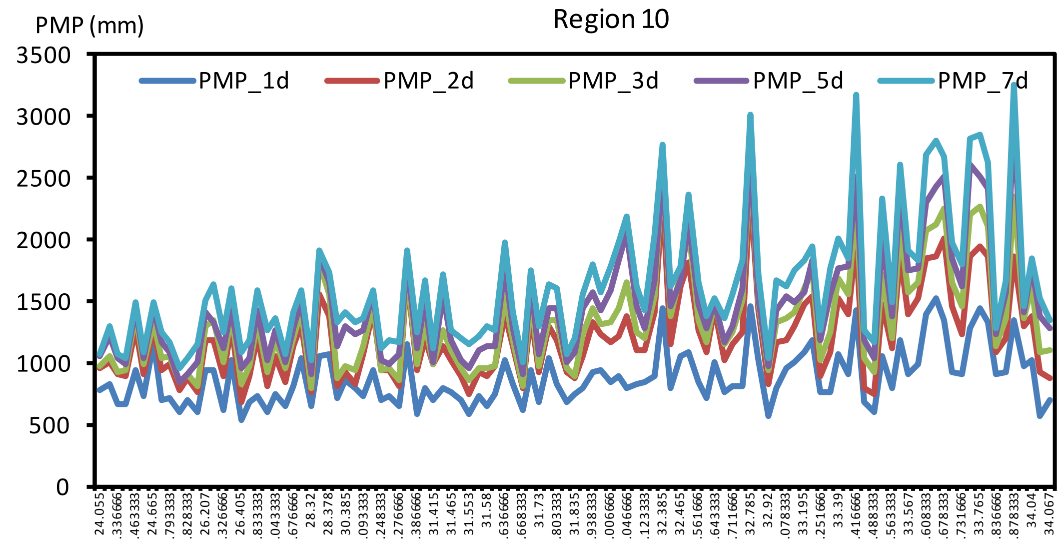

(b)

Figure 6-42: Point statistical PMP estimates for Region 10: **(a)** by station name, and **(b)** by latitudes

6.5.11 *All regions*

Figure 6-43 illustrates the statistical 1-day PMP plots for the whole Japan. The statistical PMP estimates are consistent with the historical records of extreme and record-breaking rainfall events in Japan. The PMP estimated are also correlated to the means of the annual maximum series of each station, this is presented in Figure 6-44. Higher PMPs are estimated mostly within regions facing the Pacific Ocean and are exposed directly against typhoons which are regions on the South-West.

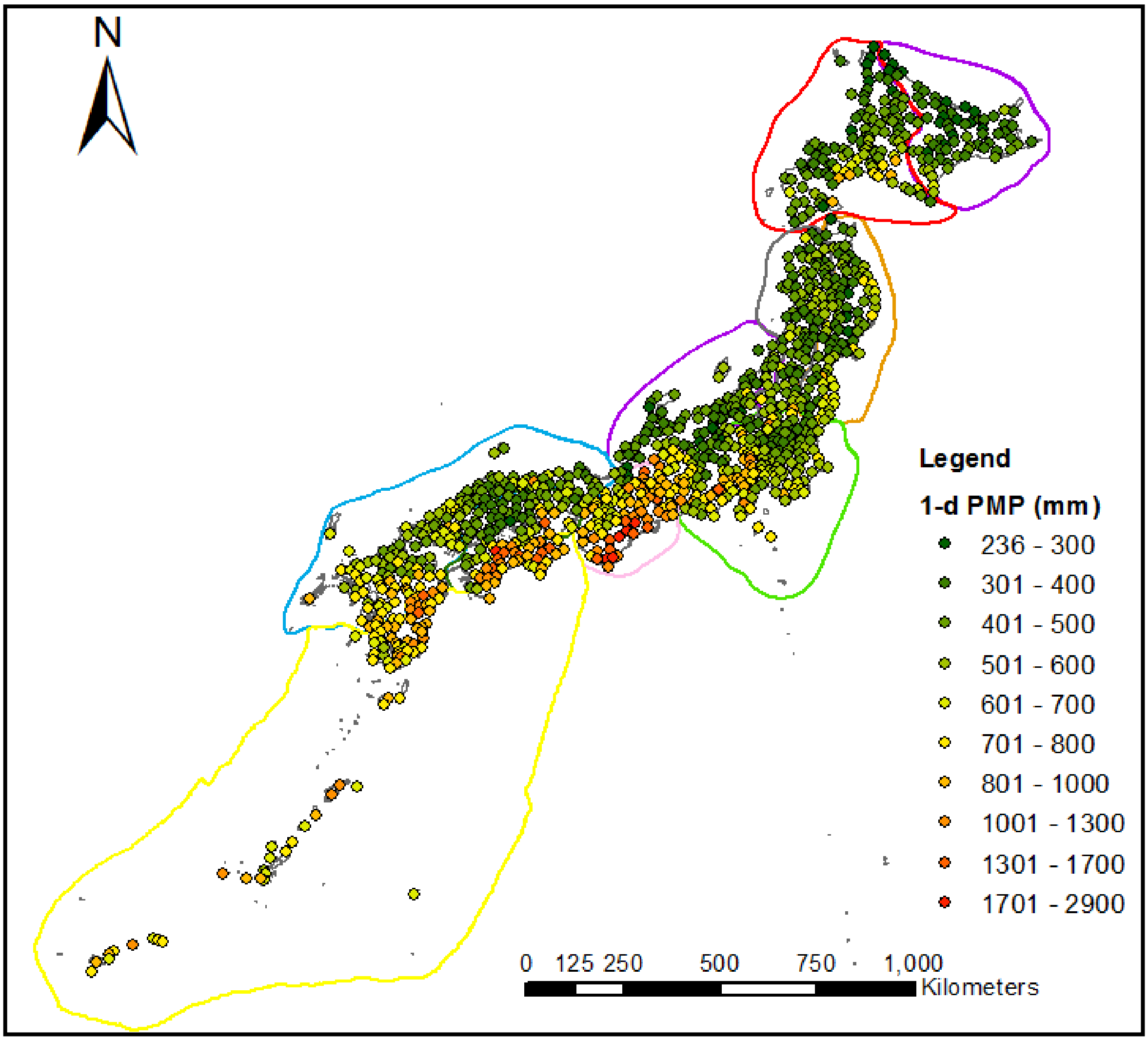

Figure 6-43: Point statistical 1-day PMP estimates for whole Japan

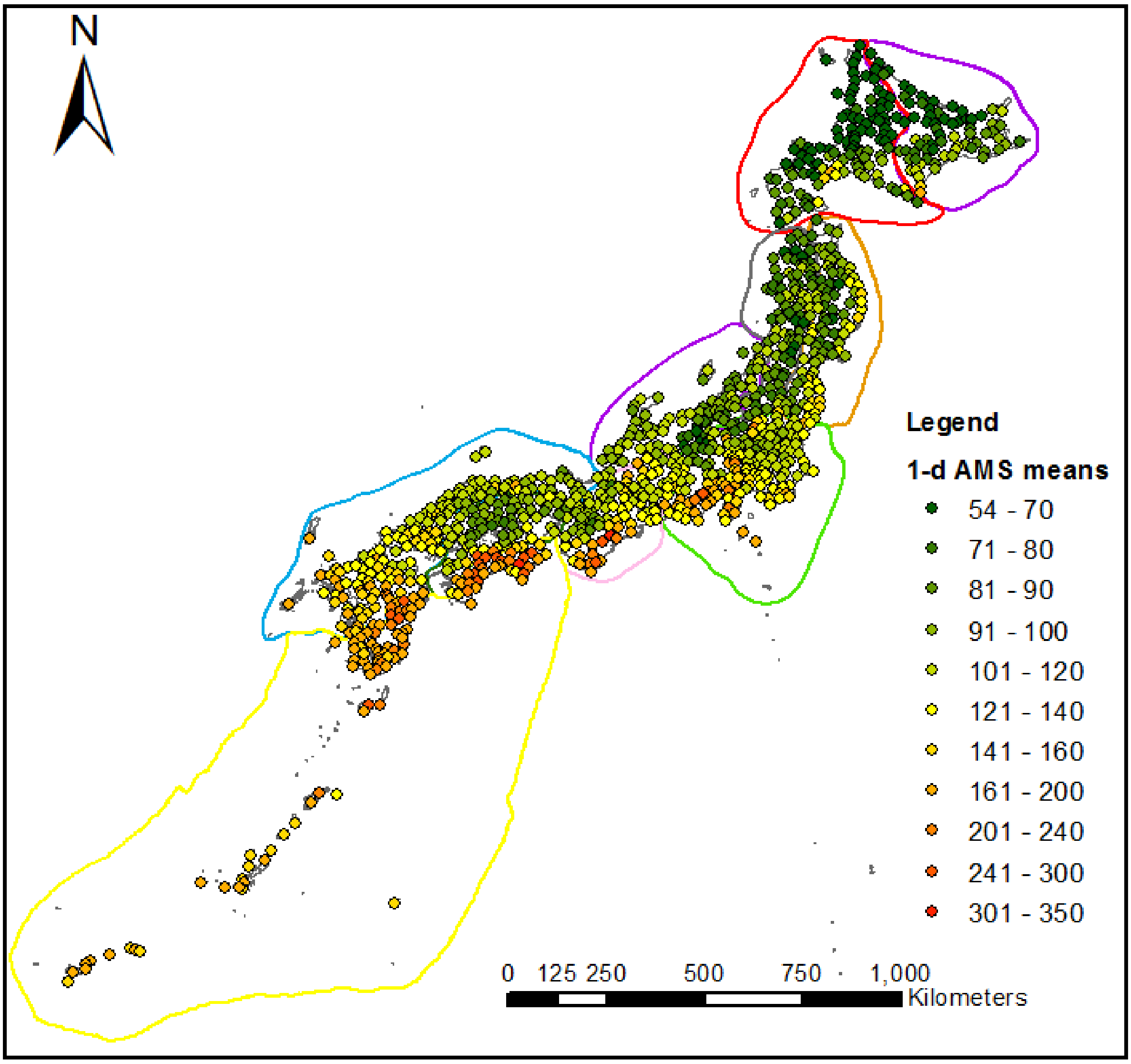

Figure 6-44: Means of the annual maximum series, X_n for whole Japan

Chapter 7 Summary and Conclusion

7.1 Summary of the research findings

Summaries of the analyses conducted from previous chapters are presented. Some of the results obtained in the chapters were related. There are nine main outcomes summarized as follows:

I. **Limitation of conventional frequency analysis and the importance of probable maximum precipitation estimates.**

Conventional frequency analysis of extreme rainfalls can under-estimate its quantiles. In some extreme rainfall events were observed to occur more than once within its estimated return period. This is due to the existence of extreme outliers in the rainfall datasets. The condition will be more wide-spread in the future because of global warming. Several extreme outliers identified in the Japanese rainfall records are from Kochi and Hikone. Analysis conducted in Section 3.2 shows that the quantiles of the 500-year and 1000-year for Kochi is around 500 mm to 750 mm using the generalized extreme value, Gumbel and Log-normal 3-parameters models. Values selected for designing critical structures such as dams and hazardous land-fills would fall into that range. However in real situation, a maximum rainfall of 628.5 mm had occurred, thus increasing the possibility that the design limit would be exceeded. Thus, it is surely safer to assume a much higher benchmark. This is where the purpose of the probable maximum precipitation (PMP) is significant. PMP estimates provide an optimum value to represent a maximum rainfall. The statistical PMP estimated for Kochi is 908 mm. This surely increases the precaution measure for the design.

II. **A simple quantile plot with PMP as upper boundary.**

The analysis regarding frequency analysis and PMP as upper boundary was discussed in Section 3.3. A sample of data is first fitted to a distribution function. Using the fitted parameters, the return periods of quantiles (until the maximum value of the sample) and the PMP estimate are calculated. Based on the relationship between the return periods, its quantiles and the PMP, a non-linear regression equation (NLR) were produced. The NLR appear to reduce the return period of the quantiles near the PMP value. It can be concluded that GEV overestimates the return periods for high quantiles values (more than 700 mm) because GEV's upper bound is infinite. The NLR with upper bound given by PMP stabilizes the return period estimates. In other words, we can avoid (or reduce) overestimation by using the NLR.

III. The extreme-rainfall homogeneous regions for Japan.

The construction of the homogeneous regions using the *L*-moments regional frequency analysis method uses the Japan Meteorological Agency's (JMA) 1053 AMeDAS stations with data from 1976 to 2008, and surface stations with data from as far as 1896 to 2008. Ten extreme-rainfall homogeneous regions were identified. A heterogeneity test and discordance test were used to assess the homogeneity of sites inside the regions. All of the regions were proven to be homogeneous with 0% to 30% of high discordances' sites. Some of the high discordances' sites are due to local extreme storms and orographic effects. If the events occurred at the discordances sites are equally likely to affect any of the sites within the same region in the future, then it is correct to treat the entire group of sites as a homogenous region, even though some sites appear to be discordant with the region as a whole. The homogeneous regions could be divided into three major sections according to their moisture source. The sections are separated by the Japanese mountain ranges. The borders of the 10 homogeneous regions are illustrated in Figure 4-4 in Section 4.4. All of the regions except have very good heterogeneity assessment, thus research considering them as homogenous regions can be conducted with high level of assurance. However, for Region 2, Region 6 and Region 9, modification of the homogeneous regions can be made by introducing sub-regions or analysis using seasonal data.

IV. Fitting extreme outliers using regional frequency analysis.

There are extreme outliers found within the annual maximum daily-rainfall distribution of several sites in Japan. Using conventional frequency analysis, the outliers were not able to be fitted into the frequency analysis models, consequence to underestimation of the quantile values. Six sites were chosen for the at-site frequency analysis (conventional frequency analysis) and two homogenous regions for the regional frequency analysis. They are Hikone, Kyoto and Miyagawa located within homogeneous region, Region 7; and Kochi, Yanase and Miyazaki located within Region 10. The analyses use the station-years method in which the sample size is equal to the total number of observation years of all the sites within the homogeneous region. An SLSC test results prove that the regional datasets has better fit compared to using the at-site analysis. The regional frequency analysis reduces all the probability differences of the outliers quite significantly. More than 30% of reductions are obtained for the outliers (Hikone 30.24%, Kyoto 78.03%, and Kochi 58.23%), and almost all of the probability differences of the 30-year or 10-year rainfall events have a reduction around 90%. By focusing on the three stations with extreme outliers (Hikone, Kyoto and Kochi), the return period for Hikone extreme rainfall outlier of 596.9 mm was reduced from a 2000-year rain to a 500-year-rain. Similar goes to the outlier of Kyoto (288.6 mm), where its rainfall period was reduced from a 100-year-rain to a 30-year-rain. This study provides evidence of the importance to consider regional frequency analysis into quantiles estimations especially for rainfall distribution with significant extreme outliers. Better identification of the extreme-rainfall homogeneous regions provide higher assurance in estimating the quantiles of the regional frequency frequency analysis models. It is highlighted also the benefits of using regional frequency analysis for region with long historical data, not just for regions with limited data availability and number of gauged-sites.

V. Preliminary statistical PMP estimation for whole Japan.

Hershfield statistical 1-day PMP estimations were conducted for whole of Japan by using all the long-observation stations' (51 stations from JMA) daily rainfall records. The data are from the period 1986 to 2008. No transposition boundaries were used; instead the envelopment process uses all of the data from the 51 stations. According to the PMP manual (WMO, 2009) this would not be appropriate for the statistical estimation since it involves a very large area (about 400 000 km^2). However, for preliminary assessment the statistical PMP estimates for whole Japan were conducted using all available long-observation records. Results are presented by comparing the highest observed rainfall at one point (or site) against the PMP estimated at the same point. Small differences were observed at areas which have the top record-breaking daily rainfalls in Japan. Instead, at other locations, there are very high percentage differences. This shows the non-uniformity of the K_m values being transposed. Therefore, it would be more accurate to consider a focused region such as a river basin area or some administrative regions as recommended by the PMP manual by the world meteorological organization. Another way is to use a homogeneous region which are tested and proposed in this thesis.

VI. Improving statistical PMP estimates considering extreme-rainfall homogeneous regions.

The transposition boundaries for the conventional statistical PMP analysis usually are taken from the river basin or administrative-regions. Possibility of a higher observed rainfall outside those boundaries being over looked could occur. This study proposes to consider extreme-rainfall homogeneous region (obtained by regional frequency analysis) for the statistical PMP analysis. In the analysis, the transposition boundaries used for the conventional statistical PMP estimation are from two river basins and six administrative regions, while for the new approach are from two homogeneous regions of Region 7 and Region 10. The analysis uses data from the AMeDAS and surface station network ranging from the year 1896 to 2008. Results show that by using the homogeneous region, we can obtain optimal frequency factor K_m for the transposition. The improved K_m values produce PMP estimates that were higher than the current record-breaking rainfall events. This study also proves the new approach can compensate data limitations by comparing conventional PMP results using short (1976 - 2008) and long (1896-2008) observation-period to the PMP estimated by the new approach. The PMPs estimated by the conventional method using shorter observation data are very low compared to the PMPs estimated using the longer one. By adopting homogeneous region as the transposition boundary and using short observation data (1976 - 2008), the PMPs were comparable to the PMPs from longer observation data. Thus, this study recommends the highest PMP value within the homogeneous region to be used for flood defence structures intended for any site within the same region.

VII. Validation of the statistical PMP estimates using the new approach

This study validates the PMP estimates using data until 2008 to current rainfall records up to 2014. At Kamikitayama point the conventional PMP analysis considers Nara prefecture as the transposition boundary. The conventional PMP estimated has the same value as the record breaking rainfall of 661 mm in 21/8/2011. However, when the homogeneous region was used as the boundary, the PMP estimated becomes 978 mm. The optimal PMP value leaves higher precautions for designing flood-defence structures. Similar assessment can be made for point Fukuharaasahi, and Miyaji. The PMPs estimated using conventional method for both points are very close to their record-breaking rainfall events, 542 mm and 301 mm PMP estimates to 641 mm and 283 mm record-breaking rainfall event respectively. For Fukuharaasahi, the conventional PMP estimates were even exceeded by the 641 mm -rainfall in 19/7/2011. When the new method was considered, the statistical PMP estimated to be 860 mm which is higher than the record-breaking rainfall event. Thus, by considering the homogeneous region, improvements of the PMP estimated can be obtained.

VIII. Multiple durations PMP estimates using a 1-point envelopment

Two techniques to transpose the observed frequency factor, K_m used in statistical PMP estimation were analyzed. They are: 1) Using maximum observed frequency factor, K_m (1-point envelopment); and 2) using a regression line (2-point or multiple point envelopment). The 1-point envelopment used in this study considers the highest observed K_m values for all the sites and rainfall-periods in a homogeneous region, while the 2-point envelopment used has different envelope for each rainfall periods. Results show that it is more reasonable to adopt a 1-point envelopment technique compared to 2-point envelopment when estimating multiple durations PMP values. When using the 2-point envelopment technique, a 1-day PMP estimates can be higher than a 2-day PMP estimates at similar site. This is because different transposition factors were used. The 1-point envelopment also gives better correlation of the PMPs and annual maximum means. This is because the frequency factor K_m for all the stations are transposed to a constant K_m value resulting to sites with higher annual maximum means producing higher PMP values.

IX. **Projected PMP estimates based on the MRI-AGCM3.2 (20km)**

Three time slices (1979 - 2008, 2014 - 2044, and 2075 - 2104) of an atmospheric general circulation model (AGCM) were used for the PMP projections. Annual maximum daily rainfalls (AMS) were extracted from the AGCM outputs. First, bias corrections were conducted using AMS from the AGCM within the year 1979 - 2008. The means of the bias-corrected AMS have good correlations with the observed data (R square value of 0.761). Using similar bias corrections, future PMPs were estimated using projected climate data of the time-periods 2014 - 2044 and 2075 - 2104. The future PMP values are comparable to the improved PMP values estimated using data from 1979 - 2008. From the results, it is acknowledged that; 1) the PMPs estimated by the GCM data have an error variability of about 24% by the R square value of 0.761; 2) The range of PMPs estimated by the near-future (2014-2044) and far-future scenario (2075-2104) has not much difference as compared to the present condition (1979-2008); 2) It is suggested that the PMP estimated using the homogeneous regions and the 1-point envelopment for Region 7 of Japan has been proven not just from record-breaking rainfall events but also using projections of an atmospheric general circulation model.

7.2 **Conclusions and Future Works**

Outcomes of extreme precipitation analysis influence improvements on flood protection and flood risk management. As mentioned in the background and problem statements, reports show an increase in extreme precipitation around the world due to global warming. The existence of extreme rainfall values or outliers influences the quality of the quantile values calculated using conventional frequency analysis. This is because the outliers were not fitted to the frequency model. In future, this problem will be more significant for many regions which receive–much higher rainfall intensities than usual. There are various steps and approaches that can contribute to the preparation of future extreme events. One of them is prediction of the probability of occurrence of an extreme rainfall event, and the other is estimation of the highest rainfall amount by estimating the probable maximum precipitation (PMP). Both approaches are important. However, estimation of reliable quantiles and PMP estimates are quite difficult for regions with limited resources or data-records containing extreme outliers. In order to solve the problems, the thesis proposes a method that could improve the quantiles and the PMP considering data limitations.

The analyses in the study use data from around 1050 stations belonging to the Japan Meteorological Agency (JMA) of surface stations (1896 to 2008) and AMeDAS network (1976 - 2008). The analyses include conventional frequency analysis, regional frequency analysis, determination of Japanese extreme-rainfall homogeneous regions, and the Hershfield statistical PMP estimates. First, extreme-rainfall homogeneous regions for Japan were identified by using the *L*-moments regional frequency analysis method. Using the regions, based on a station-year method, analysis was conducted to see whether by applying the homogeneous regions, improvement of the quantiles and fittings of extreme outliers were achieved. Results show that the extreme outliers were able to fit in the regional frequency distribution. The statistical PMP estimates were also improved by considering the homogeneous regions as the transposition boundaries. Finally, the PMP results were validated by using recent record-breaking rainfall events (up to March 2014) and the projected climate data of the atmospheric general circulation model (AGCM3.2s-20 km).

Results obtained from this study prove the benefits of considering regional frequency analysis for extreme rainfall. Summary of the conclusions are: 1) For the statistical PMP estimation, it is recommended to use the homogeneous regions as the transposition boundaries in order to compensate for data limitations; 2) It is suggested that, the highest PMP value within a homogeneous region can be used to represent the PMP value for flood-mitigation projects intended for any site in the same region; 3) It is demonstrated that PMP estimates are also important to represent extreme rainfall values for designing critical infrastructures (e.g., dams or hazardous waste landfills) in addition to using quantiles from frequency analysis; 4) The improved statistical PMP estimates show convincing results since most of the current record-breaking rainfalls were not exceeded compared to using the conventional method; 5) the PMPs estimated using the new approach are comparable to the projected PMPs based on the MRI-AGCM3.2s model output.

For future research, in order to acquire more understanding of the improved statistical PMP method, detailed tests using hourly rainfall data may be conducted. This research recommends tests on regions with much less data availability. Such implementation can be conducted for Malaysia. Recently, Malaysia has record-breaking rainfalls every year from 2010 until 2014. Being a tropical climate region and located very near to the equator, the extreme climate conditions in Malaysia are notably influenced by global warming effects.

7.3 Research contributions

The main contributions from this research are as follows:

a) This thesis proposed ten extreme-rainfall homogeneous regions for Japan, which have not been proposed before, by using an *L*-moments regional frequency analysis. The regions can be used for future research in relation to extreme rainfall analysis.
b) This thesis introduces an improved method for statistical PMP estimation. The method considers extreme-rainfall homogeneous regions as the transposition boundaries. Hydro-meteorological PMP estimation method needs long records of meteorological data besides rainfall. If statistical PMP estimates using only precipitation data can provide satisfactory maximum rainfall estimates, it will benefit countries with limited data availability.
c) This research presents the statistical PMP estimates for Japan using the new approach. There is no previous research on PMP for Japan which use the Hershfield statistical method. Since long-term observation records are available, using statistical methods are suitable.
d) A FORTRAN program code for the Hershfield statistical PMP estimation was developed from this research. Using program-codes for calculation will shorten analysis time for detailed and extensive preliminary PMP estimation.
e) This thesis proves the Japanese atmospheric general circulation model, MRI-AGCM 3.2 (20 km) outputs to perform adequately in terms of the means of annual maximum series (X_n) by using a simple bias correction method. The AGCM outputs also produce acceptable PMP estimates. The PMPs estimated by the new approach are comparable to PMPs estimated using projected climate data up to the year of 2104.

References

Alias, N.E., Takara, K., 2012. Probability Distribution for Extreme Hydrological Values-Series in the Yodo River Basin, Japan and Kuala Lumpur, Malaysia, International Conference on Water Resources 2012 (ICWR), Langkawi, Malaysia.

ASCE, WEF, 2012. Design of Urban Stormwater Controls. Mc Graw Hill.

Awadallah, A.G., 2013. Regional intensity-duration-frequency curves for Jeddah region, Saudi Arabia, using ordinary and L-moments approaches. Journal of Flood Risk Management.

B.O.M, A., 2011. Report to Queensland Floods Commision of Inquiry. Bureau of Meteorology.

B.O.M, A., 2012. Annual Australian Climate Statement 2010/2011. Bureau of Meteorology Australia.

Bhatia, S. et al., 2010. Protecting Development Gains-Reducing Disaster Vulnarability and Building Resilience in Asia and the Pacific, ESCAP,UNISDR, Bangkok, Thailand.

Brunetti, M., Buffoni, L., Maugeri, M., Nanni, T., 2000. Precipitation intensity trends in northern Italy. International Journal of Climatology, 20(9): 1017-1031.

Brunetti, M., Colacino, M., Maugeri, M., Nanni, T., 2001. Trends in the daily intensity of precipitation in Italy from 1951 to 1996. International Journal of Climatology, 21(3): 299-316.

Cannarozzo, M., Noto, L.V., Viola, F., 2006. Spatial distribution of rainfall trends in Sicily (1921–2000). Physics and Chemistry of the Earth, Parts A/B/C, 31(18): 1201-1211.

Casas, M.C., Rodríguez, R., Nieto, R., Redaño, A., 2008. The Estimation of Probable Maximum Precipitation. Annals of the New York Academy of Sciences, 1146(1): 291-302.

Casas, M.C., Rodríguez, R., Prohom, M., Gázquez, A., Redaño, A., 2011. Estimation of the probable maximum precipitation in Barcelona (Spain). International Journal of Climatology, 31(9): 1322-1327.

Chaffe, P.L.B. et al., 2013. Mapping of Japanese areas susceptible to snow cover change. Hydrological Sciences Journal, 58(8): 1718-1728.

Chow, V.T., 1951. A general formula for hydrologic frequency analysis. Transactions, American Geophysical Union, 32(2): 231-237.

Chow, V.T., 1964. Manual of Applied Hydrology. Mc Graw Hill.

Dasgupta, S. et al., 2010. Three thousand years of extreme rainfall events recorded in stalagmites from Spring Valley Caverns, Minnesota. Earth and Planetary Science Letters, 300(1–2): 46-54.

Desa M, M.N., Noriah, A.B., Rakhecha, P.R., 2001. Probable maximum precipitation for 24 h duration over southeast Asian monsoon region—Selangor, Malaysia. Atmospheric Research, 58(1): 41-54.

Desa M, M.N., Rakhecha, P.R., 2007. Probable maximum precipitation for 24-h duration over an equatorial region: Part 2-Johor, Malaysia. Atmospheric Research, 84(1): 84-90.

Deshpande, N.R., Kulkarni, B.D., Verma, A.K., Mandal, B.N., 2008. Extreme rainfall analysis and estimation of Probable Maximum Precipitation (PMP) by statistical methods over the Indus river basin in India. Journal of Spatial Hydrology, 8(1): 22-35.

Duan, W. et al., 2014. Anomalous atmospheric events leading to Kyushu's flash floods, July 11–14, 2012. Natural Hazards: 1-13.

Ekström, M., Fowler, H.J., Kilsby, C.G., Jones, P.D., 2005. New estimates of future changes in extreme rainfall across the UK using regional climate model integrations. 2. Future estimates and use in impact studies. Journal of Hydrology, 300(1–4): 234-251.

Elíasson, J., 1997. A statistical model for extreme precipitation. Water Resour. Res., 33(3): 449-455.

Emanuel, K.A., 2011. Cyclones- Tropical cyclones. In: Schneider, S.H., Root, T.L., Mastrandrea, M.D. (Eds.), Encyclopedia of Climate and Weather. OXFORD UNIVERSITY PRESS, pp. 352-358.

Fowler, H.J., Kilsby, C.G., 2003. A regional frequency analysis of United Kingdom extreme rainfall from 1961 to 2000. International Journal of Climatology, 23(11): 1313-1334.

Fu, G. et al., 2013. Temporal variation of extreme rainfall events in China, 1961–2009. Journal of Hydrology, 487(0): 48-59.

Fujibe, F., Yamazaki, N., 2006. Long-term changes of heavy precipitation and Dry weather in Japan (1901-2004). Journal of the Meteorological Society of Japan, 84(6): 1033-1046.

Fujibe, F., Yamazaki, N., Katsuyama, M., Kobayashi, K., 2005. The increasing Trend of Intense Precipitation in Japan Based on Four-hourly data for a Hundred Years. SOLA, 1: 041-044.

Greenwood, J.A., Landwher, J.M., Matalas, N.C., Wallis, J.R., 1979. Probability weighted moments: Definition and relation to parameters of several distributions expressable in inverse form. Water Resour. Res., 15(No.5): 1049-1054.

Guha-Sapir, D., Vos, F., Below, R., Ponserre, S., 2012. Annual Disaster Statistical Review 2011: The Numbers and Trends, Brussels: CRED.

Hailegeorgis, T.T., Thorolfsson, S.T., Alfredsen, K., 2013. Regional frequency analysis of extreme precipitation with consideration of uncertainties to update IDF curves for the city of Trondheim. Journal of Hydrology, 498(0): 305-318.

Hassan, B.G.H., Ping, F., 2012. Regional Rainfall Frequency Analysis for the Luanhe Basin – by Using L-moments and Cluster Techniques. APCBEE Procedia, 1(0): 126-135.

Hershfield, D.M., 1961. Estimating the probable maximum precipitation. Journal of Hydraulics Division: Proceedings of the American Society of Civil Engineers, 87: 99-106.

Hershfield, D.M., 1965. Method for Estimating Probable Maximum Precipitation. Journal of the American Waterworks Association, 57: 965-972.

Hosking, J.R.M., Wallis, J.R., 1997. Regional Frequency Analysis. Cambridge University Press, United Kingdom.

Huang, G., 2006. Characterization of flood inundation in Sanjo City, Japan on July 13, 2004. Journal of Hydrodynamics, Ser. B, 18(3, Supplement): 295-299.

IPCC, 2007. Summary for Policymakers. In: Climate Change 2007: The Physical Science Basis. Contribution of Working Group I to the Fourth Assessment Report of the Intergovernmental Panel on Climate Change [Solomon, S., D. Qin, M. Manning, Z. Chen, M. Marquis, K.B. Averyt, M.Tignor and H.L. Miller (eds.)], Cambridge University Press, Cambridge, United Kingdom and New York, NY, USA.

J.M.A, 2014. 歴代全国ランキング (in Japanese).
Jarvis, A., Reuter, H.I., Nelson, A., Guevara, E., 2008. Hole-filled seamless SRTM data V4. International Centre for Tropical Agriculture (CIAT).
Jones, M., Fower, H.J., C.G.Kilsby, S.Blenkinsop, 2010. An updated regional frequency anaysis of United Kingdom extreme rainfall from 1961-2009, BHS Third International Symposium, Managing Consequences of a Changing Global Environment, Newcastle 2010. British Hydrological Society.
Jothityangkoon, C., Hirunteeyakul, C., Boonrawd, K., Sivapalan, M., 2013. Assessing the impact of climate and land use changes on extreme floods in a large tropical catchment. Journal of Hydrology, 490(0): 88-105.
Kanda, J.A., 1981. New Extreme Value Distribution With Lower and Upper Limits For Earthquake Motions and Wind Speeds. Theoretical and Applied Mechanics, 31: 351-354.
Karl, T.R., Knight, R.W., Plummer, N., 1995. Trends in high-frequency climate variability in the 20th century. Nature, 377: 217-220.
Kim, S., Nakakita, E., 2010. Reproducibility of AGCM20 Precipitation Output and Its Dependency on Topography. Annuals of Disaster Prevention Research Institute, Kyoto University, No. 53B.
Koutsoyiannis, D., 1999. A probabilistic view of hershfield's method for estimating probable maximum precipitation. Water Resour. Res., 35(4): 1313-1322.
Kunkel, K.E. et al., 2013. Probable maximum precipitation and climate change. Geophysical Research Letters, 40(7): 1402-1408.
Kysely, J., Picek, J., 2007. Regional growth curves and improved design value estimates of extreme precipitation events in the Czech Republic. Climate Research, 33(3): 243-255.
Makkonen, L., 2006. Plotting Positions in Extreme Value Analysis. Journal of Applied Meteorology and Climatology, 45(2): 334-340.
Mason, S., Waylen, P., Mimmack, G., Rajaratnam, B., Harrison, J.M., 1999. Changes in Extreme Rainfall Events in South Africa. Climatic Change, 41(2): 249-257.
McCuen, R.H., 1998. Hydrologic Analysis and Design. Prentice-Hall.
Miyajima, J., Fujibe, F., 2011. Climatology of Extreme Precipitation in Japan for Different Time Scales. SOLA, 7: 157-160.
Mizuta, R. et al., 2012. Climate Simulation Using MRI-AGCM3.2 with 20-km Grid. . Journal of the Meteorological Society of Japan, 90A: 233-258.
Murazaki, K., Kurihara, K., Sasaki, H., 2010. Dynamical Downscaling of JRA-25 Precipitation over Japan Using the MRI-Regional Climate Model. 6: 141−144.
NAHRIM, 2007. NAHRIM TECHNICAL RESEARCH PUBLICATION (TRP) NO. 1 – DERIVATION OF PROBABLE MAXIMUM PRECIPITATION FOR DESIGN FLOODS IN MALAYSIA, National Hydraulic Research Institute (NAHRIM).
NOAA, H., 2007. Responses to email regarding uses and understanding of 500-year and 1000-year estimates. National Oceanic and Atmospheric Administration, NOAA.
Nobilis, F., Haiden, T., Kerschbaum, M., 1991. Statistical considerations concerning Probable Maximum Precipitation (PMP) in the Alpine Country of Austria. Theoretical and Applied Climatology, 44(2): 89-94.
Osborn, T.J., Hulme, M., Jones, P.D., Basnett, T.A., 2000. Observed trends in the daily intensity of United Kingdom precipitation. International Journal of Climatology, 20(4): 347-364.
Pal, I., Al-Tabbaa, A., 2009. Trends in seasonal precipitation extremes – An indicator of 'climate change' in Kerala, India. Journal of Hydrology, 367(1–2): 62-69.

Pal, I., Al-Tabbaa, A., 2010. Regional changes in extreme monsoon rainfall deficit and excess in India. Dynamics of Atmospheres and Oceans, 49(2–3): 206-214.

Papalexiou, S.M., Koutsoyiannis, D., 2006. A probabilistic approach to the concept of Probable Maximum Precipitation. Advances in Geosciences, 7: 51–54.

Plummer, N. et al., 1999. Changes in Climate Extremes Over the Australian Region and New Zealand During the Twentieth Century. Climatic Change, 42(1): 183-202.

Rakhecha, P.R., Soman, M.K., 1994. Estimation of probable maximum precipitation for a 2-day duration: Part 2 — north Indian region. Theoretical and Applied Climatology, 49(2): 77-84.

Rezacova, D., Pesice, P., Sokol, Z., 2005. An estimation of the probable maximum precipitation for river basins in the Czech Republic. Atmospheric Research, 77(1–4): 407-421.

Sasaki, H. et al., 2006. Preliminary results from the coupled atmosphereocean Regional Climate Model at the Meteorological Research Institute. J.Meteor. Soc. Japan, 84: 389-403.

Shabri, A., Jemain, A.A., 2013. Regional flood frequency analysis for Southwest Peninsular Malaysia by LQ-moments. Journal of Flood Risk Management, 6(4): 360-371.

Sherif, M., Almulla, M., Shetty, A., Chowdhury, R.K., 2013. Analysis of rainfall, PMP and drought in the United Arab Emirates. International Journal of Climatology: n/a-n/a.

Slade, J.J., 1936. An asymmetric probability function. Transactions, American Society of Civil Engineers, 101: 481–490.

Subash, N., Singh, S.S., Priya, N., 2011. Extreme rainfall indices and its impact on rice productivity—A case study over sub-humid climatic environment. Agricultural Water Management, 98(9): 1373-1387.

Suhaila, J., Deni, S.M., Zin, W.Z.W., Jemain, A.A., 2010. Trends in Peninsular Malaysia Rainfall Data During the Southwest Monsoon and Northeast Monsoon Seasons: 1975–2004. Sains Malaysiana, 39(4): 533-542.

Suppiah, R., Hennessy, K.J., 1998. Trends in total rainfall, heavy rain events and number of dry days in Australia, 1910–1990. International Journal of Climatology, 18(10): 1141-1164.

Takara, K., Stedinger, J.R., 1994. Recent Japanese Contributions to Frequency Analysis and Quantile Lower Bound Estimators. Stochastic and Statistical Methods in Hydrology and Environmental Engineering, 1: 217-234.

Takara, K., Tosa, K., 1999. Storm and Flood Frequency Analysis Using PMP/PMF Estimates, International Symposium on Floods and Droughts, Nanjing, China, pp. 7-17.

Trenberth, K., 1998. Atmospheric Moisture Residence Times and Cycling: Implications for Rainfall Rates and Climate Change. Climatic Change, 39(4): 667-694.

Tsonis, A.A., Salinger, M.J., Kularatne, I., 2011. Climate. In: Schneider, S.H., Root, T.L., Mastrandrea, M.D. (Eds.), Encyclopedia of Climate and Weather. Oxford University Press, New York.

UNISDR, 2013. www.PreventionWeb.net.

WMO, W.M.O., 2009. Manual for Estimation of Probable Maximum Precipitation, Geneva.

Yang, T. et al., 2010. Regional frequency analysis and spatio-temporal pattern characterization of rainfall extremes in the Pearl River Basin, China. Journal of Hydrology, 380(3–4): 386-405.

Yevjevich, V., 1972. Probability and Statistics in Hydrology. Water Resources Publications, Colorado.

Zhan, D., Zhou, J., 1984. Recent developments on the probable maximum precipitation (PMP) estimation in China. Journal of Hydrology, 68(1–4): 285-293.

Lists of Publications and Conferences

Publications

Alias, N. E., Luo, P., & Takara, K. (2013). A Basin-scale Spatial Distribution of Probable Maximum Precipitation for the Yodo River Basin, Japan, *Annuals of Disas. Prev. Res. Inst., Kyoto Univ. No.56B, 2012,pp.65-72.*

Alias, N. E., Luo, P., & Takara, K. (2013). Probable maximum precipitation using statistical method for the Yodo river basin, *Annual Journal of Hydraulic Engineering*, JSCE, Vol.57, 2013,pp. 157-162.

Duan, W., He. B., Takara, K., Luo, P., Hu, M., Alias, N. E., Ishihara, M., Wang, Y., (2014). Climate Change Impacts on Wave Characteristics along the Coast of Japan from 1986 to 2012. Journal of Coastal Research.

Conference Presentations

Alias, N. E. & Takara, K. Estimating the probable maximum precipitation (PMP) of Kuala Lumpur, Malaysia and Yodo River basin, Japan using Statistical Methods. Poster presentation in the *GCOE-ARS International Symposium*, Uji Campus, Kyoto University, 3-4 August 2012.

Alias, N. E. & Takara, K . Probability Distribution for Extreme Hydrological Values-Series in the Yodo River Basin, Japan and Kuala Lumpur, Malaysia. *International Conference on Water Resources 2012 (ICWR)*, Langkawi, Malaysia, 5-9 November 2012.

Alias, N. E., Luo, P., & Takara, K. (2012). A Basin-scale Spatial Distribution of Probable Maximum Precipitation for the Yodo River Basin, Japan, *DPRI Annual Meeting 2012*, Kyoto University, Uji Campus, 19-20 February 2013.

Alias, N. E., Luo, P., & Takara, K. (2013). Probable maximum precipitation using statistical method for the Yodo river basin. *Annual Meeting of Hydraulic Engineering, Japan Society of Civil Engineering (JSCE)* 2013, Nagoya, 5-7 March 2013.

Alias, N. E. . *Extreme rainfall in Japan and Malaysia*. Internship presentation for the School of Civil Engineering and Geosciences, Newcastle University, Newcastle Upon Tyne, UK, 30 September 2013.

Alias, N. E. & Takara, K . Assessing probable maximum precipitation (PMP) and Extreme rainfall trend in Japan. Poster presentation in the *Final GCOE-ARS International Symposium*, Uji Campus, Kyoto University, 1-3 December 2013.

APPENDICES

A-1

Format of the input file for the ANNMAX.FOR and HERSHPMP.FOR program containing the list of stations (Example: Station_list.txt)

```
AKITA.txt
ASAHIKAWA.txt
FUKUI.txt
FUKUOKA.txt
FUKUSHIMA.txt
FUSHIKI.txt
GIFU.txt
HAMADA.txt
HAMAMATSU.txt
HIKONE.txt
IIDA.txt
ISHIGAKIJIMA.txt
ISHINOMAKI.txt
KAGOSHIMA.txt
KOBE.txt
KOCHI.txt
KOFU.txt
KUMAMOTO.txt
KYOTO.txt
MAEBASHI.txt
MATSUMOTO.txt
MATSUYAMA.txt
MITO.txt
MIYAZAKI.txt
NAGANO.txt
NAGASAKI.txt
NAGOYA.txt
NAHA.txt
NAZE.txt
NEMURO.TXT
OBIHIRO.txt
OITA.txt
OSAKA.txt
SAPPORO.txt
SHIMONOSEKI.txt
SUTTSU.txt
TADOTSU.txt
TOKUSHIMA.txt
TOKYO.txt
TSU.txt
TSURUGA.txt
UTSUNOMIYA.txt
WAKAYAMA.txt
YAMAGATA.txt
YOKOHAMA.txt
```

Page 1 of 1

A-2

Format of the input file for the ANNMAX.FOR and HERSHPMP.FOR program containing the date and rainfall data (Example: J_47407.txt for daily data)

```
19010101        240000  2
19010102        240000  1.9
19010103        240000  1.7
19010104        240000  0.2
19010105        240000  0
19010106        240000  0
19010107        240000  0
19010108        240000  0
19010109        240000  0
19010110        240000  0
19010111        240000  3.7
19010112        240000  6.2
19010113        240000  0.5
19010114        240000  0
19010115        240000  1.6
19010116        240000  2.7
19010117        240000  3.6
19010118        240000  0.2
19010119        240000  0.9
19010120        240000  4.6
19010121        240000  0
19010122        240000  0
19010123        240000  0
19010124        240000  4.4
19010125        240000  1.9
19010126        240000  1.4
19010127        240000  2.6
19010128        240000  3.5
19010129        240000  1.5
19010130        240000  5.7
19010131        240000  0.5
19010201        240000  1
19010202        240000  0.1
19010203        240000  0.6
19010204        240000  0
19010205        240000  0
19010206        240000  0.3
19010207        240000  0
19010208        240000  1.1
19010209        240000  1.1
19010210        240000  1.7
19010211        240000  0
19010212        240000  1.3
19010213        240000  0
19010214        240000  0.8
19010215        240000  0.4
19010216        240000  0
19010217        240000  0
19010218        240000  0.5
19010219        240000  0.1
19010220        240000  0.1
19010221        240000  0
19010222        240000  0
19010223        240000  0
19010224        240000  0.1
19010225        240000  0
19010226        240000  1.3
```

Page 1 of 693

A-3

Format of the input file for the ANNMAX.FOR and HERSHPMP.FOR program containing the date and rainfall data (Example: Akita.txt for hourly data)

1976	1	1	1	0
1976	1	1	2	0
1976	1	1	3	0
1976	1	1	4	0
1976	1	1	5	0
1976	1	1	6	0
1976	1	1	7	0
1976	1	1	8	0
1976	1	1	9	0
1976	1	1	10	0
1976	1	1	11	1
1976	1	1	12	0
1976	1	1	13	0
1976	1	1	14	0
1976	1	1	15	0
1976	1	1	16	0
1976	1	1	17	0
1976	1	1	18	1
1976	1	1	19	0
1976	1	1	20	1
1976	1	1	21	0
1976	1	1	22	0
1976	1	1	23	0
1976	1	1	24	0
1976	1	2	1	2
1976	1	2	2	1
1976	1	2	3	3
1976	1	2	4	0
1976	1	2	5	0
1976	1	2	6	0
1976	1	2	7	0
1976	1	2	8	0
1976	1	2	9	0
1976	1	2	10	0
1976	1	2	11	0
1976	1	2	12	0
1976	1	2	13	0
1976	1	2	14	0
1976	1	2	15	0
1976	1	2	16	0
1976	1	2	17	0
1976	1	2	18	0
1976	1	2	19	0
1976	1	2	20	0
1976	1	2	21	0
1976	1	2	22	0
1976	1	2	23	0
1976	1	2	24	0
1976	1	3	1	0
1976	1	3	2	0
1976	1	3	3	0
1976	1	3	4	0
1976	1	3	5	0
1976	1	3	6	0
1976	1	3	7	0
1976	1	3	8	0
1976	1	3	9	0
1976	1	3	10	0
1976	1	3	11	0
1976	1	3	12	0
1976	1	3	13	0
1976	1	3	14	0
1976	1	3	15	0
1976	1	3	16	0
1976	1	3	17	0

Page 1 of 4451

A-4

HERSHPMP.FOR program codes (for the daily data)


```
!   @@@@@@@@@@@@@@@@
!   @  Programmer: Nor Eliza Alias @
!   @  Date:15 June 2012          @
!   @                             @
!   @   ~~^o^~~  ~~^o^~~          @
!   @@@@@@@@@@@@@@@@
!
!This program calculates the ann_max and Hershfield statistical PMP parameters for all rain periods

program HERSHPMP
implicit none
integer,parameter::max=100000  ! the maximum number of line per file
integer::N,N2,N3,N5,N7,NE,i,j,k,p,m,h,l,NumbLine,SY,EY,Numb_Yr,Numb_Stn,N_stn  !SY=Starting year,
EY=Ending year, Numb_Yr =number of Av_Yr ,Numb_Stn = Number of station to analyse
real,allocatable,dimension(:)::Ln,R,Ann_max,Ann_max2,Ann_max3,Ann_max5,Ann_max7,R2,R3,R5,R7,z,z2,
z3,z5,z7,Km_S,Xn_S,Sn_S,New_Km,PMP  ! Ln=line, R=daily rainfall, R2=2d-rain-, R3=3d-rain-, R5=5d-rain
real,allocatable,dimension(:)::Km_S2,Xn_S2,Sn_S2,New_Km2,PMP2,Km_S3,Xn_S3,Sn_S3,New_Km3,PMP3
real,allocatable,dimension(:)::Km_S5,Xn_S5,Sn_S5,New_Km5,PMP5,Km_S7,Xn_S7,Sn_S7,New_Km7,PMP7
real,dimension(400)::R_yr          !R_yr=rainfall data in specific year
integer,allocatable,dimension(:)::Yr,Mth,Day,Hr,Av_Yr,Numb_R,Numb_R2,Numb_R3,Numb_R5,Numb_R7 !
Yr=year,Mth=month,Hr=hour,Av_Yr= Available year, Numb_R = No. of recorded days
real::Sn,Sn2,Sn3,Sn5,Sn7,AVGAM,AVGAM2,AVGAM3,AVGAM5,AVGAM7
real::AVGEX,AVGEX2,AVGEX3,AVGEX5,AVGEX7,SnEX,SnEX2,SnEX3,SnEX5,SnEX7,Km,Km2,Km3,Km5,K
m7
real::X2,X2_2,X2_3,X2_5,X2_7,Y1,Y1_2,Y1_3,Y1_5,Y1_7
integer,dimension(1)::max_loc1,max_loc2,max_loc3,max_loc5,max_loc7 !max_loc1=max value location
integer,dimension(1)::Y1_loc,X2_loc,Y1_loc2,X2_loc2,Y1_loc3,X2_loc3,Y1_loc5,X2_loc5,Y1_loc7,X2_loc7
real,dimension(1)::X1,Y2,Reg_M,Reg_C,X1_2,Y2_2,Reg_M_2,Reg_C_2
real,dimension(1)::X1_3,Y2_3,Reg_M_3,Reg_C_3,X1_5,Y2_5,Reg_M_5,Reg_C_5
real,dimension(1)::X1_7,Y2_7,Reg_M_7,Reg_C_7
character(30)::ListName
character(30),allocatable,dimension(:)::fname

print*,'Please enter the number of stations to analyse:'
read*,N_stn
print*,'Please enter the file name containing the lists of stations to be analyse:'
read*,ListName
open(10,file=ListName)
open(20,file='output.txt',STATUS='REPLACE')


allocate(Km_S(N_stn))
allocate(Xn_S(N_stn))
allocate(Sn_S(N_stn))
allocate(New_Km(N_stn))
allocate(PMP(N_stn))
allocate(Km_S2(N_stn))
allocate(Xn_S2(N_stn))
allocate(Sn_S2(N_stn))
```

HERSHPMP

```
allocate(New_Km2(N_stn))
allocate(PMP2(N_stn))
allocate(Km_S3(N_stn))
allocate(Xn_S3(N_stn))
allocate(Sn_S3(N_stn))
allocate(New_Km3(N_stn))
allocate(PMP3(N_stn))
allocate(Km_S5(N_stn))
allocate(Xn_S5(N_stn))
allocate(Sn_S5(N_stn))
allocate(New_Km5(N_stn))
allocate(PMP5(N_stn))
allocate(Km_S7(N_stn))
allocate(Xn_S7(N_stn))
allocate(Sn_S7(N_stn))
allocate(New_Km7(N_stn))
allocate(PMP7(N_stn))
allocate(fname(N_stn))

do h=1,N_stn

   read(10,*)fname(h)
   print*,'now reading',fname(h)
!---allocating the number of data------------------------

   open(30,file=fname(h))
   Do 100 i=1,max
      N=N+1
   READ(30,*,END=120)
      NumbLine=N
100 CONTINUE
120 NumbLine=i-1
   close(30)
   write(20,*),''
   write(20,*),'----------------Station Number**',h,'','File name','**',fname(h),'------------------------------------------'
   write(20,*),'The number of LINE is:',NumbLine

   allocate(Ln(NumbLine))
   allocate(R(NumbLine))
   allocate(R2(NumbLine-1))
   allocate(R3(NumbLine-2))
   allocate(R5(NumbLine-4))
   allocate(R7(NumbLine-6))
   allocate(Yr(NumbLine))
   allocate(Mth(NumbLine))
   allocate(Day(NumbLine))
   allocate(Hr(NumbLine))

!-----reading data from file----------------------------------
```

Page 2

HERSHPMP

```
   open(30,file=fname(h))

   do i=1,NumbLine
   read(30,'(I4,I2,I2,x,I6,x,F7.2)')Yr(i),Mth(i),Day(i),Hr(i),R(i)
   end do

   SY=Yr(1)
   EY=Yr(numbline)
   Numb_Yr = EY-SY+1

   allocate(Av_Yr(Numb_Yr))
   allocate(Numb_R(Numb_Yr))
   allocate(Numb_R2(Numb_Yr))
   allocate(Numb_R3(Numb_Yr))
   allocate(Numb_R5(Numb_Yr))
   allocate(Numb_R7(Numb_Yr))
   allocate(Ann_max(Numb_Yr))
   allocate(Ann_max2(Numb_Yr))
   allocate(Ann_max3(Numb_Yr))
   allocate(Ann_max5(Numb_Yr))
   allocate(Ann_max7(Numb_Yr))

   write(20,*)''
   write(20,*)'Available years are :'
   do i=1,Numb_Yr
      Av_Yr(i)=SY
      SY=SY+1
   If(SY==EY) then
   go to 220
   End if
220 End do

!**calculating the Number of data per year***

   do j=1,Numb_Yr
      N=1
      do i=1,NumbLine
      if (Yr(i)==Av_Yr(j)) then
      Numb_R(j)=N
      N=N+1
      else
      go to 320
      End if
320    end do
   end do

   write(20,*)'      Year   Recorded number of days'
   do j=1,Numb_Yr
```

Page 3

```
   write(20,*)Av_Yr(j),Numb_R(j)
   end do

!calculating the Number of data per year for R2,R3,R5,R7 **

   do j=1,Numb_yr
      if (j==Numb_yr) then
         Numb_R2(j)=Numb_R(j)-1
         Numb_R3(j)=Numb_R(j)-2
         Numb_R5(j)=Numb_R(j)-4
         Numb_R7(j)=Numb_R(j)-6
         Else
         Numb_R2(j)=Numb_R(j)
         Numb_R3(j)=Numb_R(j)
         Numb_R5(j)=Numb_R(j)
         Numb_R7(j)=Numb_R(j)
      End if
   end do

!-------calculating Rainfall 2-day,3-day,5-day,7-day --------------------

!******2-day rainfall*******
   N2=Numbline-1
   do i=1,N2
      R2(i)=R(i)+R(i+1)
   end do
!******3-day rainfall*******
   N3=Numbline-2
   do i=1,N3
      R3(i)=R(i)+R(i+1)+R(i+2)
   end do
!******5-day rainfall*******
   N5=Numbline-4
   do i=1,N5
   R5(i)=R(i)+R(i+1)+R(i+2)+R(i+3)+R(i+4)
   end do
!******7-day rainfall*******
   N7=Numbline-6
   do i=1,N7
      R7(i)=R(i)+R(i+1)+R(i+2)+R(i+3)+R(i+4)+R(i+5)+R(i+6)
   end do
!-----calculate AnnMax ----------------------------

!******1-day rainfall AnnMax*******
   p=0
   do j=1,Numb_yr
      Ann_max(j)= 0.000011
      m=1+p
      p=p+Numb_R(j)
```

```
       do k=m,p
       if (R(k)>Ann_max(j)) then
         Ann_max(j)=R(k)
       Else
         Ann_max(j)=Ann_max(j)
       End if
       End do
    End do
!******2-day rainfall AnnMax*******
    p=0
    do j=1,Numb_yr
       Ann_max2(j)= 0.000011
       m=1+p
       p=p+Numb_R2(j)
       do k=m,p
       if (R2(k)>Ann_max2(j)) then
          Ann_max2(j)=R2(k)
       Else
          Ann_max2(j)=Ann_max2(j)
       End if
       End do
    End do

!******3-day rainfall AnnMax*******
    p=0
    do j=1,Numb_yr
       Ann_max3(j)= 0.000011
       m=1+p
       p=p+Numb_R3(j)
       do k=m,p
       if (R3(k)>Ann_max3(j)) then
          Ann_max3(j)=R3(k)
       Else
          Ann_max3(j)=Ann_max3(j)
       End if
       End do
    End do

!******5-day rainfall AnnMax*******
    p=0
    do j=1,Numb_yr
       Ann_max5(j)= 0.000011
       m=1+p
       p=p+Numb_R5(j)
       do k=m,p
       if (R5(k)>Ann_max5(j)) then
          Ann_max5(j)=R5(k)
       Else
          Ann_max5(j)=Ann_max5(j)
```

```
      End if
      End do
   End do

!******7-day rainfall AnnMax*******
   p=0
   do j=1,Numb_yr
      Ann_max7(j)= 0.000011
      m=1+p
      p=p+Numb_R7(j)
      do k=m,p
      if (R7(k)>Ann_max7(j)) then
         Ann_max7(j)=R7(k)
      Else
         Ann_max7(j)=Ann_max7(j)
      End if
      End do
   End do

!*******Searching for zero Annual Maximums*****
   NE=0
   do i=1,Numb_yr
   if (Ann_max(i)==0.000011) then
      NE=NE+1
   Else
      NE=NE
   End if
   End do

!**printing the annual maximum**********

   !print*,'The annual maximums are:'
   !print*,'Year     d      2-d      3-d       5-d      7-d'
   write(20,*)'The number of years are:',Numb_yr
   write(20,*)'The annual maximums are:'
   write(20,*)'Year      d       2-d        3-d        5-d        7-d'
      do j=1,Numb_yr
      !write(*,'(I4,5F10.2)')Av_Yr(j),Ann_max(j),Ann_max2(j),Ann_max3(j),Ann_max5(j),Ann_max7(j)
      write(20,'(I4,5F10.2)')Av_Yr(j),Ann_max(j),Ann_max2(j),Ann_max3(j),Ann_max5(j),Ann_max7(j)
      End do
   print*,'There are',NE,'years with 0 ann max'

!-------------Calculating the PMP using Hershfield Statistical Method------------------------------------------

!CALCULATE Sn,Xn-1,Sn-1,Km
!Xn=AVGAM       = average annual maximum
!Sn             = the standard deviation
!Xn-1= AVGEX    = the average of the series excluding the maximum value in the series
!Sn-1= SnEX     = the standard deviation of the series excluding the maximum value in the series
```

```
!Km          = the frequency factor of Hershfield method

   allocate(z(Numb_Yr))
   allocate(z2(Numb_Yr))
   allocate(z3(Numb_Yr))
   allocate(z5(Numb_Yr))
   allocate(z7(Numb_Yr))

   AVGAM=sum(Ann_max)/(Numb_Yr-NE)
   AVGAM2=sum(Ann_max2)/(Numb_Yr-NE)
   AVGAM3=sum(Ann_max3)/(Numb_Yr-NE)
   AVGAM5=sum(Ann_max5)/(Numb_Yr-NE)
   AVGAM7=sum(Ann_max7)/(Numb_Yr-NE)

   max_loc1=maxloc(Ann_max)
   max_loc2=maxloc(Ann_max2)
   max_loc3=maxloc(Ann_max3)
   max_loc5=maxloc(Ann_max5)
   max_loc7=maxloc(Ann_max7)

   write(20,*)'The highest annual maximum 1d is on the year',Av_Yr(max_loc1)
   write(20,*)'The highest annual maximum 2d is on the year',Av_Yr(max_loc2)
   write(20,*)'The highest annual maximum 3d is on the year',Av_Yr(max_loc3)
   write(20,*)'The highest annual maximum 5d is on the year',Av_Yr(max_loc5)
   write(20,*)'The highest annual maximum 7d is on the year',Av_Yr(max_loc7)

   write(20,*)'Xn is:'
   write(20,*)'    1d          2d          3d          5d          7d'
   write(20,*)AVGAM,AVGAM2,AVGAM3,AVGAM5,AVGAM7

!****** Calculate Sn ************
!--Sn 1-d---
   do i=1,Numb_Yr
      z(i)=(ABS(Ann_max(i)-AVGAM))**2.0
   end do
   Sn=sqrt(1.0/(Numb_Yr-1)*sum(z))

!--Sn 2-d---
   do i=1,Numb_Yr
      z2(i)=(ABS(Ann_max2(i)-AVGAM2))**2.0
   end do
   Sn2=sqrt(1.0/(Numb_Yr-1)*sum(z2))

!--Sn 3-d---
   do i=1,Numb_Yr
      z3(i)=(ABS(Ann_max3(i)-AVGAM3))**2.0
   end do
   Sn3=sqrt(1.0/(Numb_Yr-1)*sum(z3))
```

HERSHPMP

```
!--Sn 5-d---
   do i=1,Numb_Yr
      z5(i)=(ABS(Ann_max5(i)-AVGAM5))**2.0
   end do
   Sn5=sqrt(1.0/(Numb_Yr-1)*sum(z5))

!--Sn 7-d---
   do i=1,Numb_Yr
      z7(i)=(ABS(Ann_max7(i)-AVGAM7))**2.0
   end do
   Sn7=sqrt(1.0/(Numb_Yr-1)*sum(z7))
!---------
   write(20,*)'Sn is:'
   write(20,*)'    1d          2d          3d          5d          7d'
   write(20,*)Sn,Sn2,Sn3,Sn5,Sn7

!****** Calculate Xn-1  ************
   AVGEX=(sum(Ann_max)-maxval(Ann_max))/(Numb_Yr-1-NE)     !1-d
   AVGEX2=(sum(Ann_max2)-maxval(Ann_max2))/(Numb_Yr-1-NE)  !2-d
   AVGEX3=(sum(Ann_max3)-maxval(Ann_max3))/(Numb_Yr-1-NE)  !3-d
   AVGEX5=(sum(Ann_max5)-maxval(Ann_max5))/(Numb_Yr-1-NE)  !5-d
   AVGEX7=(sum(Ann_max7)-maxval(Ann_max7))/(Numb_Yr-1-NE)  !7-d
   write(20,*)'Xn-1 is: '
   write(20,*)'    1d          2d          3d          5d          7d'
   write(20,*)AVGEX,AVGEX2,AVGEX3,AVGEX5,AVGEX7

!****** Calculate Sn-1  ************

!--Sn-1 1-d---
   do i=1,Numb_Yr
      if (i==max_loc1(1)) then
         z(i)=0.0
      else
         z(i)=(ABS(Ann_max(i)-AVGEX))**2.0
      end if
   end do
   SnEX=sqrt(1.0/(Numb_Yr-2)*sum(z))

!--Sn-1 2-d---
   do i=1,Numb_Yr
      if (i==max_loc2(1)) then
         z2(i)=0.0
      else
         z2(i)=(ABS(Ann_max2(i)-AVGEX2))**2.0
      end if
   end do
   SnEX2=sqrt(1.0/(Numb_Yr-2)*sum(z2))

!--Sn-1 3-d---
```

Page 8

```
  do i=1,Numb_Yr
    if (i==max_loc3(1)) then
      z3(i)=0.0
    else
      z3(i)=(ABS(Ann_max3(i)-AVGEX3))**2.0
    end if
  end do
  SnEX3=sqrt(1.0/(Numb_Yr-2)*sum(z3))

!--Sn-1 5-d---
  do i=1,Numb_Yr
    if (i==max_loc5(1)) then
      z5(i)=0.0
    else
      z5(i)=(ABS(Ann_max5(i)-AVGEX5))**2.0
    end if
  end do
  SnEX5=sqrt(1.0/(Numb_Yr-2)*sum(z5))

!--Sn-1 7-d---
  do i=1,Numb_Yr
    if (i==max_loc7(1)) then
      z7(i)=0.0
    else
      z7(i)=(ABS(Ann_max7(i)-AVGEX7))**2.0
    end if
  end do
  SnEX7=sqrt(1.0/(Numb_Yr-2)*sum(z7))

!-------------------------------------
  write(20,*),'Sn-1 is: '
  write(20,*),'    1d          2d          3d          5d          7d'
  write(20,*),SnEX,SnEX2,SnEX3,SnEX5,SnEX7

!****** Calculate Km  ************
  Km=(maxval(Ann_max)-AVGEX)/SnEX
  Km2=(maxval(Ann_max2)-AVGEX2)/SnEX2
  Km3=(maxval(Ann_max3)-AVGEX3)/SnEX3
  Km5=(maxval(Ann_max5)-AVGEX5)/SnEX5
  Km7=(maxval(Ann_max7)-AVGEX7)/SnEX7
  write(20,*),'Km is: '
  write(20,*)'    1d          2d          3d          5d          7d'
  write(20,*)Km,Km2,Km3,Km5,Km7

!-----Clarifying the Km and Xn for every station----------------------------------------

  Km_S(h)= Km
  Xn_S(h)= AVGAM
  Sn_S(h)=Sn
```

```
    Km_S2(h)= Km2
    Xn_S2(h)= AVGAM2
    Sn_S2(h)=Sn2

    Km_S3(h)= Km3
    Xn_S3(h)= AVGAM3
    Sn_S3(h)=Sn3

    Km_S5(h)= Km5
    Xn_S5(h)= AVGAM5
    Sn_S5(h)=Sn5

    Km_S7(h)= Km7
    Xn_S7(h)= AVGAM7
    Sn_S7(h)=Sn7

    deallocate(Ln)
    deallocate(R)
    deallocate(R2)
    deallocate(R3)
    deallocate(R5)
    deallocate(R7)
    deallocate(Yr)
    deallocate(Mth)
    deallocate(Day)
    deallocate(Hr)
    deallocate(Av_Yr)
    deallocate(Numb_R)
    deallocate(Numb_R2)
    deallocate(Numb_R3)
    deallocate(Numb_R5)
    deallocate(Numb_R7)
    deallocate(Ann_max)
    deallocate(Ann_max2)
    deallocate(Ann_max3)
    deallocate(Ann_max5)
    deallocate(Ann_max7)
    deallocate(z)
    deallocate(z2)
    deallocate(z3)
    deallocate(z5)
    deallocate(z7)


  end do

    write(20,*)'**********************HERSHFIELD PARAMETERS**************************************************'
```

HERSHPMP

```
    write(20,*)'The Hershfield parameters for 1-day rainfall are:'
    write(20,*)'       No.        Station              Km              Xn              Sn'
  do h=1,N_stn
    write(20,*),h,fname(h),Km_S(h),Xn_S(h),Sn_S(h)
  end do

    write(20,*)'The Hershfield parameters for 2-day rainfall are:'
    write(20,*)'       No.        Station              Km              Xn              Sn'
  do h=1,N_stn
    write(20,*),h,fname(h),Km_S2(h),Xn_S2(h),Sn_S2(h)
  end do

    write(20,*)'The Hershfield parameters for 3-day rainfall are:'
    write(20,*)'       No.        Station              Km              Xn              Sn'
  do h=1,N_stn
    write(20,*),h,fname(h),Km_S3(h),Xn_S3(h),Sn_S3(h)
  end do

    write(20,*)'The Hershfield parameters for 5-day rainfall are:'
    write(20,*)'       No.        Station              Km              Xn              Sn'
  do h=1,N_stn
    write(20,*),h,fname(h),Km_S5(h),Xn_S5(h),Sn_S5(h)
  end do

    write(20,*)'The Hershfield parameters for 7-day rainfall are:'
    write(20,*)'       No.        Station              Km              Xn              Sn'
  do h=1,N_stn
    write(20,*),h,fname(h),Km_S7(h),Xn_S7(h),Sn_S7(h)
  end do


  print*,'---------------------- PMP HERSHFIELD (mm)-------------------------------'
  write(20,*),''
  write(20,*),'----------------------------------------PMP
HERSHFIELD(mm)-----------------------------------------------------'
!  write(20,*)' For 1-day rainfall the PMP parameters are:'
! print*,'       No.     Km          Xn '
! write(20,*)'       No.     Km          Xn'

! do h=1,N_stn

!     print*,h,Km_S(h),Xn_S(h),Km_S2(h),Xn_S2(h)
!     write(20,*)h,Km_S(h),Xn_S(h),Km_S2(h),Xn_S2(h)
!  end do


  !****** Plotting Km and determine Envelope --- 1-day rain ******
```

Page 11

HERSHPMP

```
!Y = m X + C
! m = (Y1-Y2)/(X1-X2)
! X1=Xn for the max Km
! Y1=Max Km
! X2=Max Xn
! Y2=Km for the max Xn
! C= Y1-m*X1
!PMP=Xn+Sn*Km

Y1= maxval(Km_s)
Y1_loc= maxloc(Km_s)
X1=Xn_S(Y1_loc)

X2=maxval(Xn_S)
X2_loc= maxloc(Xn_S)
Y2= Km_s(X2_loc)

Reg_M=(Y1-Y2)/(X1-X2)
Reg_C=Y1-Reg_M*X1


!print*,'max Km is', Y1
!print*,'location of the max Km is', Y1_loc
!print*,'Xn for the max Km is', X1

!print*,'max Xn is', X2
!print*,'location of the max Xn is', X2_loc
!print*,'Km for the max Xn is',Y2

print*,'Reg_M for the Envelope=',Reg_M
print*,'Reg_C for the Envelope=',Reg_C
print*,'The PMPs are:'
write(20,*)'Reg_M for the Envelope=',Reg_M
write(20,*)'Reg_C for the Envelope=',Reg_C
write(20,*)'The PMPs are:'


do h=1,N_stn

   New_Km(h)=Reg_M(1)*Xn_S(h)+Reg_C(1)
   PMP(h)=Xn_S(h)+Sn_S(h)*New_Km(h)
   print*,h,PMP(h)
   write(20,*),h,PMP(h)
end do

!****** Plotting Km and determine Envelope --- 2-day rain ******

Y1_2= maxval(Km_s2)
```

Page 12

HERSHPMP

```
 Y1_loc2= maxloc(Km_s2)
 X1_2=Xn_S2(Y1_loc2)

 X2_2=maxval(Xn_S2)
 X2_loc2= maxloc(Xn_S2)
 Y2_2= Km_s2(X2_loc2)

 Reg_M_2=(Y1_2-Y2_2)/(X1_2-X2_2)
 Reg_C_2=Y1_2-Reg_M_2*X1_2

 print*,'Reg_M (2d)for the Envelope=',Reg_M_2
 print*,'Reg_C (2d)for the Envelope=',Reg_C_2
 print*,'The PMPs for 2-day are:'
 write(20,*)'Reg_M (2d)for the Envelope=',Reg_M_2
 write(20,*)'Reg_C (2d)for the Envelope=',Reg_C_2
 write(20,*)'The PMPs for 2-day are:'


 do h=1,N_stn

    New_Km2(h)=Reg_M_2(1)*Xn_S2(h)+Reg_C_2(1)
    PMP2(h)=Xn_S2(h)+Sn_S2(h)*New_Km2(h)
    print*,h,PMP2(h)
    write(20,*),h,PMP2(h)

 end do

!****** Plotting Km and determine Envelope --- 3-day rain ******

 Y1_3= maxval(Km_s3)
 Y1_loc3= maxloc(Km_s3)
 X1_3=Xn_S3(Y1_loc3)

 X2_3=maxval(Xn_S3)
 X2_loc3= maxloc(Xn_S3)
 Y2_3= Km_s3(X2_loc3)

 Reg_M_3=(Y1_3-Y2_3)/(X1_3-X2_3)
 Reg_C_3=Y1_3-Reg_M_3*X1_3

 print*,'Reg_M (3d)for the Envelope=',Reg_M_3
 print*,'Reg_C (3d)for the Envelope=',Reg_C_3
 print*,'The PMPs for 3-day are:'
 write(20,*)'Reg_M (3d)for the Envelope=',Reg_M_3
 write(20,*)'Reg_C (3d)for the Envelope=',Reg_C_3
 write(20,*)'The PMPs for 3-day are:'


 do h=1,N_stn
```

Page 13

```
        New_Km3(h)=Reg_M_3(1)*Xn_S3(h)+Reg_C_3(1)
        PMP3(h)=Xn_S3(h)+Sn_S3(h)*New_Km3(h)
        print*,h,PMP3(h)
        write(20,*),h,PMP3(h)

    end do

!****** Plotting Km and determine Envelope --- 5-day rain ******

    Y1_5= maxval(Km_s5)
    Y1_loc5= maxloc(Km_s5)
    X1_5=Xn_S5(Y1_loc5)

    X2_5=maxval(Xn_S5)
    X2_loc5= maxloc(Xn_S5)
    Y2_5= Km_s5(X2_loc5)

    Reg_M_5=(Y1_5-Y2_5)/(X1_5-X2_5)
    Reg_C_5=Y1_5-Reg_M_5*X1_5

    print*,'Reg_M (5d)for the Envelope=',Reg_M_5
    print*,'Reg_C (5d)for the Envelope=',Reg_C_5
    print*,'The PMPs for 5-day are:'
    write(20,*)'Reg_M (5d)for the Envelope=',Reg_M_5
    write(20,*)'Reg_C (5d)for the Envelope=',Reg_C_5
    write(20,*)'The PMPs for 5-day are:'


    do h=1,N_stn

        New_Km5(h)=Reg_M_5(1)*Xn_S5(h)+Reg_C_5(1)
        PMP5(h)=Xn_S5(h)+Sn_S5(h)*New_Km5(h)
        print*,h,PMP5(h)
        write(20,*),h,PMP5(h)

    end do

!****** Plotting Km and determine Envelope --- 7-day rain ******

    Y1_7= maxval(Km_s7)
    Y1_loc7= maxloc(Km_s7)
    X1_7=Xn_S7(Y1_loc7)

    X2_7=maxval(Xn_S7)
    X2_loc7= maxloc(Xn_S7)
    Y2_7= Km_s7(X2_loc7)

    Reg_M_7=(Y1_7-Y2_7)/(X1_7-X2_7)
```

```
  Reg_C_7=Y1_7-Reg_M_7*X1_7

  print*,'Reg_M (7d)for the Envelope=',Reg_M_7
  print*,'Reg_C (7d)for the Envelope=',Reg_C_7
  print*,'The PMPs for 7-day are:'
  write(20,*)'Reg_M (7d)for the Envelope=',Reg_M_7
  write(20,*)'Reg_C (7d)for the Envelope=',Reg_C_7
  write(20,*)'The PMPs for 7-day are:'


  do h=1,N_stn

     New_Km7(h)=Reg_M_7(1)*Xn_S7(h)+Reg_C_7(1)
     PMP7(h)=Xn_S7(h)+Sn_S7(h)*New_Km7(h)
     print*,h,PMP7(h)
     write(20,*),h,PMP7(h)

  end do

print*,'****************************************************************** '


print*,'PLEASE SEE THE OUTPUT FILE NAMED "OUTPUT.TXT"'

end program
```

A-5

HERSHPMP.FOR program codes (for the hourly data)

```
!     @@@@@@@@@@@@@@@@@@@@@@@@@@@@@@@@@@@@@@@
!     @   Programmer: Nor Eliza Alias       @
!     @   Date:15 June 2012                 @
!     @                                     @
!     @     ~~^o^~~  ~~^o^~~                @
!     @@@@@@@@@@@@@@@@@@@@@@@@@@@@@@@@@@@@@@@
!This program calculates the ann_max and Hershfield statistical PMP parameters for subdaily rainfall

program HERSHPMP_hr
implicit none
integer,parameter::max=1000000000 ! the maximum number of line per file
integer::N,N2,N3,N4,N6,N12,N24,i,j,k,p,m,h,NumbLine,SY,EY,Numb_Yr,Numb_Stn,NE,N_stn   !SY=Starting year,
EY=Ending year, Numb_Yr =number of Av_Yr ,Numb_Stn = Number of station to analyse
real,allocatable,dimension(:)::Ln,Ann_max,Ann_max2,Ann_max3,Ann_max4,Ann_max6,Ann_max12,Ann_max24!
Ln=line, R=hourly rainfall, R2=2hr-rain, R3=3hr-rain, R6=6hr-rain,R12=12hr-rain,R24=24hr-rain
real,allocatable,dimension(:)::R,R2,R3,R4,R6,R12,R24,z,z2,z3,z4,z6,z12,z24,MDATA,MDATA2   !MDATA=missing
data for leap years, MDATA2=missing data for normal years
real,allocatable,dimension(:)::Km_S,Xn_S,Sn_S,New_Km,PMP,Km_S2,Xn_S2,Sn_S2,New_Km2,PMP2,Km_S3,Xn_S3,Sn_S3,
New_Km3,PMP3
real,allocatable,dimension(:)::Km_S4,Xn_S4,Sn_S4,New_Km4,PMP4,Km_S6,Xn_S6,Sn_S6,New_Km6,PMP6,Km_S12,Xn_S12
,Sn_S12,New_Km12,PMP12
real,allocatable,dimension(:)::Km_S24,Xn_S24,Sn_S24,New_Km24,PMP24
real,dimension(400)::R_yr             !R_yr=rainfall data in specific year
integer,allocatable,dimension(:)::Yr,Mth,Day,Hr,Av_Yr ! Yr=year,Mth=month,Hr=hour,Av_Yr= Available year,
Numb_R = No. of recorded days
integer,allocatable,dimension(:)::Numb_R,Numb_R2,Numb_R3,Numb_R4,Numb_R6,Numb_R12,Numb_R24
real::Sn,Sn2,Sn3,Sn4,Sn6,Sn12,Sn24,AVGAM,AVGAM2,AVGAM3,AVGAM4,AVGAM6,AVGAM12,AVGAM24
real::AVGEX,AVGEX2,AVGEX3,AVGEX4,AVGEX6,AVGEX12,AVGEX24
real::SnEX,SnEX2,SnEX3,SnEX4,SnEX6,SnEX12,SnEX24,Km,Km2,Km3,Km4,Km6,Km12,Km24
real::X2,X2_2,X2_3,X2_4,X2_6,X2_12,X2_24,Y1,Y1_2,Y1_3,Y1_4,Y1_6,Y1_12,Y1_24
integer,dimension(1)::max_loc1,max_loc2,max_loc3,max_loc4,max_loc6,max_loc12,max_loc24  !max_loc=max
value location
integer,dimension(1)::Y1_loc,X2_loc,Y1_loc2,X2_loc2,Y1_loc3,X2_loc3,Y1_loc4,X2_loc4
integer,dimension(1)::Y1_loc6,X2_loc6,Y1_loc12,X2_loc12,Y1_loc24,X2_loc24
real,dimension(1)::X1,Y2,Reg_M,Reg_C,X1_2,Y2_2,Reg_M_2,Reg_C_2
real,dimension(1)::X1_3,Y2_3,Reg_M_3,Reg_C_3,X1_4,Y2_4,Reg_M_4,Reg_C_4
real,dimension(1)::X1_6,Y2_6,Reg_M_6,Reg_C_6,X1_12,Y2_12,Reg_M_12,Reg_C_12,X1_24,Y2_24,Reg_M_24,Reg_C_24
character(30)::ListName
character(30),allocatable,dimension(:)::fname

print*,'Please enter the number of stations to analyse:'
read*,N_stn
print*,'Please enter the file name containing the lists of stations to be analyse:'
read*,ListName
open(10,file=ListName)
open(20,file='output.txt',STATUS='REPLACE')


allocate(Km_S(N_stn))
allocate(Xn_S(N_stn))
allocate(Sn_S(N_stn))
allocate(New_Km(N_stn))
allocate(PMP(N_stn))
allocate(Km_S2(N_stn))
allocate(Xn_S2(N_stn))
allocate(Sn_S2(N_stn))
allocate(New_Km2(N_stn))
allocate(PMP2(N_stn))
allocate(Km_S3(N_stn))
allocate(Xn_S3(N_stn))
allocate(Sn_S3(N_stn))
allocate(New_Km3(N_stn))
allocate(PMP3(N_stn))
allocate(Km_S4(N_stn))
allocate(Xn_S4(N_stn))
allocate(Sn_S4(N_stn))
allocate(New_Km4(N_stn))
```

```
allocate(PMP4(N_stn))
allocate(Km_S6(N_stn))
allocate(Xn_S6(N_stn))
allocate(Sn_S6(N_stn))
allocate(New_Km6(N_stn))
allocate(PMP6(N_stn))
allocate(Km_S12(N_stn))
allocate(Xn_S12(N_stn))
allocate(Sn_S12(N_stn))
allocate(New_Km12(N_stn))
allocate(PMP12(N_stn))
allocate(Km_S24(N_stn))
allocate(Xn_S24(N_stn))
allocate(Sn_S24(N_stn))
allocate(New_Km24(N_stn))
allocate(PMP24(N_stn))

allocate(fname(N_stn))


do h=1,N_stn

        read(10,*)fname(h)
        print*,'now reading',fname(h)

!---allocating the number of data------------------------

open(30,file=fname(h))

   Do 100 i=1,max

     N=N+1
     READ(30,*,END=120)
     NumbLine=N

 100 CONTINUE

120 NumbLine=i-1

close(30)

PRINT*,''
PRINT*,'The number of LINE is :',NumbLine

write(20,*),''
write(20,*),'Reading file',' ',fname(h)

write(20,*),''
write(20,*),'The number of LINE is:',NumbLine

allocate(Ln(NumbLine))
allocate(R(NumbLine))
allocate(R2(NumbLine-1))
allocate(R3(NumbLine-2))
allocate(R4(NumbLine-3))
allocate(R6(NumbLine-5))
allocate(R12(NumbLine-11))
allocate(R24(NumbLine-23))
allocate(Yr(NumbLine))
allocate(Mth(NumbLine))
allocate(Day(NumbLine))
allocate(Hr(NumbLine))


!-----reading data from file---------------------------------

open(30,file=fname(h))
```

```
PRINT*,''
PRINT*,'Please wait...Calculating..'

write(20,*),''
write(20,*),'The data are:'
write(20,*),'Year/Month/Day/Hour   Rainfall (mm)'

do i=1,NumbLine

 read(30,*)Yr(i),Mth(i),Day(i),Hr(i),R(i)

end do

!print*,'the years are:'

SY=Yr(1)
EY=Yr(numbline)
Numb_Yr = EY-SY+1

allocate(Av_Yr(Numb_Yr))
allocate(Numb_R(Numb_Yr))
allocate(Numb_R2(Numb_Yr))
allocate(Numb_R3(Numb_Yr))
allocate(Numb_R4(Numb_Yr))
allocate(Numb_R6(Numb_Yr))
allocate(Numb_R12(Numb_Yr))
allocate(Numb_R24(Numb_Yr))
allocate(Ann_max(Numb_Yr))
allocate(Ann_max2(Numb_Yr))
allocate(Ann_max3(Numb_Yr))
allocate(Ann_max4(Numb_Yr))
allocate(Ann_max6(Numb_Yr))
allocate(Ann_max12(Numb_Yr))
allocate(Ann_max24(Numb_Yr))
allocate(MDATA(Numb_Yr))
allocate(MDATA2(Numb_Yr))



!print*,'start year is = ',SY
!print*,'end year is = ',EY
!print*,'available years are :'
write(20,*)''
write(20,*)'Available years are :'

        do i=1,Numb_Yr
                Av_Yr(i)=SY
                SY=SY+1
          If(SY==EY) then
                go to 220
          End if

220 End do

        print*,'the number of years are:',Numb_Yr
        print*,''

!**calculating the Number of data every year***

        do j=1,Numb_Yr
                N=1
                do i=1,NumbLine
                if (Yr(i)==Av_Yr(j)) then
                Numb_R(j)=N
                N=N+1
                else
```

```
              go to 320
              End if
320           end do
       end do

       print*, '       Year   Rec. hrs    %Missing    %Missing(For Leap yrs)'
       write(20,*)'       Year   Rec. hrs  %Missing    %Missing(For Leap yrs)'

    !Percentage of missing data per year

       do j=1,Numb_Yr

           MDATA(j)=(8760.0-Numb_R(j))/8760.0*100.0
           MDATA2(j)=(8784.0-Numb_R(j))/8784.0*100.0
       print*,Av_Yr(j),Numb_R(j),MDATA(j),MDATA2(j)
       write(20,*)Av_Yr(j),Numb_R(j),MDATA(j),MDATA2(j)

       end do


!calculating the Number of data per year for R2,R3,R4,R6,R12,R24 **

do j=1,Numb_yr

       if (j==Numb_yr) then

       Numb_R2(j)=Numb_R(j)-1
       Numb_R3(j)=Numb_R(j)-2
       Numb_R4(j)=Numb_R(j)-3
       Numb_R6(j)=Numb_R(j)-5
    Numb_R12(j)=Numb_R(j)-11
    Numb_R24(j)=Numb_R(j)-23

       Else

       Numb_R2(j)=Numb_R(j)
       Numb_R3(j)=Numb_R(j)
       Numb_R4(j)=Numb_R(j)
       Numb_R6(j)=Numb_R(j)
    Numb_R12(j)=Numb_R(j)
       Numb_R24(j)=Numb_R(j)

       End if

end do

!-------calculating Rainfall 2-hr,3-hr,4-hr,6-hr,12-hr,24-hr --------------------

!******2-hr rainfall*******

N2=Numbline-1

do i=1,N2
 R2(i)=R(i)+R(i+1)
end do

!******3-hr rainfall*******

N3=Numbline-2
do i=1,N3
  R3(i)=R(i)+R(i+1)+R(i+2)
end do

!******4-hr rainfall*******

N4=Numbline-3
do i=1,N4
```

```
  R4(i)=R(i)+R(i+1)+R(i+2)+R(i+3)
end do

!******6-hr rainfall*******

N6=Numbline-5
do i=1,N6
  R6(i)=R(i)+R(i+1)+R(i+2)+R(i+3)+R(i+4)+R(i+5)
end do

!******12-hr rainfall*******

N12=Numbline-11
do i=1,N12
  R12(i)=R(i)+R(i+1)+R(i+2)+R(i+3)+R(i+4)+R(i+5)+R(i+6)+R(i+7)&
  +R(i+8)+R(i+9)+R(i+10)+R(i+11)
end do

!******24-hr rainfall*******

N24=Numbline-23
do i=1,N24
  R24(i)=R(i)+R(i+1)+R(i+2)+R(i+3)+R(i+4)+R(i+5)+R(i+6)+R(i+7)+R(i+8)+R(i+9)+R(i+10)
  R24(i)=R24(i)+R(i+11)+R(i+12)+R(i+13)+R(i+14)+R(i+15)+R(i+16)+R(i+17)&
  +R(i+18)+R(i+19)+R(i+20)+R(i+21)+R(i+22)+R(i+23)
end do

!-----calculate AnnMax -----------------------------

!******1-hr rainfall AnnMax*******
p=0
 do j=1,Numb_yr
        Ann_max(j)= 0.000011
        m=1+p
        p=p+Numb_R(j)
        do k=m,p
                if (R(k)>Ann_max(j)) then
                Ann_max(j)=R(k)
                Else
                Ann_max(j)=Ann_max(j)
                End if
        End do
 End do

!******2-hr rainfall AnnMax*******
p=0
 do j=1,Numb_yr
        Ann_max2(j)= 0.000011
        m=1+p
        p=p+Numb_R2(j)
        do k=m,p
                if (R2(k)>Ann_max2(j)) then
                Ann_max2(j)=R2(k)
                Else
                Ann_max2(j)=Ann_max2(j)
                End if
        End do
 End do

 !******3-hr rainfall AnnMax*******
p=0
 do j=1,Numb_yr
        Ann_max3(j)= 0.000011
        m=1+p
        p=p+Numb_R3(j)
        do k=m,p
                if (R3(k)>Ann_max3(j)) then
```

```
                Ann_max3(j)=R3(k)
                Else
                Ann_max3(j)=Ann_max3(j)
                End if
        End do
 End do

  !******4-hr rainfall AnnMax*******
p=0
 do j=1,Numb_yr
        Ann_max4(j)= 0.000011
        m=1+p
        p=p+Numb_R4(j)
        do k=m,p
                if (R4(k)>Ann_max4(j)) then
                Ann_max4(j)=R4(k)
                Else
                Ann_max4(j)=Ann_max4(j)
                End if
        End do
 End do

 !******6-hr rainfall AnnMax*******
p=0
 do j=1,Numb_yr
        Ann_max6(j)= 0.000011
        m=1+p
        p=p+Numb_R6(j)
        do k=m,p
                if (R6(k)>Ann_max6(j)) then
                Ann_max6(j)=R6(k)
                Else
                Ann_max6(j)=Ann_max6(j)
                End if
        End do
 End do

  !******12-hr rainfall AnnMax*******
p=0
 do j=1,Numb_yr
        Ann_max12(j)= 0.000011
        m=1+p
        p=p+Numb_R12(j)
        do k=m,p
                if (R12(k)>Ann_max12(j)) then
                Ann_max12(j)=R12(k)
                Else
                Ann_max12(j)=Ann_max12(j)
                End if
        End do
 End do

   !******24-hr rainfall AnnMax*******
p=0
 do j=1,Numb_yr
        Ann_max24(j)= 0.000011
        m=1+p
        p=p+Numb_R24(j)
        do k=m,p
                if (R24(k)>Ann_max24(j)) then
                Ann_max24(j)=R24(k)
                Else
                Ann_max24(j)=Ann_max24(j)
                End if
        End do
 End do
```

```
!*******Searching for zero Annual Maximums (errors) *****
NE=0
do i=1,Numb_yr

    if (Ann_max(i)==0.000011) then
        NE=NE+1
    Else
       NE=NE
    End if

End do

!**printing the annual maximum**********

print*,'The annual maximums are:'
print*,'Year   1-hr       2-hr       3-hr      4-hr     6-hr      12-hr      24-hr'
write(20,*)'The annual maximums are:'
write(20,*)'Year      1-hr      2-hr      3-hr      4-hr      6-hr      12-hr     24-hr'

do j=1,Numb_yr

write(*,'(I4,7F10.2)')Av_Yr(j),Ann_max(j),Ann_max2(j),Ann_max3(j),Ann_max4(j),Ann_max6(j),Ann_max12(j),Ann
_max24(j)

write(20,'(I4,7F10.2)')Av_Yr(j),Ann_max(j),Ann_max2(j),Ann_max3(j),Ann_max4(j),Ann_max6(j),Ann_max12(j),An
n_max24(j)
End do
print*,'There are',NE,'years with 0 ann max, the years with 0 annmax are not included for PMP analysis'

                !-------------Calculating the PMP using Hershfield Statistical
Method-----------------------------------------

                !CALCULATE Sn,Xn-1,Sn-1,Km
                !Xn=AVGAM       = average annual maximum
                !Sn             = the standard deviation
                !Xn-1= AVGEX    = the average of the series excluding the maximum value in the series
                !Sn-1= SnEX     = the standard deviation of the series excluding the maximum value in the
series
                !Km             = the frequency factor of Hershfield method

                allocate(z(Numb_Yr))
                allocate(z2(Numb_Yr))
                allocate(z3(Numb_Yr))
                allocate(z4(Numb_Yr))
                allocate(z6(Numb_Yr))
                allocate(z12(Numb_Yr))
                allocate(z24(Numb_Yr))


                AVGAM=sum(Ann_max)/(Numb_Yr-NE)
                AVGAM2=sum(Ann_max2)/(Numb_Yr-NE)
                AVGAM3=sum(Ann_max3)/(Numb_Yr-NE)
                AVGAM4=sum(Ann_max4)/(Numb_Yr-NE)
                AVGAM6=sum(Ann_max6)/(Numb_Yr-NE)
                AVGAM12=sum(Ann_max12)/(Numb_Yr-NE)
                AVGAM24=sum(Ann_max24)/(Numb_Yr-NE)

                max_loc1=maxloc(Ann_max)
                max_loc2=maxloc(Ann_max2)
                        max_loc3=maxloc(Ann_max3)
                max_loc4=maxloc(Ann_max4)
                        max_loc6=maxloc(Ann_max6)
                        max_loc12=maxloc(Ann_max12)
                max_loc24=maxloc(Ann_max24)

                write(20,*)'The highest annual maximum 1-hr is on the year',Av_Yr(max_loc1)
                write(20,*)'The highest annual maximum 2-hr is on the year',Av_Yr(max_loc2)
```

```
write(20,*)'The highest annual maximum 3-hr is on the year',Av_Yr(max_loc3)
write(20,*)'The highest annual maximum 4-hr is on the year',Av_Yr(max_loc4)
write(20,*)'The highest annual maximum 6-hr is on the year',Av_Yr(max_loc6)
write(20,*)'The highest annual maximum 12-hr is on the year',Av_Yr(max_loc12)
write(20,*)'The highest annual maximum 24-hr is on the year',Av_Yr(max_loc24)


write(20,*)'Xn is:'
write(20,*),'     1hr       2hr       3hr      4hr      6hr      12hr      24hr'

write(20,*)AVGAM,AVGAM2,AVGAM3,AVGAM4,AVGAM6,AVGAM12,AVGAM24

!print*,'the number of years is:'

!print*,Numb_Yr

!****** Calculate Sn ************

!--Sn 1-hr---

do i=1,Numb_Yr
z(i)=(ABS(Ann_max(i)-AVGAM))**2.0
end do

Sn=sqrt(1.0/(Numb_Yr-1)*sum(z))

!--Sn 2-hr---

do i=1,Numb_Yr
z2(i)=(ABS(Ann_max2(i)-AVGAM2))**2.0
end do

Sn2=sqrt(1.0/(Numb_Yr-1)*sum(z2))

!--Sn 3-hr---

do i=1,Numb_Yr
z3(i)=(ABS(Ann_max3(i)-AVGAM3))**2.0
end do

Sn3=sqrt(1.0/(Numb_Yr-1)*sum(z3))

!--Sn 4-hr---

do i=1,Numb_Yr
z4(i)=(ABS(Ann_max4(i)-AVGAM4))**2.0
end do

Sn4=sqrt(1.0/(Numb_Yr-1)*sum(z4))

!--Sn 6-hr---

do i=1,Numb_Yr
z6(i)=(ABS(Ann_max6(i)-AVGAM6))**2.0
end do

Sn6=sqrt(1.0/(Numb_Yr-1)*sum(z6))

!--Sn 12-hr---

do i=1,Numb_Yr
z12(i)=(ABS(Ann_max12(i)-AVGAM12))**2.0
end do

Sn12=sqrt(1.0/(Numb_Yr-1)*sum(z12))

!--Sn 24-hr---
```

```
do i=1,Numb_Yr
z24(i)=(ABS(Ann_max24(i)-AVGAM24))**2.0
end do

Sn24=sqrt(1.0/(Numb_Yr-1)*sum(z24))

!---------

write(20,*)'Sn is:'
write(20,*),'     1hr       2hr       3hr      4hr      6hr      12hr      24hr'
write(20,*)Sn,Sn2,Sn3,Sn4,Sn6,Sn12,Sn24


!****** Calculate Xn-1   ************


AVGEX=(sum(Ann_max)-maxval(Ann_max))/(Numb_Yr-1-NE)      !1-hr
AVGEX2=(sum(Ann_max2)-maxval(Ann_max2))/(Numb_Yr-1-NE)  !2-hr
AVGEX3=(sum(Ann_max3)-maxval(Ann_max3))/(Numb_Yr-1-NE)  !3-hr
AVGEX4=(sum(Ann_max4)-maxval(Ann_max4))/(Numb_Yr-1-NE)  !4-hr
AVGEX6=(sum(Ann_max6)-maxval(Ann_max6))/(Numb_Yr-1-NE)  !6-hr
AVGEX12=(sum(Ann_max12)-maxval(Ann_max12))/(Numb_Yr-1-NE)  !12-hr
AVGEX24=(sum(Ann_max24)-maxval(Ann_max24))/(Numb_Yr-1-NE)  !24-hr

write(20,*)'Xn-1 is: '
write(20,*),'     1hr       2hr       3hr      4hr      6hr      12hr      24hr'
write(20,*)AVGEX,AVGEX2,AVGEX3,AVGEX4,AVGEX6,AVGEX12,AVGEX24


!****** Calculate Sn-1   ************

!--Sn-1 1-hr---

do i=1,Numb_Yr
if (i==max_loc1(1)) then
        z(i)=0.0
        else
        z(i)=(ABS(Ann_max(i)-AVGEX))**2.0
        end if
end do

SnEX=sqrt(1.0/(Numb_Yr-2)*sum(z))


!--Sn-1 2-hr---

do i=1,Numb_Yr
        if (i==max_loc2(1)) then
        z2(i)=0.0
        else
        z2(i)=(ABS(Ann_max2(i)-AVGEX2))**2.0
        end if
end do

SnEX2=sqrt(1.0/(Numb_Yr-2)*sum(z2))

!--Sn-1 3-hr---

do i=1,Numb_Yr
if (i==max_loc3(1)) then
        z3(i)=0.0
        else
        z3(i)=(ABS(Ann_max3(i)-AVGEX3))**2.0
        end if
end do
```

```
SnEX3=sqrt(1.0/(Numb_Yr-2)*sum(z3))

!--Sn-1 4-hr---

do i=1,Numb_Yr
        if (i==max_loc4(1)) then
        z4(i)=0.0
        else
        z4(i)=(ABS(Ann_max4(i)-AVGEX4))**2.0
        end if
end do

SnEX4=sqrt(1.0/(Numb_Yr-2)*sum(z4))

!--Sn-1 6-hr---

do i=1,Numb_Yr
        if (i==max_loc6(1)) then
        z6(i)=0.0
        else
        z6(i)=(ABS(Ann_max6(i)-AVGEX6))**2.0
        end if
end do

SnEX6=sqrt(1.0/(Numb_Yr-2)*sum(z6))

!--Sn-1 12-hr---

do i=1,Numb_Yr
        if (i==max_loc12(1)) then
        z12(i)=0.0
        else
        z12(i)=(ABS(Ann_max12(i)-AVGEX12))**2.0
        end if
end do

SnEX12=sqrt(1.0/(Numb_Yr-2)*sum(z12))

!--Sn-1 24-hr---

do i=1,Numb_Yr
        if (i==max_loc24(1)) then
        z24(i)=0.0
        else
        z24(i)=(ABS(Ann_max24(i)-AVGEX24))**2.0
        end if
end do

SnEX24=sqrt(1.0/(Numb_Yr-2)*sum(z24))

!-----------------------------------------------------------------------------

write(20,*),'Sn-1 is: '
write(20,*),'     1hr       2hr       3hr      4hr      6hr      12hr      24hr'
write(20,*),SnEX,SnEX2,SnEX3,SnEX4,SnEX6,SnEX12,SnEX24


!****** Calculate Km  ************

Km=(maxval(Ann_max)-AVGEX)/SnEX
Km2=(maxval(Ann_max2)-AVGEX2)/SnEX2
Km3=(maxval(Ann_max3)-AVGEX3)/SnEX3
Km4=(maxval(Ann_max4)-AVGEX4)/SnEX4
Km6=(maxval(Ann_max6)-AVGEX6)/SnEX6
Km12=(maxval(Ann_max12)-AVGEX12)/SnEX12
Km24=(maxval(Ann_max24)-AVGEX24)/SnEX24
```

```
              write(20,*),'Km is: '
              write(20,*),'      1hr        2hr        3hr        4hr        6hr        12hr        24hr'
              write(20,*)Km,Km2,Km3,Km4,Km6,Km12,Km24


!-----Clarifying the Km and Xn for every station-----------------------------------------
        Km_S(h)=Km
        Xn_S(h)=AVGAM
                Sn_S(h)=Sn
                Km_S2(h)=Km2
        Xn_S2(h)=AVGAM2
                Sn_S2(h)=Sn2
                Km_S3(h)=Km3
        Xn_S3(h)=AVGAM3
                Sn_S3(h)=Sn3
                Km_S4(h)=Km4
        Xn_S4(h)=AVGAM4
                Sn_S4(h)=Sn4
                Km_S6(h)=Km6
        Xn_S6(h)=AVGAM6
        Sn_S6(h)=Sn6
               Km_S12(h)=Km12
        Xn_S12(h)=AVGAM12
        Sn_S12(h)=Sn12
        Km_S24(h)=Km24
        Xn_S24(h)=AVGAM24
                Sn_S24(h)=Sn24

        deallocate(Ln)
        deallocate(R)
        deallocate(R2)
        deallocate(R3)
        deallocate(R4)
        deallocate(R6)
        deallocate(R12)
        deallocate(R24)
        deallocate(Mth)
        deallocate(Day)
        deallocate(Hr)
        deallocate(Av_Yr)
        deallocate(Numb_R)
        deallocate(Numb_R2)
        deallocate(Numb_R3)
        deallocate(Numb_R4)
        deallocate(Numb_R6)
        deallocate(Numb_R12)
        deallocate(Numb_R24)
        deallocate(Ann_max)
        deallocate(Ann_max2)
        deallocate(Ann_max3)
        deallocate(Ann_max4)
        deallocate(Ann_max6)
        deallocate(Ann_max12)
        deallocate(Ann_max24)
        deallocate(MDATA)
        deallocate(MDATA2)
        deallocate(z)
        deallocate(z2)
        deallocate(z3)
        deallocate(z4)
        deallocate(z6)
        deallocate(z12)
        deallocate(z24)

End do

    write(20,*)'********************HERSHFIELD
```

```
PARAMETERS**************************************************'

        write(20,*)'The Hershfield parameters for 1-hr rainfall are:'
        write(20,*)'         No.          Station              Km              Xn            Sn'
    do h=1,N_stn
        write(20,*),h,fname(h),Km_S(h),Xn_S(h),Sn_S(h)
    end do

        write(20,*)'The Hershfield parameters for 2-hr rainfall are:'
        write(20,*)'         No.          Station              Km              Xn            Sn'
    do h=1,N_stn
        write(20,*),h,fname(h),Km_S2(h),Xn_S2(h),Sn_S2(h)
    end do

        write(20,*)'The Hershfield parameters for 3-hr rainfall are:'
        write(20,*)'         No.          Station              Km              Xn            Sn'
    do h=1,N_stn
        write(20,*),h,fname(h),Km_S3(h),Xn_S3(h),Sn_S3(h)
    end do

        write(20,*)'The Hershfield parameters for 4-hr rainfall are:'
        write(20,*)'         No.          Station              Km              Xn            Sn'
    do h=1,N_stn
        write(20,*),h,fname(h),Km_S4(h),Xn_S4(h),Sn_S4(h)
    end do

        write(20,*)'The Hershfield parameters for 6-hr rainfall are:'
        write(20,*)'         No.          Station              Km              Xn            Sn'
    do h=1,N_stn
        write(20,*),h,fname(h),Km_S6(h),Xn_S6(h),Sn_S6(h)
    end do

        write(20,*)'The Hershfield parameters for 12-hr rainfall are:'
        write(20,*)'         No.          Station              Km              Xn            Sn'
    do h=1,N_stn
        write(20,*),h,fname(h),Km_S12(h),Xn_S12(h),Sn_S12(h)
    end do

        write(20,*)'The Hershfield parameters for 24-hr rainfall are:'
        write(20,*)'         No.          Station              Km              Xn            Sn'
    do h=1,N_stn
        write(20,*),h,fname(h),Km_S24(h),Xn_S24(h),Sn_S24(h)
    end do


    print*,'---------------------- PMP HERSHFIELD (mm)-------------------------------'
    write(20,*),''
    write(20,*),'----------------------------------------PMP
HERSHFIELD(mm)-----------------------------------------------------'
 !   write(20,*)' For 1-day rainfall the PMP parameters are:'
 !  print*,'         No.      Km              Xn '
 !  write(20,*)'         No.      Km              Xn'

 !  do h=1,N_stn

 !       print*,h,Km_S(h),Xn_S(h),Km_S2(h),Xn_S2(h)
 !       write(20,*)h,Km_S(h),Xn_S(h),Km_S2(h),Xn_S2(h)
 !   end do


    !****** Plotting Km and determine Envelope --- 1-hr rain ******

    !Y = m X + C
    ! m = (Y1-Y2)/(X1-X2)
    ! X1=Xn for the max Km
    ! Y1=Max Km
    ! X2=Max Xn
```

```
! Y2=Km for the max Xn
! C= Y1-m*X1
!PMP=Xn+Sn*Km

Y1= maxval(Km_s)
Y1_loc= maxloc(Km_s)
X1=Xn_S(Y1_loc)

X2=maxval(Xn_S)
X2_loc= maxloc(Xn_S)
Y2= Km_s(X2_loc)

Reg_M=(Y1-Y2)/(X1-X2)
Reg_C=Y1-Reg_M*X1


!print*,'max Km is', Y1
!print*,'location of the max Km is', Y1_loc
!print*,'Xn for the max Km is', X1

!print*,'max Xn is', X2
!print*,'location of the max Xn is', X2_loc
!print*,'Km for the max Xn is',Y2

print*,'Reg_M for the Envelope=',Reg_M
print*,'Reg_C for the Envelope=',Reg_C
print*,'The PMPs are:'
write(20,*)'Reg_M for the Envelope=',Reg_M
write(20,*)'Reg_C for the Envelope=',Reg_C
write(20,*)'The PMPs are:'


do h=1,N_stn

    New_Km(h)=Reg_M(1)*Xn_S(h)+Reg_C(1)
    PMP(h)=Xn_S(h)+Sn_S(h)*New_Km(h)
    print*,h,PMP(h)
    write(20,*),h,PMP(h)
end do

!****** Plotting Km and determine Envelope --- 2-hr rain ******

Y1_2= maxval(Km_s2)
Y1_loc2= maxloc(Km_s2)
X1_2=Xn_S2(Y1_loc2)

X2_2=maxval(Xn_S2)
X2_loc2= maxloc(Xn_S2)
Y2_2= Km_s2(X2_loc2)

Reg_M_2=(Y1_2-Y2_2)/(X1_2-X2_2)
Reg_C_2=Y1_2-Reg_M_2*X1_2

print*,'Reg_M (2hr)for the Envelope=',Reg_M_2
print*,'Reg_C (2hr)for the Envelope=',Reg_C_2
print*,'The PMPs for 2-hr are:'
write(20,*)'Reg_M (2hr)for the Envelope=',Reg_M_2
write(20,*)'Reg_C (2hr)for the Envelope=',Reg_C_2
write(20,*)'The PMPs for 2-hr are:'


do h=1,N_stn

    New_Km2(h)=Reg_M_2(1)*Xn_S2(h)+Reg_C_2(1)
    PMP2(h)=Xn_S2(h)+Sn_S2(h)*New_Km2(h)
    print*,h,PMP2(h)
    write(20,*),h,PMP2(h)
```

```
    end do

!****** Plotting Km and determine Envelope --- 3-hr rain ******

    Y1_3= maxval(Km_s3)
    Y1_loc3= maxloc(Km_s3)
    X1_3=Xn_S3(Y1_loc3)

    X2_3=maxval(Xn_S3)
    X2_loc3= maxloc(Xn_S3)
    Y2_3= Km_s3(X2_loc3)

    Reg_M_3=(Y1_3-Y2_3)/(X1_3-X2_3)
    Reg_C_3=Y1_3-Reg_M_3*X1_3

    print*,'Reg_M (3hr)for the Envelope=',Reg_M_3
    print*,'Reg_C (3hr)for the Envelope=',Reg_C_3
    print*,'The PMPs for 3-hr are:'
    write(20,*)'Reg_M (3hr)for the Envelope=',Reg_M_3
    write(20,*)'Reg_C (3hr)for the Envelope=',Reg_C_3
    write(20,*)'The PMPs for 3-hr are:'


    do h=1,N_stn

        New_Km3(h)=Reg_M_3(1)*Xn_S3(h)+Reg_C_3(1)
        PMP3(h)=Xn_S3(h)+Sn_S3(h)*New_Km3(h)
        print*,h,PMP3(h)
        write(20,*),h,PMP3(h)

    end do

!****** Plotting Km and determine Envelope --- 4-hr rain ******

    Y1_4= maxval(Km_s4)
    Y1_loc4= maxloc(Km_s4)
    X1_4=Xn_S4(Y1_loc4)

    X2_4=maxval(Xn_S4)
    X2_loc4= maxloc(Xn_S4)
    Y2_4= Km_s4(X2_loc4)

    Reg_M_4=(Y1_4-Y2_4)/(X1_4-X2_4)
    Reg_C_4=Y1_4-Reg_M_4*X1_4

    print*,'Reg_M (4hr)for the Envelope=',Reg_M_4
    print*,'Reg_C (4hr)for the Envelope=',Reg_C_4
    print*,'The PMPs for 4-hr are:'
    write(20,*)'Reg_M (4hr)for the Envelope=',Reg_M_4
    write(20,*)'Reg_C (4hr)for the Envelope=',Reg_C_4
    write(20,*)'The PMPs for 4-hr are:'


    do h=1,N_stn

        New_Km4(h)=Reg_M_4(1)*Xn_S4(h)+Reg_C_4(1)
        PMP4(h)=Xn_S4(h)+Sn_S4(h)*New_Km4(h)
        print*,h,PMP4(h)
        write(20,*),h,PMP4(h)

    end do

!****** Plotting Km and determine Envelope --- 6-hr rain ******

    Y1_6= maxval(Km_s6)
    Y1_loc6= maxloc(Km_s6)
```

```
    X1_6=Xn_S6(Y1_loc6)

    X2_6=maxval(Xn_S6)
    X2_loc6= maxloc(Xn_S6)
    Y2_6= Km_s6(X2_loc6)

    Reg_M_6=(Y1_6-Y2_6)/(X1_6-X2_6)
    Reg_C_6=Y1_6-Reg_M_6*X1_6

    print*,'Reg_M (6hr)for the Envelope=',Reg_M_6
    print*,'Reg_C (6hr)for the Envelope=',Reg_C_6
    print*,'The PMPs for 6-hr are:'
    write(20,*)'Reg_M (6hr)for the Envelope=',Reg_M_6
    write(20,*)'Reg_C (6hr)for the Envelope=',Reg_C_6
    write(20,*)'The PMPs for 6-hr are:'


    do h=1,N_stn

        New_Km6(h)=Reg_M_6(1)*Xn_S6(h)+Reg_C_6(1)
        PMP6(h)=Xn_S6(h)+Sn_S6(h)*New_Km6(h)
        print*,h,PMP6(h)
        write(20,*),h,PMP6(h)

    end do


!****** Plotting Km and determine Envelope --- 12-hr rain ******

    Y1_12= maxval(Km_s12)
    Y1_loc12= maxloc(Km_s12)
    X1_12=Xn_S12(Y1_loc12)

    X2_12=maxval(Xn_S12)
    X2_loc12= maxloc(Xn_S12)
    Y2_12= Km_s12(X2_loc12)

    Reg_M_12=(Y1_12-Y2_12)/(X1_12-X2_12)
    Reg_C_12=Y1_12-Reg_M_12*X1_12

    print*,'Reg_M (12hr)for the Envelope=',Reg_M_12
    print*,'Reg_C (12hr)for the Envelope=',Reg_C_12
    print*,'The PMPs for 12-hr are:'
    write(20,*)'Reg_M (12hr)for the Envelope=',Reg_M_12
    write(20,*)'Reg_C (12hr)for the Envelope=',Reg_C_12
    write(20,*)'The PMPs for 12-hr are:'


    do h=1,N_stn
        New_Km12(h)=Reg_M_12(1)*Xn_S12(h)+Reg_C_12(1)
        PMP12(h)=Xn_S12(h)+Sn_S12(h)*New_Km12(h)
        print*,h,PMP12(h)
        write(20,*),h,PMP12(h)
    end do

!****** Plotting Km and determine Envelope --- 24-hr rain ******

    Y1_24= maxval(Km_s24)
    Y1_loc24= maxloc(Km_s24)
    X1_12=Xn_S24(Y1_loc24)
    X2_24=maxval(Xn_S24)
    X2_loc24= maxloc(Xn_S24)
    Y2_24= Km_s24(X2_loc24)
    Reg_M_24=(Y1_24-Y2_24)/(X1_24-X2_24)
    Reg_C_24=Y1_24-Reg_M_24*X1_24

    print*,'Reg_M (24hr)for the Envelope=',Reg_M_24
```

```
    print*,'Reg_C (24hr)for the Envelope=',Reg_C_24
    print*,'The PMPs for 24-hr are:'
    write(20,*)'Reg_M (24hr)for the Envelope=',Reg_M_24
    write(20,*)'Reg_C (24hr)for the Envelope=',Reg_C_24
    write(20,*)'The PMPs for 24-hr are:'

    do h=1,N_stn
        New_Km24(h)=Reg_M_24(1)*Xn_S24(h)+Reg_C_24(1)
        PMP24(h)=Xn_S24(h)+Sn_S24(h)*New_Km24(h)
        print*,h,PMP24(h)
        write(20,*),h,PMP24(h)
    end do


print*,'****************************************************************  '


print*,'PLEASE SEE  "OUTPUT.TXT"'


End program
```

A-6

Output file for the ANNMAX.FOR program

(Example of one station for hourly data)

```
Reading file AKITA.txt

The number of LINE is:      289296

The data are:
Year/Month/Day/Hour   Rainfall (mm)

Available years are :
       Year   Rec. hrs  %Missing    %Missing(For Leap yrs)
       1976       8784 -0.273972601       0.00000000
       1977       8760   0.00000000      0.273224026
       1978       8760   0.00000000      0.273224026
       1979       8760   0.00000000      0.273224026
       1980       8784 -0.273972601       0.00000000
       1981       8760   0.00000000      0.273224026
       1982       8760   0.00000000      0.273224026
       1983       8760   0.00000000      0.273224026
       1984       8784 -0.273972601       0.00000000
       1985       8760   0.00000000      0.273224026
       1986       8760   0.00000000      0.273224026
       1987       8760   0.00000000      0.273224026
       1988       8784 -0.273972601       0.00000000
       1989       8760   0.00000000      0.273224026
       1990       8760   0.00000000      0.273224026
       1991       8760   0.00000000      0.273224026
       1992       8784 -0.273972601       0.00000000
       1993       8760   0.00000000      0.273224026
       1994       8760   0.00000000      0.273224026
       1995       8760   0.00000000      0.273224026
       1996       8784 -0.273972601       0.00000000
       1997       8760   0.00000000      0.273224026
       1998       8760   0.00000000      0.273224026
       1999       8760   0.00000000      0.273224026
       2000       8784 -0.273972601       0.00000000
       2001       8760   0.00000000      0.273224026
       2002       8760   0.00000000      0.273224026
       2003       8760   0.00000000      0.273224026
       2004       8784 -0.273972601       0.00000000
       2005       8760   0.00000000      0.273224026
       2006       8760   0.00000000      0.273224026
       2007       8760   0.00000000      0.273224026
       2008       8784 -0.273972601       0.00000000
The annual maximums are:
Year      1-hr      2-hr       3-hr       4-hr      6-hr      12-hr     24-hr
1976     33.00     40.00      40.00      40.00     43.00      46.00     46.00
1977     25.00     40.00      55.00      68.00     74.00      82.00     83.00
1978     22.00     23.00      33.00      40.00     55.00      70.00     80.00
1979     44.00     50.00      59.00      82.00    109.00     122.00    124.00
1980     19.00     32.00      44.00      50.00     64.00      73.00     82.00
1981     22.00     31.00      37.00      48.00     52.00      83.00     93.00
1982     19.00     32.00      37.00      44.00     55.00      60.00     70.00
1983     18.00     26.00      32.00      37.00     52.00      73.00     75.00
1984     21.00     28.00      35.00      40.00     45.00      73.00     93.00
1985     42.00     61.00      81.00      98.00    107.00     115.00    120.00
1986     19.00     25.00      29.00      36.00     44.00      64.00     68.00
1987     52.00     57.00      57.00      58.00     89.00     119.00    127.00

                               Page 1 of 104
```

1988	30.00	43.00	53.00	59.00	62.00	68.00	99.00
1989	49.00	53.00	55.00	56.00	56.00	67.00	73.00
1990	36.00	56.00	65.00	72.00	77.00	78.00	115.00
1991	22.00	34.00	42.00	42.00	49.00	72.00	73.00
1992	22.00	31.00	39.00	42.00	48.00	69.00	76.00
1993	17.00	27.00	28.00	33.00	41.00	56.00	65.00
1994	24.00	29.00	33.00	43.00	52.00	80.00	88.00
1995	42.00	50.00	52.00	57.00	81.00	95.00	128.00
1996	25.00	26.00	31.00	37.00	40.00	53.00	77.00
1997	17.00	31.00	34.00	37.00	39.00	48.00	55.00
1998	26.00	42.00	50.00	55.00	70.00	78.00	116.00
1999	37.00	52.00	54.00	54.00	58.00	63.00	69.00
2000	14.00	21.00	30.00	36.00	45.00	52.00	67.00
2001	41.00	41.00	41.00	43.00	51.00	55.00	61.00
2002	41.00	58.00	70.00	73.00	74.00	93.00	127.00
2003	21.00	26.00	30.00	32.00	39.00	49.00	90.00
2004	21.00	31.00	34.00	42.00	51.00	70.00	83.00
2005	21.00	40.00	53.00	66.00	82.00	95.00	103.00
2006	15.00	20.00	23.00	23.00	28.00	39.00	58.00
2007	21.00	30.00	42.00	47.00	68.00	90.00	136.00
2008	19.00	22.00	25.00	28.00	29.00	40.00	53.00

```
The highest annual maximum 1-hr is on the year        1987
The highest annual maximum 2-hr is on the year        1985
The highest annual maximum 3-hr is on the year        1985
The highest annual maximum 4-hr is on the year        1985
The highest annual maximum 6-hr is on the year        1979
The highest annual maximum 12-hr is on the year        1979
The highest annual maximum 24-hr is on the year        2007
```

A-7

Output file for the ANNMAX.FOR program

(Example of one station for daily data)

```
 ----------------Station Number**          1 File
name**J_47407.txt                    ------------------------------------------
 The number of LINE is:       39447

 Available years are :
        Year   Recorded number of days
        1901         365
        1902         365
        1903         365
        1904         366
        1905         365
        1906         365
        1907         365
        1908         366
        1909         365
        1910         365
        1911         365
        1912         366
        1913         365
        1914         365
        1915         365
        1916         366
        1917         365
        1918         365
        1919         365
        1920         366
        1921         365
        1922         365
        1923         365
        1924         366
        1925         365
        1926         365
        1927         365
        1928         366
        1929         365
        1930         365
        1931         365
        1932         366
        1933         365
        1934         365
        1935         365
        1936         366
        1937         365
        1938         365
        1939         365
        1940         366
        1941         365
        1942         365
        1943         365
        1944         366
        1945         365
        1946         365
        1947         365
        1948         366
        1949         365
        1950         365
        1951         365
        1952         366
        1953         365
        1954         365
        1955         365
        1956         366
        1957         365
        1958         365
        1959         365
        1960         366
```

Page 1 of 4

1961	365
1962	365
1963	365
1964	366
1965	365
1966	365
1967	365
1968	366
1969	365
1970	365
1971	365
1972	366
1973	365
1974	365
1975	365
1976	366
1977	365
1978	365
1979	365
1980	366
1981	365
1982	365
1983	365
1984	366
1985	365
1986	365
1987	365
1988	366
1989	365
1990	365
1991	365
1992	366
1993	365
1994	365
1995	365
1996	366
1997	365
1998	365
1999	365
2000	366
2001	365
2002	365
2003	365
2004	366
2005	365
2006	365
2007	365
2008	366

The number of years are: 108

The annual maximums are:

Year	d	2-d	3-d	5-d	7-d
1901	51.90	103.50	153.10	189.30	191.32
1902	37.60	51.50	59.30	61.80	63.20
1903	62.50	62.51	90.50	114.81	118.61
1904	127.60	145.90	151.50	183.50	183.50
1905	31.50	38.60	49.50	55.50	55.50
1906	28.60	41.40	66.80	66.83	76.43
1907	51.50	59.00	59.10	60.10	61.60
1908	41.10	64.30	80.80	81.65	81.85
1909	50.70	63.20	65.90	66.10	66.20
1910	32.50	54.10	56.30	76.60	77.30
1911	79.50	79.50	79.50	104.20	104.20
1912	95.90	100.00	102.40	129.90	140.30
1913	33.10	38.50	46.60	57.70	68.60
1914	52.80	53.70	53.78	66.31	73.71
1915	64.30	71.70	78.90	80.60	86.00
1916	48.80	66.40	71.30	75.40	90.70

1917	39.10	49.50	61.60	69.10	92.80
1918	60.30	70.80	75.30	108.90	109.20
1919	69.90	117.70	117.70	149.00	149.08
1920	115.10	122.80	122.80	143.00	146.30
1921	23.70	34.90	40.20	54.30	80.40
1922	51.60	85.70	105.20	106.75	151.30
1923	61.80	76.50	81.80	82.50	95.90
1924	36.60	47.60	57.10	61.20	62.60
1925	32.80	41.70	53.20	56.30	60.60
1926	91.50	118.00	129.10	134.75	150.95
1927	49.90	52.40	54.90	71.80	99.80
1928	68.50	83.20	88.70	100.10	105.70
1929	56.60	95.70	98.80	104.30	105.00
1930	101.20	115.90	116.20	116.70	116.70
1931	67.20	67.60	67.60	67.79	80.99
1932	70.60	99.60	121.70	141.80	188.70
1933	96.10	98.90	99.60	112.50	113.90
1934	40.20	48.60	56.80	58.00	60.80
1935	63.50	63.51	83.81	118.60	138.91
1936	46.30	64.80	67.70	81.20	92.72
1937	45.10	67.60	67.60	114.10	126.70
1938	40.80	60.50	73.60	94.90	112.52
1939	53.20	78.20	103.20	120.49	144.79
1940	42.50	57.50	68.10	74.20	79.61
1941	58.20	71.30	87.50	88.30	116.10
1942	55.90	71.20	75.00	75.50	83.15
1943	41.40	49.80	53.60	72.17	100.47
1944	27.10	33.50	41.20	63.20	73.60
1945	60.50	63.80	95.10	100.40	109.10
1946	32.30	59.30	68.60	69.23	79.70
1947	79.60	100.40	100.40	100.60	111.30
1948	52.80	64.70	74.90	93.70	96.40
1949	24.70	44.60	51.20	69.70	73.50
1950	30.20	49.80	52.30	60.70	70.30
1951	47.40	75.30	100.50	110.70	117.70
1952	38.80	40.90	42.10	58.70	65.00
1953	97.80	179.50	181.00	231.50	253.40
1954	65.40	71.60	71.60	86.60	87.45
1955	184.20	216.80	225.90	276.50	281.31
1956	61.60	82.80	94.00	97.40	139.90
1957	43.80	57.90	63.00	67.30	75.30
1958	69.50	74.20	75.00	107.76	107.76
1959	57.80	63.90	63.90	77.80	88.00
1960	38.30	39.00	47.71	52.40	62.61
1961	91.90	92.17	92.23	96.76	99.93
1962	81.10	81.23	83.80	140.63	153.73
1963	115.60	121.00	121.00	125.60	126.50
1964	68.10	89.20	89.30	99.90	130.10
1965	39.10	57.90	82.60	106.10	120.50
1966	74.50	76.30	76.30	101.90	109.19
1967	48.10	56.80	60.30	64.10	65.20
1968	44.50	44.53	44.68	45.11	49.62
1969	49.50	81.00	81.50	85.01	85.51
1970	164.50	202.00	202.00	202.35	202.35
1971	67.50	80.00	80.00	80.50	80.50
1972	26.50	28.00	36.00	47.51	48.03
1973	25.50	26.00	26.60	32.56	40.54
1974	63.50	68.00	68.50	79.59	83.59
1975	53.50	90.00	103.30	140.15	140.46
1976	37.50	37.50	37.50	39.03	41.53
1977	45.50	61.00	61.00	61.14	74.14
1978	29.50	32.00	32.50	35.01	38.56
1979	53.50	53.61	53.72	56.58	56.80
1980	39.50	39.50	40.00	45.50	50.00
1981	42.50	42.50	42.50	43.50	63.50
1982	46.50	48.00	48.03	59.00	59.08
1983	25.50	40.00	40.00	40.01	40.01

1984	27.50	27.50	41.50	41.55	45.50
1985	27.50	52.00	52.00	61.00	61.50
1986	24.50	41.00	41.16	50.62	52.28
1987	28.50	28.51	29.00	34.04	43.04
1988	100.50	118.00	118.01	144.00	145.50
1989	27.50	33.00	33.01	33.08	33.67
1990	41.50	50.00	50.03	55.53	56.03
1991	36.50	36.50	36.50	36.50	50.00
1992	69.50	71.00	72.50	72.55	87.55
1993	34.50	36.00	49.50	50.06	59.63
1994	43.50	43.50	43.60	52.50	62.63
1995	40.50	51.00	51.00	51.00	51.01
1996	31.50	45.00	46.50	50.06	66.06
1997	38.50	38.50	38.66	38.86	59.37
1998	69.50	69.55	71.00	71.10	71.10
1999	44.50	44.52	51.02	56.02	56.10
2000	94.50	107.00	107.00	107.00	109.50
2001	55.50	97.00	104.50	105.42	105.47
2002	35.50	48.00	48.28	53.81	59.31
2003	23.50	26.00	26.01	27.15	28.11
2004	30.50	30.51	40.12	43.62	67.03
2005	56.50	57.14	67.64	67.64	78.14
2006	53.50	57.00	57.03	60.00	60.11
2007	21.50	24.00	26.50	31.60	42.87
2008	25.50	26.00	27.06	40.67	40.83

The highest annual maximum 1d is on the year 1955
The highest annual maximum 2d is on the year 1955
The highest annual maximum 3d is on the year 1955
The highest annual maximum 5d is on the year 1955
The highest annual maximum 7d is on the year 1955

A-8

Output file for the HERSHPMP.FOR program (Example for hourly data)

********************HERSHFIELD PARAMETERS**

The Hershfield parameters for 1-hr rainfall are:

No.	Station	Km	Xn	Sn
1	AKITA.txt	2.61139727	27.1818180	10.6256018
2	ASAHIKAWA.txt	2.30501056	20.2424240	8.91988754
3	FUKUI.txt	5.88645315	28.8787880	11.4803028
4	FUKUOKA.txt	5.03893900	40.5454559	14.9626427
5	FUKUSHIMA.txt	4.63501406	26.2121220	12.1159954
6	FUSHIKI.txt	2.14013743	35.0909081	13.6458864
7	GIFU.txt	4.04950285	38.5757561	14.0045309
8	HAMADA.txt	3.74644613	34.7575760	16.0039673
9	HAMAMATSU.txt	3.18159318	44.7272720	15.1085110
10	HIKONE.txt	4.48834229	30.7272720	9.31823635
11	IIDA.txt	2.57100677	26.3030300	7.67497873
12	ISHIGAKIJIMA.txt	4.64997339	58.5000000	17.5020733
13	ISHINOMAKI.txt	2.79234433	24.5757580	8.68558598
14	KAGOSHIMA.txt	4.45432186	48.4242439	14.6714649
15	KOBE.txt	2.57020354	28.3636360	9.81968117
16	KOCHI.txt	3.21583772	32.2424240	8.98968220
17	KOFU.txt	4.20029497	29.5151520	13.9935722
18	KUMAMOTO.txt	3.06094265	46.3333321	14.2031393
19	KYOTO.txt	3.60544229	35.7878799	11.4229975
20	MAEBASHI.txt	4.60017443	37.1515160	18.4460716
21	MATSUMOTO.txt	5.11823893	20.8787880	9.66228962
22	MATSUYAMA.txt	3.54415345	29.4848480	10.3141937
23	MITO.txt	3.01081729	32.8787880	10.7405701
24	MIYAZAKI.txt	3.55365252	44.1515160	17.1539383
25	NAGANO.txt	2.05244446	21.9696960	7.90761137
26	NAGASAKI.txt	4.08779335	48.6363640	19.4145851
27	NAGOYA.txt	3.94518948	38.6969681	17.0357800
28	NAHA.txt	3.27030873	54.6363640	15.5479460
29	NAZE.txt	2.72271633	51.7575760	16.6508827
30	NEMURO.TXT	3.02337217	19.9285717	5.09123135
31	OBIHIRO.txt	1.54285705	15.8076925	3.58908629
32	OITA.txt	3.76728606	38.6363640	13.7154531
33	OSAKA.txt	2.83214259	32.2121201	12.3408813
34	SAPPORO.txt	3.27550983	19.0909100	5.69738817
35	SHIMONOSEKI.txt	2.37088728	36.1515160	11.0711374
36	SUTTSU.txt	5.93765259	20.0909100	9.14932919
37	TADOTSU.txt	2.22960401	25.1212120	8.74913502
38	TOKUSHIMA.txt	2.52327180	42.5454559	14.2961769
39	TOKYO.txt	2.86198831	38.2424240	15.8035402
40	TSU.txt	3.83273935	37.4545441	22.2501278
41	TSURUGA.txt	2.72088909	27.0303040	7.43927479
42	UTSUNOMIYA.txt	2.78488755	39.9393921	13.8382177
43	WAKAYAMA.txt	3.07910156	33.4848480	11.4540415
44	YAMAGATA.txt	6.44862318	25.3939400	11.3659000
45	YOKOHAMA.txt	4.76980352	37.3636360	14.0974693

The Hershfield parameters for 2-hr rainfall are:

No.	Station	Km	Xn	Sn
1	AKITA.txt	2.20029187	36.6060600	12.0751276
2	ASAHIKAWA.txt	3.07955265	28.0303040	11.9986582
3	FUKUI.txt	5.07283401	40.6969681	15.4039068
4	FUKUOKA.txt	3.67656851	58.4242439	17.9722538
5	FUKUSHIMA.txt	3.07805920	36.1818199	16.8271618
6	FUSHIKI.txt	3.23908782	48.6969681	19.6110363
7	GIFU.txt	3.40713716	55.1515160	21.5118008
8	HAMADA.txt	4.25992632	53.0000000	27.7443695
9	HAMAMATSU.txt	3.66662169	63.0606079	19.1163216
10	HIKONE.txt	2.38381648	41.6363640	11.7202234
11	IIDA.txt	2.75832891	39.3030319	13.3872252
12	ISHIGAKIJIMA.txt	4.35606050	88.8437500	33.4992523
13	ISHINOMAKI.txt	2.27160525	35.3333321	10.4333210
14	KAGOSHIMA.txt	5.46061993	74.5757599	25.1756725
15	KOBE.txt	2.27339506	42.6969681	15.0633755

16	KOCHI.txt	3.63328648	46.9393921	16.9557133
17	KOFU.txt	3.27264810	39.9696960	16.4952374
18	KUMAMOTO.txt	2.60743237	71.4848480	24.6552734
19	KYOTO.txt	2.81918526	49.9090919	18.5427933
20	MAEBASHI.txt	4.88007259	50.6363640	27.0252399
21	MATSUMOTO.txt	8.37576294	29.3333340	13.5731058
22	MATSUYAMA.txt	2.31295729	41.4848480	13.0458841
23	MITO.txt	2.49575114	47.6969681	17.4722710
24	MIYAZAKI.txt	3.23766613	68.2727280	28.4410286
25	NAGANO.txt	1.65439546	28.9696960	7.05108547
26	NAGASAKI.txt	6.25297928	71.5454559	34.4774323
27	NAGOYA.txt	3.46062779	57.0909081	28.8545513
28	NAHA.txt	2.40857077	84.0000000	27.0254517
29	NAZE.txt	3.12660408	77.9393921	23.3932934
30	NEMURO.TXT	3.06856942	32.0357132	9.61665916
31	OBIHIRO.txt	2.32834196	26.1538467	6.68546104
32	OITA.txt	2.54959488	58.0606079	22.2457008
33	OSAKA.txt	4.21684742	44.7272720	16.8972511
34	SAPPORO.txt	3.01504683	28.8181820	9.98891449
35	SHIMONOSEKI.txt	1.90299368	54.6969681	17.6165485
36	SUTTSU.txt	6.38146830	27.3636360	10.7057753
37	TADOTSU.txt	2.95298028	37.6363640	14.4888277
38	TOKUSHIMA.txt	3.20564294	64.7575760	23.0190544
39	TOKYO.txt	3.13213587	54.0909081	21.8236732
40	TSU.txt	4.45136499	57.7272720	35.7747040
41	TSURUGA.txt	2.76641417	39.3636360	12.9224091
42	UTSUNOMIYA.txt	2.33565760	55.2121201	19.1780415
43	WAKAYAMA.txt	3.33362389	51.0606079	20.8325748
44	YAMAGATA.txt	3.50604248	35.1515160	13.5741510
45	YOKOHAMA.txt	3.20228934	53.2121201	18.1362152

The Hershfield parameters for 3-hr rainfall are:

No.	Station	Km	Xn	Sn
1	AKITA.txt	3.19085550	43.1212120	13.8355465
2	ASAHIKAWA.txt	3.49412394	33.0303040	14.3319683
3	FUKUI.txt	7.84684801	49.3333321	22.4953709
4	FUKUOKA.txt	3.33936524	71.1515121	19.3618851
5	FUKUSHIMA.txt	2.93490458	42.9090919	18.7389355
6	FUSHIKI.txt	3.68925500	56.1212120	23.2845955
7	GIFU.txt	3.43142962	67.7575760	27.7646675
8	HAMADA.txt	6.12988329	63.2121201	35.3604279
9	HAMAMATSU.txt	3.73383117	75.8484879	23.1788158
10	HIKONE.txt	3.29211116	48.9696960	13.5680819
11	IIDA.txt	2.48057127	47.4242439	14.1090183
12	ISHIGAKIJIMA.txt	3.85470557	106.531250	39.2469215
13	ISHINOMAKI.txt	3.77734995	41.5757561	12.7402668
14	KAGOSHIMA.txt	5.50310135	91.6363602	34.3254814
15	KOBE.txt	2.58292198	51.5151520	18.7868328
16	KOCHI.txt	2.48505712	55.6666679	19.7795143
17	KOFU.txt	2.53676987	47.9696960	16.6779881
18	KUMAMOTO.txt	2.68851638	87.0606079	30.4917412
19	KYOTO.txt	3.82421374	59.2424240	25.5563469
20	MAEBASHI.txt	4.39052916	56.9090919	29.2962933
21	MATSUMOTO.txt	7.42824888	35.2727280	14.1515741
22	MATSUYAMA.txt	3.20571566	50.3939400	18.0553627
23	MITO.txt	2.67913747	58.5151520	22.8420124
24	MIYAZAKI.txt	3.63192987	84.7272720	34.9671936
25	NAGANO.txt	1.83597934	33.3030319	7.38023043
26	NAGASAKI.txt	7.99587297	88.7272720	49.3097839
27	NAGOYA.txt	5.07403898	70.5151520	38.5657883
28	NAHA.txt	3.24826527	99.2121201	31.6363697
29	NAZE.txt	3.05110717	95.6060638	30.3901100
30	NEMURO.TXT	3.11443830	40.7142868	13.0635414
31	OBIHIRO.txt	2.57512784	33.9615402	9.36581326
32	OITA.txt	2.85073662	72.8787842	31.1505985
33	OSAKA.txt	3.48117399	51.8181801	18.2096386

34	SAPPORO.txt	2.86440539	36.3333321	14.1678925
35	SHIMONOSEKI.txt	2.69621158	66.8787842	21.7381554
36	SUTTSU.txt	4.14784956	33.8181801	12.1949120
37	TADOTSU.txt	2.87390018	46.4242439	18.4526939
38	TOKUSHIMA.txt	2.35411310	80.8484879	28.5603752
39	TOKYO.txt	3.51875854	65.3030319	26.0582085
40	TSU.txt	5.55304003	74.6363602	50.3076897
41	TSURUGA.txt	2.51109219	46.1818199	14.9571362
42	UTSUNOMIYA.txt	2.03660369	63.9090919	21.2372952
43	WAKAYAMA.txt	2.14435697	61.9393921	25.3425789
44	YAMAGATA.txt	2.77824020	41.9090919	14.6913319
45	YOKOHAMA.txt	4.08380556	66.4242401	24.0910110

The Hershfield parameters for 4-hr rainfall are:

No.	Station	Km	Xn	Sn
1	AKITA.txt	3.61428809	49.0303040	16.3219280
2	ASAHIKAWA.txt	4.38600588	37.3030319	17.7772408
3	FUKUI.txt	8.02469158	55.9090919	25.9330444
4	FUKUOKA.txt	2.68310714	80.6666641	22.3322449
5	FUKUSHIMA.txt	3.01704288	48.7878799	19.5284367
6	FUSHIKI.txt	3.10951996	63.1818199	24.8915844
7	GIFU.txt	3.65797472	77.4242401	31.9169102
8	HAMADA.txt	7.84474421	72.9696960	43.6000900
9	HAMAMATSU.txt	2.58918190	88.1515121	26.6670685
10	HIKONE.txt	4.67823887	54.7272720	15.5649300
11	IIDA.txt	2.54614234	53.9393921	15.7657452
12	ISHIGAKIJIMA.txt	3.54098630	118.375000	42.7013245
13	ISHINOMAKI.txt	3.77699518	46.7575760	14.2982311
14	KAGOSHIMA.txt	4.90738344	103.878784	41.9357796
15	KOBE.txt	2.46107626	57.6666679	20.3909683
16	KOCHI.txt	2.11181879	62.0303040	21.0200596
17	KOFU.txt	2.17835546	53.9696960	17.4919357
18	KUMAMOTO.txt	3.22326756	98.1818161	34.0068512
19	KYOTO.txt	3.63230228	65.7575760	28.3119144
20	MAEBASHI.txt	4.18609476	60.6666679	29.0631485
21	MATSUMOTO.txt	6.10340643	39.7878799	14.2450829
22	MATSUYAMA.txt	3.79001737	58.5151520	22.4027367
23	MITO.txt	2.78547835	66.1212158	27.1670246
24	MIYAZAKI.txt	3.19500136	97.4848480	40.6917686
25	NAGANO.txt	1.99924600	36.7575760	8.74653625
26	NAGASAKI.txt	8.33248138	101.666664	59.0813408
27	NAGOYA.txt	5.13237715	79.0000000	42.7346458
28	NAHA.txt	3.57746840	111.090912	35.8942566
29	NAZE.txt	3.22833562	109.757576	38.1026802
30	NEMURO.TXT	3.48874164	48.0357132	16.8555565
31	OBIHIRO.txt	2.65409017	40.6923065	11.8718796
32	OITA.txt	3.73407459	86.5454559	42.1701126
33	OSAKA.txt	3.11327434	57.9696960	18.9925747
34	SAPPORO.txt	2.98230815	43.3636360	16.7906570
35	SHIMONOSEKI.txt	2.84871912	77.6060638	24.8934441
36	SUTTSU.txt	2.68997955	39.3636360	14.8908920
37	TADOTSU.txt	2.37525225	52.7272720	20.9840298
38	TOKUSHIMA.txt	2.56703949	91.7575760	32.6736031
39	TOKYO.txt	3.50648618	74.5454559	30.8099918
40	TSU.txt	6.26773787	85.1212158	56.3026199
41	TSURUGA.txt	2.19491148	51.9696960	16.3849888
42	UTSUNOMIYA.txt	1.85198987	70.4242401	22.2472324
43	WAKAYAMA.txt	2.65630412	71.8181839	30.4738159
44	YAMAGATA.txt	2.43929672	47.9393921	16.3419323
45	YOKOHAMA.txt	3.81344795	77.1818161	28.5147495

The Hershfield parameters for 6-hr rainfall are:

No.	Station	Km	Xn	Sn
1	AKITA.txt	2.92577171	58.4545441	19.7438145
2	ASAHIKAWA.txt	3.78453159	44.4242439	22.1317501
3	FUKUI.txt	5.55123711	65.5151520	29.3354759
4	FUKUOKA.txt	1.92521477	96.0000000	29.5180035

5	FUKUSHIMA.txt	3.90047646	59.5151520	21.6508102
6	FUSHIKI.txt	2.58074880	70.8181839	26.0185699
7	GIFU.txt	5.08298588	89.3333359	36.9659157
8	HAMADA.txt	8.82864094	86.7272720	54.4181061
9	HAMAMATSU.txt	2.24054980	105.212120	30.5959129
10	HIKONE.txt	3.56918693	63.4848480	21.0239754
11	IIDA.txt	2.61240911	64.2121201	18.7412605
12	ISHIGAKIJIMA.txt	2.83646774	136.250000	50.1282234
13	ISHINOMAKI.txt	2.94106340	56.0000000	16.7275963
14	KAGOSHIMA.txt	4.23421001	124.696968	48.0081253
15	KOBE.txt	1.76189053	67.7272720	23.6976681
16	KOCHI.txt	2.45638537	71.3636398	22.8128510
17	KOFU.txt	2.77787995	66.3030319	22.2675285
18	KUMAMOTO.txt	3.51715398	115.515152	41.2887115
19	KYOTO.txt	3.39646745	77.5151520	37.1223679
20	MAEBASHI.txt	4.01752806	68.2727280	27.4991741
21	MATSUMOTO.txt	4.09961462	47.4545441	15.4577875
22	MATSUYAMA.txt	5.22883749	68.6666641	28.9078999
23	MITO.txt	2.98836040	81.4242401	33.2603645
24	MIYAZAKI.txt	3.13310695	122.333336	56.5440483
25	NAGANO.txt	2.50979447	43.2727280	12.2685385
26	NAGASAKI.txt	7.74391031	118.393936	69.7069550
27	NAGOYA.txt	5.85111380	94.3333359	51.5919456
28	NAHA.txt	4.16182041	136.151520	47.1958160
29	NAZE.txt	3.34681892	130.848480	43.4015541
30	NEMURO.TXT	4.54472399	60.5357132	23.6462841
31	OBIHIRO.txt	2.24477458	51.2692299	15.2932873
32	OITA.txt	3.27117467	109.939392	55.9441338
33	OSAKA.txt	2.79733610	67.9696960	23.0874500
34	SAPPORO.txt	4.52875328	53.7575760	23.0421219
35	SHIMONOSEKI.txt	3.39470315	91.3030319	28.1430321
36	SUTTSU.txt	1.93123341	47.4242439	16.4260273
37	TADOTSU.txt	2.44780898	62.1212120	26.6044617
38	TOKUSHIMA.txt	2.47759676	109.060608	38.4390221
39	TOKYO.txt	3.20663047	89.5757599	36.1801338
40	TSU.txt	6.19916105	100.303032	58.2395287
41	TSURUGA.txt	2.99548554	60.0909081	19.1382542
42	UTSUNOMIYA.txt	2.62379861	82.3939362	26.6996479
43	WAKAYAMA.txt	2.24045157	85.6666641	36.7105789
44	YAMAGATA.txt	2.81295729	56.7878799	19.4305763
45	YOKOHAMA.txt	4.42467594	95.5454559	38.0000763

The Hershfield parameters for 12-hr rainfall are:

No.	Station	Km	Xn	Sn
1	AKITA.txt	2.62628269	72.4242401	21.1261559
2	ASAHIKAWA.txt	2.56135035	58.5757561	28.8974781
3	FUKUI.txt	4.74691057	81.6060638	32.2169800
4	FUKUOKA.txt	2.88254642	121.333336	41.7639694
5	FUKUSHIMA.txt	5.09302902	82.8181839	33.3086472
6	FUSHIKI.txt	2.59485626	88.9393921	31.0140476
7	GIFU.txt	5.76148987	107.969696	45.7844696
8	HAMADA.txt	5.63824320	109.818184	71.4857712
9	HAMAMATSU.txt	3.28515744	126.878784	31.8460732
10	HIKONE.txt	3.92421055	78.9393921	23.6325245
11	IIDA.txt	2.34538603	88.4848480	28.3528233
12	ISHIGAKIJIMA.txt	2.52217603	176.406250	50.2129974
13	ISHINOMAKI.txt	2.06608224	77.0000000	26.1521988
14	KAGOSHIMA.txt	4.04636145	157.272720	50.5038795
15	KOBE.txt	2.25826526	88.2424240	31.3418961
16	KOCHI.txt	3.55858564	89.5151520	25.7768326
17	KOFU.txt	4.02768564	90.6363602	40.0264130
18	KUMAMOTO.txt	3.79989576	157.303024	62.9818878
19	KYOTO.txt	3.25149775	98.4242401	42.6995544
20	MAEBASHI.txt	2.58797002	84.7878799	31.1475868
21	MATSUMOTO.txt	2.31016231	66.1818161	22.2211246
22	MATSUYAMA.txt	5.58102179	89.8181839	40.4223442

Page 4 of 11

23 MITO.txt	3.48077846	107.272728	45.4500198
24 MIYAZAKI.txt	3.18512082	169.666672	68.5185394
25 NAGANO.txt	2.91120934	57.1818199	19.9287090
26 NAGASAKI.txt	6.05268574	148.000000	87.4546280
27 NAGOYA.txt	8.78121376	116.060608	73.0081100
28 NAHA.txt	4.67425013	172.121216	63.3584862
29 NAZE.txt	3.11255646	181.333328	63.5303459
30 NEMURO.TXT	4.00889301	81.8571396	33.3985062
31 OBIHIRO.txt	3.71069074	73.3461533	22.1159534
32 OITA.txt	3.04849792	147.545456	76.2033081
33 OSAKA.txt	2.98810363	87.2424240	31.0272408
34 SAPPORO.txt	5.05000401	71.4545441	29.5212727
35 SHIMONOSEKI.txt	2.89508295	115.121216	33.0385742
36 SUTTSU.txt	2.02787757	62.0606079	20.1741486
37 TADOTSU.txt	3.23455191	81.2424240	34.6184845
38 TOKUSHIMA.txt	3.12964678	136.393936	48.0435600
39 TOKYO.txt	2.69434237	119.939392	49.6845894
40 TSU.txt	5.97086716	128.939392	64.2956772
41 TSURUGA.txt	2.87723470	76.0303040	20.5707378
42 UTSUNOMIYA.txt	3.29511666	101.878784	34.6263618
43 WAKAYAMA.txt	3.91833138	113.666664	58.4105492
44 YAMAGATA.txt	2.73367047	73.4545441	24.9700966
45 YOKOHAMA.txt	3.24412847	121.757576	44.0950928

The Hershfield parameters for 24-hr rainfall are:

No. Station	Km	Xn	Sn
1 AKITA.txt	2.12560606	87.0606079	24.9661522
2 ASAHIKAWA.txt	3.30788803	70.1515121	34.7851601
3 FUKUI.txt	3.13043785	102.303032	35.4669609
4 FUKUOKA.txt	3.11287308	146.212128	47.9372978
5 FUKUSHIMA.txt	4.59030962	107.090912	43.8358879
6 FUSHIKI.txt	2.37245798	111.666664	33.5602684
7 GIFU.txt	5.35747862	133.424240	55.4819984
8 HAMADA.txt	5.16004658	130.969696	70.5795135
9 HAMAMATSU.txt	2.85408115	146.393936	38.0870209
10 HIKONE.txt	3.28833747	103.787880	30.7842884
11 IIDA.txt	2.41606092	115.757576	42.5984421
12 ISHIGAKIJIMA.txt	3.23291564	220.218750	69.3037872
13 ISHINOMAKI.txt	3.38392568	97.9393921	40.5708771
14 KAGOSHIMA.txt	3.17622519	187.242432	51.9591331
15 KOBE.txt	2.48360777	107.212120	40.9716034
16 KOCHI.txt	2.80975819	113.303032	34.9727402
17 KOFU.txt	3.68851304	117.696968	58.2545547
18 KUMAMOTO.txt	3.10769534	196.696976	79.1242981
19 KYOTO.txt	3.81549048	122.000000	47.4973679
20 MAEBASHI.txt	2.81847548	108.212120	37.3369408
21 MATSUMOTO.txt	2.82007074	86.4848480	34.3948784
22 MATSUYAMA.txt	4.00659609	112.909088	46.2914429
23 MITO.txt	3.69064641	127.515152	52.7074013
24 MIYAZAKI.txt	4.75608540	218.242432	96.1444321
25 NAGANO.txt	2.28446460	71.5454559	26.0948887
26 NAGASAKI.txt	5.41846228	176.121216	97.5236435
27 NAGOYA.txt	8.61031055	143.000000	84.1869202
28 NAHA.txt	3.56152105	214.848480	88.2978363
29 NAZE.txt	4.12431192	243.030304	102.952507
30 NEMURO.TXT	3.68343568	98.6071396	38.7483253
31 OBIHIRO.txt	3.31854558	92.5000000	34.4665031
32 OITA.txt	3.02559996	176.696976	90.2903366
33 OSAKA.txt	3.22695136	107.636360	37.0724106
34 SAPPORO.txt	4.86975622	86.5454559	36.7109451
35 SHIMONOSEKI.txt	3.84392381	143.424240	42.3313065
36 SUTTSU.txt	2.40741062	74.3636398	22.7456303
37 TADOTSU.txt	3.46478295	102.121216	44.9671783
38 TOKUSHIMA.txt	2.29513550	166.727280	60.7460251
39 TOKYO.txt	2.35881710	150.484848	59.4538307
40 TSU.txt	5.13406038	159.818176	74.0196152

```
        41 TSURUGA.txt                          2.57472682      98.2727280      28.9042320
        42 UTSUNOMIYA.txt                       3.35332441      123.545456      42.7420273
        43 WAKAYAMA.txt                         4.19306755      132.060608      73.2145538
        44 YAMAGATA.txt                         3.34529829      89.7575760      32.8719406
        45 YOKOHAMA.txt                         2.19209003      156.666672      52.8066444

 ----------------------------------------PMP
HERSHFIELD(mm)-----------------------------------------------------
 Reg_M for the Envelope=  -5.43299243E-02
 Reg_C for the Envelope=   7.82827377
 The PMPs are:
           1    94.6701965
           2    80.2599258
           3    100.737350
           4    124.716942
           5    103.805023
           6    115.898941
           7    118.856110
           8    129.819504
           9    126.286705
          10    88.1170197
          11    75.4169998
          12    139.884171
          13    80.9719162
          14    124.677536
          15    90.1027222
          16    86.8686371
          17    116.621193
          18    121.766022
          19    102.999893
          20    144.320145
          21    85.5574799
          22    93.7047729
          23    97.7730103
          24    137.289261
          25    74.4340210
          26    149.317749
          27    136.241638
          28    130.197586
          29    135.283203
          30    54.2717590
          31    40.8216248
          32    117.214432
          33    107.222366
          34    57.7822495
          35    101.074478
          36    81.7275314
          37    81.6707153
          38    121.414352
          39    129.121719
          40    166.357788
          41    74.3420029
          42    118.241142
          43    102.312698
          44    98.6883392
          45    119.105133
 Reg_M (2hr)for the Envelope=  -6.75462037E-02
 Reg_C (2hr)for the Envelope=   10.3571186
 The PMPs for 2-hr are:
           1    131.812622
           2    129.584274
           3    157.892853
           4    173.640457
           5    169.338074
           6    187.304321
```

```
           7   197.814407
           8   241.028305
           9   179.624557
          10   130.062408
          11   142.416092
          12   234.768524
          13   118.491974
          14   208.505524
          15   155.267090
          16   168.792313
          17   166.278961
          18   207.793701
          19   179.448090
          20   238.105728
          21   143.018448
          22   140.046173
          23   172.368073
          24   231.682220
          25   88.2011108
          26   262.015839
          27   244.669861
          28   210.566620
          29   197.072266
          30   110.827194
          31   83.5854721
          32   201.219360
          33   168.684845
          34   112.830544
          35   172.068039
          36   118.457031
          37   150.865463
          38   202.480347
          39   200.385544
          40   288.755310
          41   138.843628
          42   182.319366
          43   194.975540
          44   143.510803
          45   175.864471
Reg_M (3hr)for the Envelope= -0.232597888
Reg_C (3hr)for the Envelope=   28.6336479
The PMPs for 3-hr are:
           1   300.514191
           2   333.297485
           3   435.327332
           4   305.119690
           5   392.448029
           6   418.894562
           7   425.182648
           8   555.805603
           9   330.617279
          10   282.929565
          11   295.783447
          12   257.816528
          13   283.172180
          14   342.872223
          15   364.340942
          16   365.922150
          17   339.434174
          18   342.689209
          19   438.856018
          20   507.975708
          21   324.379303
          22   355.748505
          23   401.674072
```

```
         24   396.853668
         25   187.457092
         26   483.002014
         27   542.250793
         28   275.019135
         29   289.977539
         30   291.058624
         31   228.154785
         32   436.786224
         33   353.749451
         34   322.278107
         35   351.165680
         36   287.077362
         37   375.536652
         38   361.553009
         39   415.637421
         40   641.774475
         41   313.792725
         42   356.315369
         43   422.480042
         44   319.364899
         45   384.028320
Reg_M (4hr)for the Envelope= -0.286772758
Reg_C (4hr)for the Envelope=   37.4877090
The PMPs for 4-hr are:
          1   431.406647
          2   513.559143
          3   612.289734
          4   401.239502
          5   507.641174
          6   545.304016
          7   565.259705
          8   795.073853
          9   413.709961
         10   393.940308
         11   401.091003
         12   269.579773
         13   391.043396
         14   426.704742
         15   484.867218
         16   476.106720
         17   438.978912
         18   415.528259
         19   593.214966
         20   644.550049
         21   411.265869
         22   522.412170
         23   569.416016
         24   485.346985
         25   272.447296
         26   593.960754
         27   712.868530
         28   313.170624
         29   338.839508
         30   447.720978
         31   347.203613
         32   620.791504
         33   454.222778
         34   464.006561
         35   456.793091
         36   429.494476
         37   522.076294
         38   456.856812
         39   570.897644
         40   821.405396
```

```
         41   422.011841
         42   455.122375
         43   586.588257
         44   435.896820
         45   514.999207
Reg_M (6hr)for the Envelope= -0.120998450
Reg_C (6hr)for the Envelope=   19.3225060
The PMPs for 6-hr are:
          1   300.308289
          2   353.101105
          3   399.800964
          4   323.485046
          5   321.950378
          6   350.611877
          7   404.035645
          8   567.165222
          9   306.900452
         10   308.223633
         11   280.728760
         12   278.437073
         13   265.874329
         14   327.980957
         15   331.425690
         16   315.178650
         17   317.924805
         18   336.217834
         19   446.633728
         20   372.457947
         21   257.380249
         22   387.056702
         23   396.409851
         24   377.932892
         25   216.094391
         26   466.721252
         27   502.338898
         28   270.583282
         29   282.321777
         30   344.238586
         31   251.901993
         32   446.723633
         33   324.200623
         34   349.109711
         35   324.186066
         36   270.559448
         37   376.211761
         38   344.551208
         39   396.527222
         40   518.811951
         41   290.737488
         42   332.114868
         43   414.482300
         44   298.723053
         45   390.488892
Reg_M (12hr)for the Envelope=  -8.68457332E-02
Reg_C (12hr)for the Envelope=   18.8605824
The PMPs for 12-hr are:
          1   337.997925
          2   456.595978
          3   460.910828
          4   468.947357
          5   471.469360
          6   434.329681
          7   542.183899
          8   776.304443
          9   376.606201
```

```
          10   362.648651
          11   405.357422
          12   354.182953
          13   395.362762
          14   419.999878
          15   439.180908
          16   375.291870
          17   530.494629
          18   484.776428
          19   538.778625
          20   442.895294
          21   357.566864
          22   536.899719
          23   541.066101
          24   452.357483
          25   334.082947
          26   673.376160
          27   757.160400
          28   420.016937
          29   379.075134
          30   474.344330
          31   349.591705
          32   608.338440
          33   437.352264
          34   445.048035
          35   407.935364
          36   333.824219
          37   489.914520
          38   473.436401
          39   539.493835
          40   621.620850
          41   328.179749
          42   448.587189
          43   638.726013
          44   385.115540
          45   487.149628
Reg_M (24hr)for the Envelope=  -1.84585974E-02
Reg_C (24hr)for the Envelope=   8.61031055
The PMPs for 24-hr are:
           1   261.905914
           2   324.619293
           3   340.709808
           4   429.590576
           5   397.879028
           6   331.456238
           7   474.499084
           8   568.054077
           9   371.415253
          10   309.874268
          11   391.522339
          12   535.230896
          13   373.922241
          14   455.043854
          15   378.908142
          16   341.286682
          17   492.727539
          18   590.701172
          19   424.005432
          20   355.116333
          21   327.727844
          22   415.014771
          23   457.282166
          24   658.762939
          25   261.768890
          26   698.785522
```

27	645.657471
28	624.948608
29	667.638550
30	361.714508
31	330.418488
32	659.635803
33	353.185242
34	343.992065
35	395.841614
36	238.988831
37	404.538788
38	502.820374
39	497.253540
40	578.790771
41	294.715546
42	394.095459
43	583.988892
44	318.333008
45	458.639587